

Importance of the IL-6 / STAT3 signalling
pathway in prostate cancer stem cells

Paula Kroon

PhD

University of York

Biology

September 2012

Abstract

Prostate cancer is the most diagnosed cancer in men in the Western world. Currently, most treatments are directed towards an androgen receptor-expressing cell, which encompasses the majority of prostate tumours. Unfortunately, the tumour recurs in the majority of patients. This recurrence is thought to arise due to the presence of a rare population of prostate cancer stem cells. These cells are also hypothesized to be responsible for tumour initiation, maintenance, recurrence and metastasis. It is therefore important to develop novel therapies to target these tumour-initiating cells.

Interleukin-6 (IL-6) is a pro-inflammatory cytokine, which is involved in the regulation of a multitude of cellular functions, including proliferation, apoptosis, and differentiation. IL-6 and the associated JAK-STAT signalling pathway have been implicated in the development and progression of a variety of tumours, including prostate cancer.

In this study we have demonstrated that these stem-like cells, selected from primary prostate cancer cultures have elevated IL-6 levels and express the IL-6 receptor, suggesting that these cells are constitutively active. Targeting IL-6, and downstream activation of STAT3, resulted in a significant decrease in colony forming ability of these stem-like cells. Moreover, treatment with a small molecule inhibitor of STAT3 resulted in a modest inhibition of tumour growth, with a significant increase in the proportion of CD24⁺ luminal cells. Whilst the impact on established tumours was modest, LLL12 abolished tumour initiation, suggesting that activation of STAT3, through IL-6, is important for the maintenance of the undifferentiated stem-like cells within prostate tumours. Targeting the JAK-STAT signalling pathway in this cell population might result in a more durable response to current standard of care therapies.

Table of Contents

1.1.1.1. List of figures and tables	7
1.1.1.2. Acknowledgements	10
1.1.1.3. Author's declaration	11
1. Introduction	14
1.1. The prostate and prostate cancer	14
1.1.1. Anatomy and development of the human prostate	14
1.1.2. Prostate epithelial stem cells	18
1.1.3. Prostate cancer	23
1.1.3.1. Prostate cancer incidence	23
1.1.3.2. Diseases of the prostate	24
1.1.3.3. Diagnosis of prostate cancer	24
1.1.3.4. Treatment of prostate cancer	27
1.1.4. Development of prostate cancer	29
1.1.4.1. Castrate resistant prostate cancer	33
1.1.5. Prostate cancer stem cells	35
1.1.6. Prostate cancer stem cells and therapy resistance	39
1.1.7. Models for studying prostate cancer	41
1.1.7.1. Cell lines	41
1.1.7.2. Primary cells	42
1.1.7.3. Mouse models	42
1.2. Inflammation and cancer	45
1.2.1. Inflammation and prostate cancer	48
1.2.2. JAK-STAT signalling pathway	50
1.2.2.1. STAT3 activation and prostate cancer	54
1.2.2.2. IL-6 and prostate cancer	56
1.2.3. Targeting the JAK-STAT signalling pathway in prostate cancer stem cells	58
1.3. Main research strategies and aims	61
2. Materials and Methods	63
2.1. Mammalian cell culture	63
2.1.1. Cell lines	63
2.1.2. Primary cell culture	63
2.1.3. Isolation of subpopulations from primary prostate epithelial cell cultures	65
2.1.4. Isolation of lymphocytes from patients peripheral blood samples	66
2.1.5. Determination of live cell number	66
2.2. Transcriptional expression	67
2.2.1. RNA extraction	67
2.2.2. RT-PCR	67
2.2.3. Quantitative RT-PCR	68
2.3. Protein expression	69

2.3.1.	Primary prostate cells	69
2.3.1.1.	SDS-PAGE and Western blot	69
2.3.1.1.1.	Preparation of whole cell lysates	69
2.3.1.1.2.	Preparation of cytoplasmic and nuclear extracts	69
2.3.1.1.3.	BCA assay for the determination of protein concentrations	70
2.3.1.1.4.	SDS-PAGE gel electrophoreses and Western blotting	70
2.3.1.2.	Enzyme-Linked Immunosorbent spot (ELISPOT) assay	71
2.3.1.3.	Enzyme-Linked ImmunoSorbent Assay (ELISA)	72
2.3.1.4.	Cell-Based ELISA	72
2.3.1.5.	Flow cytometry	73
2.3.1.5.1.	Detection of cell surface protein(s)	73
2.3.1.5.2.	Detection of intracellular antigen(s)	74
2.3.1.5.3.	Data analysis	74
2.3.1.6.	Immunofluorescence with fixed cells	75
2.3.2.	Prostate tissue	75
2.3.2.1.	Preparation of tissue blocks and sections	75
2.3.2.2.	Hematoxylin & eosin (H&E) staining	75
2.3.2.3.	Immunohistochemistry	76
2.3.2.4.	Immunofluorescence	76
2.4.	Functional analysis	77
2.4.1.	Clonogenic recovery assay	77
2.5.	In Vivo studies	78
2.5.1.	General animal husbandry	78
2.5.2.	Subcutaneous xenotransplantation of prostate tumour cells	78
2.5.2.1.	Depletion of mouse endothelial and lineage positive blood cells	78
2.5.2.2.	Engraftment of prostate tumour cells	79
2.5.3.	Intraperitoneal injection of drug into Rag2 ^{-/-} γC ^{-/-} mice	80
2.5.4.	Ex vivo treatment of human xenograft cells	80
2.5.5.	Analyses of treatment response	81
3.	Results I	83
3.1.	IL-6 expression in primary prostate cells	83
3.1.1.	IL-6 mRNA expression in selected populations	83
3.1.2.	Summary of IL-6 mRNA expression in selected populations of primary prostate cells	86
3.1.3.	IL-6 protein expression in selected populations	88
3.1.3.1.	Levels of secreted IL-6 in selected populations of primary prostate cells, using ELISPOT assay	88
3.1.3.2.	Levels of secreted IL-6 in selected populations of primary prostate cells, using ELISA	90
3.1.3.2.1.	Optimization of the High Sensitivity Human IL-6 ELISA	90
3.1.3.2.2.	HS ELISA for IL-6 on selected populations of primary prostate cells	90

3.1.3.2.3.	Analysis of secreted IL-6 levels from a series of primary prostate cell cultures	93
3.2.	IL-6 receptor expression in primary prostate cells	95
3.2.1.	IL-6 receptor expression in prostate cell lines by Western blot	95
3.2.2.	IL-6 receptor expression in benign prostate tissue	97
3.2.2.1.	Immunohistochemistry for IL-6 receptor	97
3.2.2.2.	Immunofluorescence for IL-6 receptor	97
3.2.3.	Leukemia Inhibitory Factor receptor expression in benign prostate tissue	100
3.2.4.	IL-6 receptor expression on selected primary prostate cells	102
3.2.4.1.	Immunofluorescence staining for IL-6 receptor	102
3.2.4.2.	Flow cytometry analysis for IL-6 receptor	105
3.3.	Activation of the JAK-STAT signaling pathway	110
3.3.1.	STAT3 phosphorylation in primary prostate cells	110
3.4.	Inhibition of STAT3 phosphorylation in primary prostate cells	112
3.4.1.	Inhibition of STAT3 phosphorylation using pyridone-6	112
3.4.2.	Inhibition of the JAK-STAT pathway using neutralizing antibodies	117
3.4.2.1.	Inhibition of the JAK-STAT pathway using commercially available neutralizing antibodies to IL-6, LIF and OSM	117
3.4.2.2.	Inhibition of STAT3 phosphorylation using CNTO 328	119
3.4.3.	Inhibition of STAT3 phosphorylation using a direct inhibitor, LLL12	124
3.4.3.1.	Optimization of treatment with LLL12	124
3.4.3.2.	Change in cell morphology following treatment with LLL12	126
3.4.3.3.	Western blot analysis for pSTAT3 in primary prostate cells treated with LLL12	126
3.4.3.4.	Flow cytometry analysis of primary prostate cells treated with LLL12	126
3.5.	Importance of the JAK-STAT signalling pathway for cell survival	130
3.5.1.	Colony formation efficiency following treatment with P6	130
3.5.1.1.	Using a Rho-associated kinase inhibitor to improve colony formation efficiency	134
3.5.2.	Summary of results on the effect of treatment with the JAK inhibitor (P6) on colony forming recovery	136
3.5.3.	The effect of the IL-6 neutralizing antibody CNTO 328 on Colony forming efficiency of prostate primary cells	139
3.5.4.	The effect of treatment with the STAT3 inhibitor, LLL12 on colony forming efficiency	139
4.	Results II	142
4.1.	Optimisation of protocol to determine the effect of LLL12 on tumour growth in a ‘near patient’ xenograft	142
4.2.	Levels of STAT3 phosphorylation in a panel of ‘near patient’ xenografts	144
4.3.	Inhibition of tumour growth using the pSTAT3 inhibitor LLL12	146

4.3.1.	Treatment of tumours derived from Y019 xenograft with LLL12	146
4.3.2.	Treatment of tumours derived from Y018 xenograft with LLL12	151
4.3.2.1.	Histological analysis of Y018 xenograft post treatment	154
4.3.2.2.	Flow cytometry analysis of Y018 xenograft post treatment.....	154
4.3.2.3.	Levels of phosphorylated STAT3 in Y018 xenograft post treatment.....	159
4.3.3.	Flow cytometry analysis for levels of phosphorylated STAT3 in xenograft tumour cells	161
4.4.	Tumour initiation frequency following ex vivo treatment of xenograft tumour cells.....	163
4.4.1.	Ex vivo treatment of xenograft cells with LLL12	163
4.4.2.	Effect of ex vivo treatment of the STAT3 inhibitor LLL12 on tumour initiation of Y019 xenograft.....	165
4.4.3.	Flow cytometry analysis of xenograft tumours initiated following ex vivo treatment	165
5.	Discussion	169
5.1.	IL-6 is highly expressed by undifferentiated prostate cancer cells.....	169
5.2.	IL-6 receptor is expressed in a rare subpopulation of undifferentiated prostate cancer cells	171
5.3.	STAT3 is constitutively activate in primary prostate cells	174
5.4.	Successful inhibition of STAT3 phosphorylation, using an anti-IL-6 antibody and small molecule inhibitor.....	176
5.5.	Inhibition of STAT3 phosphorylation resulted in a decrease in the cell survival of the undifferentiated stem-like cells from primary cancer samples	179
5.6.	In vivo inhibition of STAT3 phosphorylation, using LLL12, resulted in a decrease in tumour growth	181
5.7.	Treatment of Y018 xenograft with LLL12 resulted in an increase in cells with a luminal phenotype.....	184
5.8.	Ex vivo treatment of xenograft tumour cells with LLL12 resulted in improved survival.....	185
5.9.	Summary.....	188
	Abbreviations	191
	Appendices.....	195
	References	207

1.1.1.1. List of figures and tables

Table 1. Prostate cancer treatment: current target and therapy resistance.....	28
Table 2. Common mutation and genes involved in the initiation and development of prostate cancer.	31
Table 3. Cyan ADP flow cytometry lasers.....	74
Table 4. Percentage of α_2^{hi} and α_2^{low} cells from several primary prostate cancer cell cultures.	105
Table 5. Tumour initiation frequency of “near patients” xenografts used in this study.	142
Table 6. Tumour initiation frequency of Y019 xenograft, following <i>ex vivo</i> treatment.	165
Figure 1.1. Schematic representation of the location of the human prostate gland.....	14
Figure 1.2. Schematic representation of the anatomy and organisation of the human prostate gland.	15
Figure 1.3. Schematic representation of the architecture of the human prostate epithelium.....	17
Figure 1.4. Schematic representation of the human prostate epithelium as a hierarchical pathway.	21
Figure 1.5. Fractionation of prostate epithelial cells.....	21
Figure 1.6. The ten most commonly diagnosed male cancer in the UK (2009),	23
Figure 1.7. Gleason grading system for prostatic adenocarcinoma.....	26
Figure 1.8. Pathway of the progression of human prostate cancer.	30
Figure 1.9. Schematic representation of the fractionation of human prostate biopsies.....	38
Figure 1.10. Schematic representation of the JAK-STAT signalling pathway.....	51
Figure 1.11. Schematic representation of STAT3 activation through the IL-6 family of cytokines.	55
Figure 1.12. Schematic representation of inhibitors of the JAK-STAT signalling pathway.....	60
Figure 3.1. qRT-PCR analysis for IL-6 expression in primary prostate cells.	85
Figure 3.2. Overall results of IL-6 mRNA expression in a series of primary prostate cancer and benign cultures.....	87
Figure 3.3. Levels of secreted IL-6 in selected populations of primary prostate cells, using ELISPOT.	89
Figure 3.4. Optimisation of ELISA assay to analyse levels of secreted IL-6.....	91
Figure 3.5. IL-6 levels from conditioned medium of primary prostate cell cultures.....	92
Figure 3.6. Overall results of IL-6 levels in a series of primary prostate cancer and benign cultures.....	94

Figure 3.7. IL-6 receptor expression in prostate cell lines and primary prostate cells, by Western blot.....	96
Figure 3.8. IL-6 receptor staining of BPH paraffin embedded tissue sections.	98
Figure 3.9. IL-6 receptor and CK-5 co-staining of BPH paraffin embedded tissue sections.....	99
Figure 3.10. LIF receptor staining of BPH paraffin embedded sections.	101
Figure 3.11. IL-6 receptor staining on selected cells from primary prostate cultures..	103
Figure 3.12. Flow cytometry analysis for the IL-6 receptor, CD49b and CD133 on primary prostate cells.....	106
Figure 3.13. Flow cytometry analysis for CD133 on primary prostate cancer cells. ...	108
Figure 3.14. Flow cytometry analysis for the IL-6 receptor and CD133 from pre-selected $\alpha_2\beta_1^{hi}$ and $\alpha_2\beta_1^{low}$ cells.....	109
Figure 3.15. Levels of phosphorylated STAT3 in primary prostate cells.....	111
Figure 3.16. Effect of Pyridone-6 on phosphorylated STAT3 levels in a series of primary prostate cells.....	113
Figure 3.17. Time course of treatment of primary prostate cancer cells with Pyridone-6.	116
Figure 3.18. Effect of neutralizing antibodies against IL-6, LIF and OSM on phosphorylated STAT3 levels.....	118
Figure 3.19. Effect of CNTO 328 on phosphorylated STAT3 levels.	120
Figure 3.20. Effect of CNTO 328 on phosphorylated STAT3 levels in a series of primary prostate cancer cells.....	122
Figure 3.21. Optimization of primary prostate cells treated with LLL12 to inhibit phosphorylation of STAT3.	125
Figure 3.22. Effect of LLL12 on phosphorylated STAT3 levels in primary prostate cells.....	127
Figure 3.23. Images of colonies derived from single stem-like cells.....	131
Figure 3.24. Colony forming efficiency of primary prostate cells derived from prostate cancer and benign disease, following treatment with P6.....	132
Figure 3.25. Colony forming efficiency of primary prostate cancer cells, following treatment with P6, + / - ROCK inhibitor.....	135
Figure 3.26. Overall results on colony forming efficiency of a series of primary prostate cancer cell cultures, following treatment with the JAK inhibitor, P6.....	138
Figure 3.27. Colony formation efficiency of primary prostate cancer cells following treatment with CNTO 328 and LLL12.	140
Figure 4.1. Overview of the <i>in vivo</i> protocol to determine the effect of LLL12 on tumour growth.	143
Figure 4.2. Levels of phosphorylated STAT3 in a series of 'near patient' xenografts.	145

Figure 4.3. Growth curve of Y019 xenograft after treatment with LLL12.	147
Figure 4.4. Flow cytometry gating strategy.	148
Figure 4.5. Flow cytometry analysis of Y019 xenograft tumour cells after treatment with LLL12.	150
Figure 4.6. Growth curve of Y018 xenograft after treatment with LLL12.	152
Figure 4.7. Survival curves of Y018 xenograft after treatment with LLL12.	153
Figure 4.8. H&E staining of Y018 xenograft paraffin embedded tissue sections.	155
Figure 4.9. Flow cytometry analysis of Y018 xenograft tumour cells after treatment with LLL12.	157
Figure 4.10. Effect on phosphorylated STAT3 levels after <i>in vivo</i> treatment of Y018 xenograft tumours.	160
Figure 4.11. Flow cytometry analysis, of xenograft tumour cells, for levels of phosphorylated STAT3.	162
Figure 4.12. Effect on the viability of xenograft tumour cells, following <i>ex vivo</i> treatment.	164
Figure 4.13. Survival curve of Y019 xenograft, following <i>ex vivo</i> treatment of tumour cells.	166
Figure 4.14. Flow cytometry analysis, of xenograft tumour initiated after overnight <i>ex vivo</i> treatment.	167
Figure 5.1. <i>In vivo</i> pre-clinical model for testing prostate cancer stem cells therapeutics.	187
Figure 5.2. Proposed model of STAT3 activation in prostate cancer.	190

1.1.1.2. Acknowledgements

I would like to thank Yorkshire Cancer Research for funding this project and my supervisor Norman Maitland for giving me the opportunity to carry out this work in his laboratory.

I would especially like to thank my co-supervisor Anne Collins who supported me throughout this thesis with her patience and knowledge, especially towards the end when I needed the most encouragement and whilst writing this thesis

I would also like to thank Paul Berry for assisting me with the *in vivo* experiments and continuing the work whilst I was away or writing my thesis. Also, thanks to Alan Haigh for his training and advice whilst carrying out the *in vivo* experiments. I would also like to thank Katy Hyde and Hannah Walker for their help over the years whilst working in the tissue culture lab as well as the main lab. And Fiona Frame for being there to talk to, science related or not, especially late in the evenings and occasionally trying to make me go to the gym and not think about science. A special thanks to my fellow PhD students Guillermo Rivera and Emma Oldridge for their support during the years, they made this PhD easier as we were in the same situation together. However, everyone, past and present members, of the YCR CRU lab deserves a special thanks for making this a very welcoming and relaxing work environment.

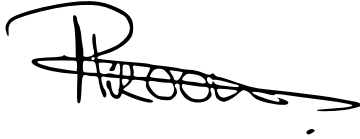
I would also like to thank members of the technology facility and the BSF for their advice and training on the confocal and flow cytometer, where I spend many hours, and the support provided by the animal facility. Tom Li for kindly providing me with the STAT3 inhibitors as well as J&J for the agreement to use their antibody.

Also, a special thanks all my friends and family, they made sure I stayed sane during my PhD and were always there for me when I was visiting.

Last, but certainly not least, I would like to extend my appreciation to all those patients from York District Hospital and Castle Hill Hospital (Hull) who kindly donated their tissue and the surgeons for their cooperation, and therefore supporting cancer research.

1.1.1.3. Author's declaration

I declare that this thesis represents my own unaided work, except where acknowledged otherwise in the text, and that this work has not been submitted previously in consideration for a degree at this, or any other university.

A handwritten signature in black ink, appearing to read 'Paula Kroon', with a large, stylized initial 'P'.

Paula Kroon

September 2012

This work has been presented at the following scientific meeting

- White Rose Stem Cell meeting, May 2009, oral presentation.
- YCR annual scientific meeting, June 2009, poster presentation.
- 3rd International symposium Stem Cells, Development and Regulation, October 2009, poster presentation.
- White Rose Stem Cell meeting, December 2009, oral presentation.
- YCR annual scientific meeting, June 2010, poster presentation.
- Young Prostate Research Symposium, November 2010, poster presentation.
- Stem Cells, Cancer and Metastasis Keystone Symposium, March 2011, poster presentation.
- YCR annual scientific meeting, June 2011, oral presentation.
- YCR annual scientific meeting, June 2012, poster presentation.
- EACR22 – from Basic Research to Personalized Cancer Treatment, July 2012, poster presentation.

Parts of this work have been under consideration for publishing.

Cancer Stem Cells in Prostate Cancer. 2011. Paula Kroon, Davide Pellacani, Fiona M Frame, Norman J Maitland, Anne T Collins. In *Cancer Stem Cells in Solid Tumors*, A.L. Allan, ed. (Springer Science + Business Media), p99 -116.

JAK-STAT blockade inhibits tumour-initiation and clonogenic recovery of prostate cancer stem cells. Paula Kroon, Paul A. Berry, Michael J. Stower, Greta Rodrigues, Vincent M. Mann, Matthew Simms, Deepak Bhasin, Pui-Kai Li, Chenglong Li, Norman J. Maitland, Anne T. Collins. *Manuscript in preparation*.

Chapter 1

Introduction

1. Introduction

1.1. The prostate and prostate cancer

1.1.1. Anatomy and development of the human prostate

The prostate is located towards the base of the bladder surrounding the urethra (Figure 1.1). The main function of the prostate is to produce hormones and secrete proteins for semen production and is therefore essential for the reproductive system. It also functions as an endocrine gland, as it helps the rapid metabolism of testosterone to dihydrotestosterone (DHT), which is a more effective androgen (Kumar and Majumder, 1995).

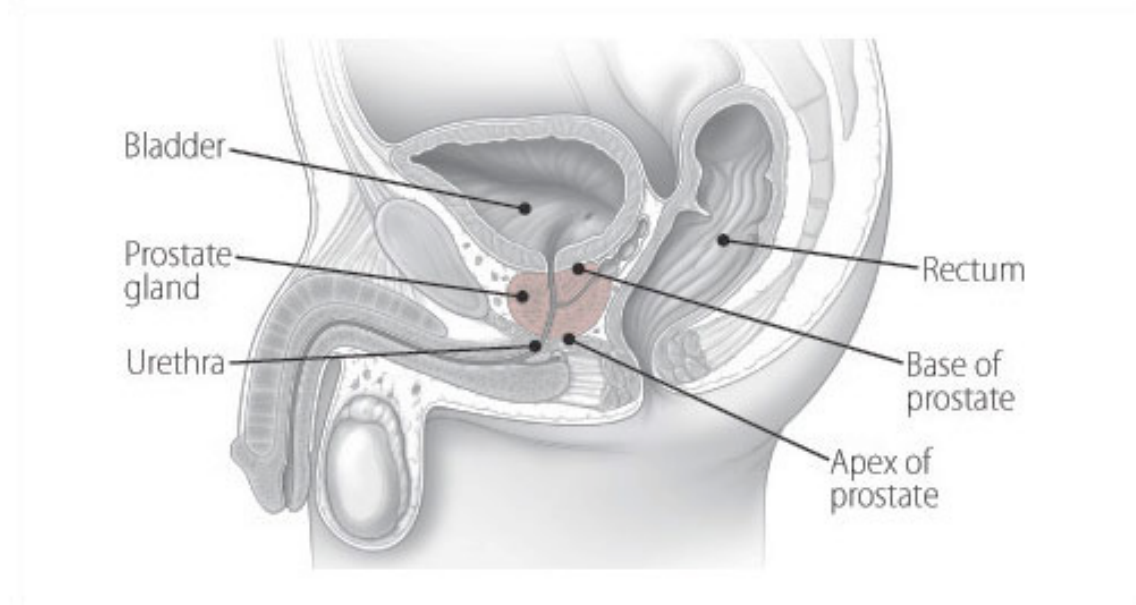


Figure 1.1. **Schematic representation of the location of the human prostate gland.**The walnut sized prostate is located in front of the rectum and towards the base of the bladder, surrounding the urethra. Image taken from ¹

¹ www.harvardprostateknowledge.org/prostate-basics

The human adult prostate is a complex tubulo-alveolar gland composed of an epithelial parenchyma embedded within a connective tissue matrix. The epithelial cells are arranged in glands composed of ducts that branch out from the urethra and terminate into acini. The human prostate is a heterogeneous organ, which can be divided into central, transition and peripheral zones. In a young adult prostate gland, the peripheral zone is the largest zone (70% of the glandular tissue) and surrounds the urethra. The second largest zone (25%) is the central zone, which surrounds the ejaculatory ducts. The transition zone makes up only 5% of the volume (Figure 1.2A). The whole organ is encapsulated in a fibrous capsule (McNeal, 1981). The majority of prostate cancers arise in the peripheral zone (70%) compared to 20% in the transition zone and 10% within the central zone, whereas Benign Prostatic Hyperplasia (BPH) mainly occurs within the transitional zone (McNeal et al., 1988).

Each glandular zone has specific architectural and stromal features, as in all zones of the prostate the acini are distributed evenly with columnar secretory luminal cell lining the lumen. In the human prostate, basal cells line the basement membrane (Figure 1.2B). However, within the different zones of the prostate there are differences in the parenchymal components of the prostate as there is a variation in size, shape and number of acini and in compactness and looseness of stroma (McNeal, 1981; Amin et al., 2010).

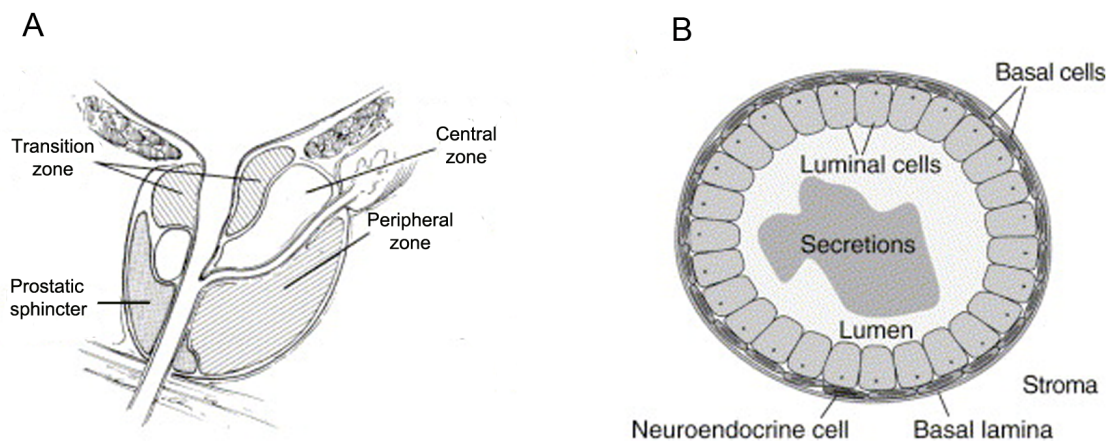


Figure 1.2. **Schematic representation of the anatomy and organisation of the human prostate gland.**A. Zonal anatomy of the human prostate gland of a young adult, consisting of the peripheral zone (70%), central zone (25%) and transition zone (5%), according to (McNeal, 1981). B. Organisation of the prostate duct, consisting of epithelial cells: basal cells layer, neuroendocrine cells and secretory luminal cells, and stromal cells. Adapted from (Abate-Shen and Shen, 2000).

The development of the human prostate begins during the ninth week of embryogenesis (Kellokumpu-Lehtinen et al., 1979), in response to testosterone stimulation. It starts with the outgrowth of epithelial buds from the urogenital sinus epithelium into the surrounding urogenital sinus mesenchyme (UGM) (Cunha et al., 1987). By the 11th week, some of the prostatic outgrowths acquire a lumen (Kellokumpu-Lehtinen et al., 1980). Mesenchymal cells differentiate into smooth muscle, fibroblasts and blood vessels, and the epithelial buds form ducts that elongate, branch out and terminate into acini, whilst the stroma of the glands thin (Kellokumpu-Lehtinen et al., 1980). From the 20th week of gestation up to puberty, the immature prostatic acini and ducts are lined by multiple layers of immature cells with round nuclei and very little cytoplasm. In the immature epithelium, cytokeratins (CK) of simple and stratified epithelium are expressed (primary cytokeratins; numbers 7, 8, 18 and 19) (Wernert et al., 1987). During puberty, where the levels of testosterone increase again (Coffey and Pienta, 1987), the prostate undergoes dramatic morphological changes as the immature multilayered epithelium differentiates into a two-layered epithelium consisting of peripheral flattened to cuboidal basal cells and inner secretory cylindrical epithelium (Kellokumpu-Lehtinen et al., 1981; Aumuller, 1991). In parallel with epithelial differentiation, the epithelial-mesenchymal interaction induces UGM to proliferate and differentiate into prostatic smooth muscle and interfascicular fibroblasts (Cunha et al., 1992).

The main cell types within the mature prostate gland are basal, secretory luminal and neuroendocrine cells (Aumuller, 1991) (Figure 1.3). The luminal epithelial cells represent the major cell type in normal prostate. They are terminally differentiated, express high levels of androgen receptor (AR) (Sar et al., 1990) and are dependent upon androgens for their survival (Kyprianou and Isaacs, 1988b). The luminal cells are the 'factory' within the epithelium generating secretory products like prostate-specific antigen (PSA) and prostatic acid phosphatase (PAP) (Lilja and Abrahamsson, 1988). Basal cells are relatively undifferentiated, express low/undetectable levels of AR (Bonkhoff and Remberger, 1993) and are androgen-independent for their survival (Kyprianou and Isaacs, 1988b). The basal cells lack secretory activity but, unlike luminal cells, are able to proliferate, indicating a role of basal cells in epithelial renewal, and the development of hyperplastic and neoplastic disorders in the human prostate (Bonkhoff et al., 1994). Rare neuroendocrine cells are located within the basal layer and they are terminally differentiated and androgen-insensitive (Bonkhoff et al., 1995). The neuroendocrine cells secrete a variety of hormones, including serotonin, calcitonin and chromogranin family of peptides (di Sant'Agnes, 1998; Abrahamsson, 1999). The neuroendocrine cells are essential for the growth and differentiation, and for the

homeostatic regulation of the secretory processes in the mature prostate gland (di Sant'Agnes, 1992). Closely associated with the basal cell surface is the basement membrane, which is a layer of specialized matrix that surrounds the normal prostate gland and acts as a barrier separating epithelial cells from connective tissue (Bonkhoff et al., 1991). Because of the basement membrane, the epithelium normally lacks the supply of blood vessels and lymphatic ducts, and therefore totally relies on the stroma for its metabolic needs. The stromal cells within the normal prostate gland consist of a mixture of cell types, including myofibroblasts, fibroblasts and smooth muscle cells, which express the AR. The stromal cells are responsible for prediction of epithelial cell development, maintenance and differentiation as they supply nutrients and growth factors (Kassen et al., 1996; Hayward et al., 1997; Berry et al., 2008).

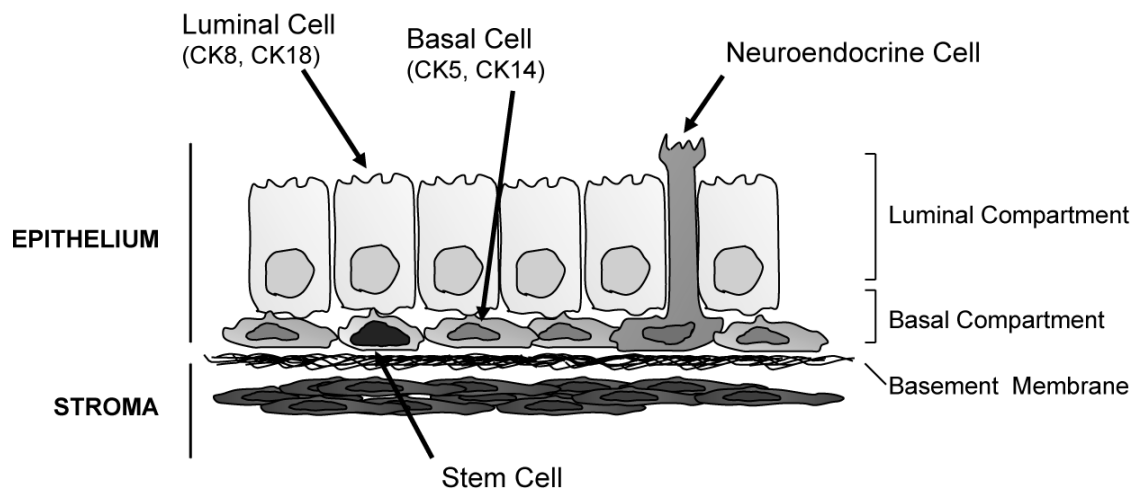


Figure 1.3. **Schematic representation of the architecture of the human prostate epithelium.** The human prostate epithelium consists of the basal layer of relatively undifferentiated basal cells and a luminal layer of terminally differentiated secretory luminal cells, separated from stromal cells by the basement membrane. Taken from (Kroon et al., 2011).

1.1.2. Prostate epithelial stem cells

Adult stem cells are an essential component of tissue homeostasis, as they support ongoing tissue regeneration, and replacing terminally differentiated cells with a short lifespan or lost cells due to apoptosis or injury. Due to this important function, these stem cells need to be able to self-renew and differentiate throughout the lifespan of an adult. In self-renewing epithelial tissue, the rare stem cell population has the capacity for unlimited growth and its progeny are either stem cells or cells with more limited proliferative capacity, named transit amplifying (TA) cells. These transit amplifying (progenitor) cells divide to maintain tissue balance, but are limited to a fixed number of cell divisions before they terminally differentiate (Potten, 1981; Hall and Watt, 1989). Initial studies on stem cells focused on tissues with rapid cell turnover, such as skin and intestine (Potten, 1981; Hall and Watt, 1989). However other epithelia, such as the liver and pancreas, have a slow cell turnover under normal conditions but do have special adaptation for regeneration (Finegood et al., 1995; Alison et al., 1997; Slack, 2000). These studies have provided evidence that all epithelial tissue contain cells that are capable of repopulating during a normal lifespan or at least under circumstances of tissue repair (Slack, 2000).

The prostate is an androgen-dependent organ, which normally undergoes very limited regeneration or turnover. The prostate undergoes involution following castration, but can completely regenerate if androgen levels are restored (Isaacs and Coffey, 1989). Isaacs showed that this cycle of involution, followed by regeneration, can be repeated numerous times and postulated the existence of a population of long-lived, androgen-independent stem cells (SC) responsible for regeneration of the gland (Isaacs, 1985). This led to a model of prostate lineage in which androgen-independent SCs give rise to androgen-responsive transit amplifying cells, which differentiate into secretory luminal cells, which are both androgen-dependent and terminally differentiated (Isaacs and Coffey, 1989).

Basal and luminal cells can be discriminated on the basis of their localization, morphology and expression of specific cytokeratins (Figure 1.3). For example, CK5 and CK14 are expressed by basal cells, whereas the luminal cells of the prostate predominantly express CK8 and CK18 (Sherwood et al., 1991). Keratin expression patterns in the prostate have provided evidence of epithelial cells that are phenotypically intermediate between basal and luminal cells. Cells have been identified, in the luminal layer, that express both CK5 and CK18 while some basal cells lack CK14 expression, but express low levels of CK18 and CK5 (Verhagen et al., 1992;

Xue et al., 1998; van Leenders et al., 2000). These results indicate that basal and luminal cells are linked in a hierarchical pathway.

Although the overall organization of the murine prostate differs from that of the human prostate gland, studying the murine prostate provides a unique opportunity to study the biology of the human prostate. Sugimura *et al.* have shown that the proliferating cells are located at the tips of ducts (Sugimura et al., 1986) and suggested that prostatic stem cells are located in the distal region (Kinbara et al., 1996). However, quiescent cells were subsequently shown to be located in the proximal region of the duct nearest the urethra. These cells also have a high proliferative potential and are capable of reconstituting large, branched glandular structures in collagen gels (Tsujiura et al., 2002). Tsujiura and co-workers proposed that the stem cells migrate distally towards the proliferating tips where they terminally differentiate (Tsujiura et al., 2002).

The proposal that prostate stem cells are located within the basal layer of epithelial cells is supported by evidence provided by Signoretti *et al.*, who has shown that p63, which is expressed by basal cells (Yang et al., 1998), is essential for normal prostate development in the mouse (Signoretti et al., 2000). With histological examination, they found that new born p63^(-/-) male mice do not develop a prostate, suggesting that p63 is necessary for the formation of ducts or epithelial budding structures (Signoretti et al., 2000).

Recently, using the murine haematopoietic stem cell marker Sca-1 (Spangrude et al., 1988), it was shown that Sca-1⁺ prostate cells can self-renew (in a sphere-forming assay) for several generations. Moreover Sca-1⁺ cells can differentiate *in vivo* to produce prostatic tubule structures containing basal and luminal cells. Sca1⁺ cells are also localized to the basal cell layer within the proximal region of the murine prostate (Lawson et al., 2007). Leong and colleagues also showed enrichment of stem cells within the proximal region of the mouse prostate. They determined that lin⁻/Sca-1⁺/CD133⁺/CD44⁺/CD177⁺ cells (localized to the basal compartment of mouse prostate) can generate a prostate after transplantation *in vivo* (Leong et al., 2008). The regenerated prostate had a branching morphology with epithelial tubules composed of basal, luminal and neuroendocrine cells. Nonetheless, there is still some controversy as to whether stem cells are located within the basal layer. The *Nkx3.1* gene regulates prostate epithelial differentiation, and is expressed within the luminal cells and rare basal cells, in the mouse prostate. Expression is rapidly lost after castration and is restored following prostate regeneration when androgen levels are restored. Wang and colleagues (2009) showed that, in the castrate-resistant state, *Nkx3.1* expression is restricted to the luminal cells and only those genetically marked. They observed that

Nkx3.1-marked luminal cells were able to give rise to both basal and luminal cells following androgen-induced regeneration (Wang et al., 2009b).

In the human prostate, several studies have revealed that prostatic basal cells can differentiate into luminal cells *in vitro* (Liu et al., 1997; Robinson et al., 1998). Basal epithelial cells, isolated on the basis of high surface expression of $\alpha_2\beta_1$ -integrin, are clonogenic *in vitro* (Hudson et al., 2000; Collins et al., 2001) and have the potential to regenerate a fully differentiated human prostate epithelium *in vivo* (Collins et al., 2001). Using the CD133 antigen, which was first identified as a marker for human haematopoietic stem cells (Yin et al., 1997), further enriched for the stem cell population (Richardson et al., 2004). The cells expressing CD133 are restricted to the $\alpha_2\beta_1^{\text{hi}}$ population and are located within the basal layer. Richardson and colleagues showed that these $\alpha_2\beta_1^{\text{hi}}/\text{CD133}^+$ cells had a greater colony-forming ability and proliferative potential *in vitro* than $\alpha_2\beta_1^{\text{hi}}/\text{CD133}^-$ cells. Moreover, when grafted together with prostate stromal cells, which is necessary for a functional and morphological differentiated prostate (Lang et al., 2001), into nude mice $\alpha_2\beta_1^{\text{hi}}/\text{CD133}^+$ generated prostatic acini, unlike the $\alpha_2\beta_1^{\text{hi}}/\text{CD133}^-$ cells (Richardson et al., 2004).

With the use of lineage-tracking lentiviruses it has been shown that the basal stem cells have the capacity to differentiate through a hierarchy of cells (Frame et al., 2010). All together, the observations suggest that basal and luminal cells are linked in a hierarchical pathway, which is most accurately described as a continuum with different stages of change, rather than a single switch from one cell type to another (Figure 1.4) (Oldridge et al., 2012).

Thus, with the use of different cell surface markers, the following cells types can be isolated from human prostate tissue: basal ($\text{CD44}^+\text{CD24}^-$), luminal ($\text{CD44}^-\text{CD24}^+$) and stromal cells. With the use of cell surface marker, the basal cell population can be subdivided into stem cells ($\alpha_2\beta_1^{\text{hi}}/\text{CD133}^+$), transit-amplifying ($\alpha_2\beta_1^{\text{hi}}/\text{CD133}^-$) and committed basal cells ($\alpha_2\beta_1^{\text{low}}$) as shown in Figure 1.5.

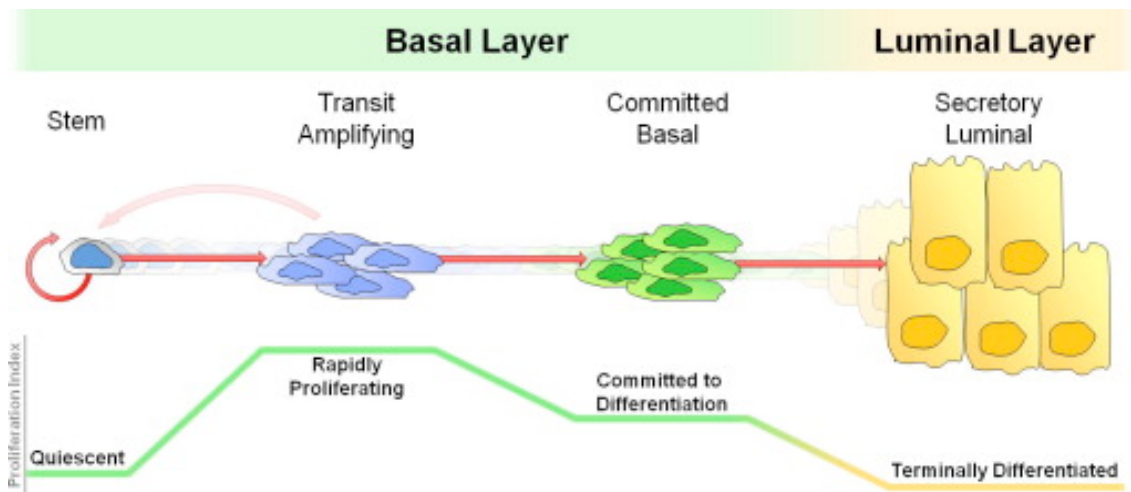


Figure 1.4. **Schematic representation of the human prostate epithelium as a hierarchical pathway.** Stem cells are mostly quiescent and generate the rapidly proliferating transit amplifying cells. Although these cells maintain a degree of multipotency, they are largely committed to differentiation and give rise to committed basal cells. Through the differentiation process, terminally differentiated secretory luminal cells are then formed. Taken from (Oldridge et al., 2012).

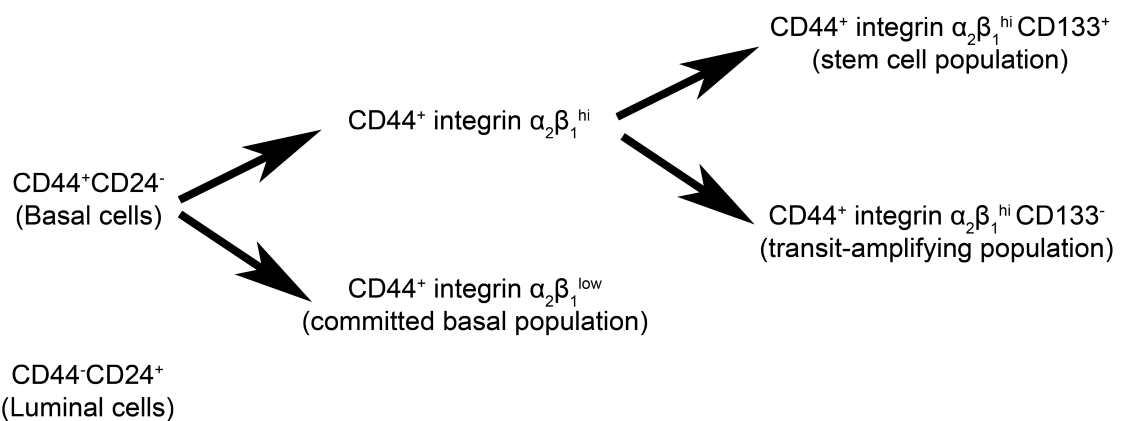


Figure 1.5. **Fractionation of prostate epithelial cells.** Cells can be separated into basal cells (CD44⁺CD24⁻) and terminally differentiated luminal cells (CD44⁻CD24⁺). The basal cells can be further separated into a committed basal population (integrin $\alpha_2\beta_1^{\text{low}}$), transit-amplifying population (integrin $\alpha_2\beta_1^{\text{hi}}$ CD133⁻) and stem cell population (integrin $\alpha_2\beta_1^{\text{hi}}$ CD133⁺), on the basis of expression of cell surface markers integrin $\alpha_2\beta_1$ and CD133.

The identification and characterization of stem cells in the normal prostate is important, because they may represent a major target for carcinogenesis as well as a potential source of BPH (De Marzo et al., 1998). It was hypothesized in the 1960s that cancers exist in a hierarchy consisting of cells with different proliferative potentials (Southam and Brunshwig A., 1961; Bruce and Van Der Gaag, 1963). The cancer stem cell (CSC) hypothesis presumes that the bulk population of cancerous cells arise from CSCs (Hamburger and Salmon, 1977), defined as a rare population of cells that maintain the rest of the population. Normal stem cells and cancer stem cells have shared properties, such as the capacity to self-renew and differentiate to give rise to multi-cellular lineages (Wicha et al., 2006). These properties are important for CSCs to maintain and promotes spread of the tumour.

1.1.3. Prostate cancer

1.1.3.1. Prostate cancer incidence

In the United Kingdom (UK), over 40,000 men were diagnosed with prostate cancer in 2009 and over 10,000 men died from prostate cancer in 2010, according to the most recent statistics. Prostate cancer is the most frequently diagnosed cancer in men, in economically developed countries, as it accounts for 25% of the male cases in the UK (Figure 1.6) (Source: Cancer Research UK). Even though there has been a large increase (>25 fold) in the incidence of prostate cancer in many countries worldwide, there has been little change or even a small decline in mortality. This is because of the wide utilization of PSA testing, which detects clinically important tumours as well as slow-growing tumours that might otherwise escape diagnosis. Prostate cancer incidence is strongly related to age, as 80% of prostate tumours are diagnosed in men over the age of 65. However race (black) and family history also remain well-established risk factors for prostate cancer (Hsing and Chokkalingam, 2006; Jemal et al., 2011).

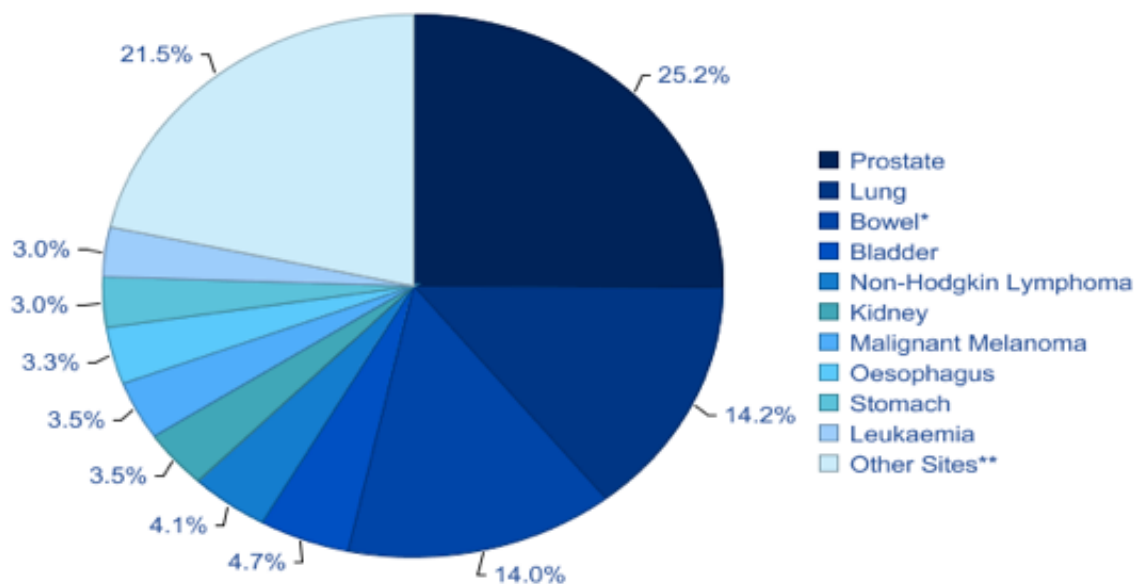


Figure 1.6. **The ten most commonly diagnosed male cancer in the UK (2009)**, with prostate cancer being the most commonly diagnosed male cancer at 25.2%. Taken from Cancer Research UK.

1.1.3.2. Diseases of the prostate

Even though prostate cancer is the cause of 7% of all cancer deaths in the UK, it is not the only disease of the prostate. Other problems of the prostate include Prostatitis and BPH. Prostatitis describes a combination of infectious diseases (acute and chronic bacterial prostatitis), a chronic pelvic pain syndrome and asymptomatic inflammation of the prostate (Drach et al., 1978; Krieger et al., 2008), which usually occurs in the peripheral zone of the prostate gland (Blacklock, 1991). Prostatitis has been most commonly diagnosed in 36 - 65 year old men and can be easily treated with antibiotics, or nonsteroidal anti-inflammatory drugs (Stevermer and Easley, 2000), although there are many potential causes of the disease.

Benign prostate hyperplasia is a non-malignant enlargement of the prostate, which can be associated with lower urinary tract symptoms (LUTS). Histologic BPH shows microscopic evidence of prostate stromal and epithelial hyperplasia, which only occurs in the transition zone of the prostate gland (McNeal, 1988). The microscopic nodules undergo further hyperplastic changes and increase in size, ultimately developing into macroscopic nodules. Because of these changes, the original anatomy of the prostate becomes distorted and the BPH tissue enlarges significantly during this stage, however during this stage the symptoms might not be apparent. The final stage of BPH development is the occurrence of clinical symptoms, as a result of this enlargement of the prostate, i.e. LUTS (decrease in the force and calibre of urinary stream and the sensation of incomplete bladder emptying) (Oesterling, 1991). Almost half of men at the age of 60 exhibit histological evidence of BPH, and almost 90% of men develop histological BPH by the age of 90 (Roehrborn, 2002). However only between 15 and 30% of these men have symptoms. The development of BPH requires both ageing and androgens (Coffey and Walsh, 1990; Lepor, 2004) and the most effective treatment for BPH is transurethral resection of the prostate (TURP) to reduce the enlargement of the prostate and reduce the symptoms. However it has also been shown that treatment with finasteride, which is a competitive inhibitor of 5 α -reductase, resulted in sustained decrease in serum dihydrotestosterone concentration as well as a decrease in PSA levels and prostatic volume (Gormley et al., 1992). So, treatment of finasteride is beneficial to men with BPH.

1.1.3.3. Diagnosis of prostate cancer

The diagnosis of prostate cancer is currently based on the quantification of serum levels of the prostate secretory protein; PSA. The prostate gland normally produces

PSA as it functions as a serine protease to maintain the fluidity of seminal fluid (Watt et al., 1986). In general, PSA levels of < 4 ng/mL are considered normal, however when the PSA levels are above 4 ng/mL, a biopsy is usually taken for further examination. Although PSA testing has led to an increase in the detection of prostate cancer, it has substantial drawbacks. There is a lack of specificity within the range of 4 – 10 ng/mL, which is a diagnostic grey zone in which prostate cancer is only present in 25% of the patients. Most patients with prostate cancer with PSA level less than 10 ng/mL have early-stage disease, whilst more than 50% of the patients with PSA levels higher than 10 ng/mL have advanced disease (Catalona et al., 1994). Patients with prostate cancer also have significantly lower levels of free-PSA circulating in their blood. Thus, the use of the free-PSA percentage can enhance the specificity of PSA screening and decrease the number of unnecessary biopsies. If biopsies are only performed on patients with less than 25% free-PSA, with PSA levels between 4 – 10 ng/mL, it would detect 95% of the cancers and spare 20% of patients (with BPH) from biopsy (Catalona et al., 1998). However it has also been shown that 15% of patients with PSA levels less than 4 ng/mL had detectable prostate cancer in the biopsy (Thompson et al., 2004). Thus it is important to identify and characterize prostate cancer biomarkers that could supplement PSA testing, and studies have already shown evidence for such specific biomarkers, such as PCA3 (Laxman et al., 2008; Wu et al., 2011).

Once the initial testing of the patients' serum indicate an increase in the levels of PSA, other methods are used to examine the size and shape of the prostate, such as a Digital Rectal Examination (DRE) or transrectal ultrasonography (TRUS). However to confirm the presence of prostate cancer, a biopsy is taken and histologically analysed and graded according to the Gleason tumour grading system (Gleason, 1966). Prostate cancers are stratified into five grades on the basis of the glandular pattern and degree of differentiation (Figure 1.7), with 1 representing normal cellular histology and 5 representing a high malignant phenotype. The five grade patterns are used to generate a histological score, which can be arranged from 2 to 10, by adding the primary grade pattern and the secondary grade pattern, whereby the primary grade pattern is the most predominant and the secondary pattern is the second most common pattern. A patient with prostate cancer with a Gleason score above 7 usually has a poor clinical outcome.

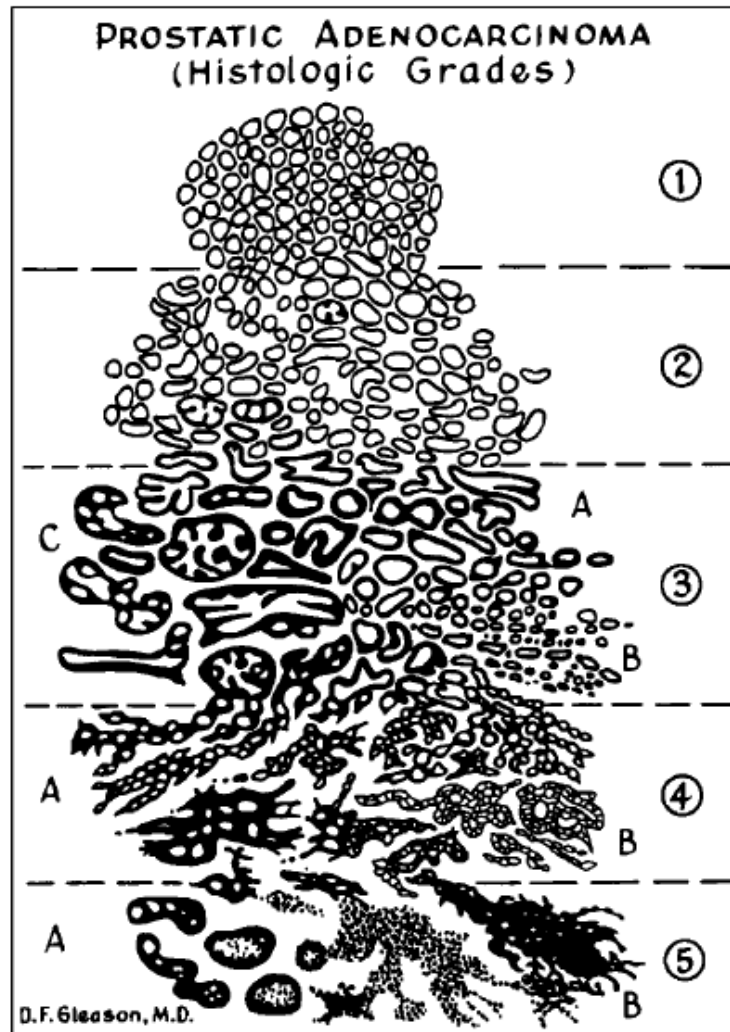


Figure 1.7. **Gleason grading system for prostatic adenocarcinoma.** Grades are from 1 to 5 depending on the degree of differentiation. These grades are assigned to the primary and secondary pattern within a surgical specimen. Taken from (Gleason, 1966).

1.1.3.4. Treatment of prostate cancer

The treatment options for prostate cancer depend on the stage of the disease and the androgen responsive status of the tumour. If the cancer is still confined to the prostate, known as localized disease, a “watchful waiting” treatment strategy is often recommended. These patients are monitored closely and active treatment is postponed until it is required. This therapeutic alternative has emerged in men with low risk prostate cancer (Chodak et al., 1994) and it has been demonstrated that at 10 years, these men have a prostate cancer-specific survival of 97% (Klotz et al., 2010).

Radical prostatectomy, removal of the entire prostate gland, is the only treatment for localized prostate cancer that has shown a reduction in metastasis and therefore prostate cancer-free survival (Bill-Axelsson et al., 2008). The radical prostatectomy options include retropubic and perineal approaches as well as minimal invasive, robotic or laparoscopic, surgery. However, surgical removal of the prostate increases the chance of these patients experiencing erectile dysfunction, although this risk has been significantly reduced with the introduction of nerve-sparing surgery (Walsh, 2007).

Another treatment option for localised prostate cancer is radiotherapy, which uses radiation to cause DNA damage within the tumour cells. There are two types of radiotherapy; external beam radiotherapy or internal radiation. The external beam method uses 3-dimensional conformal radiotherapy, intensity-modulated radiotherapy, or image-guided radiotherapy, and a more recently developed technique of 4-dimensional conformal radiotherapy, which takes organ motion into account. All these methods have the advantage to escalate the radiation dose while minimizing the toxicity to the surrounding normal tissue. It has been shown that there is an increased efficiency when an increased dose of radiation is applied (Zietman et al., 2005). Internal radiotherapy, also known as brachytherapy, involves implantation of radioactive seeds into the patients, providing radiation from the inside of the prostate.

Beside radical prostatectomy and radiotherapy, cryosurgical ablation of the prostate and high-intensity focussed ultrasound (HIFU) has emerged as alternative therapeutic approaches in patients with localised prostate cancer. These therapies are known as “minimal invasive therapies” as these have similar chances of a positive outcome but with fewer side effects (Aus, 2006; Ahmed et al., 2012).

Hormone therapy is a well-established form of treatment for the various stages of prostate cancer, which has escaped the prostatic capsule. The most common target being the androgen receptor, as the primary tumour is dependent on androgens for its growth and survival. It was shown in the late 60s that orchiectomy induced the regression of prostate cancer (Huggins, 1967) and since this discovery, androgen ablation therapy has been the main treatment of hormone-sensitive prostate cancer (Balk, 2002). The tumour initially responds well to androgen ablation therapy, as the main cell type within prostate carcinoma is the AR-positive secretory luminal cell (Nagle et al., 1987). Therefore a reduction in tumour growth is observed initially but ultimately, and in most cases, the therapy fails and the prostate cells become castrate-resistant (Feldman and Feldman, 2001). Treatment failure can also be explained by the presence of tumour initiating cells or cancer stem cells (described in sections 1.1.5), as these cells are independent of androgens for their survival (Collins et al., 2005) and it has been suggested that these cells are more resistant to radiation (Phillips et al., 2006) and chemotherapies (Dean et al., 2005).

Chemotherapy is a treatment option for advanced prostate cancer with metastasis and when hormone therapy fails (Beedassy and Cardi, 1999). This therapy targets rapidly dividing cells within the tumour mass, but unfortunately chemotherapy affects all the cells of the body as it circulates through the blood stream and therefore has many severe side effects. This being the reason that chemotherapy is usually only recommended as a last treatment option.

In summary, when prostate cancer is confined to the prostatic capsule, it can be managed effectively using “watchful waiting” or with radical surgery intervention. However, if the cancer is not detected early or in a more aggressive form of the disease, there is no effective treatment for advanced prostate cancer. This is because the treatment strategies are designed for a homogeneous mass of cells. However, as prostate cancer is heterogeneous, new treatment strategies are needed to target the therapy-resistant tumour initiating cells (**Table 1**).

Table 1. Prostate cancer treatment: current target and therapy resistance.

Therapy	Target	Resistance
Surgery	Removal of the entire prostate gland	Residual tumour
Radiotherapy	Highly proliferating cells	Tumour initiating cells divide slowly
Chemotherapy	Highly proliferating cells	Tumour initiating cells divide slowly
Hormone therapy	Androgen Receptor expressing cells	Tumour initiating cells do not express the AR

1.1.4. Development of prostate cancer

Studies in the 1960s showed that cancers are composed of a heterogeneous population of cells with differences in their potential to self-renew and reconstitute the tumour upon transplantation (Bruce and Van Der Gaag, 1963; Hamburger and Salmon, 1977; Stahel et al., 1985). These studies led to the development of two theories to explain these observations: stochastic and hierarchical models. The stochastic model predicts cancer cells of many different phenotypes have the potential to proliferate extensively. Whilst the hierarchical model predicts that only a subset of cancer cells, termed cancer stem cells, have the ability to proliferate extensively and form new tumours, whilst most cancer cells have limited proliferative potential (Reya et al., 2001). This model, i.e. that only cancer stem cells are able to initiate tumour growth and metastasize, explains the failure of current therapies to eradicate the entire tumour. However, resistance to therapy in many cancers may also be explained by an accumulation of epigenetic and genetic differences in tumorigenic cancer cells that lack any hierarchical organisation, described by the clonal evolution model (Nowell, 1976; Shackleton et al., 2009). This model was proposed in the 1970s, as mutations in oncogenes and tumour suppressor genes were found to cause most human cancers. This model of clonal evolution proposes that most neoplasms arise from single “mutated” cells-of-origin and that tumour progression results from subsequently additional genetic changes within the original clone, allowing selection of a more aggressive subline, so tumour cells are more genetically unstable than normal cells. This genetic instability and associated selection progress results in advanced human malignancy being highly individual; karyotypically and biologically. Hence each person might require individualized therapy (Nowell, 1976; Clevers, 2011). Thus, in a single tumour there might be multiple cancer stem cell clones that are genetically distinct, but they will always have a common ancestor: the cancer cell-of-origin which sustained the first oncogenic mutation.

Because tissue stem cells and cancer stem cells share characteristics, such as the ability to self-renew and differentiate, it is thought that the cancer stem cell might arise from mutation(s) of the tissue stem cells (Bonnet and Dick, 1997). This is not surprising as normal stem cells are long-lived by nature and therefore more likely to be subjected to the accumulation of multiple mutations that are required for carcinogenesis. The initial mutation will provoke a multistep process which will lead to the development of prostate cancer: progressing from normal epithelia to high-grade prostate intraepithelial neoplastic lesions (PIN) to invasive carcinoma, and potentially to metastatic prostate cancer (Figure 1.8) (Abate-Shen and Shen, 2000). Common mutations that are implicated with the initiation and progression of prostate cancer are shown in **Table 2**.

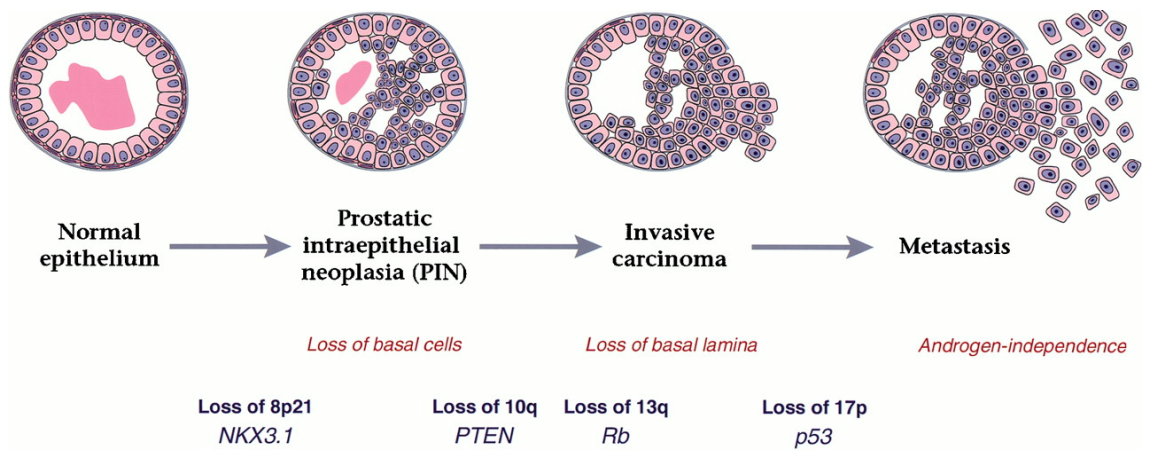


Figure 1.8. **Pathway of the progression of human prostate cancer.** The different stages of the progression from normal prostate epithelium to high-grade prostatic intraepithelial neoplasia to invasive carcinoma to metastatic prostate cancer. Taken from (Abate-Shen and Shen, 2000).

Table 2. Common mutation and genes involved in the initiation and development of prostate cancer.

Affected gene	Phenotype	Reference
Androgen-receptor	Expression is maintained even in an androgen-independent tumours (amplified or mutated)	(Marcelli et al., 1990; Visakorpi et al., 1995)
C-Cam	Expression is decreased in PIN and lost in carcinoma	(Kleinerman et al., 1995)
C-met	Expression is increased in PIN, carcinoma and metastasis	(Pisters et al., 1995)
E-cadherin	Decreased expression in PIN and carcinoma	(Umbas et al., 1994)
FGFs	Overexpression in carcinoma	(Kwabi-Addo et al., 2004)
Integrins	Decreased expression	(Cress et al., 1995)
Myc	Amplified In carcinoma	(Thompson et al., 1989)
NKX3.1	Mutation causes prostatic epithelial hyperplasia and dysplasia	(Bhatia-Gaur et al., 1999)
P53	Frequently mutated in metastatic prostate cancer	(Eastham et al., 1995)
PTEN	Expression is lost in advanced prostate cancer	(Li et al., 1997)
Telomerase	Reduced telomere length and increased telomerase activity in PIN and carcinoma	(Sommerfeld et al., 1996)
TGF β	Decreased expression in prostate cancer metastasis	(Djakiew, 2000)

Prostate cancer is thought to arise from high-grade PIN (Zynger and Yang, 2009) or a hyper-proliferative lesion known as proliferative inflammatory atrophy (PIA), possibly by hormonal imbalances, exposure to environmental factors, such as infectious agents and dietary carcinogens, leading to the development of chronic inflammation (De Marzo et al., 1999). The risk of developing prostate cancer increases with age, as the largest numbers of cases are diagnosed within the age range 72 - 74, but ethnicity and family history and even diet are also thought to play a role (Snowdon et al., 1984; Gronberg, 2003).

1.1.4.1. Castrate resistant prostate cancer

Prostate cancer cells are initially dependent on androgens, and therefore androgen ablation has been the key treatment for this stage of prostate cancer. Initially the treatment shows good results, and there is usually a significant clinical regression and biochemical response as measured by the decrease in serum PSA in 80 - 90% of patients. The treatment does lead to remission that lasts 2 - 3 years, however almost all patients progress to an androgen-independent prostate cancer, also referred to as castrate resistant prostate cancer (CRPC), resulting in death within 16 – 18 months (Feldman and Feldman, 2001; Pienta and Bradley, 2006). At present, there is no effective treatment for this stage of the disease, and in order to develop new drugs and to optimize androgenic suppression in CRPC, it is important to identify and characterize the mechanisms that result in this stage of the disease. It has been shown that in CRPC patients, the serum levels of androgens are still sufficient for AR activation, and subsequently cancer cell survival. It is thought that these androgens arise from the direct synthesis of androgens in prostate cancer cells due to the up-regulation of synthetic enzymes, to produce testosterone and DHT (Mohler et al., 2004). It has also been shown that there is an increased expression of the AR, allowing for enhanced ligand binding in the presence of low levels of androgens (Visakorpi et al., 1995). Although the wild-type AR can only be activated by testosterone and DHT, the specificity of the AR has been shown to be expanded by mutations. Because of these mutations, the AR can be activated by non-androgenic steroid molecules that are normally present in the circulation (Veldscholte et al., 1992; Buchanan et al., 2001). Another mechanism for the development of CRPC is the activation of different signal transduction pathway in the castrate resistant cancer cells. It has been shown that deregulated growth factors, including epidermal growth factors, insulin-like growth factors and cytokines, including IL-6, are able to enhance the activation of the AR in the absence, or of low levels, of androgens (Culig et al., 1994; Culig et al., 2002). A more recently accepted mechanism for the development of CRPC is the presence of prostate cancer stem cells, as these cells are resistant to current therapies, and most important are AR-negative and therefore independent of androgens for survival (Collins et al., 2005). So it is thought that these cells are responsible for maintaining tumour growth and development of prostate cancer.

Patients with CRPC have only limited treatment options. Since 2004, the chemotherapeutic docetaxel has been used in patients with CRPC, however this only shows a median survival benefit of 2 - 3 months (Tannock et al., 2004). Since then, multiple new therapy strategies have been developed for patients with CRPC, including

Abiraterone. This drug is a potent and highly selective inhibitor of androgen biosynthesis that blocks the synthesis of DHT (inhibitor of CYP17A1). Even though phase III studies have shown prolonged survival of patients with CRPC, the median survival was only extended by 4 months (de Bono et al., 2011).

Apart from newly developed drugs that are able to reduce circulating levels of androgens, other treatment methods that are beneficial for patients with CRPC include non-hormonal approaches such as, bisphosphonates and denosumab which are treatments that benefit patients with bone metastasis (most common metastasis for prostate cancer patients), chemotherapies and a vaccine: sipuleucel-T (Amaral et al., 2012). However, the survival benefit of these therapy strategies in CRPC is modest. Therefore it is important to design new treatment strategies, and it is crucial to take the different cell types into account, including prostate cancer stem cells as current therapies are not aimed for this relatively quiescent, AR-negative cell type (Collins et al., 2005; Maitland and Collins, 2008b).

1.1.5. Prostate cancer stem cells

The origin of prostate cancer is still controversial. As prostate cancer mainly consists of luminal cells, it has been the prevailing view that these AR-expressing luminal cells are the tumour-initiating cells (Nagle et al., 1987; Maitland and Collins, 2008b). The observation that telomerase is expressed within the luminal compartment in high-grade PIN, thus extending the lifespan of these cells, has added weight to this proposal (Meeker et al., 2002). Others have suggested that an intermediate cell, which expresses both basal and luminal keratin markers, could give rise to prostate cancer (Verhagen et al., 1992).

However, it has been shown, with the use of a phosphatase and tensin homolog (PTEN) knockout mouse, that not only the tumour microenvironment can enhance the stemness and growth potential of tumour initiating cells but that the tumour initiating cell strongly expresses the basal marker p63 (Liao et al., 2010), confirming that the cell of origin of prostate cancer has a basal origin. It is more plausible that normal tissue stem cells are the targets for transformation given their longevity. This has been definitively demonstrated by Bonnet and Dick, in 1997 they showed that the tumour initiating cells, in acute myeloid leukaemia (AML), shared cell surface markers with normal hematopoietic stem cells (Bonnet and Dick, 1997). More recently, Barker and colleagues showed that crypt stem cells are the cells of origin of intestinal cancer (Barker et al., 2009). This study demonstrated a rapid transformation of stem cells, through loss of adenomatous polyposis coli (APC), toward initiating intestinal adenomas (Barker et al., 2009). This has been supported by studies that used lineage tracing of cells in mice and showed that a subset of normal (stem) cells drives tumour growth, including glioma stem cells (Chen et al., 2012), crypts stem cells (Schepers et al., 2012) and epidermal stem cells (Driessens et al., 2012).

There are several lines of evidence that support the proposal that prostate cancer stem cells arise from prostate epithelial stem cells. Metastases often include rare cells that are phenotypically undifferentiated, expressing basal cell markers, such as cytokeratins 5 and 14. (Liu et al., 2002; Lang et al., 2009). Advanced prostate cancers can respond to low levels of androgens, but the castrate resistant state results from clonal expansion of androgen-independent cells that are present at a frequency of 1 per 10^5 - 10^6 androgen-responsive cells (Craft et al., 1999). Cancer stem cells share numerous markers with normal stem cells. More recent work from our laboratory compared isolated populations, from primary prostate cancers, for clonogenic potential. It was shown that only the most primitive cells ($CD44^+/\alpha_2\beta_1^{hi}/CD133^+$), which were identical phenotypically to normal prostate epithelial stem cells, could self-renew *in vitro* (Collins

et al., 2005). Additionally, under differentiating conditions, AR⁺/PAP⁺/CK18⁺ luminal cells could be identified in these cultures suggesting that they were derived from the more primitive population. In support of this finding, the CD44⁺ population from xenograft tumours and cell lines has enhanced proliferative potential and tumour-initiating ability *in vivo* compared to CD44⁻ cells (Patrawala et al., 2006). The CD44⁺ cells are likewise AR⁻ and express higher mRNA levels of stemness genes, such as OCT3/4 and BMI-1. Using clonally derived human prostate cancer epithelial cells, expressing human telomerase reverse transcriptase (hTERT) Gu and co-workers (Gu et al., 2007) demonstrated that these lines could regenerate tumours in mice that resembled the original patient tumour with respect to Gleason score. The tumours contained luminal, basal and neuroendocrine cells, implying that the clone of origin could differentiate into the epithelial cells lineages of the prostate. In this case, the tumour initiating cell was AR⁻ and p63⁻ and expressed the stem cell genes Oct-4, Nanog, Sox2, nestin, CD44, CD133 and c-kit. Moreover, Sca-1 sorted cells, enriched for cells with prostate-regenerating activity, showed evidence of basal and luminal lineage.

A recurrent genomic alteration in prostate cancer is the expression of *TMPRSS2-ETS* fusion genes (Tomlins et al., 2005), with *TMPRSS2-ERG* being the most frequently detected (Demichelis and Rubin, 2007). The presence of the fusion is associated with PSA biochemical failure (Demichelis and Rubin, 2007) and occurs with a frequency of approximately 50% (Tomlins et al., 2005). Identification of the *TMPRSS2.ETS* fusion gene in approximately 20% of PIN lesions suggests that it is an early event in prostate tumorigenesis (Cerveira et al., 2006) and recent findings that *TMPRSS2.ERG* is expressed in $\alpha_2\beta_1^{\text{hi}}$ /CD133⁺ cells from prostate tumours (Birnie et al., 2008) supports the hypothesis that the cell of origin of prostate cancer is a stem cell.

The ultimate evidence for the identification of the cell or origin of cancer, also termed cancer stem cells, is serial xenotransplantation. This assay will show that these cells have the ability to initiate a tumour that can be serially transplanted and is identical to the parental tumour from which it was derived. It has been confirmed that the strongest tumour-initiating fraction, where less than 100 cells have the capacity to initiate new tumour growth in immunocompromised mice, has a basal phenotype (Maitland et al., 2011).

Based on this evidence, the cell culture model that is used in our laboratory are primary tumour cells, derived from patient biopsies, which can be sorted on the basis of the expression of the following cell surface markers: $\alpha_2\beta_1$ integrin and CD133 (Figure 1.9).

This is based on the finding that human prostate biopsies can be fractionated into basal, luminal and progenitor cells as first described in the normal prostate (Richardson et al., 2004), and that this can also be applied to malignant tissue as the same fractions can be identified (Collins et al., 2005), but in different proportions. The basal cell fraction accounts for approximately 1% of the tumour mass, however they are expanded in *in vitro* culture. Although the $\alpha_2\beta_1^{\text{hi}}/\text{CD133}^+$ population has the potential to self renew and proliferate and differentiate to recapitulate the phenotype of the original tumour *in vitro* (Collins et al., 2005), it has currently not been demonstrated *in vivo* that these cells are able to initiate tumour growth. Therefore in this study they are labelled as follows: $\alpha_2\beta_1^{\text{hi}}/\text{CD133}^+$ are stem-like cells, $\alpha_2\beta_1^{\text{hi}}/\text{CD133}^-$ are transit amplifying cells (TA: progeny of the stem-like cells) and $\alpha_2\beta_1^{\text{low}}$ are committed basal cells (CB) derived from malignant tissue from prostate biopsies.

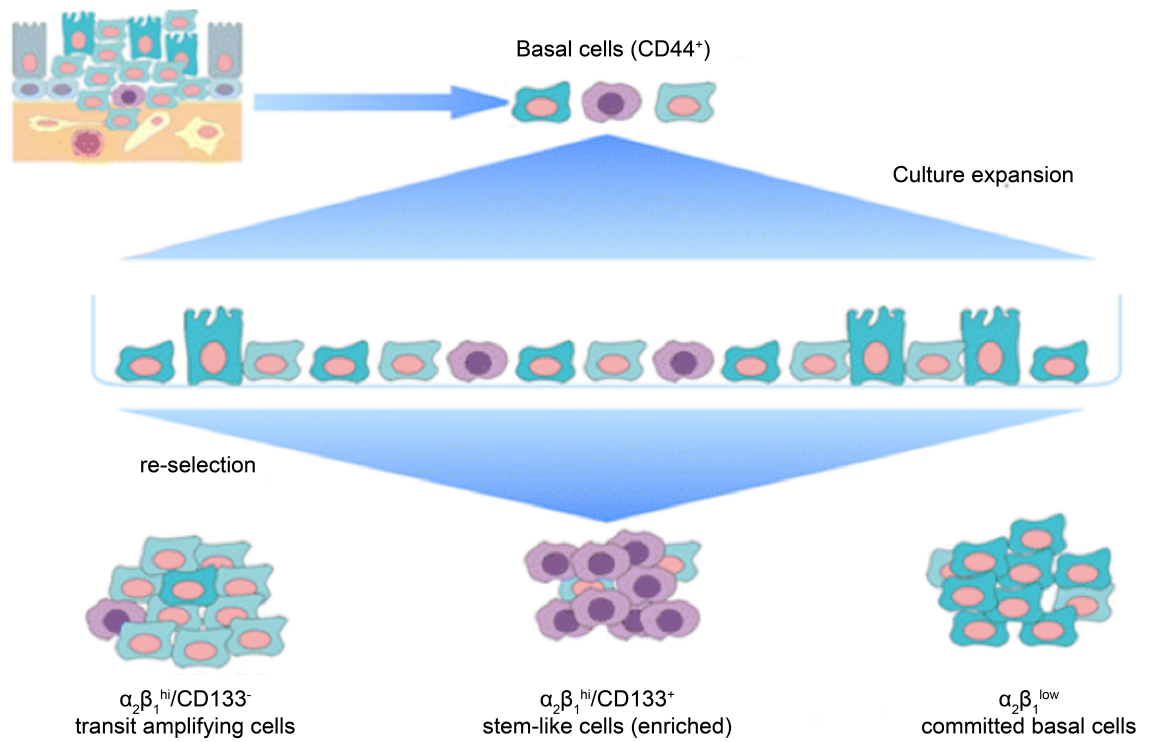


Figure 1.9. **Schematic representation of the fractionation of human prostate biopsies.** Cell fractionation of enriched stem-like cells ($\alpha_2\beta_1^{\text{hi}}/\text{CD133}^+$), transit amplifying cells ($\alpha_2\beta_1^{\text{hi}}/\text{CD133}^-$) and committed basal cells ($\alpha_2\beta_1^{\text{low}}$), following expansion *in vitro*, from malignant tissue derived from prostate biopsies. Modified from (Maitland et al., 2011).

1.1.6. Prostate cancer stem cells and therapy resistance

In the last decade, there has been an explosion in the number of papers published on cancer stem cells, and there has now been a consensus; that CSCs must be taken into consideration when developing new therapies, particularly with tumours that are prone to relapse (Dean et al., 2005; Lee and Herlyn, 2007; Eyer and Rich, 2008; Fabian et al., 2009; Winquist et al., 2009; Frank et al., 2010). However, before targeting prostate CSCs specifically, there needs to be proof that they are resistant to current therapies and preferably an explanation of the mechanism of resistance. Ultimately, it is important to design diagnostic test(s) to determine whether, when the CSC component of a tumour is eliminated, that this results in tumour eradication or cure (Drewa and Styczynski, 2008; Woodward et al., 2009).

Very little is known about therapy resistance of prostate CSCs, and most studies are based on cancer cell lines and tissue sections. However, increasing numbers of studies are now using primary epithelial cell cultures from patient samples, a focus of which is the response of epithelial cells to DNA damage caused by radiotherapy or chemotherapeutic agents. In terms of DNA repair, homologous recombination (HR), nucleotide excision repair (NER), base excision repair (BER) and mismatch repair (MMR) have all been examined. There are reduced levels of MMR proteins, including hMLH1 and hMSH2, in various prostate cancer cell lines (Yeh et al., 2001). More significantly, there are defects in MMR in prostate tumour foci as indicated by the absence of PMS1 and PMS2 proteins (Chen et al., 2003). In contrast, another study found increased levels of PMS2 in recurrent prostate cancer patients and suggested this to be of use as a marker with prognostic potential (Norris et al., 2009). Increased expression of this protein has been associated with increased mutation frequency and resistance to apoptosis. Even though conflicting results have been observed regarding an increase or decrease in repair protein, it does indicate that these proteins have the potential to cause mutations that may be involved in tumour progression. Combination of radiotherapy with inhibitors of DNA repair has been explored by Bristow *et al.* (Bristow et al., 2007). Mutations in BRCA1 and BRCA2, key proteins in the double-strand break (DSB) response, have been found in familial prostate cancers (Dong, 2006; Levy-Lahad and Friedman, 2007). Cells with these mutations are defective in DSB repair and are more sensitive to radiation (Farmer et al., 2005). Other DSB response proteins, such as ATM, have an increased expression in prostate tumours and p53 is frequently mutated in (advanced) prostate cancer (Angele et al., 2004; Cuddihy and Bristow, 2004). Mutations of Chk2 have also been observed (Dong, 2006). These proteins are involved in cell cycle checkpoints, abrogation of which can

lead to radioresistance and metastasis (Bristow et al., 2007). An altered BER pathway and response to oxidative stress have also been implicated in prostate cancer (Xu et al., 2002; Chen et al., 2003; Rybicki et al., 2004; Trzeciak et al., 2004).

With the study of CSCs, the prostate field can follow the lead of other fields. CD133⁺ cells from hepatocellular carcinoma are resistant to doxorubicin and fluorouracil, which is due to expression of bcl-2, Akt and PKB; components of an anti-apoptotic survival pathway (Ma et al., 2008). Glioma stem cells are resistant to chemotherapeutic agents (Murat et al., 2008) and have increased activation of DNA damage checkpoints and more efficient DNA repair in response to irradiation, with inhibition of Chk1 and Chk2 kinase restoring radio sensitivity (Bao et al., 2006). These studies on cell lines and whole populations of primary epithelial cells can be used as a basis for studies on prostate CSCs, as we now have the ability to isolate these cells and analyse their response, which is likely to be significantly different to the more differentiated cells. Ultimately, in cancer cells there is an upset in control of DNA repair and cell cycle checkpoints, and depending on the mutation the cells may be more sensitive to treatment or resistant to treatment. Therefore it is imperative to explore the specific response of prostate CSCs to different treatments, in order to manipulate therapy. This would allow for prediction of success of certain therapies and also for manipulation of treatments to exploit defects in the prostate CSCs.

1.1.7. Models for studying prostate cancer

1.1.7.1. Cell lines

One of the limitations of prostate cancer research is the difficulty in generating permanent cell lines for *in vitro* studies (Abate-Shen and Shen, 2000). This limitation is related to the inherently slow growth of most prostate tumours and the slow proliferation rate of normal prostatic epithelial cells (Isaacs and Coffey, 1989). There have been several spontaneously immortalized prostate cells lines, derived from metastatic lesions, which are commonly used: DU145 (Stone et al., 1978), PC-3 (Kaighn et al., 1979) and LNCaP (Horoszewicz et al., 1980). Unfortunately, expanded primary prostate cells only survive and proliferate short-term in culture and rarely immortalize spontaneously. Therefore, there are several prostate cell lines that are immortalized using different viral transformation genes, such as simian virus (SV40), human papillomavirus-18 (HPV) or telomerase (hTERT) (Webber et al., 1996). More recently, prostate cell lines have been spontaneously immortalized from trans-rectal needle biopsy of the prostate of patients with advanced, metastatic CRPC. Not only are these newly established cell lines from the primary tumour, unlike the cell lines that were derived in the late 70s, the cells show an intermediate phenotype, express basal markers with some luminal and cancer-marker gene expression that are commonly present in prostate tumours and these cells express stem-cell markers which makes them a more representative pre-clinical model for studying CRPC (Attard et al., 2009).

The advantage of using cell lines is that the cells are immortalized and therefore have the ability to grow indefinitely in culture. However, the most commonly used cell lines have been established from metastatic lesions, and therefore do not accurately simulate the biological behaviour of primary tumours. Also, the established cell lines do not reflect the full spectrum of heterogeneity that is observed in prostate cancer. This accounts for the failure of many clinical-trials, as these are based on results obtained in pre-clinical studies using immortalized cell lines. Therefore it is important to perform pre-clinical *in vitro* studies on a more accurate model that is more closely related to the heterogeneity observed in the patients' tumour.

1.1.7.2. Primary cells

Due to the limitations of immortalized prostate cell lines, it is important to use primary cell cultures, which are a better representation of the patients' tumour as they contain a mixture of several different cell phenotypes. They also have the advantage that a given observation can be confirmed by studying cell cultures derived from numerous patients (reviewed in (Peehl, 2005)). These cell cultures are derived from prostate (needle) biopsies, from radical prostatectomy or TURP, of malignant and benign tissue. However, these cell cultures have a limited life span before they senesce, which is an added difficulty compared to working with immortalized cell lines.

Primary cell cultures can be derived from benign tissue, which acts as a "normal" control as well as all grades of prostate cancer, including CRPC. However there is currently no cancer-specific cell surface antigen that can sort live cancer cells from non-cancerous cells. However, cells can be screened for TMRSS2 fusion (Birnie et al., 2008). It was also shown in this publication that the gene expression profile of the malignant cells clustered away from the normal gene expression profile. Histological analysis and xenografts derived from the same tissue has shown that the majority of the cells are malignant (Maitland et al., 2011).

1.1.7.3. Mouse models

Even though cell lines provide a model for identifying prospective target genes in a quick and efficient manner it is important to extend the knowledge that has been obtained in *in vitro* studies into a pre-clinical *in vivo* model. Moreover, mouse models have provided valuable information about the biology and pathology of prostate cancer, as well as being a useful system for assessing novel treatment strategies *in vivo*.

There are two main classes of mouse models for studying prostate cancer: xenografts or genetically engineered mouse models (GEMMs). The xenograft model uses an immunocompromised mouse as a recipient of human tumour tissue or cell lines. Because of their immune-deficient nature, these mice are not able to mount an immunological response to foreign tissue and this allows the growth of human tumours. The most commonly used immunocompromised mouse models are NUDE mice, which lack T lymphocytes (Flanagan, 1966), SCID mice, which lack B and T lymphocytes (Custer et al., 1985) and NOD/SCID mice, which lack B and T lymphocyte and have low levels of natural killer (NK) cell activity (Shultz et al., 1995). Residual immune response, in particular NK cells, severely inhibit the efficient uptake of human tumour

tissue and cells. Therefore the xenograft model used in this study is the Rag2 $\gamma^{-/-}$ C $\delta^{-/-}$ mouse, which lack B and T lymphocytes and most importantly NK cells activity (Goldman et al., 1998).

There are two main sites used for engraftment of tumour tissue in xenograft models: subcutaneous and orthotopic implantation. Orthotopic implantation, i.e. at the original site of the tumour, has been suggested to be more representative due to the interaction of tumour cells with their relevant organ environment (Fidler, 1990), which is more relevant for the progression of prostate cancer. Orthotopic implantation of prostate cancer cell lines results in reproducible formation of metastasis, whilst metastasis is rarely achieved with subcutaneous implantation (Rembrink et al., 1997). However subcutaneous implantation is technically simple and it results in an easy to palpate and measurable tumour.

Xenografts that are established with the use of prostate cell lines have a high degree of predictability and rapid tumour formation. However most cell lines have been maintained for decades *in vitro*, thus lack the architectural and cellular complexity of *in vivo* tumours. Therefore, the resulting xenograft does not represent the genetics and histology of the human tumour (Becher and Holland, 2006). Currently no mouse model fully recapitulates all features of prostate cancer (Valkenburg and Williams, 2011). However in this study 'near-patient' xenografts were used whereby tumour biopsies of patients with primary prostate cancer were engrafted into Rag2 $\gamma^{-/-}$ C $\delta^{-/-}$ mice. The advantage of this mouse strain was that limiting numbers of cells could be engrafted with high efficiency (Maitland et al., 2011). As the tumour shares more similarities with the patients' tumour, compared to cell lines, it is a more predictable model that can be used in developing new therapeutic agents.

The GEMM allow for the development of mice carrying genetic modifications equivalent to those associated with human tumours. This model validates if a specific genetic modification is important for tumour initiation or progression, but it also provides an improved model for the development and testing of new therapeutic agents (Valkenburg and Williams, 2011). This was initially done with the introduction of DNA constructs, under the control of a prostate-specific promoter, that were designed to induce the expression of proteins, for example the transgenic adenocarcinoma of the mouse prostate (TRAMP) model. In this model, the SV40 tumour antigens were regulated by the prostate-specific rat probasin promoter, and these mice develop epithelial hyperplasia at 8 weeks, which progresses to PIN by 18 weeks and at 28 weeks these mice have developed metastasis (Greenberg et al., 1995; Gingrich et al.,

1996). The introduction of oncogenes usually results in a mild phenotype and rarely progresses to metastasis, for example the transgenic RAS mouse, which develops PIN and could therefore serve as a tool for the study of early events in prostate cancer (Scherl et al., 2004). Apart from transgenic mouse models, there are also traditional and conditional knockout mouse models. In the traditional (whole body) knockout mouse model, a tumour suppressor gene is deleted, for example PTEN. The PTEN knockout mouse showed that PTEN is essential for early embryonic development, as homozygous knockouts were lethal. Heterozygous knockouts were viable, however they did develop PIN and therefore showed that PTEN is a critical early regulator of prostate cancer development (Di Cristofano et al., 1998). The conditional model knocks out the same genes that are used in the traditional model, however the modifications are localized to a specific tissue. The main advantage is that it allows for studying specific genes in specific tissue, and for studying genes that would result in embryonic lethality in the traditional knockout model; for example PTEN. This conditional knockout for prostate cancer results in PIN formation which progresses to invasive adenocarcinoma, and it is therefore a more appropriate model of prostate cancer (Wang et al., 2003). Although the GEMM provide insights of the importance of a single gene in the development of prostate cancer, the mutation does occur in the entire body or tissue and is present from early development. However this is not the case for human cancer development, as mutations occur randomly and most probably in a single (stem) cell, resulting in focal disease development (Valkenburg and Williams, 2011).

1.2. Inflammation and cancer

Inflammation is a critical component in the development of a tumour. Many cancers arise from sites of infection, chronic irritation and inflammation. This link between chronic inflammation and cancer was first observed in 1863, by Rudolf Virchow, when he observed leukocytes within neoplastic tissue. From this observation he hypothesized that inflammatory cells might enhance cancer cell proliferation (Balkwill and Mantovani, 2001). Although it is now known that proliferation of cells alone does not cause cancer, sustained cell proliferation in an environment rich in inflammatory cells, growth factors, activated stroma and DNA-damage promoting factors does have the potential to promote neoplastic risk (Coussens and Werb, 2002). Inflammation is the biological response of vascular tissue to harmful stimuli, such as pathogens, damaged cells or irritants. It involves the activation and directed migration of leukocytes (neutrophils, monocytes and eosinophils) from the circulating blood systems to the region where there is damage. Acute inflammation is self-limiting, because the production of anti-inflammatory cytokines is quickly followed by the pro-inflammatory cytokines based on antigen specificity and timing of activation. There are two components of the acute immune system: innate and adaptive. Innate immune cells include dendritic cells, NK-cells, macrophages, neutrophils, basophils, eosinophils and mast cells, which are the first cells to respond to foreign pathogens. Adaptive immune cells, including B and T lymphocytes, have a more specific and larger response due to their long-lived memory (de Visser et al., 2006).

When tissues are chronically stressed, the interaction between innate and adaptive immune cells can be disturbed, for example adaptive immune responses can cause ongoing and excessive activation of innate immune cells (de Visser et al., 2006). Chronic inflammation is due to persistence of the initiation factors or failure of the mechanisms that is required for resolving the inflammatory response (Coussens and Werb, 2002).

Chronic inflammation accounts for 15 - 20% of deaths from cancer worldwide (Balkwill and Mantovani, 2001) and inflammation is linked to all types of human cancers, including, lung, bladder, pancreas, colorectal, skin and prostate cancer (Cook, 1992; Farrow and Evers, 2002; De Marzo et al., 2007; Michaud, 2007; Engels, 2008; Terzic et al., 2010). Chronic inflammation can be triggered by many environmental causes, for example, 20% of chronic inflammation related cancers are caused by tobacco (Parkin, 2011) and 35% can be attributed to dietary factors (20% of cancer burden is linked to obesity) (Aggarwal et al., 2009). It is also well known that chronic inflammation can be triggered by bacterial and viral infections; *Helicobacter pylori* infection can cause

gastric cancer (Uemura et al., 2001) and HPV causes cervical cancer (Walboomers et al., 1999). It has been shown that treatment with non-steroidal anti-inflammatory agents can decrease the incidence and mortality of several types of cancer, although this effect only occurs after long-term (15 - 20 years) treatment (Baron and Sandler, 2000).

The hallmark of cancer-related inflammation is the presence of inflammatory cells and inflammation mediators (including chemokines and cytokines) in tumour tissue, tissue remodelling and angiogenesis, which is similar to what is seen in chronic inflammatory responses and tissue repair. Inflammatory cells are present in the microenvironment of all tumours even if the initiation of the tumour is related to the activation of oncogenes. This led to the hypothesis that two separate pathways connect inflammation and cancer: an extrinsic and intrinsic pathway (Mantovani et al., 2008). The extrinsic pathway is driven by inflammatory conditions that facilitate the development of cancer, such as inflammatory bowel disease as these patients have a high risk of developing colorectal cancer (Ekobom et al., 1990). The intrinsic pathway is driven by genetic events that cause the cancer cells to produce inflammatory mediators, therefore creating an inflammatory microenvironment in tumours that do not have an underlying inflammation condition, such as the RET/PTC1 oncogene. This has been shown to induce the expression of inflammatory chemokines and cytokines in normal human thyrocytes and chronic inflammatory thyroiditis has been linked to tumour progression (Borrello et al., 2005).

Tumour-associated macrophages (TAM) are a major component of the inflammatory response in malignant tissue, and are derived from circulating monocytes, by chemotactic cytokines released by malignant and stromal tumour cells (Mantovani et al., 1992). TAMs have been shown to have both pro- and anti-tumour activity. It has been demonstrated that when macrophages are activated classically (also called an M1 response), through stimulants such as interferon gamma (INF- γ) or lipopolysaccharide (LPS), they produce large amounts of pro-inflammatory cytokines that have the potential to kill neoplastic cells (Bingle et al., 2002). However, as these stimulants are rarely present at the tumour site, it is more likely that TAMs are activated alternatively (M2 response), mainly through interleukin-10, and this phenotype is able to promote tumour growth by the secretion of various cytokines, which promote cancer cell survival and proliferation (Sica et al., 2000). Additionally, TAMs are also involved with angiogenesis, invasion and metastasis (Mantovani et al., 1992). Moreover, high levels of TAMs in tumours are often associated with poor prognosis (Bingle et al., 2002).

The nuclear factor- κ B (NF- κ B) pathway is an important regulator of TAM function, as it is the central mechanism that maintains the alternative phenotype (M2) of TAMs (Hagemann et al., 2008). It has been shown that during chronic inflammation, NF- κ B activation in TAMs triggers the release of certain pro-inflammatory cytokines, such as IL-6, which has been linked to tumour growth (Libermann and Baltimore, 1990; Schafer and Brugge, 2007). Even though NF- κ B activity has mainly been associated with a pro-inflammatory phenotype, it has also been shown that inhibition of IKK β (upstream activator of NF- κ B) activity in TAMs is able to reverse the M2 phenotype and re-educate them to an M1 phenotype activating the TAMs to kill cancer cells, which resulted in regression of the tumour (Hagemann et al., 2008). Due to this plasticity of the TAM phenotype and the complex role of NF- κ B, there is conflicting view of the role of NF- κ B in inflammation. Nevertheless, targeting NF- κ B, or downstream effectors, could be a potential therapy to block the tumour promoting role of TAMs in cancer tissue and possible restoring their intrinsic anti-tumour activity (Mancino and Lawrence, 2010).

1.2.1. Inflammation and prostate cancer

Chronic inflammation has been associated with many types of cancer, including prostate cancer, where it often occurs in the peripheral zone of the prostate gland (Blacklock, 1991). An increase in hyper proliferative epithelial cells is observed in focal atrophy lesions, also known as PIA (De Marzo et al., 1999). As PIA, high-grade PIN and carcinoma occur with preference in the peripheral zone of the prostate, and cells that are associated with these disease stages have a very similar phenotype. It is hypothesized that PIA is a precursor of high-grade PIN (De Marzo et al., 1999; Putzi and De Marzo, 2000).

There are several different aetiological agents that are thought to contribute to the initiation of prostatic inflammation, such as infections, dietary factors, hormonal changes and urine reflux. It is known that several pathogenic organisms can infect and induce an inflammatory response in the prostate, including sexually transmitted organisms and non-sexually transmitted organisms (Poletti et al., 1985; Cohen et al., 2005). Also, the correlation between an increased risk of developing more advanced prostate cancer and the consumption of dietary fat and/or high fat animal products, such as red meat, and a decreased risk with a high intake of fruit, vegetables, fibres and soy products has been established for some time (Giovannucci et al., 1993), as is the link between hormonal changes, such as increased levels of oestrogens, and the development of prostate cancer. An increase in oestrogen levels can result in architectural alterations in the prostate (Risbridger et al., 2003). Another aetiological agent that has been proposed to be involved in the development of chronic inflammation in the prostate, is chemical irritation from urine reflux (Persson and Ronquist, 1996). It has been shown that crystalline uric acid, which is released from dying cells, is able to directly engage the caspase-1 activating NALP3 “inflammasome”, which results in the production of inflammatory cytokines (Martinon et al., 2006). All these mechanisms of chronic epithelial injury may result in a break of the apparent immune “tolerance” of the prostate due to the release of antigens by damaged prostate epithelial cells, causing a chain reaction that further sustains and stimulates the inflammatory response and increases the prostatic inflammatory infiltrates (De Marzo et al., 2007).

The inflammatory network is a complex interaction of genes and transcription factors that are involved in the innate and adaptive immune system. Recently, studies have shown an association between one or multiple single nucleotide polymorphisms (SNPs) in inflammation related pathways, and their relation to an increased risk of

prostate cancer (Zheng et al., 2006). There has been an association between a SNP in the promoter region of alpha-1-antichymotrypsin (ACT), which is an acute-phase protein that is upregulated in response to inflammation, and an increased risk of prostate cancer. (Licastro et al., 2008). Another study showed that individuals carrying a SNP in IL-8 (47CT) or simultaneous SNPs in IL-1B(511CC) and IL-10(1082GG) had a significant increased risk in developing aggressive prostate cancer compared to individuals who did not carry these genotypes (Zabaleta et al., 2009).

Thus multiple pro-inflammatory cytokines, and their related pathways have been identified as potential mediators in the development from prostatic inflammation to prostate carcinoma, such as IL-1, TNF α and IL-6 and the JAK-STAT signalling pathway, which can be activated through IL-6. These cytokines have been shown to be upregulated in PIN and prostate cancer (Hobisch et al., 2000).

1.2.2. JAK-STAT signalling pathway

One of the most common cytokine signalling pathways is the Janus-kinase (JAK)-signal transducer and activator of transcription (STAT) pathway, which was discovered through studies of transcription activation by interferons (Darnell et al., 1994). The binding of cytokines to a cell-surface receptor results in receptor dimerization and subsequently activation of JAK tyrosine kinases. Specific tyrosine residues on the receptor are then phosphorylated by activated JAKs and create docking sites for the SH-domains that occur in all STATs. The receptor bound STAT is then phosphorylated by JAKs, dimerizes and leaves the receptor to translocate to the nucleus, where they activate gene transcription (Darnell, 1997) (Figure 1.10).

The mammalian JAK family has four members: JAK1, JAK2, JAK3 and tyrosine kinase 2 (TYK2) and there are seven members of the STAT family: STAT1, STAT2, STAT3, STAT4, STAT5a, STAT5b and STAT6. JAKs and STATs have specific functions in various immune responses (Shuai and Liu, 2003). The JAK-STAT signalling pathway can be regulated at many steps by distinct mechanisms. Key regulators include the suppressor of cytokine signalling (SOCS) proteins, protein inhibitor of activated (PIA) STATs family, as well as protein tyrosine phosphatases (PTPs). SOCS proteins are generally expressed at low levels in unstimulated cells and are rapidly induced by cytokine stimulation. Thus, SOCS proteins inhibit the JAK-STAT signalling pathway, by a direct inhibition of JAK enzymatic activity, forming a classic negative feedback loop. However, SOCS protein can also regulate signalling downstream of other cytokines (cross talk) (Crocker et al., 2008). There are several PTPs that have been indicated to regulate JAKs, including SPH1, SPH2 and CD45. The PTP regulate the JAK-STAT signalling pathway by dephosphorylation of JAKs, however specific PTPs dephosphorylate specific JAKs (Shuai and Liu, 2003). The last key regulator of the JAK-STAT signalling pathway, PIAs, interact with phosphorylated STAT3 and inhibit its DNA binding or the transactivating capacity (Shuai, 2006; Hoefer et al., 2012). Both PTPs and PIA are constitutively present in cells and therefore represent the first level of regulation, whilst SOCSs proteins are the second level of control.

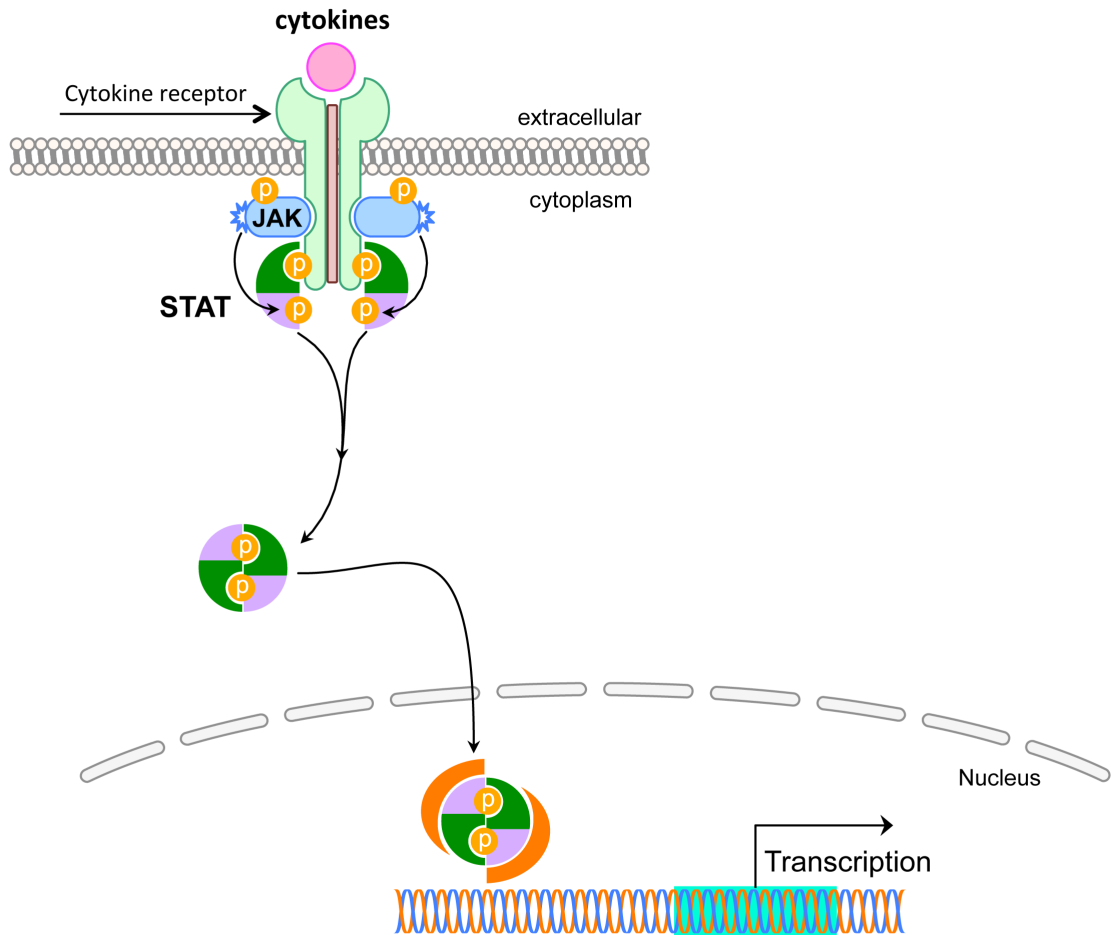


Figure 1.10. **Schematic representation of the JAK-STAT signalling pathway.** The pathway becomes activated after binding of cytokines to a cell-surface receptor, which dimerizes and activates JAKs. This creates docking sites for STATs, which are then phosphorylated, dimerize and translocate to the nucleus to activate gene transcription.

Dysregulation of the JAK-STAT signalling pathway has been implicated in many types of disease, including immune diseases and cancer. It has been shown that STATs are constitutively activated in many cancers, including leukemia (Weber-Nordt et al., 1996), breast (Watson and Miller, 1995), ovarian (Huang et al., 2000), head and neck (Grandis et al., 1998), lung (Song et al., 2003), colorectal (Corvinus et al., 2005), glioblastoma (Rahaman et al., 2002) and prostate cancer (Dhir et al., 2002). Constitutive activation of STATs in cancer is accompanied by hypermethylation of SOCS genes (Yoshikawa et al., 2001; He et al., 2003; Sutherland et al., 2004). These results suggest that SOCS proteins might act as tumour suppressors. This is confirmed by experimental overexpression of SOCS proteins in cancer cells, which resulted in decreased levels of STAT activity, inhibition of phosphorylation, induction of apoptosis and inhibition of tumour growth (Iwahori et al., 2011).

It is particularly STAT3 that is constitutively activated in many types of cancer, including prostate cancer (Bromberg, 2002; Mora et al., 2002). The first evidence showing a direct link between STAT3 and oncogenesis was from a study by Yu and colleagues. They showed that STAT3 is constitutively activated in cells transformed by an oncogene, Src (Yu et al., 1995). Direct evidence was shown with a constitutively active STAT3 mutant, which transformed fibroblasts in culture, and the transformed cells were able to form tumours in NUDE mice (Bromberg et al., 1999). The first evidence that showed the importance of STAT3 activation in cancer cells was shown in multiple myeloma. It was shown that activated STAT3 plays an essential role in preventing apoptosis in these cancer cells through the activation of anti-apoptotic proteins Bcl-xL (Catlett-Falcone et al., 1999). Since then many other proteins have been found that are crucial for cancer cell proliferation and survival, and are also regulated by STAT3, such as survivin, Cyclin D1 and c-myc (Kiuchi et al., 1999; Masuda et al., 2002; Kanda et al., 2004). More evidence that STAT3 is implicated in cancer cell survival is that inhibition of STAT3 has been shown to result in an increase of apoptotic cells and growth inhibition *in vivo*. (Burke et al., 2001; Iwamaru et al., 2007).

Not only is STAT3 implicated in inflammation and cancer, it has also been shown to be important for embryonic development. STAT3 is the only embryonic lethal knockout within the STAT family (Takeda et al., 1997) This is not surprising, as it has subsequently been shown that STAT3 activation is important for the self-renewal of pluripotent mouse embryonic stem (ES) cells (Niwa et al., 1998; Matsuda et al., 1999). However activation of STAT3 is not required to maintain human ES cells in their undifferentiated state or their ability to self-renew (Humphrey et al., 2004; Ying et al.,

2008). However, it also has been shown that STAT3 is important for stem cell maintenance (of adult tissue stem cells), including neural stem cells (Gu et al., 2005) and small-intestine crypt stem cells (Matthews et al., 2011). More recently it has become apparent that STAT3 is involved in the maintenance of cancer stem-like cells, including breast cancer (Zhou et al., 2007), liver cancer (Tang et al., 2008), colon (Lin et al., 2011) and glioblastoma (Sherry et al., 2009). Inhibition of STAT3 resulted in a decrease of viable stem-like cells as well as a decrease in tumorigenicity. In summary, constitutive activation of STAT3 is observed in many types of cancer. In addition, STAT3 is important for the maintenance of mES cells, adult tissue stem cells as well as cancer stem-like cells in a variety of tissue.

1.2.2.1. STAT3 activation and prostate cancer

It has been shown that STAT3 is constitutively activated in human prostate tumours, as well as prostate cell lines (Mora et al., 2002). This study also showed that increased levels of activated STAT3 were highly correlated with more aggressive prostate tumours, determined by Gleason score. Moreover, STAT3 is active in 77% of lymph node and 67% of bone metastasis of clinical prostate cancers, and activation of STAT3 in prostate cell lines resulted in a 33-fold increase in lung metastasis (Abdulghani et al., 2008). Inhibition of STAT3 in prostate cells induced significant growth inhibition and apoptosis as well as inhibition of tumour growth (Ni et al., 2000; Mora et al., 2002).

In prostate cancer, STAT3 is a target of the IL-6 family of cytokines, which includes IL-6, IL-11, leukemia inhibitory factor (LIF), oncostatin M (OSM), ciliary neurotrophic factor (CNTF), cardiotrophin1 and 3 (CT1, CT2), cardiotrophin-like cytokine (CLC) and IL-31 (Pflanz et al., 2002; Heinrich et al., 2003; Dillon et al., 2004). Apart from IL-31, the cytokines share a common receptor subunit; glycoprotein 130 (gp130), and IL-6, IL-11 and CNTF have a specific non-signalling α -receptor. IL-6 and IL-11 signal via gp130 homodimers, whilst the remaining IL-6 family of cytokines signal via heterodimers of gp130 and LIF receptor, gp130 and OSM receptor or gp130 and IL-27 receptor. Additionally, OSM has the exceptional capacity to recruit two different receptor complexes (Figure 1.11) (Heinrich et al., 2003; Cornelissen et al., 2012). The activation of STAT3 is initiated by the binding of a ligand to its receptor, which leads to the dimerization of the cytoplasmic domain of the receptor and activation of associated JAKs, this leads to the phosphorylation of STAT3, which allows for the dimerization of STAT3 and translocation to the nucleus. STAT3 is predominantly phosphorylated by a tyrosine kinase (Tyr705) in the carboxyl-terminal domain, however STAT3 phosphorylation is supplemented by phosphorylation of a specific serine residue (Ser727) (Wen et al., 1995).

STAT3 inhibitors have been emerging as promising anticancer therapies, and the most popular strategy to inhibit STAT3 activity is by disrupting the upstream tyrosine kinases. JAK2 inhibitors have been used in clinical trials, and have found to be very tolerable with no adverse impact on quality of life. Moreover, the phase I/II clinical trials, using JAK2 inhibitors for treatment of patients with myeloproliferative disorders has shown promising initial results (Bellido and Te Boekhorst, 2012; Shodeinde and Barton, 2012).

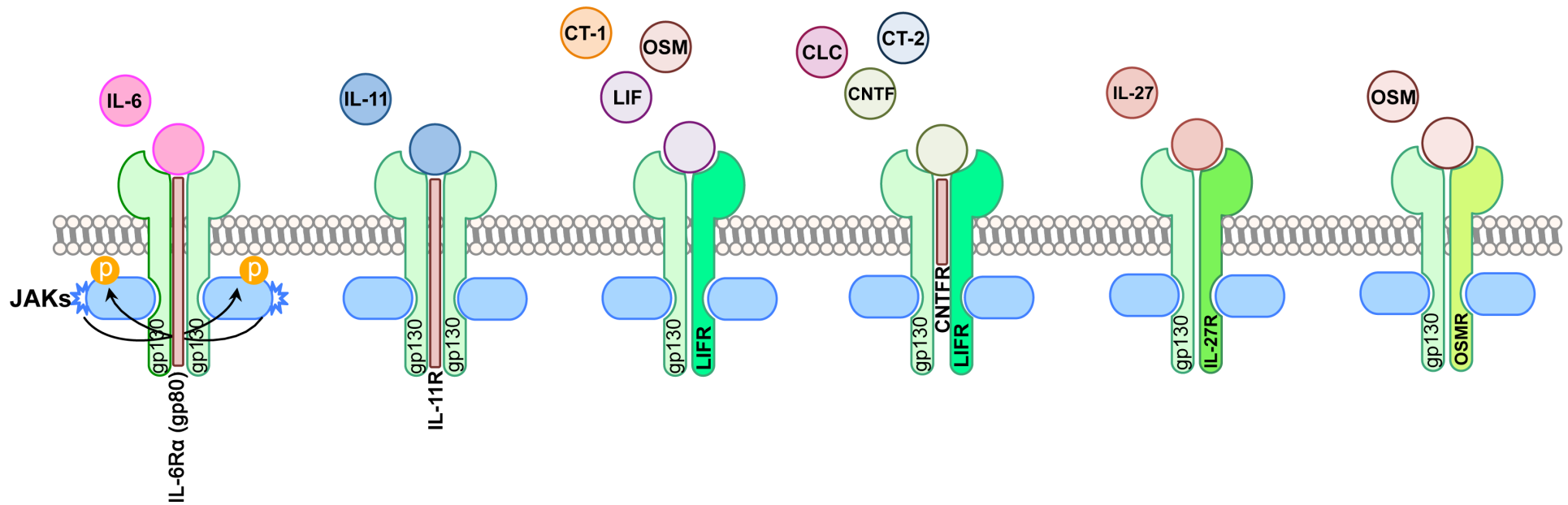


Figure 1.11. **Schematic representation of STAT3 activation through the IL-6 family of cytokines.** IL-6 and IL-11 bind their specific receptor component prior to binding to gp130, which then forms a homodimer complex. Whilst the other IL-6 family of cytokines interact with a heterodimers complex, consisting of gp130 and LIF receptor, IL-27 α receptor or OSM receptor. The LIF receptor/gp130 complex can be subdivided according to the presence of absence of CNTF receptor within its receptor complex.

1.2.2.2. IL-6 and prostate cancer

That STAT3 is constitutively activated in prostate cancer is not unexpected as it has been shown in many studies that the associated cytokine IL-6 is overexpressed in patients with prostate cancer (Smith and Keller, 2001).

The first implication that IL-6 was involved in the progression of prostate cancer was a study by Siegall and colleagues. They showed that prostate cancer cells secreted IL-6 and expressed the IL-6 specific receptor, gp80 (Siegall et al., 1990), so it was thought that IL-6 might act as a growth factor for prostate cancer cells. Since then, multiple studies have demonstrated that IL-6 is elevated in sera of patients' with prostate cancer (Twillie et al., 1995; Adler et al., 1999). Moreover, it has been shown that IL-6 is elevated in serum from men with metastatic CRPC compared to normal control, BPH or localized prostate cancer (Drachenberg et al., 1999). Additionally, the IL-6 specific receptor gp80 is highly expressed by prostate cancer cells compared to benign disease (Chung et al., 1999; Hobisch et al., 2000; Giri et al., 2001). So, not only does IL-6 act as a growth factor for prostate cells, it also plays a role in the progression of localized prostate cancer to the CRPC stage of the disease. It is thought that IL-6 undergoes a functional transition from paracrine growth inhibitor to autocrine growth stimulator in the progression of prostate cancer to a hormone-castration phenotype (Chung et al., 1999).

The biological activity of IL-6 is initiated through binding of a specific IL-6 receptor gp80 and the common receptor subunit gp130. However some cells that express lower levels of the IL-6 transmembrane receptor, can bind to a soluble form of the IL-6R (sIL-6R), which subsequently binds to gp130 and activates STAT3. High levels of sIL-6 is associated with high-grade prostate cancer, therefore it was suggested that it could be a potential circulating biomarker for prostate cancer (Terracciano et al., 2011).

It has also been shown that IL-6-mediated activation of STAT3 is able to increase the levels of PSA and activate several androgen-responsive promoters, in the absence of androgens. Suggesting that IL-6 is able to activate the AR in androgen-independent prostate cancer cells (Chen et al., 2000; Lin et al., 2001). In addition, overexpression of IL-6 protects prostate cancer cells from undergoing apoptosis induced by androgen deprivation therapy, this effect is mediated through activation of STAT3 (Lee et al., 2004). More recently it has been shown that IL-6 contributes to resistance to bicalutamide treatment (Feng et al., 2009). These results show that IL-6 is an important factor in prostate cancer progression and therapy resistance and is therefore an important therapeutic target.

In addition to the JAK-STAT signalling pathway, through activation of STAT3, IL-6 is also able to activate Ras, MAPK, Cox-2, Wnt and the PI3K/AKT pathway (Heinrich et al., 2003; Guo et al., 2012). However due to the high levels of secreted IL-6, IL-6 receptor and constitutively activated STAT3 in prostate cancer cells (and the ability of IL-6 to activate the AR in the absence of androgens) the focus of this and many other studies is the activation of STAT3, through IL-6 signalling in prostate cancer.

Because IL-6 is implicated in prostate cancer growth and progression, it is important to target IL-6 signalling. Various compounds that antagonize IL-6 production, including non-steroidal anti-inflammatory agents, oestrogens, and cytokines have been used, however these drugs also have effects on cancer cells that go far beyond their anti-IL-6 properties (Tripathi et al., 2003). Thus, a more specific anti-IL-6 neutralizing antibody is required. One of the most widely used neutralizing antibodies against IL-6 is CNTO 328, which is a murine-human chimeric monoclonal antibody (also known as siltuximab). The main advantage of this neutralizing antibody is that it has shown no life-threatening side effects and has a long half-life of 17.8 days (van Zaanen et al., 1998; Tripathi et al., 2003). The results with CNTO 328 have shown it to be capable of neutralizing IL-6's functions in a variety of human cancers, including multiple myeloma (Voorhees et al., 2007), ovarian cancer (Guo et al., 2010), and prostate cancer (Steiner et al., 2006; Fizazi et al., 2012).

As expected, treatment of prostate cancer cells with the anti-IL-6 antibody CNTO 328 resulted in significant inhibition of cell viability in vitro as well as modest growth inhibition in vivo, using LNCaP-IL-6⁺ cells (Steiner et al., 2006). Furthermore, treatment with CNTO328 inhibited the conversion of androgen-dependent prostate cancer to androgen-independent prostate cancer in vivo (Wallner et al., 2006). Phase I clinical trials did show that CNTO 328 is safe to use in patients with prostate cancer and it resulted in down regulation of genes that are associated with prostate cancer (Karkera et al., 2011). Unfortunately, phase II clinical trials with patients' with metastatic CRPC did not show an improved clinical outcome over chemotherapy (Fizazi et al., 2012).

1.2.3. Targeting the JAK-STAT signalling pathway in prostate cancer stem cells

Due to the failure of current therapies against prostate cancer, especially CRPC, it is important to develop new treatment strategies. Since prostate cancer stem cells are at the root of the tumour and are not targeted with current therapies, as well as being responsible for metastasis, elimination of these CSCs offers the potential to completely eradicate the tumour (Lou and Dean, 2007; Maitland and Collins, 2008b; van den Hoogen et al., 2010; Wang et al., 2012). One approach could be differentiation therapy, which attempts to end the cycle of self-renewal by encouraging the cells to differentiate into a more committed cell type. Cancer stem cells rely highly on certain signalling pathway in order to maintain the ability to self-renew and differentiate and understanding these mechanisms could be a potential target to inhibit these functions in cancer stem cells (Hu and Fu, 2012).

It has been shown, in gene expression profiling study, that JAK-STAT signalling is a key process in the $\alpha_2\beta_1^{\text{hi}}/\text{CD133}^+$ (stem-cell like) population of prostate cancer (Birnie et al., 2008). As IL-6 is mainly associated with prostate cancer as a growth factor or AR activator in the absence of androgens it is involved in the majority of tumour cells. However in the stem cell population, where the AR is not expressed, but IL-6 is highly expressed, it is thought to act here as a cell survival factor (Maitland and Collins, 2008a).

It has been shown that targeting the JAK-STAT signalling pathway, either through targeting IL-6 or STAT3 phosphorylation, has a promising effect on the cancer stem cell phenotype. For example, glioblastoma stem cells (GSC) express significantly higher levels of the IL-6 specific receptor compared to the non-stem glioma cells, suggesting that these cells require IL-6 signalling. When the IL-6 receptor is targeted, using shRNA, it was shown that GSC had a decreased percentage in proliferating cells, viable cells as well as a loss to serial passage neurospheres (assay for self-renewal) in the knockdown GSCs. As the GSCs are the tumour-initiating cells it was encouraging that there was an increase in survival of mice bearing glioblastoma xenografts that had the IL-6 or IL-6R knockdown. Moreover, treatment with an anti-IL-6 antibody also resulted in an inhibition of growth of a human glioma xenograft (Wang et al., 2009a). A similar result was observed for colon cancer-initiating cells. It was shown that the CD133^+ cells expressed higher levels of IL-6 and STAT3 compared to the CD133^- population. With the use of a novel STAT3 inhibitor, LLL12, it was shown that the CD133^+ cells had decrease cell viability and tumoursphere-forming capacity as well as an overall reduction in cell number after inhibition of STAT3. Moreover, treatment

with LLL12 resulted in a decreased ability of the cancer-initiating CD133⁺ cells to form tumours (Lin et al., 2011). Both these studies show that constitutively activating STAT3, through IL-6, is important for the survival and proliferation of tumour-initiating cells. There is preliminary evidence that this also might be important for prostate cancer-initiating cells, due to high expression of IL-6 and several components of the JAK-STAT signalling pathway in the stem cells population of malignancy (Birnie et al., 2008).

In most studies, inhibiting the JAK-STAT signalling pathway is done by targeting upstream targets, such as JAKs or IL-6. A widely used JAK inhibitor is pyridine-6 (P6), which is a reversible ATP inhibitor and has been found to inhibit the JAKs in the low nanomolar range (Lucet et al., 2006). It has been shown that P6 is a more sensitive inhibitor compared to AG490, another commonly used JAK2 inhibitor (Pedranzini et al., 2006). It has been shown previously that P6 successfully inhibits STAT3 activation in prostate cancer cells (Azare et al., 2007). A recently developed inhibitor, named LLL12, which is specifically directed against phospho-STAT3 (Tyr705), was also used in this study. This molecule has been derived from curcumin, which is a compound that has been used in cancer chemoprevention (Cheng et al., 2001). Treatment with LLL12 resulted in inhibition of STAT3 and inhibition of proliferation in a variety of cancer cells, including breast, pancreatic and glioblastoma (Lin et al., 2010). An overview of the three inhibitors, and their targets, used in this study are shown in Figure 1.12.

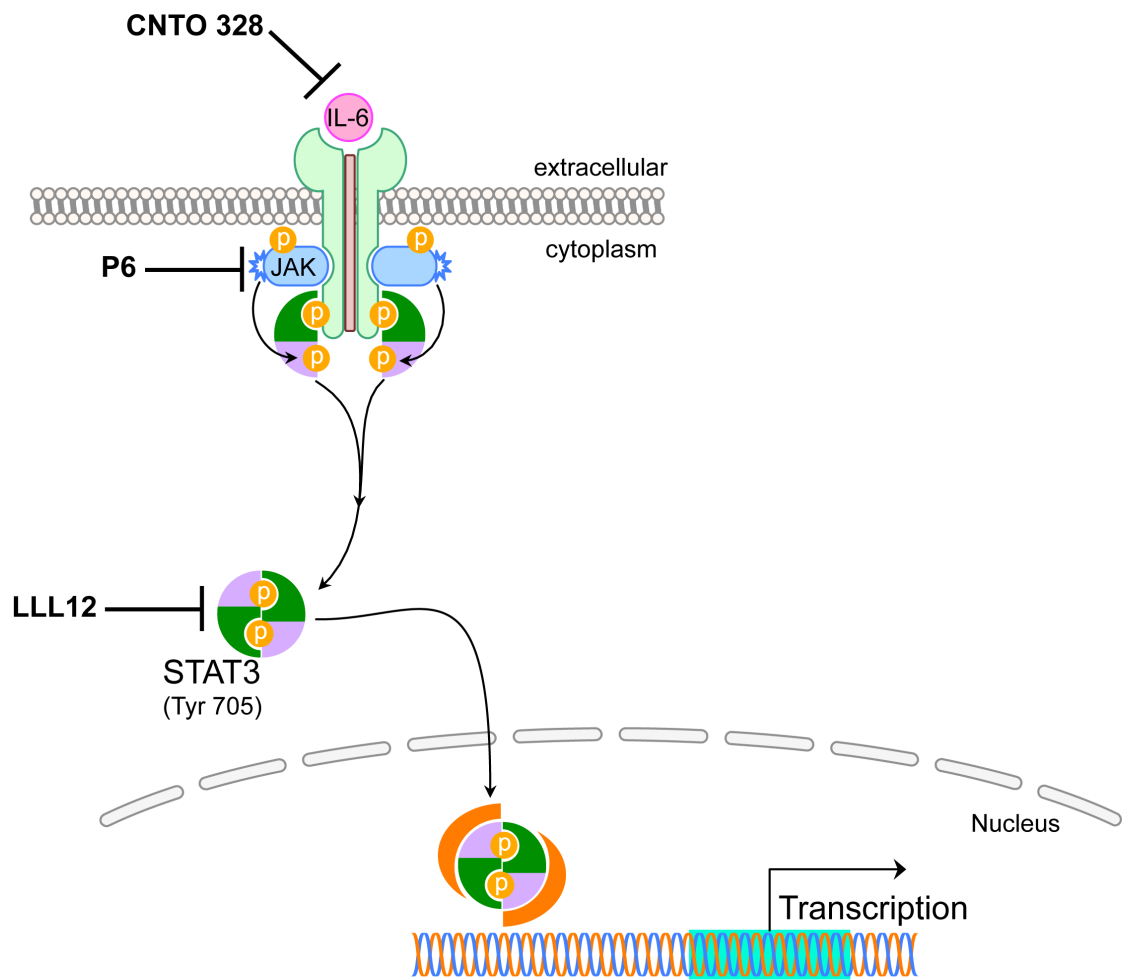


Figure 1.12. **Schematic representation of inhibitors of the JAK-STAT signalling pathway.** (1) CNTO 328 is an anti-IL-6 antibody which binds and prevents IL-6 activation of the IL-6R (gp80), (2) P6 is a pan-JAK inhibitor which binds via an induced fit mechanism, buried within a narrow JAK-ATP binding pocket., and (3) LLL12 is a specific phospho-STAT3 (Tyr705) inhibitor, which binds directly to the phosphoryl tyrosine 705 binding site of the STAT3 monomer. The levels of pSTAT3 after treatment will determine the efficiency of these inhibitors.

1.3. Main research strategies and aims

Currently there is no effective therapy for advanced prostate cancer. This is potentially due to the presence of undifferentiated cancer stem cells, which are not targeted in the current therapy strategies for prostate cancer. Thus it is important to develop new strategies that target these slow cycling, AR-negative cells, in order to eradicate the entire tumour mass. One strategy to target these cancer stem cells is through perturbation of a signalling pathway that the cells depend on for the maintenance of the undifferentiated stem cell phenotype. Disruption of this pathway could lead to perturbation of stem cell self-renewal directing the cells to terminal differentiation or making them more amenable to current standard of care therapies. One of the signalling pathways that has shown to be important for cancer stem cell maintenance and viability is the JAK-STAT signalling pathway, through activation of STAT3 (Zhou et al., 2007; Wang et al., 2009a; Lin et al., 2011).

Using gene expression profiling, components of the JAK-STAT signalling pathway were found to be overrepresented in the $\alpha_2\beta_1^{\text{hi}}/\text{CD133}^+$ (stem-like) population of primary prostate cancer cell cultures (Birnie et al., 2008). The focus of this study was to validate these findings and determine the importance of the JAK-STAT signalling pathway for the maintenance of prostate cancer stem cells using *in vitro* and *in vivo* techniques. The following questions were addressed:

- *Do the prostate cancer stem-like cells signal through an autocrine IL-6/STAT3 signalling pathway?*
- *Is STAT3 activation important for maintenance of the prostate cancer stem-like cells?*
- *What is the effect of phospho-STAT3 inhibition on tumour growth and tumour initiation?*

Chapter 2

Materials and Methods

2. Materials and Methods

2.1. Mammalian cell culture

2.1.1. Cell lines

All human cell lines were purchased from American Type Culture Collection (ATCC, USA) or the European Collection of Animal Cell Culture (ECACC, UK), except for P4E6, PNT1a and PNT2-C2, which were derived in our laboratory (Berthon et al., 1995; Maitland et al., 2001). PNT1a, PNT2-C2 and LNCaP cells were cultured in Roswell Park Memorial Institute-1640 (RPMI) (Invitrogen) supplemented with 10% Fetal Calf Serum (FCS) (PAA) and 2 mM L-Glutamine (Invitrogen) (**R10**). PC-3 cells were cultured in Ham's F-12 medium (Lorza) supplemented with 7% FCS and 2 mM L-glutamine (**H7**). P4E6 cells were cultured in Keratinocyte Serum-Free Medium (KSFM) (Invitrogen) supplemented with 2% FCS, 2 mM L-glutamine, 5 ng/mL Epidermal Growth Factor (EGF), 50 µg/mL bovine pituitary extract (Invitrogen) (**K2**). All cells were cultured in cell-culture tissue flasks (Corning) and cells were routinely cultured in T25 flask at 37 °C in 5% CO₂. List of different cell culture medium that have been used is shown in appendix 1.

2.1.2. Primary cell culture

Patient prostate tissue was collected with ethical permission from York District Hospital (York) and Castle Hill Hospital (Cottingham, Hull). Prostate tissue was obtained only from patients who had given informed consent. The Local Research Ethics Committees approved use of patient tissue. Prostate tissue was taken from patients undergoing transurethral resection of the prostate, radical prostatectomy (open and laparoscopic) or cystectomy (for bladder cancer), and all patient samples were anonymized. For patients undergoing radical prostatectomy, we received three core biopsies per side, which were taken from the right and left apex and base of the prostate using a core biopsy needle (14G). For each biopsy side: one core was fixed in OCT (Fisher Scientific) or 10% (v/v) formalin for histology, one core was engrafted into Rag2^{-/-}γC^{-/-} mice and the remaining core (or two when the sample was not required for engraftment) was digested for further culturing. From patients undergoing TURP, a small piece (~5 mm³) of tissue was taken and was placed in OCT or formalin for histology. For this study patients with BPH were used as controls as well as those patients undergoing cystectomies for bladder cancer if there were no indications of

tumour spread to the prostate. Details of patient's samples (including Gleason grade) are listed in appendix 2.

Prostate tissue biopsies were transported, the same day from the hospital, in transport medium (RPMI supplemented with 5% FCS and 2 mM L-Glutamine (**R5**) containing an antibiotic-antimycotic mixture containing 100 U/mL Penicillin, 100 µg/mL streptomycin, and 0.25 µg/mL Fungizon (ABM, Invitrogen)) at 4°C. The biopsies were placed in a Petri dish and washed with 10 mL phosphate buffered saline (PBS). 200 U/mL collagenase (Lorne laboratories Ltd) was dissolved in 2.5 mL KSFM (supplemented with 5 ng/mL EGF, 50 µg/mL bovine pituitary extract, 2 mM L-Glutamine) and 5 mL R10 containing ABM. The solution was then passed through a 0.22 µm filter unit (Millipore) prior to use. This mixture was added to the biopsy tissue, which was finely chopped (1 mm³) with a disposable scalpel (Swann Morton). The tissue was then transferred to an Erlenmeyer flask and treated overnight in the 200 U/mL collagenase solution in an orbital shaker at 37°C at 80 Revolutions Per Minute (RPM). After this incubation period the cell suspension was transferred to a universal and mechanically disrupted by tituration through a 21G blunt needle (Kendall Tyco Healthcare). The suspension was then centrifuged for 10 minutes at 2000RPM, washed in 10 mL PBS and centrifuged for a further 10 minutes at 2000RPM. This wash step was repeated once more. Organoids were separated from the stromal cells by differential centrifugation (800RPM for 1 minute), which resulted in a pellet of organoids, cells and supernatant containing stromal cells. The organoids were collected using a wetted Pasteur pipette. This step was repeated until all organoids were collected. Stromal cells were transferred to a T25 flask in R10 containing ABM and maintained for culture. This differential centrifugation step, to separate the stromal cells from the epithelial cells, does not apply to high Gleason grade cancer, due to the lack of organoids. The organoids were washed with 10 mL PBS, centrifuged for 3 minutes at 1300RPM, resuspended in 5 mL 0.05% Trypsin/EDTA (Invitrogen) and incubated in an orbital shaker for 30 minutes at 37°C at 80RPM. After this incubation step, 10 mL R10 was added to inactivate the trypsin, and the suspension was centrifuged for 3 minutes at 1300RPM resulting in a pellet of epithelial cells. Epithelial cells were cultured in the presence of irradiated (60 gray (Gy)) mouse embryonic fibroblasts (STO) mouse feeder cells on collagen-I coated plastic ware (BD biosciences) in KSFM supplemented with 5 ng/mL EGF, 50 µg/mL bovine pituitary extract, 2 mM L-glutamine, 2 ng/mL stem cell factor (First Link Ltd, UK), 1 ng/mL granulocyte-macrophage colony-stimulating factor (GM-CSF, Miltenyi Biotec) and 100 ng/mL cholera toxin (Sigma-Aldrich) (Stem Cell Medium, **SCM**). Cells were cultured at 5% CO₂ at 37°C and medium was changed

every 2 - 3 days until they reached 80% confluency, which was when cells were split at a standard ratio of 1:2.

2.1.3. Isolation of subpopulations from primary prostate epithelial cell cultures

After expansion of primary prostate cells in culture, the cells were washed once with PBS and 0.05% Trypsin/EDTA was added followed by ~5 minute incubation at 5% CO₂ at 37°C. Detached cells were collected in 10 mL R10 and two washes with PBS to ensure all cells were collected. Cell suspension was centrifuged for 3 minutes at 1300RPM and the cell pellet was resuspended in 5 mL SCM. The cells were then selected for $\alpha_2\beta_1$ integrin high expression using rapid adhesion to the substrate; Type I collagen, for 20 minutes at 37°C. The Collagen-I coated plates were pre-treated with 0.3% Bovine Serum Albumin (BSA) (Sigma Aldrich) for 1 hour at 37°C, to minimise non-specific binding. Non-adherent cells ($\alpha_2\beta_1^{\text{low}}$; the 20min+ fraction) were collected by at least three washes with PBS. The cells were subsequently resuspended in SCM. Adherent cells ($\alpha_2\beta_1^{\text{hi}}$) were detached using 0.05% trypsin/EDTA, after 5 - 10 minutes incubation at 5% CO₂ at 37°C all the cells were collected using two washes of PBS to ensure all cells are collected. The $\alpha_2\beta_1^{\text{hi}}$ cells were further enriched for CD133 expression using a CD133 microbead kit, according to the manufacturer's protocol (Miltenyi Biotec). Briefly, cells were resuspended in 300 μL MACS buffer (PBS supplemented with 2 mM EDTA and 0.5% FCS), and incubated with 100 μL FcR blocking buffer and 100 μL CD133-microbeads, at 4°C for 30 minutes. The cell suspension was washed once with 4 mL MACS buffer and centrifuged for 3 minutes at 1300RPM. The cell pellet was resuspended in 500 μL MACS buffer and applied to a pre-prepared MS column. The column was washed three times with 3 mL MACS buffer, which resulted in a flow through of CD133⁻ cells and elute of CD133⁺ cells. The purity of CD133⁺ cells was further enriched over a second MS column. Cells were washed once with R10, centrifuged for 3 minutes at 1300RPM and resuspended in SCM for further use. This procedure resulted in three cell populations: $\alpha_2\beta_1^{\text{hi}}/\text{CD133}^+$ (stem-like cells), $\alpha_2\beta_1^{\text{hi}}/\text{CD133}^-$ (transit amplifying cells) and $\alpha_2\beta_1^{\text{low}}$ (committed basal cells).

2.1.4. Isolation of lymphocytes from patients peripheral blood samples

Blood samples were taken from patients, who had given informed consent as described in section 2.1.2. The lymphocytes isolated from the blood samples could be used for genotyping, as a reference. Blood was taken using blood collection tubes and stored at 4°C until transported. Blood was transferred to a 15 mL falcon tube and diluted 1:1 with PBS and slowly layered onto 5 mL Lymphocyte Separation Medium (LSM) (MP Biomedical) followed by centrifugation for 30 minutes at 1800RPM with the brake off. Using a Pasteur pipette, the lymphocyte layer, which is a narrow creamy layer in between the yellow-orange layer of plasma and clear layer of LSM, was gently aspirated off and transferred to a fresh 15 mL tube. The lymphocytes were washed once with PBS and centrifuged for 5 minutes at 2100RPM. The cells could be used for further analysis, but were usually stored at -80°C for future use in genotyping analysis using a PowerPlex® 16 System (Promega). Analysis was performed by miss Hannah Walker.

2.1.5. Determination of live cell number

To determine live cell counts, cell suspensions were mixed in a 1:1 ratio with 0.4% Trypan Blue Stain (Sigma) in a total volume of approximately 20 µL. After mixing, the cell number was counted using a haemocytometer (10 µL per chamber), which resulted in a live cell number (non-stained cells) and total cell number (stained and non-stained cells). To calculate dead cells, the live cell number was subtracted from the total cell number.

In addition, two alternative methods were used to determine the cell number of the $\alpha_2\beta_1^{hi}/CD133^+$ fraction due to limited cells (0.01% of the total culture). (1) All adherent cells were counted, using an eyepiece graticule (NE11a – 20 mm) or (2) 10 µL from a 100 µL cell suspension, was diluted 1:1 with 0.4% Trypan blue and was then counted on a haemocytometer. Instead of counting only the cells that were within the grid, the entire area of the haemocytometer was counted for all live cells contained in the 10 µL. This resulted in a more accurate estimate of total live cells per 100 µL.

2.2. Transcriptional expression

2.2.1. RNA extraction

RNA extraction was performed using an RNeasy Mini Kit (Qiagen) according to the manufacturer's protocol. Briefly, cells were resuspended in 350 μ L RTL buffer, apart from the $\alpha_2\beta_1^{\text{hi}}/\text{CD133}^+$ population, which was resuspended in 100 μ L due to low cell numbers. The cell lysate was added onto a column and centrifuged for 2 minutes at full speed to remove cell debris. A one-time volume of 70% EtOH was added to the flow through and this mixture was added onto a binding column. Column, with bound RNA, was washed three times and RNA was eluted using 30 μ L RNase-free water. RNA quality was checked using a Nanodrop spectrophotometer and RNA was stored at -80°C .

2.2.2. RT-PCR

Reverse transcription was performed using up to 5 μ g RNA, in a total volume of 12 μ L that contained 100 ng random hexamer primers (Invitrogen) and 10 mM dNTPs (Invitrogen). This mixture was heated to 65°C , for 5 minutes followed by 2 minutes on ice. The following enzymes were then added: 1x First Strand buffer (Invitrogen), 0.1 M dithiothreitol (DTT) (Invitrogen), 40 U RNase Inhibitor (RNaseOUT, invitrogen) and 200 U reverse transcriptase II (Invitrogen) in a total volume of 20 μ L. The reaction was incubated at 25°C for 10 minutes, 42°C for 50 minutes and 70°C for 15 minutes. Synthesized cDNA was stored at -20°C .

One tenth of cDNA (or ddH₂O as a negative control) was added to a PCR reaction mix containing: 1 μ M forward and reverse primers (Appendix 3a), 1.5 mM MgCl₂ (Promega), 0.2 mM dNTPs, 1 U GoTaq polymerase (Promega), 25 U GoTaq buffer (Promega). The standard PCR cycle profile details are shown below:

94°C for 2 minutes	}	30 cycles
94°C for 30 seconds		
60°C for 30 seconds		
72°C for 30 seconds		
72°C for 2 minutes		

The annealing temperature (60°C) was for glyceraldehyde 3-phosphate dehydrogenase (GAPDH), but the annealing temperature to detect IL-6 was 54°C. The reaction was carried out using GeneAmp PCR system 9700 thermal cycler (Applied Biosystems).

10 µL of the resulting PCR reaction was added onto a 1.5% (w/v) agarose (Invitrogen) gel, together with a 100 base pair (bp) marker (Invitrogen) to assess product size. Gels were visualized using the GeneGenius UV transilluminator (Syngene).

2.2.3. Quantitative RT-PCR

RNA, from selected $\alpha_2\beta_1^{\text{hi}}/\text{CD133}^+$, $\alpha_2\beta_1^{\text{hi}}/\text{CD133}^-$ and $\alpha_2\beta_1^{\text{low}}$ primary prostate cells, was isolated as described in section 2.1.3. and cDNA reverse transcription was performed as described in section 2.2.2. qRT-PCR reaction was performed using 2 µL cDNA, 1x Taqman PCR mastermix (AB Applied Biosystems), 1x TaqMan gene expression assay (AB Applied Biosystems) (Appendix 3b) in a total volume of 20 µL per well. Reactions were run in triplicate wells on an ABI 700 real-time PCR machine (provided by the Technology Facility (TF)), and expression levels were standardized to RPLP0.

2.3. Protein expression

2.3.1. Primary prostate cells

2.3.1.1. SDS-PAGE and Western blot

2.3.1.1.1. Preparation of whole cell lysates

Primary prostate cells, at a density of 2×10^5 cells per well of a 6-well collagen I-coated plate, were washed once with PBS, and whole cell lysate was prepared by adding 500 μ L Cytobuster protein extraction reagent (Novagen) per well followed by an incubation step for 5 minutes at room temperature (RT). Occasionally, cell lysates were prepared from a confluent 10 cm² collagen-I plate, which required 1 mL cytobuster protein extraction reagent. The cells were harvested from the plate, using a cell scraper, and centrifuged for 5 minutes at 14,000xg at 4°C. The supernatant was collected and 1x complete protease inhibitor (Roche) and 1x PhosSTOP (phosphatase inhibitor cocktail, Roche) was added. Samples were stored at -80°C.

2.3.1.1.2. Preparation of cytoplasmic and nuclear extracts

Primary prostate cells, at a density of 2×10^5 cells per well of a 6-well collagen I-coated plate were washed once with PBS. Cells were harvested using 0.05% trypsin/EDTA and after R10 was added to neutralise the trypsin, all cells were collected with one PBS wash and the cells were centrifuged for 3 minutes at 1300RPM. Cytoplasmic and nuclear extracts were prepared using the nuclear and cytoplasmic extraction reagent from Thermo Scientific, according to the manufacturer's protocol. Briefly, cell pellets were resuspended in ice-cold CER-I buffer, 1x complete protease inhibitor, 1x PhosSTOP and rigorously vortexed for 15 seconds and placed on ice for 10 minutes. Buffer CER-II was added, rigorously vortexed, incubated on ice for one minute, vortexed again for 5 seconds and centrifuged for 5 minutes at 14,000 xg. Supernatant (cytoplasmic extract) was transferred to a pre-chilled tube and immediately stored at -80°C. The cell pellet was washed once with PBS and resuspended in ice cold NER buffer, vortexed for 15 seconds and place on ice for 10 minutes and vortexed again for 15 seconds every 10 minute, for a total of 40 minutes. The cell suspension was centrifuged for 10 minutes at 14,000 xg the supernatant (nuclear extract) was transferred to a pre-chilled tube and immediately stored at -80°C.

2.3.1.1.3. BCA assay for the determination of protein concentrations

Protein concentrations were determined using the bicinchoninic acid (BCA) protein assay (Thermo Scientific) according to the manufacturer's protocol. Briefly, 10 μ L of unknown protein lysate was added to 200 μ L of WR buffer (in triplicate) to a 96 well plate including a BSA standard, ranging from 0 – 2000 μ g/mL. After 30 minutes incubation at 37 °C, absorbance was measured at a wavelength of 544 nm on a BMG Labtech POLARstar OPTIMA plate reader.

2.3.1.1.4. SDS-PAGE gel electrophoreses and Western blotting

Sodium dodecyl sulphate (SDS) loading buffer (10% (v/v) glycerol, 1% SDS, 0.125 M Tris-HCl pH 6.8, 2.5% β -mercaptoethanol and bromophenol blue to colour) was added to protein lysates (~15 μ g) and heated for 5 minutes at 100°C. The mixture was rigorously vortexed for 10 seconds and loaded onto a 10% Tris-SDS acrylamide gel, using the mini-PROTEAN Tetra Cell system (Biorad). Precision plus kaleidoscope (Biorad) and biotinylated (Cell signalling technologies) protein markers were included to determine the molecular weight of the protein samples. Gels were run for 2 hours at 80 volt (V) in SDS running buffer (25 mM Tris, 0.19 M Glycine, 3.5 mM SDS). When finished, gels were submerged in transfer buffer (48 mM Tris, 39 mM Glycine, 10% (v/v) Methanol (MeOH)) for 15 minutes. Proteins were immediately transferred onto an (MeOH pre-treated) Immobilon-P membrane (Millipore) for 2 hours at 100 V at RT (or overnight at 30 V at 4°C) in transfer buffer. Membrane was air-dried, re-wet using MeOH, and washed twice in Tris-buffered saline (TBS: 150 mM NaCl, 50 mM Tris/HCl, pH 7.5). Non-specific sites were blocked using 5% (w/v) non-fat skimmed milk (Marvel) for 1 hour at RT. Primary antibodies (Appendix 4A) were incubated for 1 hour at RT or overnight at 4°C. Membranes were washed twice with TBS/0.1%Tween-20 (TBS-T) and once with 2.5% (w/v) Marvel. This was followed by a one-hour incubation step with peroxide-labelled secondary antibodies (Appendix 4C, 1:5000 anti-IgG peroxide and 1:5000 anti-biotin-HRP; Cell signalling technologies). Membranes were washed four times with TBS-T, followed by chemiluminescent detection using the BM Chemiluminescence Western Blotting Substrate (POD) system (Roche). Bound antibody was visualised using ECL Hyperfilm (Amersham) and these were manually processed using developer and fixer solutions (GBX, Kodak).

When multiple probing of the same membrane was required, the membrane was stripped of antibody by incubation in stripping buffer (20 mM Tris/HCl, 0.05% (v/v) SDS,

20 mM DTT)) for 30 - 50 minutes at RT. Membranes were washed at least three times with TBS-T, and membrane probing was resumed from the blocking step above.

2.3.1.2. Enzyme-Linked Immunosorbent spot (ELISPOT) assay

The ELISPOT assay was performed using a human IL-6 Elispot kit (Abcam, #ab46548) according to the manufacturer's protocol. Briefly, a 96 PVDF-bottomed-well plate (Millipore) was incubated with 70% ethanol for 30 seconds at RT, washed three times with PBS and incubated with human IL-6 capture antibody overnight at 4 °C. The following day, the wells were washed once with PBS, blocked with 2% skimmed milk for 2 hours at RT, emptied and washed again with PBS, before cells were added to the wells. If necessary, the plate could be stored at 4°C after wells were left to air-dry, before cells were added. Cells were added at a range between 1000 – 100,000 cells per well, in triplicate, the plate was covered and placed for 15 - 20 hours in a 5% CO₂ incubator at 37°C. It was important for the plates not to be moved during this incubation period, as this might result in inaccurate read out. After the incubation time, the wells were emptied, incubated with PBS/0.1% tween-20 for 10 minutes at 4°C and washed four times with PBS/0.1% tween-20. Detection antibody, diluted in PBS/1% BSA, was added and incubated for 1 - 2 hours at RT, followed by three washes with PBS/0.1% tween-20. Streptavidin-Alkaline phosphatase (1:5000) was added, incubated for 1 hour at 37 °C and wells were washed three times with PBS/0.1% tween-20. This was followed by an extra step, to prevent high background, this included washing both sides of the PVDF membrane under running distilled water and removing residual buffer by repeated tapping on absorbent paper. Nitro-blue tetrazolium chloride / 5-bromo-4-chloro-3'-indolyphosphate p-toluidine salt (NBT/BCIP) was used for visualisation, this was added to the wells and incubated for 2 - 10 minutes at RT until the spots became visible. The wells were rinsed three times with distilled water, dried and left overnight at 4 °C for the spots to become sharper. Spots were analysed using an ELISPOT reader (AID EliSpot Reader System), provided by St. James' Hospital in Leeds.

2.3.1.3. Enzyme-Linked ImmunoSorbent Assay (ELISA)

Unselected or selected ($\alpha_2\beta_1^{\text{hi}}/\text{CD133}^+$, $\alpha_2\beta_1^{\text{hi}}/\text{CD133}^-$ and $\alpha_2\beta_1^{\text{low}}$) primary prostate cells were plated at low cell density (500 - 1000 cells), in triplicate, onto a collagen-I coated 96-well plate (BD biosciences), in the presence of irradiated STO cells. Included were wells containing only irradiated mouse feeder cells or medium, which were the negative controls. Conditioned medium was collected from cultures after 48 hours incubation at 5% CO₂ at 37°C, and immediately stored at -20°C. The concentration of secreted IL-6 in the conditioned medium was measured using the Quantikine High Sensitive ELISA (R&D systems, #HS600B), according to the manufacturer's protocol. Briefly, conditioned medium or IL-6 standards were added to a 96-well polystyrene microplate coated with a mouse monoclonal antibody against IL-6, and incubated for 2 hours at RT on a horizontal orbital microplate shaker (Titertek). Wells were washed six times with washing buffer, and IL-6 conjugate was added to each well and incubated for 2 hours at RT on the microplate shaker. This was followed by six washes, and substrate solution was then added to the wells and incubated for 1 hour at RT. Amplifier solution was then added to each well and incubated for 30 minutes at RT followed by stop solution. The optical density of each well was determined within 30 minutes using the BMG Labtech POLARstar OPTIMA microplate reader at 485 nm and 620 nm. The readings from 485nm were corrected against those from 620 nm as this corrected for optical imperfections of the plate. Analysis was performed relative to the negative control wells (medium only).

2.3.1.4. Cell-Based ELISA

A Cell-Based ELISA was used to measure the levels of phosphorylated STAT3 (Tyr705) and total STAT3 simultaneously in primary prostate cells (R&D systems, #KCB4606), and performed according to the manufacturer's protocol. Briefly, primary prostate cells were plated onto black, collagen I coated 96-well plates in triplicate, at an optimal cell density of 10,000 cells per well. Cells were left overnight in a 5% CO₂ incubator at 37°C, to adhere. Cells were washed once with PBS and fixed with 4% (w/v) paraformaldehyde (PFA) for 20 minutes at RT. Cells were washed twice with PBS and the fixed cells could be stored for up to 2 weeks at 4°C in PBS. PBS was aspirated off and the wells were washed three times for 5 minutes with 1x washing buffer. Quenching buffer (0.6% Hydrogen Peroxide (H₂O₂) in 1x washing buffer) was added and incubated for 20 minutes at RT. Cells were washed three times for 5 minutes with washing buffer, incubated with blocking buffer for 1 hour at RT and washed again three times for 5 minutes. Primary antibody mixture (1:100 phospho-STAT3 (Tyr705)

antibody + 1:100 total STAT3 antibody) was added to the wells and incubated overnight at 4°C. Primary antibody mixture was removed, and cells were washed three times, for 5 minutes with washing buffer. Secondary antibody (1:100 HRP-conjugated antibody + 1:100 AP-conjugated antibody) was then added for 2 hours at RT. The wells were washed twice with washing buffer, followed by a further two washes in PBS. Substrate F1 was added, for 20 - 60 minutes at RT and substrate F2 was added for an additional 20 - 40 minutes at RT. The fluorescence intensity was measured using the BMG Labtech POLARstar OPTIMA microplate reader at a wavelength of 540, representing the amount of phosphorylated STAT3, and at a wavelength of 360 nm, representing the amount of total STAT3 in the cells. The relative fluorescence units (RFUs) from the control wells (secondary antibody alone) were subtracted from all sample wells. The phosphorylated STAT3 fluorescence at 540 nm in each well was normalized to that of total STAT3 fluorescence at 360 nm.

2.3.1.5. Flow cytometry

2.3.1.5.1. Detection of cell surface protein(s)

For this set of experiments either primary prostate cells or tumour cells from xenografts were used. For primary cells, a semi-confluent 10 cm² collagen-I coated plate of primary cells was harvested using 0.05% Trypsin/EDTA. For the xenografts, mouse cells were firstly depleted as described in section 2.5.2.1. Harvested cells were washed once with MACS buffer and subsequent cell labelling was performed on a MACSmix Tube Rotator (Miltenyi Biotec). If unconjugated primary antibodies were used, cells were initially incubated in 20% serum (from the second antibody species) for 10 minutes at 4°C to inhibit non-specific binding. Cells were incubated with either primary antibodies (Appendix 4A), unlabelled, or non-specific isotype as negative controls (Appendix 4B), and 20% FcR blocking buffer (Miltenyi Biotec) in a total volume of 100µL MACS buffer, for 10 minutes at 4°C. For dual labelling of multiple membrane markers, antibodies were added simultaneously in a total volume of 100 µL. Secondary antibodies (Appendix 4C) were added and incubated for 30 minutes at 4°C and cells were then resuspended in MACS buffer and 1:1000 SYTOX blue cell dead stain (Invitrogen) was added 5 minutes before analysis on a Cyan ADP flow cytometer (DAKO.), using 405, 488 and 633 lasers (Table 3). Results were analysed using Summit v4.3 software (Beckman Coulter).

2.3.1.5.2. Detection of intracellular antigen(s)

For the detection of intracellular antigens, cell suspensions were initially incubated with 1:1000 LIVE/DEAD Fixable Violet Dead Cell Stain (Invitrogen) for 30 minutes at 4°C. For the detection of cell surface antigens, cells were then labelled with membrane antibodies as described in section 2.1.3.5.1, followed by fixing the cells in 0.5% PFA (w/v) (or 1.5% (v/v) formaldehyde for xenograft cells) for 5 - 10 minutes at 4°C. Cells were permeabilised with 0.1% saponin (or ice-cold MeOH for xenograft cells) for 10 minutes at 4°C. Cells were subsequently labelled with intracellular antibody for 30 minutes at 4°C, washed twice with MACS buffer and resuspended in 500 µL and then analysed on the Cyan ADP flow cytometer, using 405, 488 and 633 lasers (**Table 3**). Results were analysed using Summit v4.3 software.

Table 3. Cyan ADP flow cytometry lasers.

Secondary antibody	Excitation	Emission
FITC	488	510 - 550
Alexa 288	488	510 - 550
PE	488	560 - 590
Violet 1	405	425 - 475
Violet 2	405	510 - 550
APC	633	645 - 685
Alexa 647	633	645 - 685

2.3.1.5.3. Data analysis

All events were analysed using the following gates; i) pulse width to exclude doublets and exclude debris, ii) Violet 1 channel to exclude dead cells as cells were labelled with either a live/dead stain, or Sytox blue which emits at a wavelength of 405nm and iii) FS/SS dot plot which depicts granularity and cell size. All other gates were set to the unlabelled or isotype control and fluorescence cells were analysed using the FITC-, PE and APC channel. Due to spectral overlap of the FITC detector into the PE detector (Table 3), compensation was performed when analysing cells that were dual labelled with a FITC and PE antibody.

2.3.1.6. Immunofluorescence with fixed cells

Primary prostate cells were selected as described in section 2.1.3 and plated onto collagen-I coated 8 well chamber slides (BD bioscience), at a maximum density of 5×10^4 cells per chamber. Cells were left for 2 - 3 hours to adhere, washed once with PBS and blocked in 10% serum for 30 minutes on ice. Primary antibodies (Appendix 4A) were added, incubated for 1 hour on ice and washed twice with PBS. Cells were fixed with 4% (w/v) PFA for 20 minutes at RT and washed twice for 10 minutes with 50 mM NH₄Cl. Alternatively, cells were left overnight in 50 mM NH₄Cl. Cells were washed twice with PBS and incubated with secondary antibody (Appendix 4C) for 1 hour at RT in the dark. After two washes in PBS, slides were mounted in Vectashield with DAPI (Vector laboratories) and visualised using a Zeiss LSM 510 meta confocal microscope (provided by the TF).

2.3.2. Prostate tissue

2.3.2.1. Preparation of tissue blocks and sections

Prostate tissue was fixed in 10% (v/v) formalin for at least 24 hours and was then transferred to 70% ethanol (EtOH). The tissue was then placed in an embedding cassette (Cell Path) and submerged in fresh 70% EtOH for 10 minutes, on a shaker. The cassette was placed in fresh absolute EtOH and incubated for 10 minutes on a shaker; this was repeated two more times. The cassette was submerged into fresh isopropanol for two times 10 minutes, submerged in fresh xylene (Fisher Scientific) for four times 10 minutes and excess xylene was removed and the cassette was placed into Histoplast Paraffin at 60 - 65°C (Thermo Scientific) for four times 15 minutes. Samples were embedded in moulds with molten wax and allowed to set on a cold plate at -10°C. Paraffin-embedded sections of tissues were prepared using APES-coated (2% (3'aminopropyl triethoxysilane) (v/v) (Sigma) in acetone) SuperFrost Plus slides (Merck), sections were cut using a microtome and were 5 µm in thickness. Mrs. Katy Hyde carried out these procedures.

2.3.2.2. Hematoxylin & eosin (H&E) staining

Paraffin embedded tissues sections, as described in section 2.3.2.1. were dewaxed in xylene for 2x 10 minutes and 2x 1 minute, xylene was refreshed after each step. Sections were re-hydrated using EtOH (3x 1 minute absolute EtOH followed by 1

minute in 70% EtOH), washed for one minute under running tap water, and were then placed in hematoxylin (Harris) for 4 minutes. Slides were washed for one minute under running tap water and placed for 5 seconds in 70% EtOH/1% hydrochloric acid and washed again for one minute under running tap water. Slides were placed in Eosin (Harris) for one minute and washed again for one minute under running tap water. Slides were dehydrated for one minute with 70% EtOH, 3x 1 minute absolute EtOH and 2x 1 minute Xylene and mounted in DPX mounting medium (Sigma). Mrs. Katy Hyde carried out this procedure.

2.3.2.3. Immunohistochemistry

Slides with paraffin embedded tissue sections, as described in 2.3.2.1, were dewaxed in xylene and re-hydrated in EtOH as described in section 2.3.2.2. Antigen retrieval was performed by boiling twice for 6 minutes in 0.01 M Citrate buffer in a microwave, at 900W. Sections were equilibrated to RT and rehydrated for 5 minutes in TBS, and a PAP-pen was used to draw around the tissue sections. Sections were blocked for 15 minutes in 5% serum (depending on which species secondary antibody was raised in) at RT, incubated with primary antibodies (Appendix 4A) or an isotype control (Appendix 4B), for 1 hour at RT and washed three times in TBS. Biotinylated secondary antibodies were added (Appendix 4C: 1:200 (DAKO)), incubated for 30 minutes at RT and slides were washed three times in TBS and incubated with streptavidin-HRP conjugate (1:200 (DAKO)) for 30 minutes at RT. After three washes in TBS, 3,3'-Diaminobenzidine (DAB) substrate (Sigma) was added for approximately 5 minutes, slides were washed twice with ddH₂O, counterstained with Haematoxylin QS (Vector Laboratories) and mounted in DPX mounting medium (Sigma). Images were taken using an Olympus BX51 light microscope.

2.3.2.4. Immunofluorescence

Slides with paraffin embedded tissue sections, as described in 2.3.2.1, were baked for 20 minutes at 60°C, dewaxed in xylene as described in 2.3.2.2., and antigen retrieval was performed by boiling for 3x 10 minutes in 0.01 M Citrate buffer in a microwave at 900W. Sections were equilibrated to RT and washed three times in PBS, and a PAP-pen was used to draw around the sections. Sections were blocked in 10% serum for 30 minutes at RT, and incubated with primary antibodies (Appendix 4A) overnight at 4 °C. Sections were washed four times in PBS, incubated with secondary antibodies (Appendix 4C) for 1 hour minutes at RT in the dark, and washed three times with PBS.

Slides were mounted using Vectashield with DAPI and visualised using a Zeiss LSM 510 meta confocal microscope.

2.4. Functional analysis

2.4.1. Clonogenic recovery assay

Semi-confluent, primary prostate epithelial cells derived from patients with cancer and benign disease, were treated with the drug/antibody of interest at the optimal concentration and time. Following treatment, the cells were selected for $\alpha_2\beta_1^{\text{hi}}/\text{CD133}^+$ (stem-like), $\alpha_2\beta_1^{\text{hi}}/\text{CD133}^-$ (TA) and $\alpha_2\beta_1^{\text{low}}$ (CB) cells as described in section 2.3.1. or for CD133^+ (stem-like) and CD133^- (progenitor) cells. The sorted fractions were counted and plated, in triplicate, onto 35 cm² collagen-I coated dishes (BD Biosciences) at a density of 100 live cells/well together with irradiated STO feeder cells, which is required for colony initiation of prostate epithelial cells. SCM was changed every two days and STOs were added when required. Colonies were counted as for the following sizes: 1 - 7 cells, 8 - 15 cells, 16 - 31 cells or >32 cells (5 population doublings), which was usually between 10 - 14 days. Colony formation efficiency (CFE) (# of colonies/number of cells plated x 100%) was normalised to the CFE generated from cells treated with vehicle alone.

2.5. In Vivo studies

2.5.1. General animal husbandry

All animal work was carried out in the Biological Service Facility (BSF), at the University of York according to the scientific procedures act of 1986. Under this act mice undergoing any procedure were checked daily for any adverse clinical signs of tumour cell engraftment and/or treatment.

All animal work was approved by the University of York Animal Procedures and Ethics Committee and performed under a United Kingdom Home Office Licence. All procedures were carried out under Personal Licence number 60/12977 and Project license number 60/3701 with training provided by Dr. Anne Collins (project licence holder), Mr. Alan Haigh and Mr. Paul Berry.

2.5.2. Subcutaneous xenotransplantation of prostate tumour cells

2.5.2.1. Depletion of mouse endothelial and lineage positive blood cells

Tumours from serially transplantable xenografts were taken once the tumour size reached 15 mm. The mice were humanely euthanized using a schedule I method and tumours were harvested and placed into transport medium (R10 + ABM + 10 nM DHT). The tumour was placed in a Petri dish and washed once with PBS before adding 200 U/mL collagenase dissolved in 2.5 mL KSFM supplemented with 5 ng/mL EGF, 50 µg/mL bovine pituitary extract and 2 mM L-Glutamine and 5 mL R10 containing ABM and 5 nM (DHT), which was passed through a 0.22 µm filter unit (Millipore) prior to use. Tumour tissue was finely chopped (~1 mm³) with a disposable scalpel. The tissue was then transferred to an Erlenmeyer flask and treated overnight in 200 U/mL collagenase in an orbital shaker at 37°C at 80RPM. After this incubation period the cell suspension was transferred to a universal and mechanically disrupted by tituration through a 21G blunt needle. The suspension was then centrifuged for 10 minutes at 2000RPM, washed in 10 mL PBS and centrifuged for a further 10 minutes at 2000RPM, this wash step was repeated once more. The pellet was resuspended in 5 mL 0.05% Trypsin/EDTA, incubated for 30 minutes at 37°C, R10 was added to inactivate the trypsin and the cell suspension was centrifuged for 3 minutes at 1300RPM. The cell pellet was resuspended in 10 mL R10, passed through a 21G blunt needle, and a 40

μm cell strainer (BD Biosciences). The cell strainer was washed three times with R10, and cells were centrifuged for 3 minutes 1300RPM. The tumour cell pellet was resuspended in 15 mL R10 and to further separate viable cells from dead cells and tissue debris, the tumour cell suspension was separated by density centrifugation using Ficoll-Paque Plus (MP Biomedicals). An underlayer of Ficoll-Paque Plus was created by pipetting 15 mL of Ficoll-Paque Plus slowly below the cell suspension being careful not to mix the two layers. The cell suspension and Ficoll layer were centrifuged for 30 minutes at 1800RPM with the brake turned off. The cells at the interface of the Ficoll-Paque Plus and cell dissociation buffer were collected and transferred to a fresh 50 mL tube. Fresh R10 was added to the cell suspension to dilute it 1:3 (e.g. 20 mL R10 added to 10 mL of cell suspension). The cells were collected by centrifugation for 10 minutes at 1300RPM and the media decanted. The cell pellet was then resuspended in 80 μL MACS buffer, 20 μL anti-mouse biotin antibody cocktail (Miltenyi Biotec), and 5 μL CD31:biotin antibody (AbD serotec) and incubated for 10 minutes at 4°C using MACSmix Tube Rotator. 60 μL MACS buffer and 40 μL anti-biotin Microbeads (Miltenyi Biotec) were added and further incubated for 15 minutes at 4°C on mixer. The cell suspension was washed once with 5 mL MACS buffer, the cell pellet was resuspended in 500 μL and added onto a pre-prepared LS column and the column was washed three times with 3 mL MACS buffer. The elute of Lin⁻CD31⁻ cells (human) was collected for further use.

2.5.2.2. Engraftment of prostate tumour cells

Lin⁻CD31⁻ tumour cells were counted and the required cell number was added to a fresh 1.5 mL Eppendorf tube together with 2×10^5 irradiated STO cells. The cell suspension was centrifuged for 4 minutes at 1600RPM in a bench top centrifuge. The cell pellet was then resuspended in 50 μL ice-cold Matrigel basement membrane complex (BD biosciences) and kept on ice. Cells were injected subcutaneously, using a 1 mL insulin syringe (27G) (BD Biosciences), into the left flank of a Rag2^{-/-} $\gamma\text{C}^{-/-}$ mouse supplemented with a 17.5 mg 5 α -DHT tablet (Innovative Research of America): 90 days slow-release of androgens, which was subcutaneously placed under the right flank. These surgical procedures were carried out under general anaesthesia of 2.5% Isoflurane (Abbott) along with oxygen and prior to surgery mice were given 4.5 mg/kg Rimadyl (Pfizer) as a local anaesthetic. Mice were monitored the following day to ensure the procedure was performed successfully and after that weekly to monitor tumour growth.

Tumour volume was measured every 2 - 3 days. Tumours were measured using digital calliper (Duratool DC150), and tumour volume (mm^3) was calculated using the

Ellipsoidal formula: $\frac{1}{2}(\text{length} \times \text{width}^2)$. For all treatments, unless otherwise indicated, treatment commenced once the tumour volume had reached 5 mm.

2.5.3. Intraperitoneal injection of drug into Rag2^{-/-}γC^{-/-} mice

LLL12, synthesized and obtained from the laboratory of Prof. Pui-Kai (Tom) Li, was prepared at a stock solution of 5 mg/mL in dimethyl sulfoxide (DMSO). The stock solution stored at -20°C in aliquots of 500 μL was prepared fresh (daily) using a vehicle of 10% DMSO, 5% Tween-80 (Sigma), 10% poly(ethylene glycol)400 (PEG400) (Sigma) and warm sterile 0.9% sodium chloride solution (Sigma) to prepare a solution of 0.5 mg/mL. This was sonicated for 10 minutes at 37°C using a water bath sonicator, and diluted 1:1 with vehicle control to create a 0.25 mg/mL solution and drug mixtures were kept at 37°C until injection. Mice were randomized into three groups of 10, which were either treated with (1) vehicle control, (2) 5 mg/kg LLL12 or (3) 2.5 mg/kg LLL12. The drug was administered via intraperitoneal (IP) injection, at 10 mL/kg body weight (BW) using a 1mL insulin syringe. Animals were kept under 2.5% isoflurane anaesthetics when this procedure was performed as it was thought to be better for the health and wellbeing of the animal.

2.5.4. Ex vivo treatment of human xenograft cells

Xenograft tumours were depleted for mouse endothelial and lineage positive blood cells as described in section 2.5.2.1. and Lin⁻CD31⁻ tumour cells were counted. Equal tumour cell numbers were resuspended in 1 mL SCM and treated with either vehicle control or LLL12. The cell suspension was placed in a 48-well collagen-I coated plate (BD biosciences) and incubated overnight at 37°C at 5% CO₂. The following day, the cell suspension was counted and equal number of live cells, usually in a limited dilution curve from 10⁵ – 10¹ cells, was added to a fresh 1.5 mL Eppendorf tube together with 2 x 10⁵ irradiated STO cells. The suspension was centrifuged for 4 minutes at 1600RPM in a bench top centrifuge. The cell pellet was resuspended in 50 μL Matrigel, and injected subcutaneously as described in section 2.5.2.2.

2.5.5. Analyses of treatment response

Tumours were measured every 2 - 3 days and tumour volume (mm³) was measured using the Ellipsoidal formula: $\frac{1}{2}(\text{length} \times \text{width}^2)$. The difference between two measurements was then calculated as a percentage increase. Due to variance in tumour size at the start date, usually varying from 5 – 8 mm, the tumour volume at the start date was adjusted to 100 mm³ and the percentage increase was then used to calculate tumour growth. Some tumours were not measureable at the start of treatment, this was observed in the control as well as the treatment groups therefore we concluded that this was a random effect and not due to treatment. Therefore the tumour growth rate was normalized to the same start date as the mice that had measurable tumours at the start of treatment. Once the tumour growth was standardized for each mouse, the tumour volumes were then averaged per treatment group. The growth curves were generated and the error bars represented the standard error of the mean (SEM).

The Kaplan-Meier survival curve was created using Sigmaplot software (Systat Software, Inc), with a dot representing a censored event. This was most likely due to weight loss or inflammation around the tumour. The software provides a 95% confidence interval and a Log-Rank test for statistical analysis.

Tumour initiation frequency was calculated using L-Calc Limited Dilution Analysis Software (StemSoft Software, Inc). This software provided a 95% confidence interval and includes the Pearson's chi-square test for statistical analysis.

Chapter 3

Results I

3. Results I

***In vitro* analysis of interleukin-6 and phosphorylated STAT3, as a potential therapeutic target, in prostate cancer (stem-like) cells**

3.1. IL-6 expression in primary prostate cells

3.1.1. IL-6 mRNA expression in selected populations

Previous work from our laboratory of an expression profile of the $\alpha_2\beta_1^{hi}/CD133^+$ population determined that IL-6 is overexpressed. This study was based on 12 patients with prostate cancer, Gleason grade seven and over and was compared to seven patients with benign disease (Birnie et al., 2008). In order to validate these findings, qRT-PCR was performed on a number of primary cultures derived from patients with benign and malignant disease.

To verify that the cDNA synthesis had worked, especially because of the limited amount of starting RNA from the $\alpha_2\beta_1^{hi}/CD133^+$ population, a standard PCR for GAPDH was performed for the different populations: $\alpha_2\beta_1^{hi}/CD133^+$ (stem-like cells), $\alpha_2\beta_1^{hi}/CD133^-$ (transit amplifying cells) and $\alpha_2\beta_1^{low}$ (committed basal cells), which from now on will be referred to as stem-like, TA and CB. Results are shown for representative samples of primary prostate cells derived from patients with cancer (Gleason 7, Gleason 8, CRPC) and benign disease (Figure 3.1A). The control PCR for GAPDH confirmed that cDNA synthesis was successful for each cell population, and bands were not due to contamination, as the H₂O controls were negative.

The qRT-PCR results demonstrated that IL-6 expression was indeed higher within the stem-like population in Gleason 7 ($P < 0.05$) and Gleason 8 cancers ($P < 0.005$), whereas there was no significant difference in expression between the populations in CRPC and benign disease (Figure 3.1B).

The overall levels of IL-6 expression were low in benign disease, Gleason 7 and CRPC compared to the Gleason 8 sample. However, the results show that within the Gleason 7 samples there was a 1.7-fold increase in IL-6 expression in the stem-like population

compared to the CB population. Furthermore, the Gleason 8 sample showed a 17-fold and 2.3 fold increase, in IL-6 expression in the stem-like and TA population respectively compared to the CB population. Interestingly, the results also show that primary prostate cells derived from a CRPC patient had low or undetectable levels of IL-6.

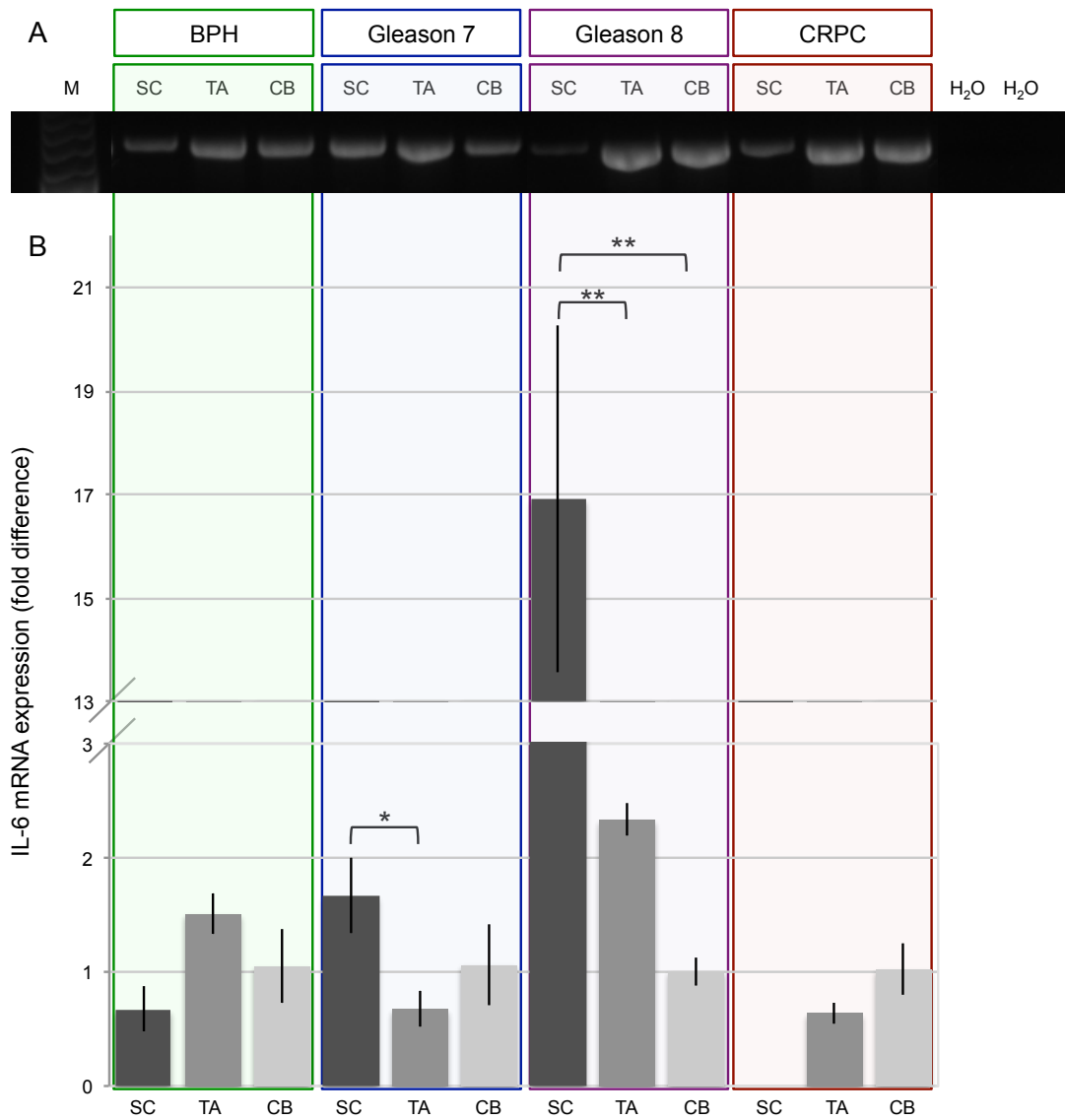


Figure 3.1. **qRT-PCR analysis for IL-6 expression in primary prostate cells.** A. Bands showing controls PCR for GAPDH to check cDNA quality, a 100 bp Marker (M) and negative controls (H_2O) for cDNA synthesis and a second H_2O control was for the PCR cycle. B. Quantification of qRT-PCR of IL-6 expression of a series of primary prostate cell populations (SC (stem-like cells), TA, CB) derived from patients with BPH (green), Gleason 7 (blue) Gleason 8 (purple) and CRPC (red) disease. Only one representative sample is shown for each group. The results are expressed as relative to the housekeeping gene RPLP0 and then normalized to the ΔCt of the CB population, which was set to one. The student's t-test was used to determine differences between each population * $P < 0.05$ and ** $P < 0.005$.

3.1.2. Summary of IL-6 mRNA expression in selected populations of primary prostate cells

Further samples were analysed to confirm the initial findings shown in Figure 3.1B. The results from a further analysis of patients with benign disease (n=5), high Gleason grade hormone naïve cancer (n=5) and CRPC (n=3) confirmed the initial findings (Figure 3.2). In high Gleason grade hormone-naïve cancers (Gleason 7 and above) the more undifferentiated stem-like and TA cells had an average of ~30 fold change in IL-6 mRNA expression, which was 6-fold higher compared to the more differentiated CB cells (~5 fold change), although this data was not significant which was likely due to patient variability. As indicated by the different symbols, each patient showed a distinct pattern: high IL-6 expression in the undifferentiated stem-like population and lower IL-6 expression in the more differentiated CB population. In contrast, the pattern of high IL-6 expression in the undifferentiated cells was not observed in cells derived from benign disease or CRPC, and the IL-6 mRNA expression levels were overall lower compared to that observed in high Gleason grade hormone-naïve cancers. This implies that IL-6 plays an important role in cancer and specifically the more undifferentiated stem-like cells within this disease, although these IL-6 expression levels needed to be confirmed at the protein level.

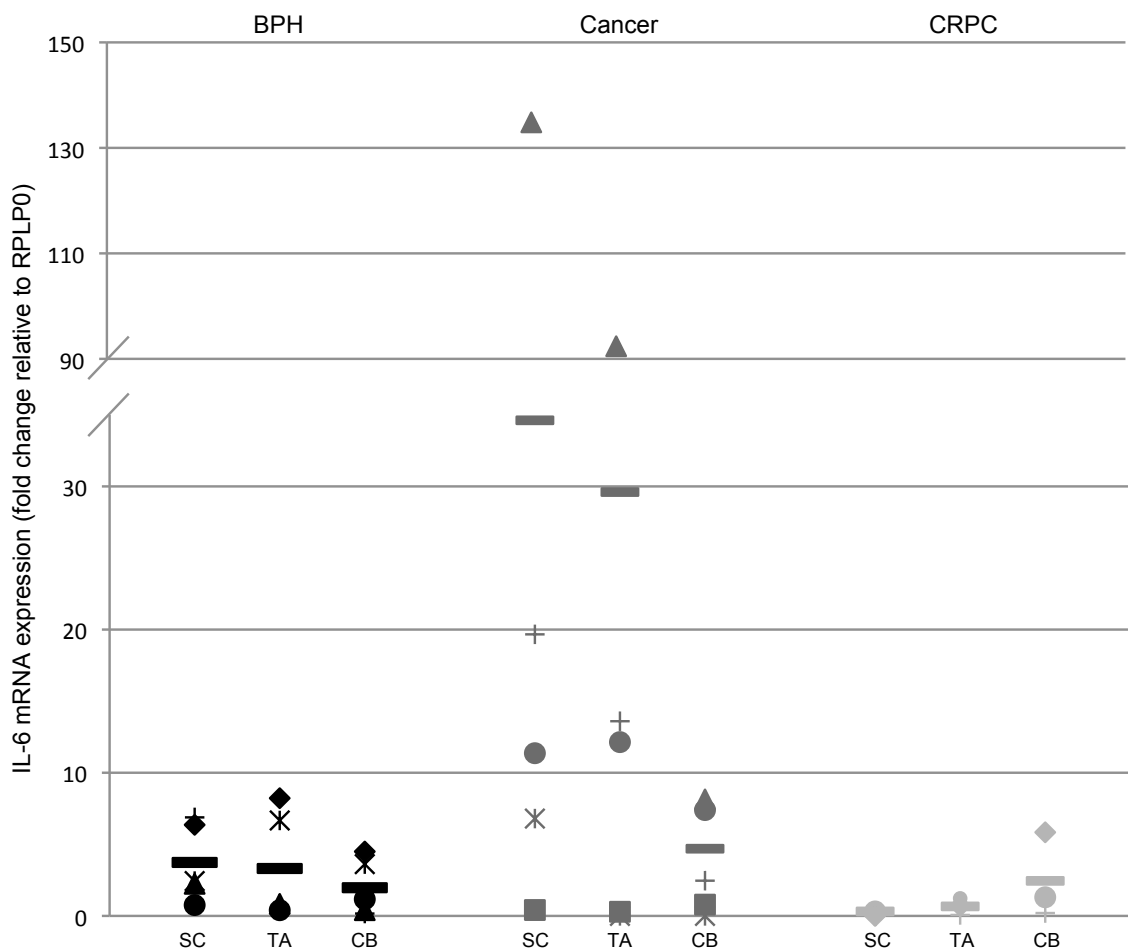


Figure 3.2. **Overall results of IL-6 mRNA expression in a series of primary prostate cancer and benign cultures.** qRT-PCR of IL-6 expression on selected stem-like cell (SC), TA and CB cells derived from patients with benign disease (n=5) (black), high Gleason grade hormone-naïve cancer (n=5) (grey) and CRPC (n=3) (light grey). The results are expressed as relative to the housekeeping gene RPLP0 and the fold difference is normalised to the average Ct-value of the CB population from benign samples. Each symbol represents a different patient and the bar represents the average within each group.

3.1.3. IL-6 protein expression in selected populations

3.1.3.1. Levels of secreted IL-6 in selected populations of primary prostate cells, using ELISPOT assay

As IL-6 is a secreted protein, the ELISPOT assay was used. This method is able to identify the levels of IL-6 secretion at a single cell level. So, this method is very sensitive, which is important when working with the rare stem-like population. The number of cells secreting IL-6 is determined by counting the number of spots and the amount of IL-6 secreted is determined by spot size.

Firstly, the method needed to be optimized; this was done using lymphocytes in the presence of 1 µg/mL LPS to stimulate IL-6 production. The lymphocytes were plated onto PVDF-bottom plates, pre-labelled with capture IL-6 antibody, at a cell density range from 100 - 100,000 cells per well, to determine the optimal cell number. The results showed that at least 1000 - 10,000 lymphocytes were required (Figure 3.3A). As the lymphocytes were stimulated with LPS to produce IL-6 it was probable that most cells produced IL-6. However, with primary prostate cells, we wanted to determine the basal levels of secreted IL-6 from the selected primary prostate cells. Therefore, a density of 10,000 cells/well was chosen, as it was likely that not all cells would secrete IL-6. Unfortunately this cell number was not achievable for the stem-like population and all cells obtained from cell selections were plated. As the cell number could not accurately be determined the cell number was not known. It was obvious that within the TA population more cells secreted IL-6 as more spots were observed compared to the CB population; some spots were also bigger suggesting that the amount of IL-6 per cell was also higher (Figure 3.3B). Unfortunately the software was not able to distinguish between small spots and background; therefore the results were not accurate. Also the number of stem-like cells was unknown and there were not enough spots to count which meant that this population could not be taken in account when the results were analysed. Therefore it was decided that this method was not sensitive enough to determine the levels of secreted IL-6 in selected primary prostate cells.

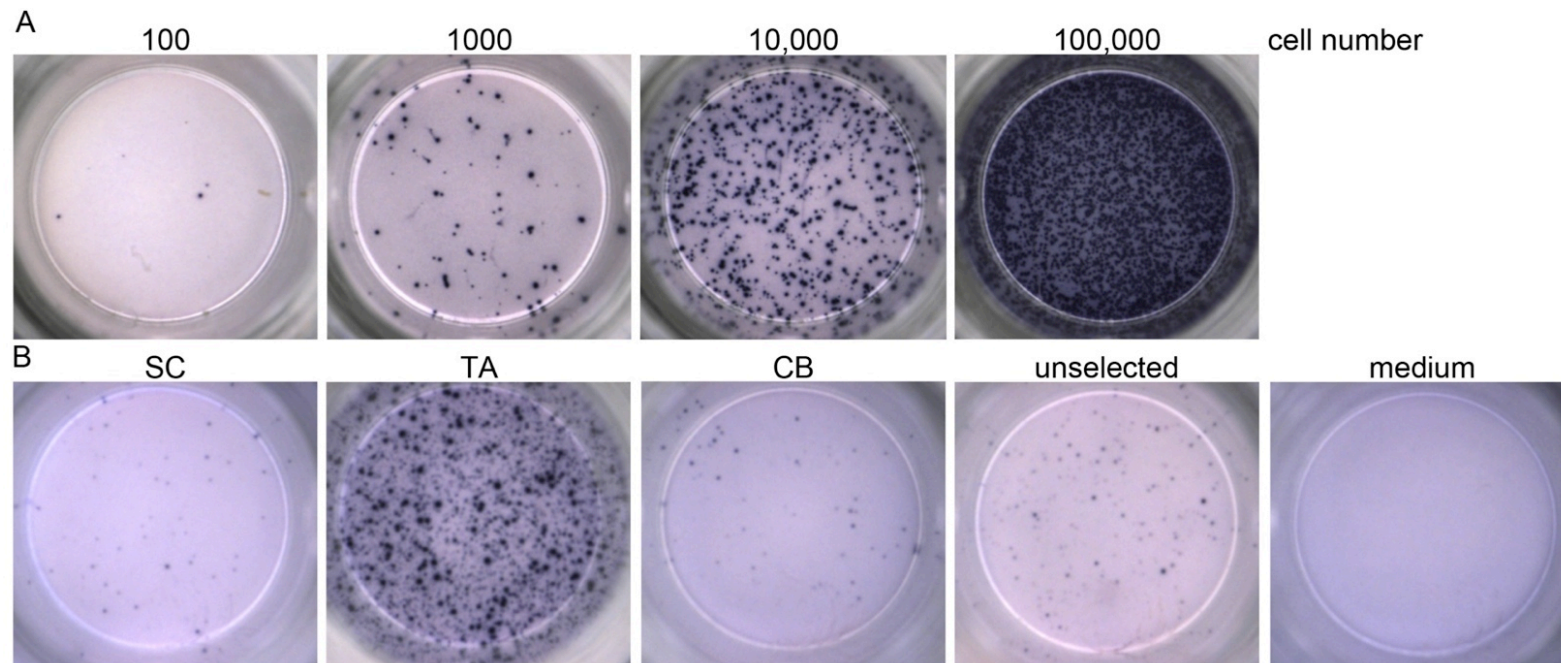


Figure 3.3. **Levels of secreted IL-6 in selected populations of primary prostate cells, using ELISPOT.** A. To determine the sensitivity of the ELISPOT assay, lymphocyte cells were plated down, in the presence of 1 $\mu\text{g}/\text{mL}$ LPS, at a density range from 100 - 100,000 cells/well. B. Representative (n=6) of primary prostate cells, derived from a cancer sample (Gleason 3+4), were selected for stem-like (SC), TA and CB cells and plated down at a density of 10,000 cells/well. Due to low yield, the cell number for the stem-like population was unknown. Controls included unselected cells and a medium control. Cells were plated down on in a PVDF-bottomed-plate pre-coated with human IL-6 capture antibody and secreted levels of IL-6 were analysed using ELISPOT assay. This data was obtained during my undergraduate project (Sept. 2007 – May 2008).

3.1.3.2. Levels of secreted IL-6 in selected populations of primary prostate cells, using ELISA

3.1.3.2.1. Optimization of the High Sensitivity Human IL-6 ELISA

Normally a commercially available ELISA has a standard range from 0 - 300 pg/mL and is used to determine the levels of cytokine from stimulated cells. As we wanted to measure the levels of IL-6 from selected, un-stimulated primary prostate cells, this assay would not have been sensitive enough. Therefore, a High Sensitivity ELISA was used, which has a standard range from 0 - 10 pg/mL and would normally be used for low levels of secreted cytokine, but in this case could also be used to determine the levels from low cell numbers.

Firstly it was important to determine the optimal cell number, hence primary prostate cells were plated at low density (500 – 2500 cells). Following 48 hours' incubation, the conditioned medium was collected and the levels of IL-6 determined by HS ELISA. As shown in Figure 3.4, as few as 500 cells were enough to analyse the levels of secreted IL-6. As the number of cells that secrete IL-6 might vary between samples, it was decided that 1000 cells should be the minimum required to accurately determine IL-6 levels. This density was used in the following experiments.

3.1.3.2.2. HS ELISA for IL-6 on selected populations of primary prostate cells

Conditioned medium from selected stem-like, TA and CB cells from primary prostate cells were analysed for IL-6 from patients with benign disease, hormone-naïve cancer and CRPC. The results show that the stem-like cells from a high Gleason grade hormone-naïve cancer had higher levels of secreted IL-6 compared to the TA and CB populations (Figure 3.5). This pattern was also observed in the CRPC sample, although the levels of IL-6 were lower compared to the hormone-naïve cancer sample. The levels of secreted IL-6, from the patient with benign disease, did not follow this pattern of high IL-6 from the more undifferentiated cells, and the IL-6 levels were also lower compared to the cancer sample. It was also confirmed that STO feeder cells did not secrete detectable levels of IL-6. These initial results were interesting and further samples were analysed to confirm this trend.

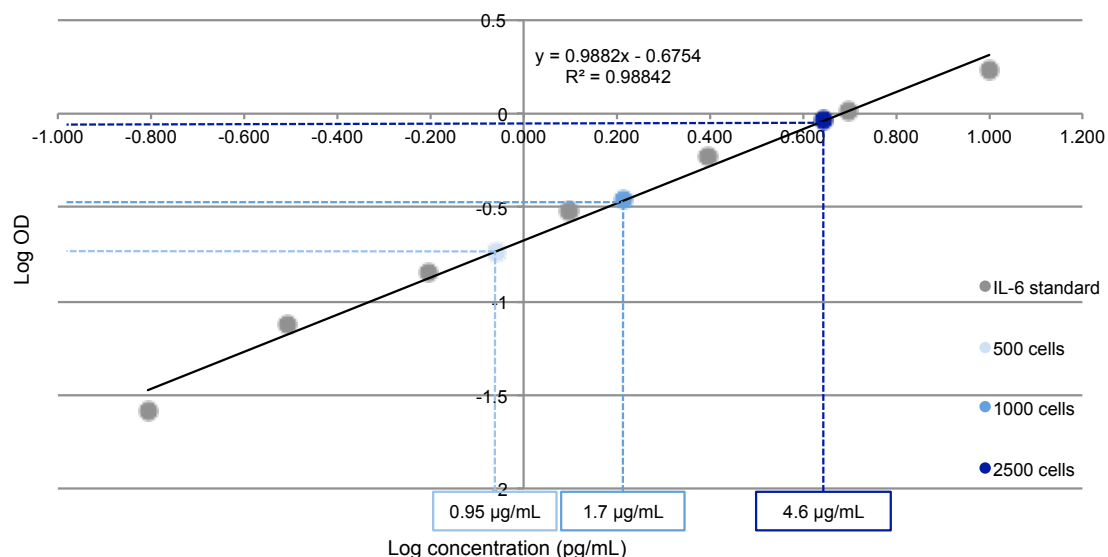


Figure 3.4. **Optimisation of ELISA assay to analyse levels of secreted IL-6.** The standard range of the High Sensitivity human IL-6 ELISA was from 0 - 10 pg/mL. Primary prostate cells were plated down at a density of 500, 1000 and 2500 cells per well in a collagen-I coated 96-well plate in the presence of irradiated STO feeder cells. After 48 hours incubation, cell medium was collected and analysed for levels of secreted IL-6. The log scale showed that conditioned medium, collected from 500 - 2500 cells was sufficient and was within the range of the standard curve. STO feeder cells, and cell-free medium were used as negative controls and had undetectable levels of IL-6.

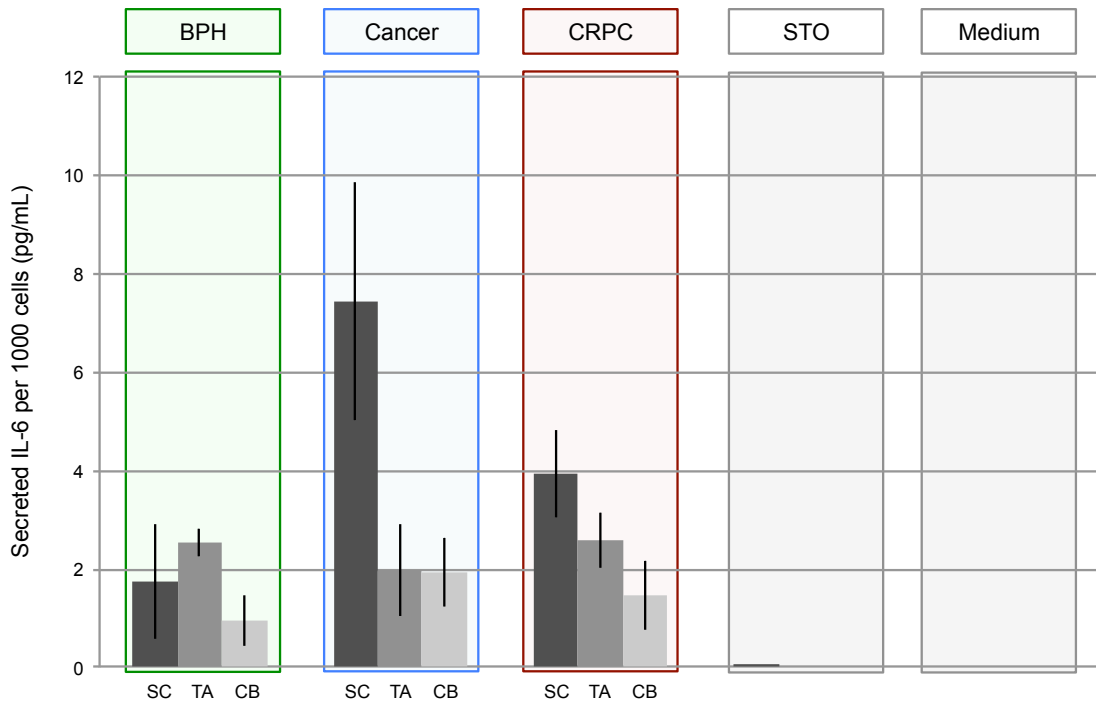


Figure 3.5. **IL-6 levels from conditioned medium of primary prostate cell cultures.** Representative samples from primary prostate cell cultures derived from benign disease (green), hormone-naïve cancer (blue) and CRPC (red). Samples were selected for stem-like (SC), TA and CB cells and were plated down at a density of 1000 cells per well in a collagen-I coated 96-well plate in the presence of irradiated STO feeder cells, STO feeder cells only or medium only were included as negative controls. After 48 hours, the conditioned medium was collected and the levels of IL-6 were analysed using a High Sensitive Human IL-6 ELISA. Levels of IL-6 are shown in pg/mL and the error bars represent the standard deviation from triplicate samples of conditioned medium.

3.1.3.2.3. Analysis of secreted IL-6 levels from a series of primary prostate cell cultures

Further analysis of IL-6 levels from a series of primary cell cultures (benign disease (n=6), hormone-naïve cancer (n=8) and CRPC (n=3)) confirmed the previous results and showed that the more undifferentiated stem-like and TA cells (from the hormone-naïve samples) had an average of 4-fold higher IL-6 levels compared to the more differentiated CB cells, which was statistically significant ($P < 0.05$). The undifferentiated stem-like and TA cells from CRPC samples showed 3-fold higher IL-6 expression compared to the more differentiated CB cells, although this was not statistically significant due mostly to patient variability and the limited number of samples that were analysed. The undifferentiated TA cells, but not stem cells, from benign disease, showed 2-fold higher IL-6 expression compared to the more differentiated CB cells although overall levels of IL-6 expression were lower compared to the hormone-naïve cancers and CRPC (Figure 3.6).

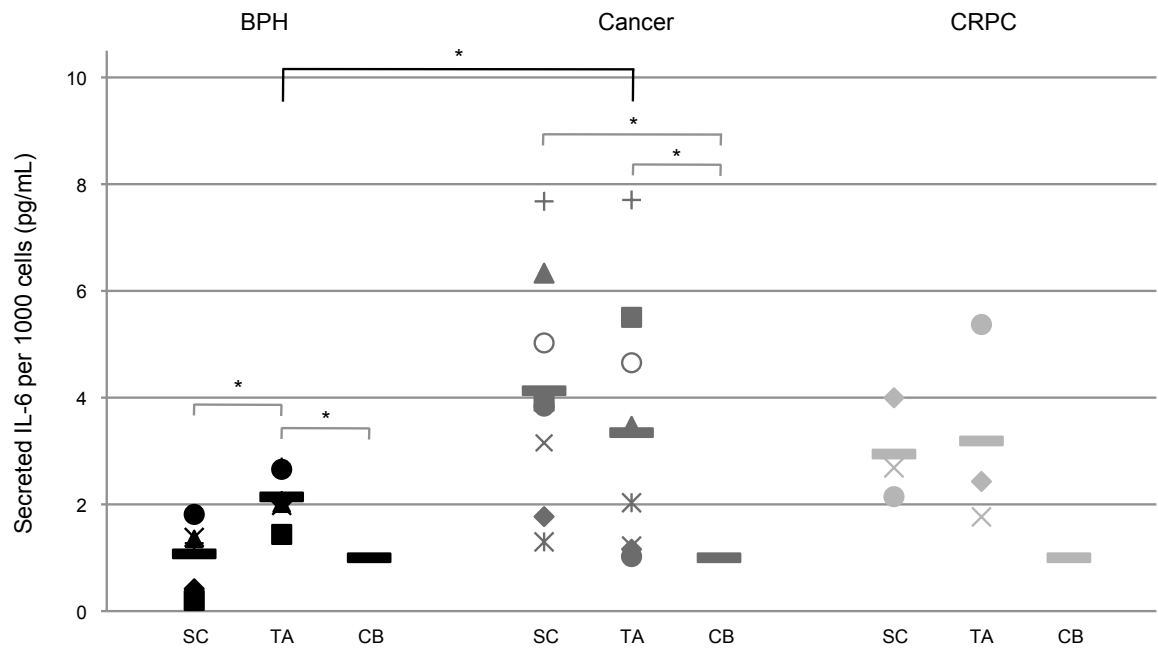


Figure 3.6. **Overall results of IL-6 levels in a series of primary prostate cancer and benign cultures.** Overall results of ELISA analysis for secreted IL-6 levels using conditioned medium collected after 48 hours incubation from 1000 pre-selected stem-like (SC), TA and CB cells. Cells were from primary prostate cell cultures derived from benign disease (n=6) (black), hormone-naïve cancer (n=8) (grey) and CRPC (n=3) (light grey). Levels of IL-6 are in pg/mL and levels are represented relative to the CB cells within each individual sample, which is represented using different symbols and a bar represents the average within each group. Statistical analysis was performed using the student's t-test, $P^* < 0.05$.

3.2. IL-6 receptor expression in primary prostate cells

3.2.1. IL-6 receptor expression in prostate cell lines by Western blot

As shown in section 3.1.3.2.3, IL-6 is more highly expressed in the undifferentiated stem-like and TA cells derived from prostate cancer samples. Therefore it is possible that these cells require IL-6, via an autocrine signaling pathway, for the maintenance of their undifferentiated phenotype. In order for IL-6 to activate the associated JAK-STAT signaling pathway, the IL-6 specific receptor, gp80 is required.

To confirm the presence of IL-6 receptor gp80, Western blot analysis was used initially, on an unselected population of prostate epithelial cells. As a positive control for this experiment, a number of prostate cell lines known to express the receptor were used. The results showed that 3 out of 5 prostate cell lines expressed the IL-6 specific receptor (Figure 3.7A), but the receptor was not detected in any of the primary cells analyzed (results not shown). As the IL-6 receptor is a large membrane protein, urea gels were used to denature the protein, but again the receptor was not detected by this method (Figure 3.7B).

As the receptor is known to be present in prostate tissue (Hobisch et al., 2000) a different method was used to verify these results.

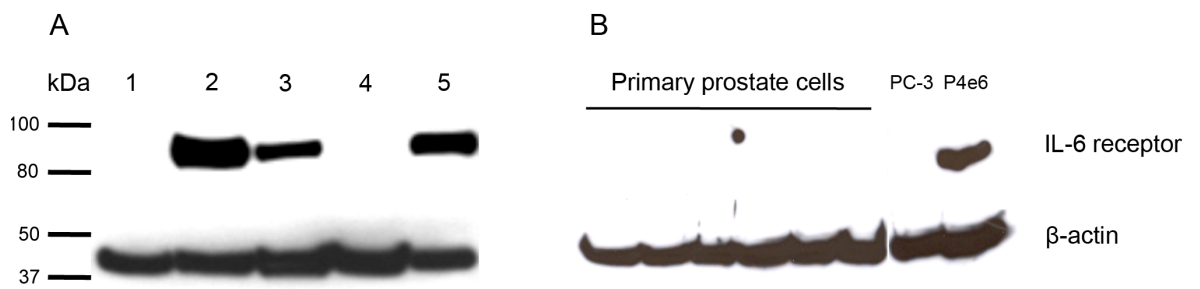


Figure 3.7. **IL-6 receptor expression in prostate cell lines and primary prostate cells, by Western blot.** Western blot analysis for the IL-6 receptor (gp80) and β -actin (loading control) in prostate cell lines: (1) PNT1a, (2) PNT2-C2, (3) P4E6, (4) PC-3 and (5) LNCaP (A) and a panel of primary prostate cells (B). PC-3 cells were included in panel B as a negative control and P4E6 cells as a positive control, the samples in the panel B were loaded onto a urea SDS-page gel.

3.2.2. IL-6 receptor expression in benign prostate tissue

3.2.2.1. Immunohistochemistry for IL-6 receptor

Immunohistochemistry was performed to confirm the presence of the IL-6 receptor in prostate tissue (Hobisch et al., 2000). As benign prostate tissue has a very organized structure, the different cell types were apparent after H&E staining was performed, which revealed the organized structure of prostate stromal cells surrounding the acini, which contain basal and luminal cells (Figure 3.8A) (McNeal, 1981). The immunohistochemical staining for the IL-6 receptor gp80 showed that all the secretory luminal cells expressed the receptor, but with a focal expression in the basal cells, although this was not very obvious from the DAB staining (Figure 3.8B). Pancytokeratin was used as a positive control to show that the technique had worked and the IgG negative control showed that the staining was specific for the IL-6 receptor (Figure 3.8C/D).

3.2.2.2. Immunofluorescence for IL-6 receptor

Immunofluorescence staining was used to get a clearer image of the basal cells expressing the IL-6 receptor. Benign prostate tissue was used, as here the basal and luminal cells are clearly defined, as shown in Figure 3.8A. Sections were co-stained with cytokeratin-5 (CK5) to define the basal cells (Sherwood et al., 1991). The images shown in Figure 3.9 confirmed that the luminal cells express the IL-6 receptor with focal expression in rare basal cells (Figure 3.9). Most of the basal cells, indicated by the cells positive for CK5, did not express the IL-6 receptor. However, rare IL-6 receptor expressing cells within the basal layer were indicated by co-expression (orange) of CK5 (red) and IL-6 receptor (green) (white arrow in Figure 3.9C). The level of staining was analyzed relative to the IgG control (Figure 3.9D).

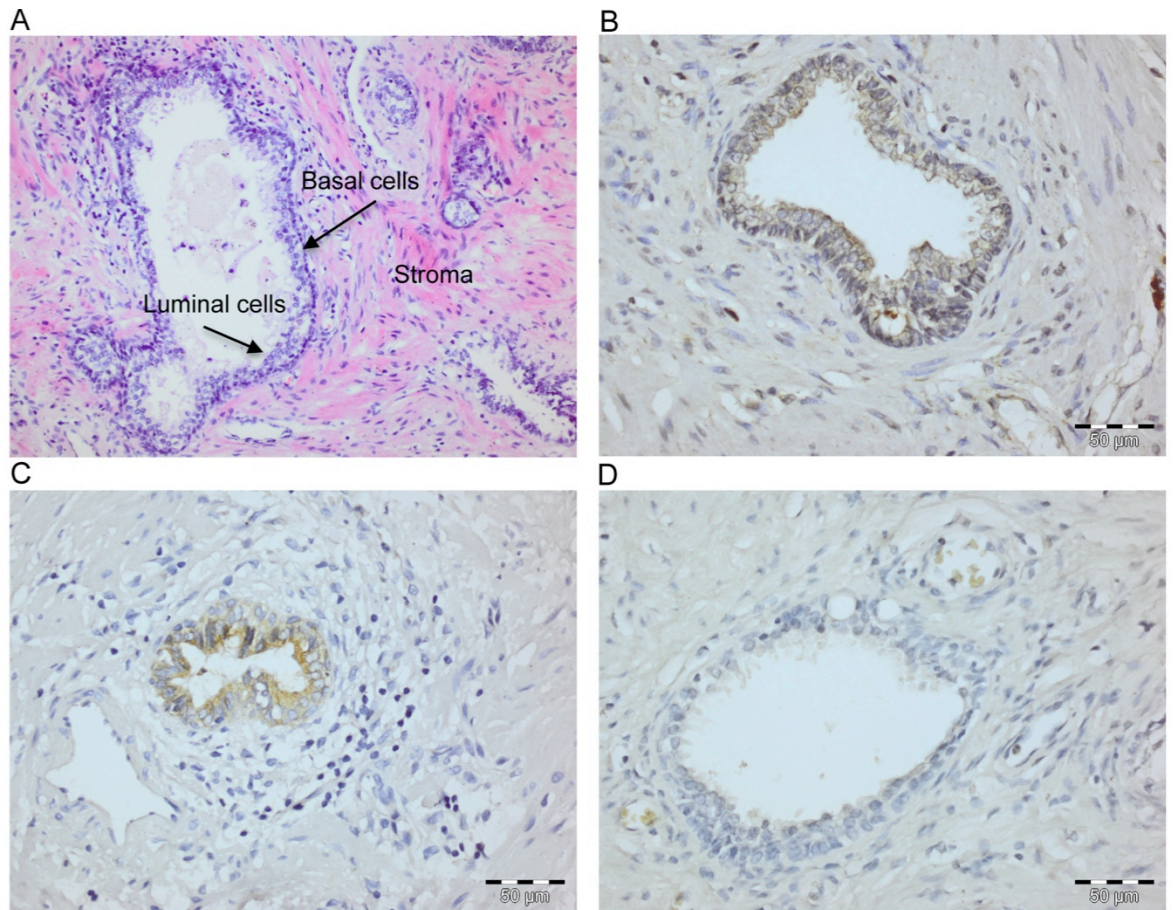


Figure 3.8. **IL-6 receptor staining of BPH paraffin embedded tissue sections.** A. H&E staining of a paraffin-embedded tissue section showing the structure and different cell types (basal, luminal and stromal cells) within benign prostate tissue. Benign prostate tissue section stained with anti-IL-6 receptor (B), pancytokeratin (C) and an isotype IgG negative control (D). Images were taken using an Olympus BX51 light microscope at 20x (A) or 40x magnification (B-D).

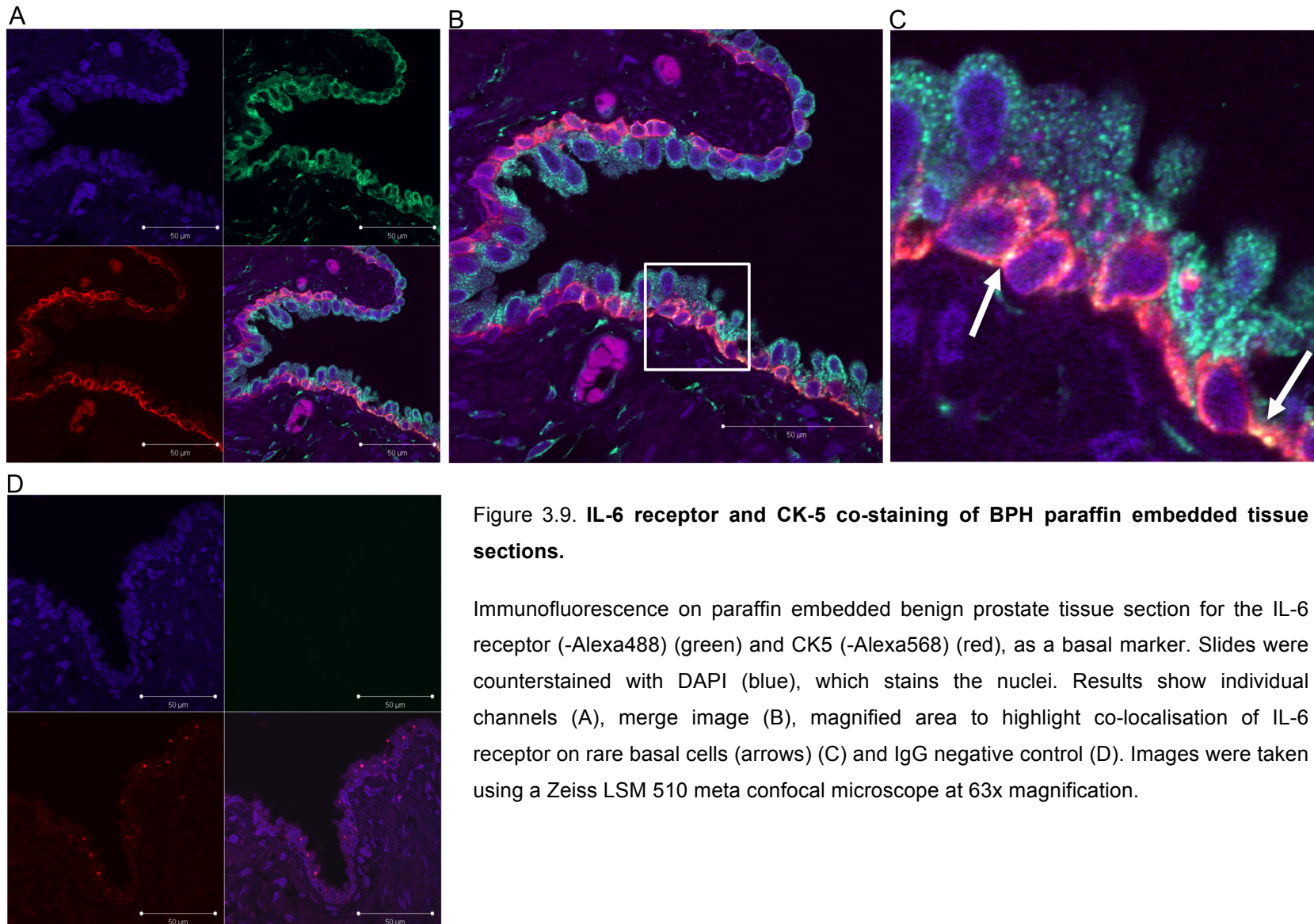


Figure 3.9. IL-6 receptor and CK-5 co-staining of BPH paraffin embedded tissue sections.

Immunofluorescence on paraffin embedded benign prostate tissue section for the IL-6 receptor (-Alexa488) (green) and CK5 (-Alexa568) (red), as a basal marker. Slides were counterstained with DAPI (blue), which stains the nuclei. Results show individual channels (A), merge image (B), magnified area to highlight co-localisation of IL-6 receptor on rare basal cells (arrows) (C) and IgG negative control (D). Images were taken using a Zeiss LSM 510 meta confocal microscope at 63x magnification.

3.2.3. Leukemia Inhibitory Factor receptor expression in benign prostate tissue

The JAK-STAT signaling pathway can be activated through a number of ligands and their receptors. The most studied receptors other than IL-6 and the IL-6 specific receptor gp80, which can activate the pathway, are LIF and OSM receptors. Therefore it was important to test for the expression of these receptors in prostate tissue. Immunohistochemical staining showed that the LIF receptor was only expressed on the secretory luminal cells within benign tissue, and not the basal cells (Figure 3.10A). The positive control, pancytokeratin and the IgG negative control showed that the staining was specific (Figure 3.10B/C).

Staining for the OSM receptor was attempted using the same technique on benign prostate tissue sections. However, despite using several different antibodies and a positive control (HeLA cells), staining for the OSM receptor was not observed on prostate tissue and a recommended positive control; HeLa cells (results not shown).

As the LIF receptor appeared to be exclusively expressed on the secretory luminal cells, no further investigation was performed for the LIF receptor, as it was unlikely that selected basal cells (stem-like, TA and CB) would express the LIF-receptor. Therefore, the focus of this study was on IL-6 and the IL-6 receptor. Further investigation on the selection cell populations was then undertaken.

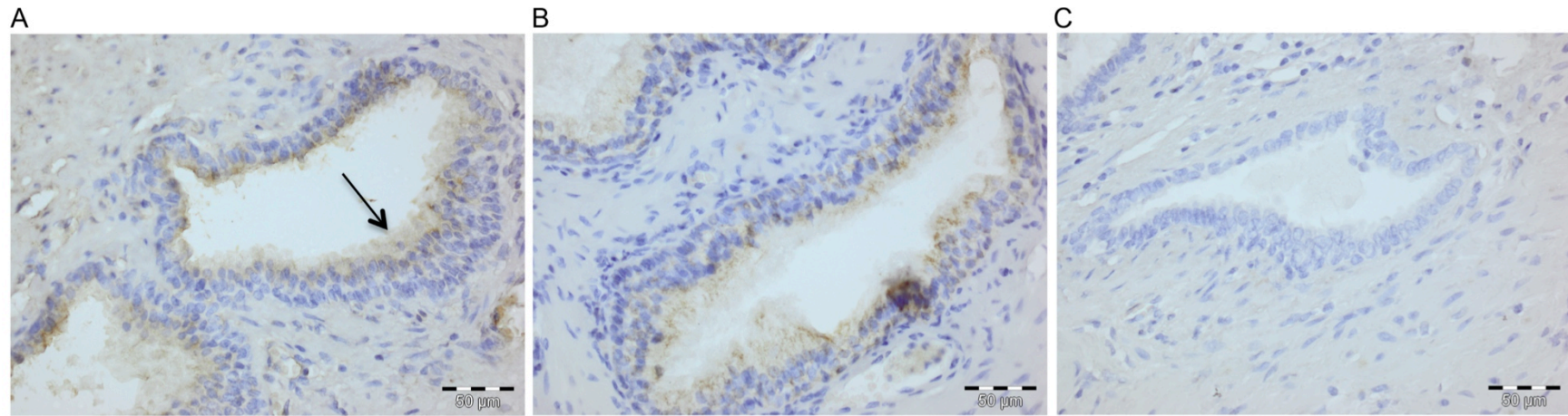


Figure 3.10. **LIF receptor staining of BPH paraffin embedded sections.** Immunohistochemistry on paraffin embedded benign prostate tissue section for the LIF receptor (A), pancytokeratin (B) and an isotype IgG negative control (C). LIF receptor staining was confined to the luminal cells indicated by the black arrow. Images were taken using an Olympus BX51 light microscope at 40x magnification.

3.2.4. IL-6 receptor expression on selected primary prostate cells

3.2.4.1. Immunofluorescence staining for IL-6 receptor

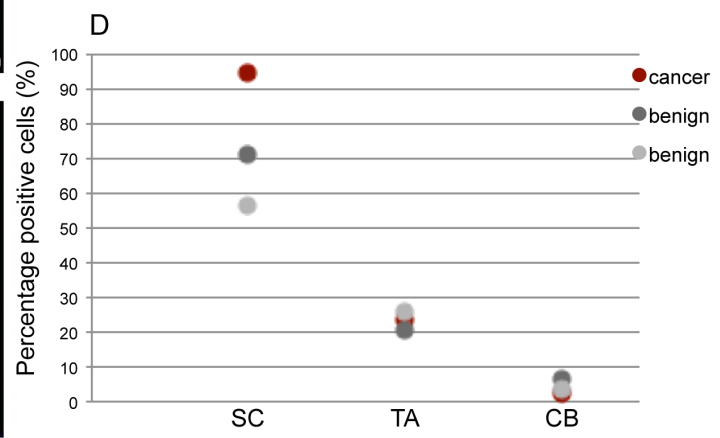
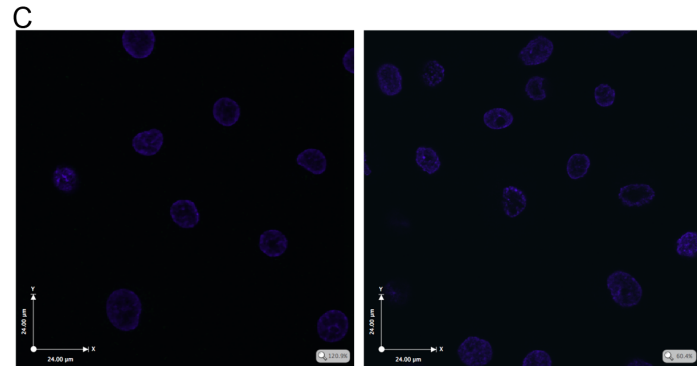
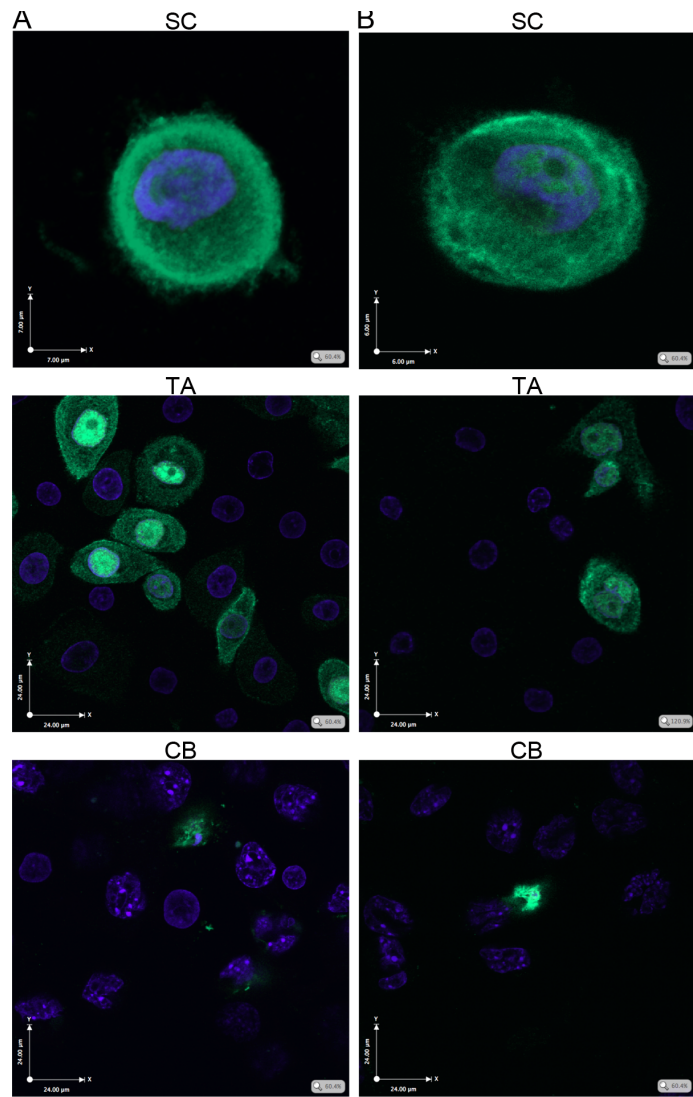
Immunofluorescence of prostate tissue sections showed that rare cells within the basal layer express the IL-6 specific receptor (gp80) (Figure 3.9C). However, prostate cancer tissue is disorganized, and consists of 99% luminal cells and 1% basal cells. Because we are mainly interested in the stem-like, TA and CB cells, which are all located within the basal compartment, immunohistochemical analysis would not be appropriate to detect the IL-6 receptor in tissue sections from a cancer sample due to the limited basal cell numbers.

To determine if the stem-like, TA and CB cells, which reside within the basal cell layer, express the receptor, immunofluorescent staining was performed on selected cells from short-term primary cultures derived from patients' samples. Although the basal cells are rare within prostate cancer tissue, in primary cultures, the basal cells expand, whilst the secretory luminal cells cannot be cultured (Peehl, 1992). Thus, the different cell types (stem-like, TA and CB cells) can be selected from cell cultures and stained, by immunofluorescence, for the IL-6 receptor gp80.

As the receptor is a plasma membrane-bound protein, we used a live-cell staining technique to determine receptor expression on the cell surface of live cells. The results show that ~60 - 95% of the stem-like cells derived from prostate cancer and benign disease, express the IL-6 receptor (Figure 3.11D). However, the TA and CB cells also express the receptor, but to a lesser extent (~20 and <10% respectively). Quantification of cells expressing the receptor show that IL-6 receptor expression reduced with differentiation (Figure 3.11D). There was no observed difference in the intensity of staining i.e. the amount of IL-6 receptors per cells.

Although the pattern of IL-6 receptor expression was similar between the different disease stages, the results did suggest that there was a higher percentage of stem-like cells, derived from patients with prostate cancer, that expressed the IL-6 receptor compared to stem cells derived from patients with benign disease, >90% relative to ~60 - 70%.

Figure 3.11. IL-6 receptor staining on selected cells from primary prostate cultures. Immunofluorescence for the IL-6 receptor on selected stem-like (SC), TA and CB cells, from primary prostate cell cultures derived from cancer (A) and benign disease (B). IgG negative control for cancer (left) and benign cells (right) (C). Cells were counterstained with DAPI to stain the nuclei before analysis on a Zeiss LSM 510 meta confocal microscope at 63x magnification. D. Quantification of Immunofluorescence for the IL-6 receptor on selected cells (stem-like, TA and CB) from primary cultures derived from prostate cancer (n=1) (red) and benign disease (n=2) (grey). Cells were counterstained with DAPI before counting 10 random fields at 63x magnification for the number of IL-6 receptor-expressing cells relative to total cells per field. Cells were scored by eye and intensity levels were relative to the IgG control. All the stem-like cells were counted due to small cell numbers. The results are expressed as the percentage of positive cells per population.



3.2.4.2. Flow cytometry analysis for IL-6 receptor

To confirm the IL-6 receptor expression in a quantitative manner, flow cytometry was used. Primary cultures were co-stained with antibodies to the IL-6R, CD49b, which marks the α_2^{hi} population that includes both the stem-like and TA cells (Collins et al., 2001), or CD133, which is a marker of stem cells.

The results of three primary cultures (from three individuals) showed that an average of 44% of cancer cells (range 29.45 – 46.54%), expressed CD49b (Figure 3.12A). These levels are similar when α_2^{hi} and α_2^{low} cells are separated by rapid collagen-I adhesion (Table 4).

Table 4. Percentage of α_2^{hi} and α_2^{low} cells from several primary prostate cancer cell cultures.

Primary prostate cells	α_2^{hi} cells (%)	α_2^{low} cells (%)
Gleason 7 (3+4)	49.1	50.9
Gleason 7 (4+3)	31.3	68.7
Gleason 9 (4+5)	65.1	34.9
Gleason 9 (4+5)	34.9	65.1
CRPC	59.9	40.1

Only a small percentage of these CD49b-positive cells (2.3%) expressed the receptor. However, those cells did not express CD133 (Figure 3.12). Indeed, all the cells expressing the receptor were not CD133 positive, by flow cytometry (Figure 3.12B). These results are in contrast to the immunofluorescence study of sorted cell populations (Figure 3.11) in which the CD133 population expressed the highest levels of receptor. Nonetheless, a small percentage of the α_2^{hi} population did express the receptor and these cells have been previously shown to encompass the stem cells and transit amplifying population (Collins et al., 2001).

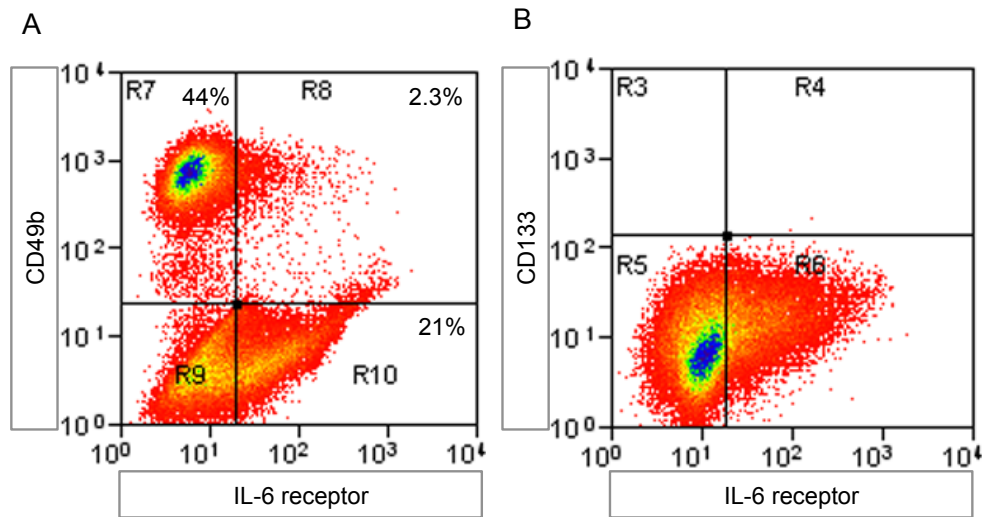


Figure 3.12. **Flow cytometry analysis for the IL-6 receptor, CD49b and CD133 on primary prostate cells.** Representative dot-plots, of three primary cultures, labelled with IL-6 receptor (-Alexa488), CD49b (-PE) and CD133 (-APC). A. Dual labelling with CD49b and FITC. B. Dual labelling with IL-6 receptor and CD133. Due to spectral overlap of the FITC detector into the PE detector, compensation was performed between single labelled samples and unlabelled to minimize the effect when analysing cells that were dual labelled for IL-6 receptor (-Alexa488) and CD49b (-PE). Analyses were performed relative to the IgG control and Sytox Blue was used to exclude dead cells.

The results shown in Figure 3.12 indicate that CD133 is not expressed in prostate cultures. However, this is not the case as single labeling with CD133 does detect a rare population (Figure 3.13). It was often observed that co-labelling with other cell surface markers 'quenched' the detection of CD133.

To exclude this possibility, primary prostate cells were pre-selected, using rapid adhesion to type I collagen, to select for $\alpha_2\beta_1^{\text{hi}}$ and $\alpha_2\beta_1^{\text{low}}$ cells, instead of labeling the cells with CD49b antibody. Cells were subsequently labeled with antibodies to CD133 and the IL-6 receptor. A representative dot-plot, of four primary cultures (from four individuals), confirmed that a small proportion of cells that rapidly adhere to type I collagen (2%) express the receptor, but unlike the previous observation (Figure 3.12) they do express CD133. These results also confirm the results shown in Figure 3.12 in which 22% of the $\alpha_2\beta_1^{\text{low}}$ cells and only 2% of the $\alpha_2\beta_1^{\text{hi}}$ cells express the IL-6 receptor (Figure 3.14A/B).

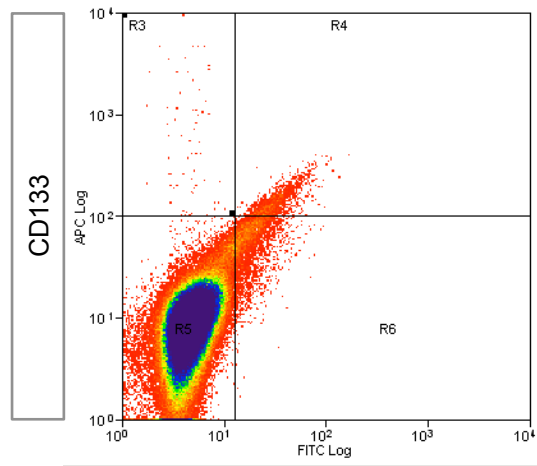


Figure 3.13. **Flow cytometry analysis for CD133 on primary prostate cancer cells.** Representative dot-plot of primary prostate cancer cells single labelled for CD133 (-APC) (y-axis). Analyses were performed relative to the IgG control and sytoxblue was used to exclude dead cells.

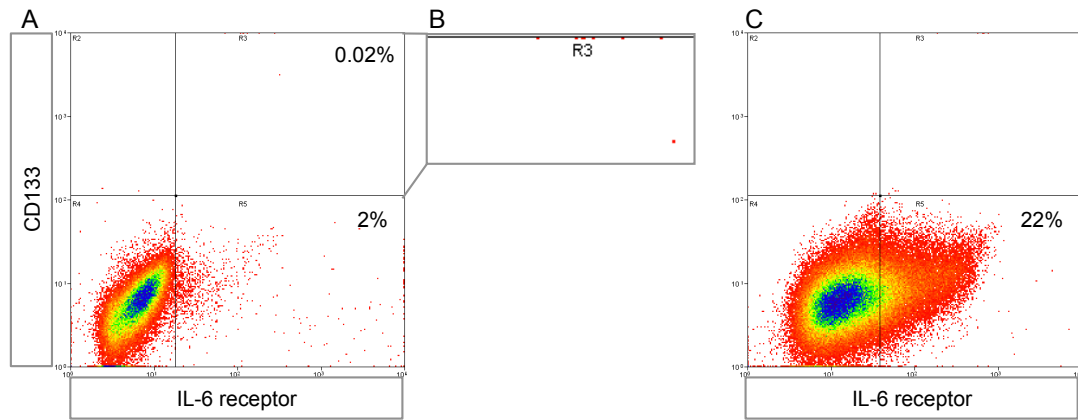


Figure 3.14. **Flow cytometry analysis for the IL-6 receptor and CD133 from pre-selected $\alpha_2\beta_1^{\text{hi}}$ and $\alpha_2\beta_1^{\text{low}}$ cells.** Representative dot-plots, of four primary cancer cultures, pre-selected by adherence to collagen-I. Non-adherent cells were selected after 20 minutes adherence to type 1 collagen and the adherent fraction was harvested by trypsin at the same time. Both fractions were then labelled with CD133 (-APC) and IL-6 receptor (Alexa-488). A. $\alpha_2\beta_1^{\text{hi}}$ cells labelled for IL-6 receptor (-Alexa488) and CD133 (-APC). B. Magnified area to highlight rare high-expressing CD133 positive cells that co-expressed the IL-6 receptor. C. $\alpha_2\beta_1^{\text{low}}$ cells labelled for IL-6 receptor (-Alexa488). Analyses were performed relative to the IgG control and sytoxblue was used to exclude dead cells.

3.3. Activation of the JAK-STAT signaling pathway

3.3.1. STAT3 phosphorylation in primary prostate cells

IL-6 signals through a receptor composed of two subunits: the common gp130 receptor, shared with the other IL-6 family cytokines, and the IL-6 specific receptor gp80. Binding of IL-6 to the IL-6 receptor induces gp130 homodimerization, followed by activation of JAK, and the cytoplasmic tail of gp130 becomes phosphorylated which creates docking sites for STAT factors, which subsequently become phosphorylated, form dimers and translocate to the nucleus (Heinrich et al., 1998). Signalling by IL-6 generally induces STAT3 phosphorylation, and it has been shown that STAT3 is constitutively active in prostate cancer cells lines and in prostate cancer tissue, using immunohistochemical staining (Dhir et al., 2002; Mora et al., 2002).

In order to determine whether the JAK-STAT signaling pathway is activated in primary prostate cells, derived from cancer and benign disease, the levels of phosphorylated STAT3 (Tyr705) was determined by Western blot analysis. Results show that all the primary prostate cell cultures that were analyzed, 2 benign and 5 cancer samples, had detectable levels of pSTAT3 (Figure 3.15A), suggesting that the pathway is constitutively active. The levels of pSTAT3 were quantified relative to total STAT3, and confirmed that 3 of the 5 primary prostate cancer samples had higher levels of pSTAT3 compared to the benign cells (Figure 3.15B).

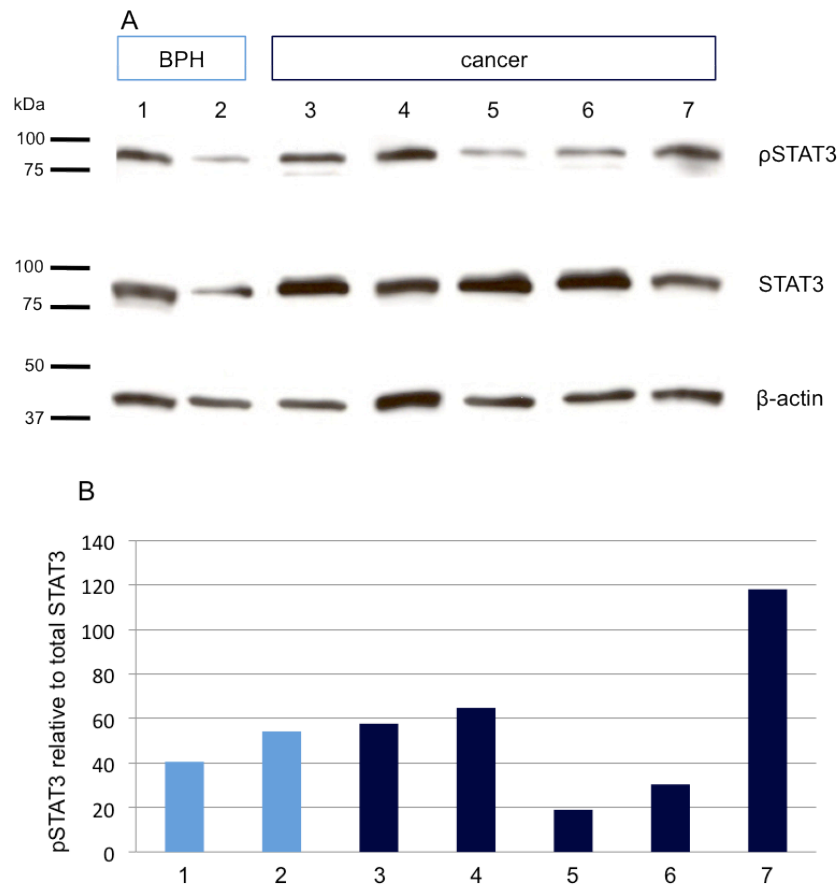


Figure 3.15. Levels of phosphorylated STAT3 in primary prostate cells. A. Western blot analysis for pSTAT3, total STAT3 and β -actin (loading control) on primary cell culture lysates derived from benign disease (n=2) and cancer (n=5). B. Quantification of Western blot, the results are expressed as levels of pSTAT3 relative to total STAT3 (benign; light blue bar and cancer; dark blue bars). Analysis was performed using Image-J software.

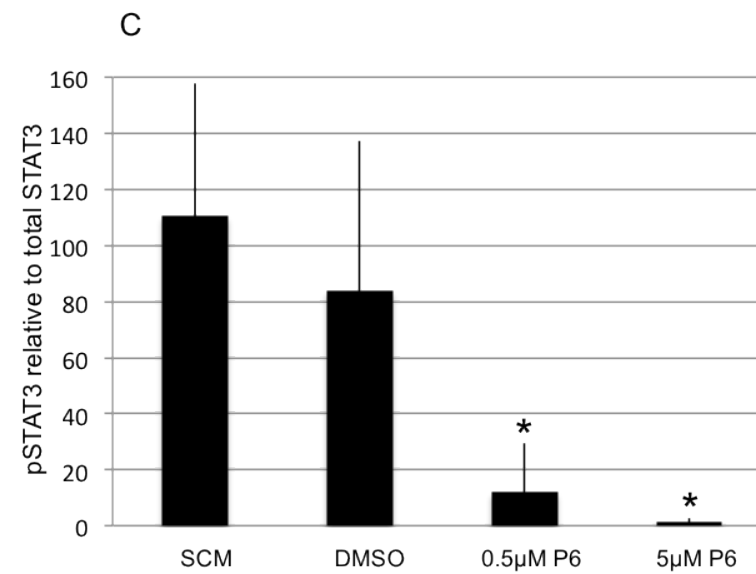
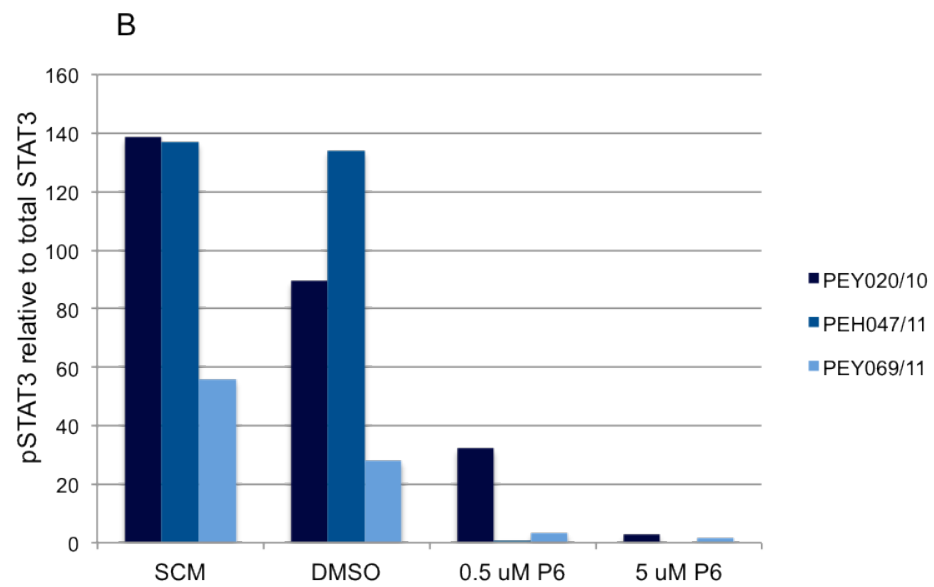
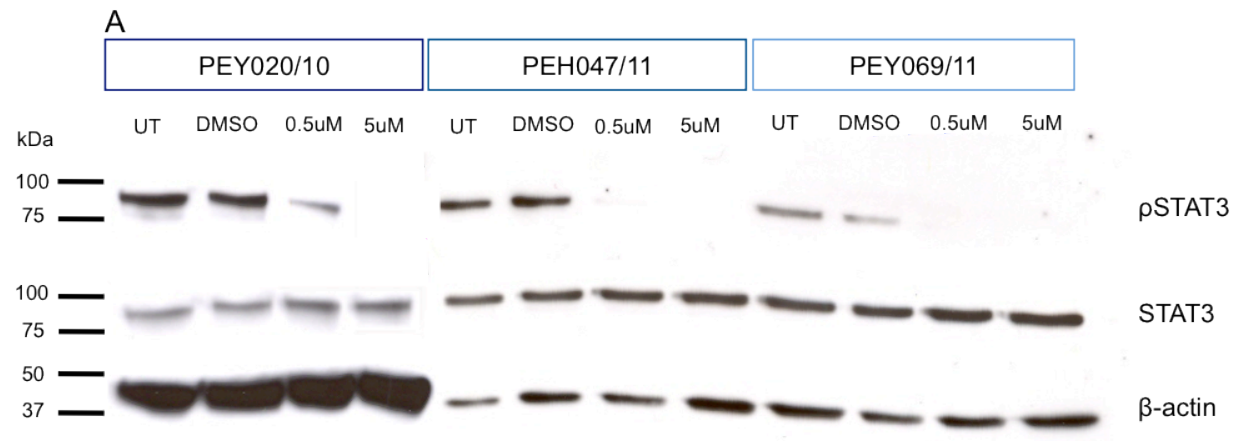
3.4. Inhibition of STAT3 phosphorylation in primary prostate cells

3.4.1. Inhibition of STAT3 phosphorylation using pyridone-6

A widely used inhibitor of JAK-STAT signaling is Pyridone-6 (P6), which is a specific pan-JAK inhibitor (Lucet et al., 2006). This inhibitor can be used at a much lower concentration and with faster kinetics than a commonly used JAK2 inhibitor, AG490, which was the first and best characterized JAK tyrosine kinase inhibitor, but was thought to be less specific compared to P6. (Pedranzini et al., 2006). It has already been shown that P6 is able to inhibit STAT3 phosphorylation in a variety of prostate cancer cell lines. However it was important to determine if inhibition of pSTAT3, using P6, could also be achieved in primary prostate cell cultures.

Firstly, the optimal concentration and treatment time was determined. Primary prostate cells, derived from cancer samples, were treated for 16 hours with 0.5 or 5 μ M P6, DMSO (P6 solvent) or medium only (SCM). The cells were subsequently lysed and loaded onto a SDS-PAGE gel for Western blot analysis. The results show that primary prostate cancer cells treated for 16 hours with P6, at both concentrations, resulted in decreased levels of pSTAT3. This result was confirmed in three different prostate cancer samples (Figure 3.16A). The levels of pSTAT3 were quantified relative to the levels of total STAT3 (Figure 3.16B). The quantified levels of phosphorylated STAT3, of three samples, were then averaged and show that there was a significant ($P < 0.005$) decrease of phosphorylated STAT3 after treatment with 0.5 μ M (85% decrease) and 5 μ M (98% decrease) P6 for 16 hours compared to the DMSO control (Figure 3.16C).

Figure 3.16. **Effect of Pyridone-6 on phosphorylated STAT3 levels in a series of primary prostate cells.** A. Western blot analysis for pSTAT3, total STAT3 and β -actin (loading control) of three primary prostate cell cultures derived from cancer samples, treated with 0.5 and 5 μ M P6, DMSO (P6 solvent) or untreated (UT) for 16 hours. B. Quantification of Western blot of three primary prostate cancer cultures, the results are expressed as the levels of pSTAT3 relative to total STAT3, following treatment with 5 μ M P6, for 16 hours. C. Average levels of pSTAT3 relative to total STAT3 (n=3) after treatment with P6, analysis was performed using Image J software and the error bars are the standard deviation of three primary cancers. Statistical analysis was performed using the students t-test, *P<0.05.



In order to have a functional effect, it is important that treatment with P6 results in inhibition of nuclear pSTAT3 as well as downstream targets. Therefore, cells were treated with 5 μ M P6, for 16 – 72 hours, to determine the levels of pSTAT3 and the downstream target SOCS3. The nuclear protein fraction was normalized against tata-binding protein (TBP), which is a transcription factor that binds to the TATA box and is a commonly used nuclear loading control. The cytoplasmic protein fraction was normalized against β -actin (Figure 3.17B). The results show that 16 hours treatment with P6 resulted in down-regulation of nuclear pSTAT3, but at that time point inhibition of SOCS3 was not observed (Figure 3.17A). However, after 48 hours, a decrease in nuclear pSTAT3 as well as the downstream target SOCS3 was observed (Figure 3.17A). This effect was maintained after 72 hours treatment with 5 μ M P6 (results not shown). Therefore, for further experiments cells were treated with 5 μ M P6, as this showed the most significant decrease in levels of pSTAT3, after 48 hours treatment without detectable cytotoxicity.

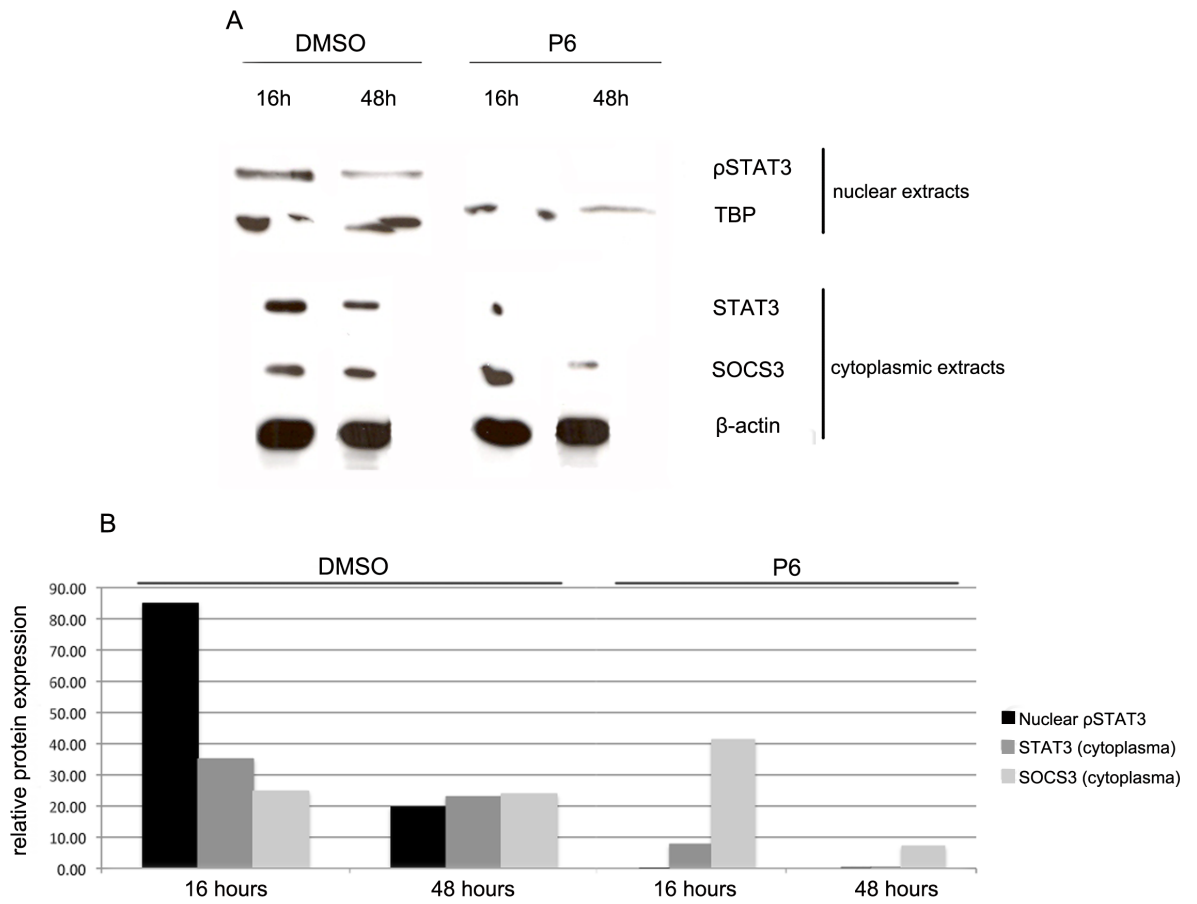


Figure 3.17. Time course of treatment of primary prostate cancer cells with Pyridone-6. A. Western blot analysis for pSTAT3, total STAT3, SOCS3, TATA-binding protein (TBP) (nuclear loading control) and β -actin (cytoplasmic loading control). Nuclear and cytoplasmic extracts of primary prostate cell cultures (derived from a cancer sample) were obtained following treatment with 5 μ M P6 or DMSO, for 16 and 48 hours. B. Quantification of Western blot. The levels of pSTAT3, total STAT3 and SOCS are expressed relative to the respective loading controls.

3.4.2. Inhibition of the JAK-STAT pathway using neutralizing antibodies

3.4.2.1. Inhibition of the JAK-STAT pathway using commercially available neutralizing antibodies to IL-6, LIF and OSM

In order to determine which ligand of the IL-6 family of cytokines activates the JAK-STAT pathway in the prostate cells were treated with neutralizing antibodies to IL-6, LIF and OSM, and the levels of pSTAT3 were subsequently analyzed using Western blotting.

Initially, primary prostate cells were treated for 48 hours with 5 µg/mL of neutralizing antibodies against IL-6, LIF, OSM or a combination of all three. As a positive control, cells were treated with 5 µM P6, and IgG controls were included as negative controls. The results indicated that there was no decrease in pSTAT3 levels following treatment with 5 µg/mL of anti-LIF, IL-6 or OSM. However, there was a decrease of ~50 % in pSTAT3 levels when the cells were treated with a combination of all three (Figure 3.18A).

As inhibition of pSTAT3 levels were not observed when the primary prostate cells were treated with 5 µg/mL of neutralizing antibodies to either LIF, IL-6 or OSM, the concentration of all antibodies was increased to 10 and 50 µg/mL (Figure 3.18). At 10 µg/ml of anti-IL-6 there was a decrease in the levels of pSTAT3 of 40% relative to the untreated control and 50% relative to the IgG control (Figure 3.18B). There was no decrease in the levels of pSTAT3 with anti-OSM relative to the untreated control or the IgG control (Figure 3.18B). When the concentration of antibodies was increased to 50 µg/ml, this inhibitory effect with anti-IL-6 was similarly observed, but there was also a decrease of 40% with the isotype control, suggesting that there was a non-specific effect (Figure 3.18C). In all experiments, treatment with 5 µM P6 reduced pSTAT3 levels (Figure 3.18).

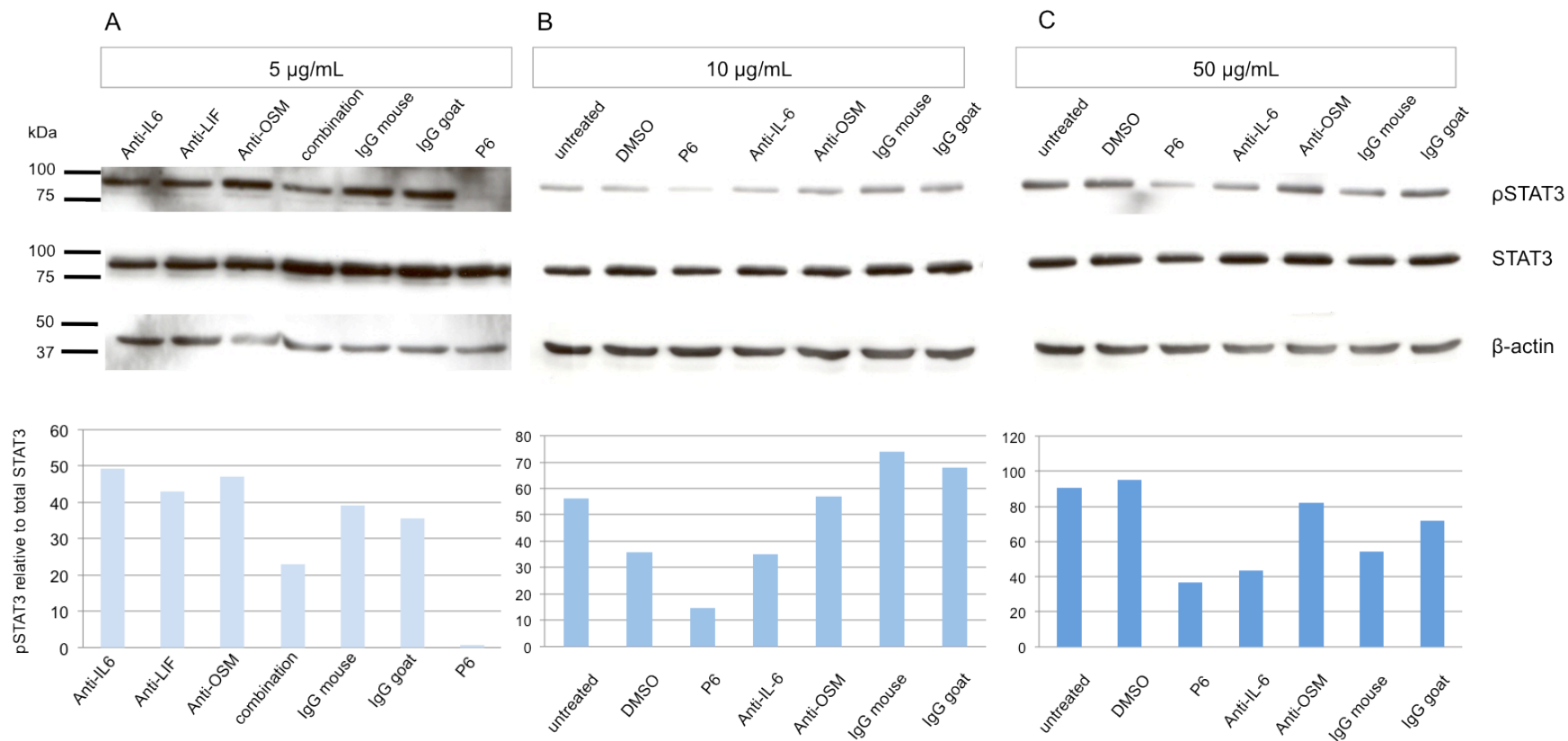


Figure 3.18. **Effect of neutralizing antibodies against IL-6, LIF and OSM on phosphorylated STAT3 levels.** Figure 30. Western blot analysis for pSTAT3, total STAT3 and β -actin (loading control) of primary cell cultures derived from prostate cancers. Cells were treated with 5 μ g/mL (A), 10 μ g/mL (B) and 50 μ g/mL (C) neutralizing antibodies against IL-6 (mouse IgG), LIF (goat IgG) and OSM (mouse IgG) for 48 hours. Included, as controls, were cells treated with 5 μ M P6, DMSO (vehicle control for P6) or IgG isotype controls. Western blots were quantified using Image J software and are expressed as relative to total STAT3 (100%).

3.4.2.2. Inhibition of STAT3 phosphorylation using CNTO 328

CNTO 328 is a neutralizing antibody against IL-6 that has been used in clinical trials for prostate cancer (Tripathi et al., 2003; Fizazi et al., 2012). It is a chimeric monoclonal which has the advantage of a long half-life (medium 18 days). This is beneficial compared to other antibodies, for example BE-8, which has a short half-life of 3 - 4 days (Tripathi et al., 2003).

CNTO 328 has been used in several phase I/II clinical trials, including for prostate cancer, although the outcome of this trial in patients with metastatic castration-resistant prostate cancer did not show a significant improvement (Tripathi et al., 2003; Fizazi et al., 2012). This antibody was used because it has been shown to have high affinity for the IL-6 receptor and has neutralizing activity (van Zaanen et al., 1996). Primary prostate cells were treated with 50 - 1 $\mu\text{g}/\text{mL}$ CNTO 328 for 24, 48 and 72 hours and the levels of pSTAT3 were determined by Western blotting. However, in these initial experiments there was no apparent difference in the levels of pSTAT3 with treatment (results not shown). The experiment was repeated for up to 6 days, as Steiner *et al.* showed that an inhibition of pSTAT3 levels was observed after 6 days treatment of prostate cancer cell lines with CNTO 328 (Steiner et al., 2006). The results show that after 4 days treatment there was a ~90% decrease in pSTAT3 levels compared to the untreated control (Figure 3.19). This effect was even greater after 6 days of treatment, where a ~95% decrease in pSTAT3 levels was obtained (Figure 3.19). This decrease in pSTAT3 was noted at concentrations from 5 – 200 $\mu\text{g}/\text{mL}$ CNTO328.

To confirm this finding, a further three primary prostate cell cultures, derived from cancer samples, were treated with 10 $\mu\text{g}/\text{mL}$ of CNTO 328 for 2, 4 and 6 days (Figure 3.20A). The results show optimal inhibition of pSTAT3 was achieved after 6 days ($P < 0.05$). The results also demonstrate the variability between patients. When the levels were averaged (from the three samples), a 90% decrease in pSTAT3 was observed after 6 days of treatment with CNTO 328 compared to the untreated control (Figure 3.20C) ($P < 0.05$).

Figure 3.19. **Effect of CNTO 328 on phosphorylated STAT3 levels.** A. Primary prostate cancer cells (Gleason 7) were treated with increasing concentrations of CNTO 328 for 2, 4 and 6 days and were then subjected to Western blot for pSTAT3, total STAT3 and β -actin (loading control). B. Quantification of Western blot for pSTAT3, which is expressed relative to total STAT3, after treatment with CNTO 328 for 2 (blue), 4 (red) and 6 (green) days. Analysis was performed using Image J software.

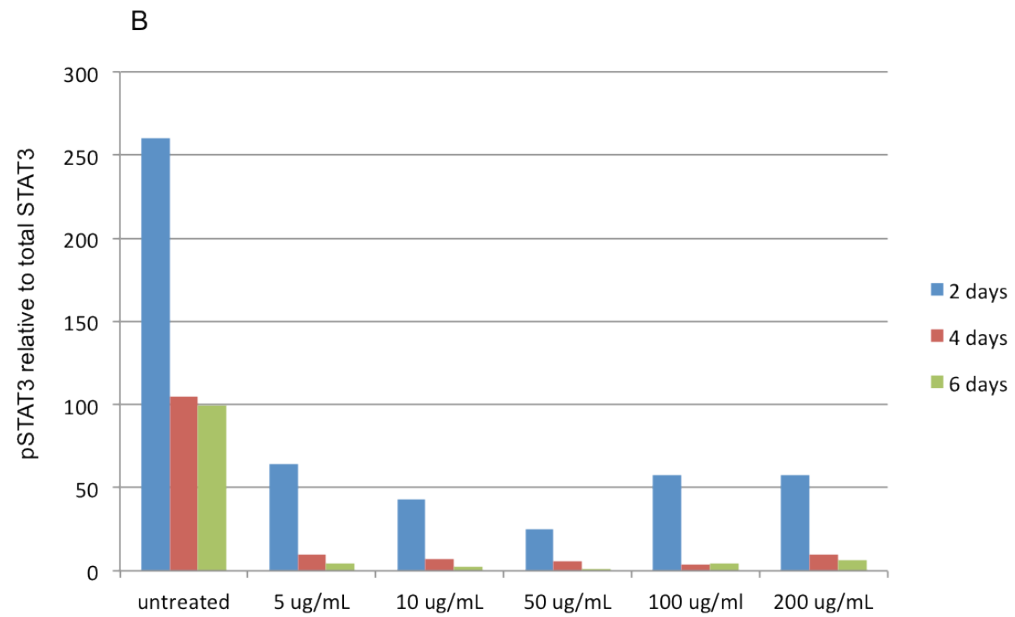
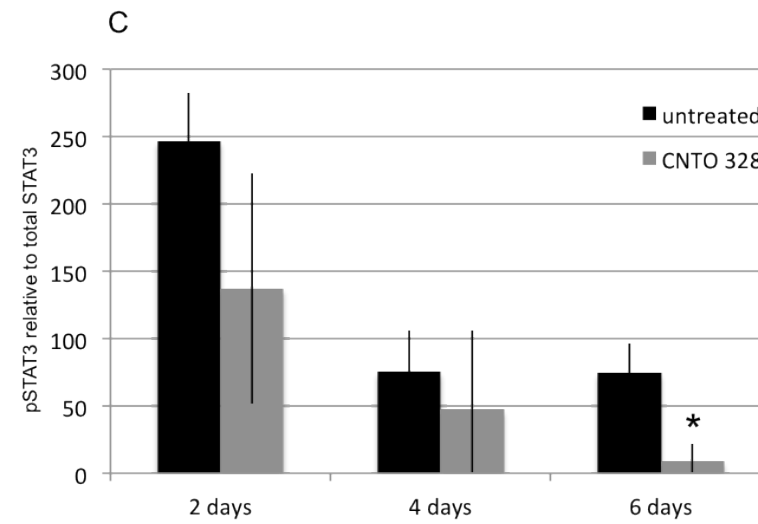
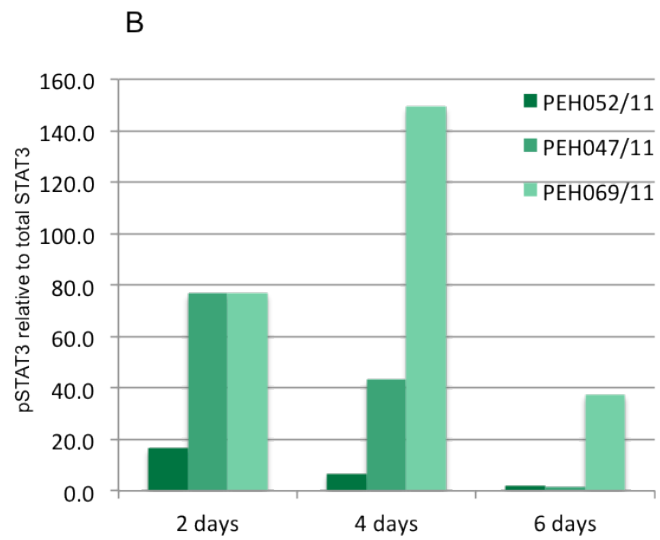


Figure 3.20. **Effect of CNTO 328 on phosphorylated STAT3 levels in a series of primary prostate cancer cells.** A. Primary cells were subjected to Western blot for pSTAT3, total STAT3 and β -actin (loading control) following treatment with CNTO 328. Three primary cell cultures derived from prostate cancer samples (Gleason 3+4 (PEH052/11 and PEH069/11)), Gleason 4+5 (PEH047/11) were treated with 10 μ g/mL CNTO (+) or untreated (-) for 2, 4 or 6 days. B. Quantification of Western blot of the three primary cultures for pSTAT3; which is expressed as relative to total STAT3 and normalized to the untreated control (100%). C. Average levels of pSTAT3 from three primary prostate cancer cultures. Results are expressed as relative to total STAT3 and are normalised to the untreated control. The results were quantified using Image J software. Statistical analysis was performed using the Students t-test, *P<0.05.



3.4.3. Inhibition of STAT3 phosphorylation using a direct inhibitor, LLL12

3.4.3.1. Optimization of treatment with LLL12

The previous section demonstrated that, JAK-STAT signaling is activated through IL-6, in the prostate. A more direct way to inhibit STAT3 phosphorylation is to target STAT3 directly. LLL12 is a specific small molecule inhibitor, which binds to the phosphoryl tyrosine 705 binding site of the STAT3 monomer (Lin et al., 2010). It has previously been shown that LLL12 inhibits STAT3 phosphorylation, subsequently affecting tumour growth in a variety of cancers, including breast cancer and glioblastoma (Lin et al., 2010; Ball et al., 2011; Wei et al., 2011).

In order to determine whether LLL12 is able to inhibit STAT3 phosphorylation in primary prostate cancer cells, we wanted to measure the levels of pSTAT3 and total STAT3 after cells were treated with increasing concentrations of the drug, at different time points. In order to do this in a fast and quantitative manner, a cell-based ELISA was used. This method measures the levels of pSTAT3 and total STAT3 simultaneously, in fixed cells. Firstly, it was important to determine the sensitivity of this assay, therefore primary prostate cells, derived from a cancer sample, were plated at different densities, up to 20,000 cells/well. The results show that at least 10,000 cells /well were required to detect pSTAT3 (Figure 3.21A).

To determine the optimal concentration of LLL12 in primary prostate cells were treated with increasing concentrations of LLL12, for up to to 72 hours. Cells were then fixed and the levels of pSTAT3 and total STAT3 were measured. The results show a statistically significant inhibition of pSTAT3 with 1 – 10 μ M LLL12, after 24 hours of treatment ($P < 0.05$) (apart from one outlier, at 5 μ M). When the treatment time was extended to 48 hours, a decrease in pSTAT3 was observed with 1 – 10 μ M, however this was not statistically significant due to the high error bars seen in the untreated control. Cells treated with 1 - 10 μ M LLL12 for 72 hours also showed a statistically significant decrease in pSTAT3 compared to the untreated control ($P < 0.05$) (Figure 3.21B).

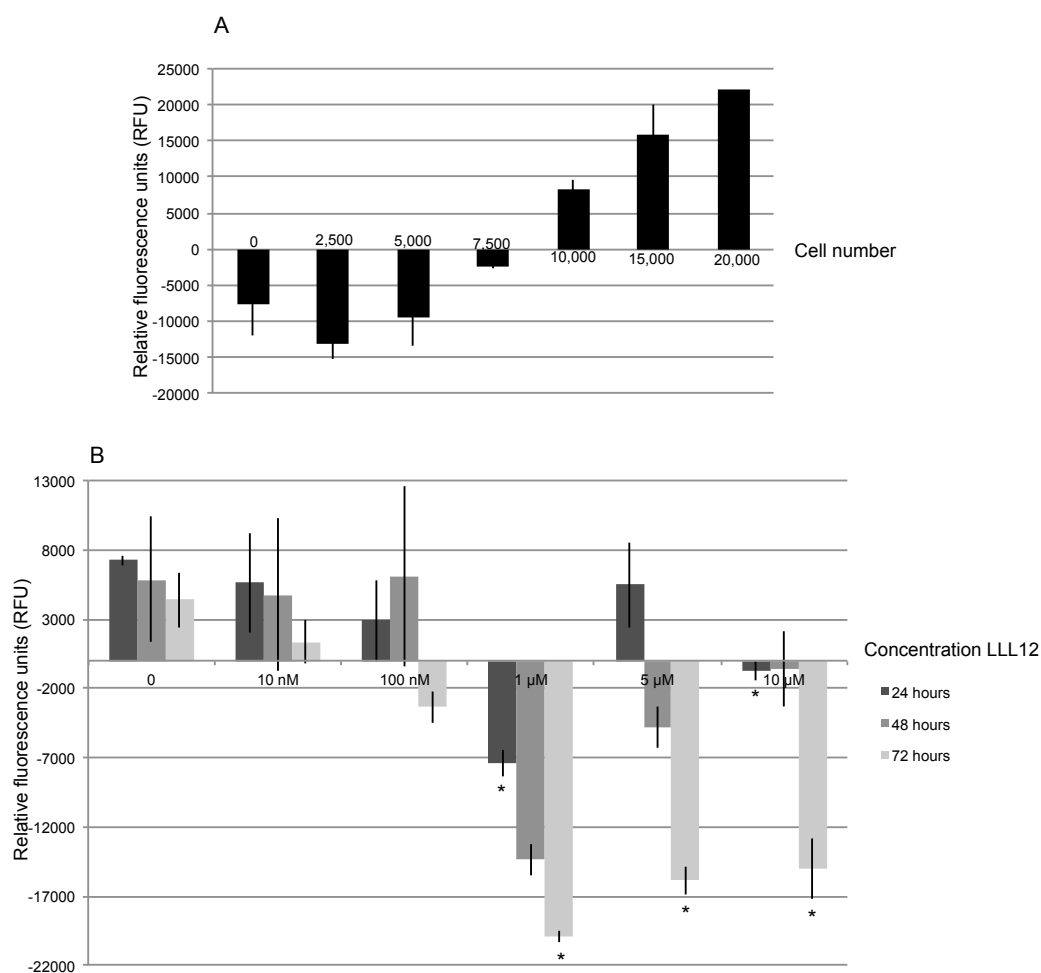


Figure 3.21. **Optimization of primary prostate cells treated with LLL12 to inhibit phosphorylation of STAT3.** A. Optimization of cell-based ELISA. Cells were plated at densities ranging from 0 - 20,000 cells per 96-well plate to determine the minimal cell number required to detect phosphorylated STAT3 and total STAT3 simultaneously. The analysis was performed by subtracting the values obtained from secondary antibody controls, resulting in relative fluorescence units (RFU). B. Cell-based ELISA for phosphorylated STAT3 relative to total STAT3. 10^4 primary prostate cells were treated with LLL12 (0 - 10 μ M), in duplicate, for 24, 48 and 72 hours. The error bars is represented by the standard deviation of duplicate values and statistical analysis was performed using the student t-test. The results were normalised to untreated cells at each time point, * $P < 0.05$.

3.4.3.2. Change in cell morphology following treatment with LLL12

It has already been shown in various cancers that LLL12 induces apoptosis (Lin et al., 2010). When primary prostate cells, derived from a cancer sample, were treated with 1 μ M LLL12 for 24 hours, the cell morphology changed significantly. More membrane blebbing and rounded, floating cells were observed with treatment (Figure 3.22A), suggesting that some cells were undergoing apoptosis. This change in morphology was different to treatment with 5 μ M P6. Those cells lost their cobblestone appearance and became more fibroblastoid (Figure 3.22A).

3.4.3.3. Western blot analysis for pSTAT3 in primary prostate cells treated with LLL12

To confirm inhibition of STAT3 phosphorylation in primary prostate cells after treatment with LLL12, Western blot analysis was performed. Primary prostate cells, derived from benign disease, were treated with 1 – 10 μ M LLL12 for 24 hours. The results showed complete inhibition of pSTAT3 after treatment with LLL12 compared to the DMSO and untreated control cells (Figure 3.22B). It was apparent from the β -actin loading control that there was less protein in each lane, but this was due to some cell death during treatment. As β -actin and total STAT3 could still be detected, although at lower levels compared to the untreated control, we could conclude that the inability to detect pSTAT3 was due to treatment with LLL12 and not due to low protein loading. Cells treated with P6 also showed inhibition of pSTAT3 following treatment, relative to the untreated controls.

3.4.3.4. Flow cytometry analysis of primary prostate cells treated with LLL12

To confirm this result, we performed flow cytometry on primary prostate cells, derived from a cancer sample, following treatment with 1 μ M LLL12, for 24 hours. Because the dead cells were gated out, using a live/dead stain, the analysis was performed solely on live cells labeled for pSTAT3. The results showed that only 5% of the primary prostate cells had detectable levels of pSTAT3 after treatment with LLL12, compared to 91% of the vehicle treated control cells (Figure 3.22C). Cells were gated relative to unlabeled cells (R12).

Figure 3.22. **Effect of LLL12 on phosphorylated STAT3 levels in primary prostate cells.** A. Images of primary prostate cells derived from a cancer after 48 hours treatment with 5 μ M P6 or 24 hours treatment with 1 μ M LLL12. The control cells were cultured in stem cell medium only. The right panel shows a magnified image of primary cells after treatment with LLL12. Images were taken on an EVOS microscope (Advanced Microscopy Group) at 10x magnification. B. Western blot analysis for pSTAT3, total STAT3 and β -actin (loading control) of primary prostate cells derived from benign disease, treated with either 1 - 10 μ M LLL12 (for 24 hours), 5 μ M P6 (positive control), DMSO (vehicle control) and untreated control (upper panel). Lower panel: quantification of Western blot, which is expressed as pSTAT3 relative to total STAT3. C. Flow cytometry histograms of primary prostate cells derived from a cancer sample for pSTAT3 (-APC) treated with a DMSO control or 1 μ M LLL12, for 24 hours. Analysis was performed relative to unlabelled cells; dead cells were excluded using a live/dead cells stain prior to fixing, permeabilizing and labelling the cells for intracellular pSTAT3.

We were able to show (using three different techniques) that treatment with LLL12, resulted in a significant inhibition of STAT3 phosphorylation in benign and cancer primary prostate cells. The results also show that >90 % of primary prostate cancer cells express pSTAT3, suggesting that this pathway is constitutively. When activation of this pathway was blocked, it had a negative effect on the viability of the cells suggesting that the cells require this pathway for their survival.

3.5. Importance of the JAK-STAT signalling pathway for cell survival

3.5.1. Colony formation efficiency following treatment with P6

It has been suggested by several groups that the JAK-STAT signalling pathway is important for stem cell self-renewal (reviewed in (Morrison and Spradling, 2008)) and CSC survival (Sherry et al., 2009; Marotta et al., 2011). As the JAK-STAT signalling pathway is constitutively active in primary prostate cells by autocrine activation via IL-6, it is likely that the pathway is important for the maintenance of these undifferentiated prostate cancer stem-like cells. In order to test this, colony forming recovery assays were performed following treatment with STAT3 inhibitors, either directly (LLL12) or indirectly (anti-IL-6 antibody and P6).

Primary prostate cells, derived from a high Gleason grade (hormone-naïve) cancer, were treated with 5 μ M P6 to inhibit STAT3 phosphorylation, or with a DMSO vehicle control. Following treatment, stem-like, TA and CB cells were selected as previously described (section 2.1.3), plated in the presence of irradiated STO feeder cells and scored for colonies after ~14 days. Stem-like colonies were considered to be >32 cells (at least 5 population doublings). Colonies smaller than 32 cells were also counted to determine the impact of STAT3 inhibition on colony forming efficiency (Figure 3.23).

The results show that, from a high Gleason grade (4+5) sample, 20.5 % of stem-like cells, 14.3% of TA and 60% of CB cells had formed colonies >32 cells. Interestingly, the stem-like cells were unable to initiate colonies, following treatment with P6. In contrast, treatment resulted in a ~2 fold increase in CFE of the TA population with a decrease in CFE of the CB population (19%) (Figure 3.24A).

The experiment was repeated with a Gleason 3+4 sample. In contrast to the Gleason grade 4+5 sample, the CFE was much lower overall, and treatment had no significant effect on the stem-like and CB cells. There was a small decrease with treatment in the TA population, but this effect was not significant. Treatment did affect colonies <32 cells, in the stem-like population, such that colonies <32 cells were not detected following treatment. This effect was not observed with either the TA or CB cells. The CFE for the TA cells showed a 3 - 4 fold increase compared to the stem-like population, however no significant difference between the DMSO (control) and P6 treated cells. Compared to the stem-like cells and TA cells, the cells from the CB population were inefficient in forming colonies, as expected (Figure 3.24B).

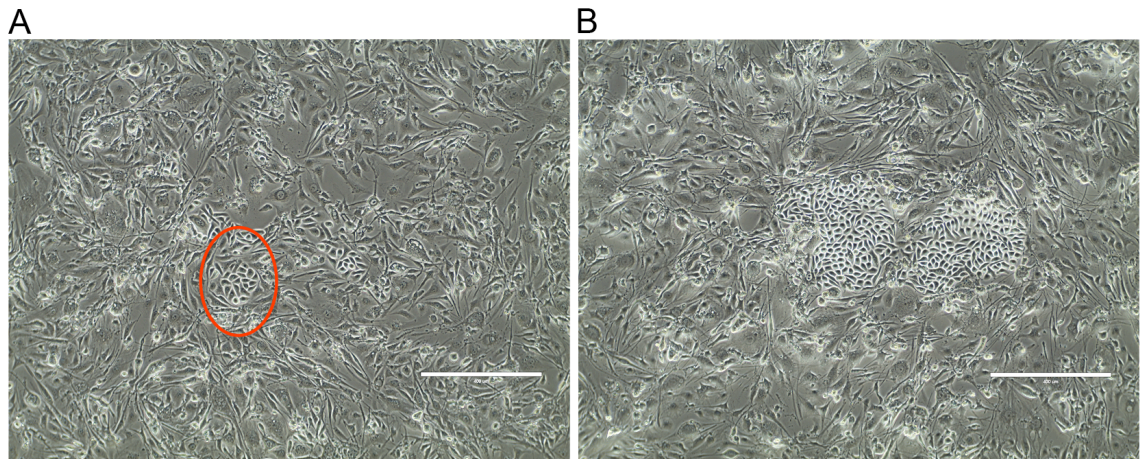
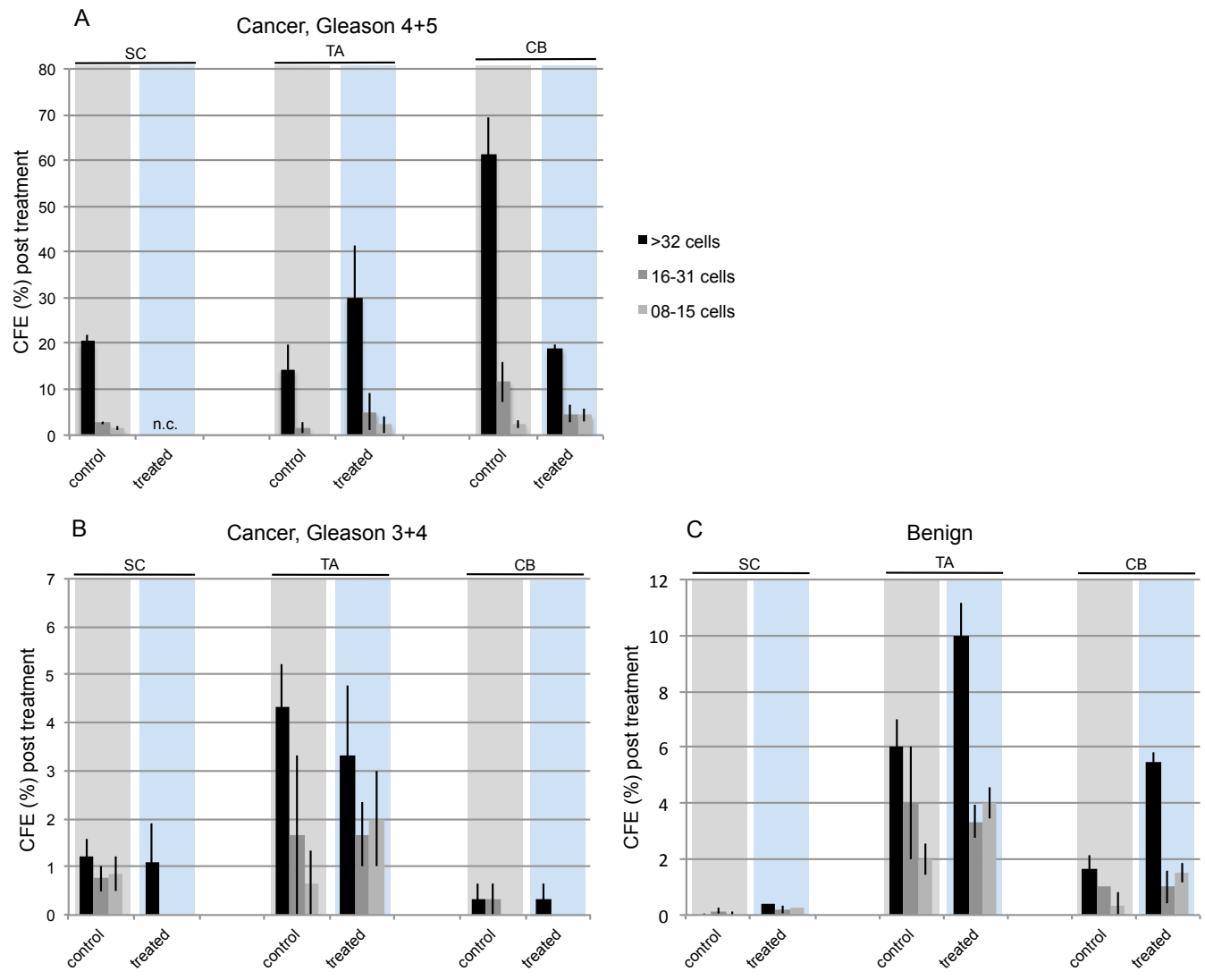


Figure 3.23. Images of colonies derived from single stem-like cells. Primary prostate cancer cells derived from a high Gleason grade hormone-naïve cancer (4+5) were treated for 48 hours with 5 μ M P6 or vehicle (DMSO) control. Stem-like, TA and CB cells were then selected and plated in triplicate, at a density of 100 cells/well in a 35mm² collagen-I coated dish, in the presence of irradiated STO feeder cells. Cells were incubated for ~14 days; until colonies were observed in the DMSO control wells. Images of a small colony (<32 cells) (A) and a larger colony (>32 cells) (B) derived from stem-like cells. Images were taken using an EVOS microscope at 10x magnification.

Figure 3.24. **Colony forming efficiency of primary prostate cells derived from prostate cancer and benign disease, following treatment with P6.** Primary prostate cells derived from a Gleason grade 4+5 (A), Gleason grade 3+4 (B) or benign disease (C) were treated for 48 hours with 5 μ M P6 or vehicle (DMSO) control. Stem-like (SC), TA and CB cells were then selected and plated in triplicate, at a density of 100 cells/well in a 35mm² collagen-I coated dish, in the presence of irradiated STO feeder cells. Cells were incubated for ~14 days; until colonies were observed in the DMSO control wells. Colony forming efficiency (CFE), was calculated using the average colony number, from triplicate. Colonies were manually counted, using a Leica light microscope at 10x magnification, and scored between 8 - 15 cells, 16 - 31 cells or > 32 cells (5 doublings) (indicated by coloured bars from light to dark respectively). The error bars are represented by the SEM. N.C. means no colonies were observed.



Treatment with P6 had no significant effect on the CFE of either the SC, TA or CB population, from a benign sample. In this sample the SC population failed to form many colonies, but colonies were observed from both the TA and CB population. The CFE of the TA population was 6% and with treatment this increased to 10% (1.5-fold increase), this was from colonies bigger than 32 cells. No difference was observed from smaller colonies. Similarly, treatment resulted in an increase in the CFE of the CB population, from 1.7% (control) to 5.5% (treatment) (3-fold increase) (Figure 3.24C).

Thus, the results for the primary prostate cells, derived from Gleason 3+4 cancer (Figure 3.24B) and benign disease (Figure 3.24C), showed a higher CFE for the TA cells compared to the stem-like population. However, there was no significant difference between P6 treatment and the control as was observed from the high Gleason grade (4+5) cancer analysed (Figure 3.24A).

3.5.1.1. Using a Rho-associated kinase inhibitor to improve colony formation efficiency

The CFE of primary cells is highly variable and in some cases (4/18 samples analysed) the efficiency was too low to include in the analysis (<5 colonies per well). The majority of these cultures were derived from benign samples. To improve efficiency, a Rho-associated kinase (ROCK) inhibitor was used; Y-27632. It has been shown that this ROCK inhibitor reduces dissociated-induced apoptosis and therefore increases colony forming efficiency. A >10-fold increase in CFE has been reported (Watanabe et al., 2007). Primary prostate cells were treated with 5 μ M P6 (or DMSO) together with 10 μ M Y-27632, for 2 days prior to selecting for stem-like, TA and CB cells. After plating, Y-27632 was added again until the assay was stopped, to count colonies. The results show that there was a 2 - 3-fold increase in CFE, when cells were treated with the ROCK inhibitor, although this effect was only observed in the TA and CB (progenitor) population (Figure 3.25). As the ROCK inhibitor did not increase the CFE of the stem-like population, no further investigation was carried out.

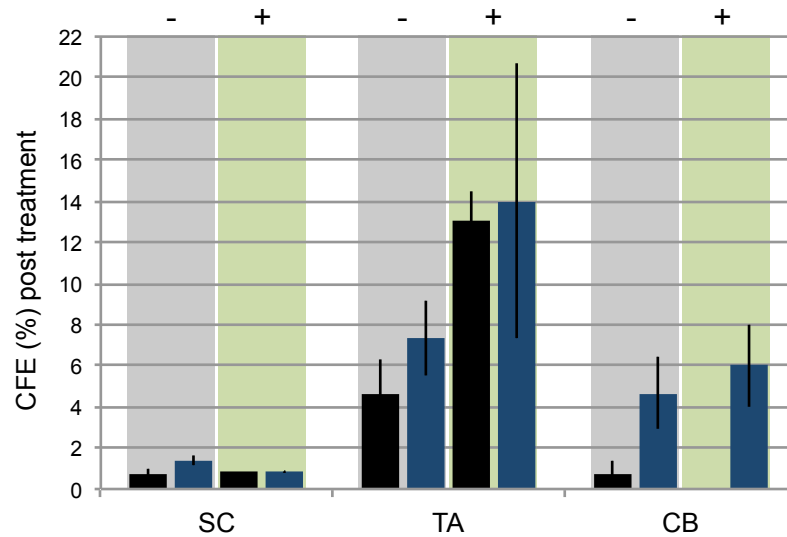


Figure 3.25. **Colony forming efficiency of primary prostate cancer cells, following treatment with P6, + / - ROCK inhibitor.** Primary prostate cells derived from a cancer sample were treated with 5 μ M P6 (blue bar) or DMSO as control (black bar) together with (+) or without (-) 10 μ M Rock inhibitor (Y-27632). Following treatment, stem-like (SC), TA and CB cells were selected and plated at a density of 100 cells/well in a 35mm² collagen-I coated dish in the presence of irradiated STO feeder cells. Colonies were manually counted, using a Leica light microscope at 10x magnification and scored if > 32 cells, at 14 days. The CFE was calculated using the average colony number, from triplicates, and the error is represented by the standard deviation.

3.5.2. Summary of results on the effect of treatment with the JAK inhibitor (P6) on colony forming recovery

Primary prostate cells, derived from benign disease, failed to initiate a sufficient number of colonies to include in the analysis. This phenomenon was observed in four different samples. Therefore only cultures derived from prostate cancer samples were analysed for their effect on CFE following treatment with P6.

In the following analysis (Figure 3.26) the TA and CB cells were grouped together as the trend was consistent following treatment with P6, in all the samples analysed. When an increase in CFE was observed in the TA population (after treatment with P6) there was also an increase in CFE for the CB population. Therefore, cell populations were grouped as CD133⁺ (stem-like cells) and CD133⁻ (progenitor cells) (Figure 3.26). Due to high patient variability, the samples were grouped into disease stages: Gleason grade 7, Gleason grade (>8) hormone-naïve, and CRPC. Most prostate cancer samples collected fall into the Gleason 7 group (n=8). Only 3 were analysed from high Gleason (hormone-naïve) grade disease and four from CRPC.

Treatment of high Gleason grade (hormone-naïve) cells, with P6 resulted in a decrease in CFE of the stem-like population, compared to the vehicle control. This was observed in 3/3 samples analysed with an average decrease of 70% CFE. However, this decrease in CFE was not significant, due to the limited number of samples analysed. The progenitor population showed an increase in CFE of 40%, following treatment with P6, however this increase was only observed in 2/3 samples, showing that there is a degree of variability within this population compared to the stem-like population.

In contrast, there was an increase (60%) in CFE of the stem-like population (following treatment with P6) from cells derived from Gleason 7 cancers. However 3/8 samples showed a decrease in CFE. Similarly, the progenitor population showed an increase (140%) in CFE following treatment.

The CRPC samples that were analysed showed, in 3/4 samples, an increase in CFE of the stem-like population, after treatment with P6. The average increase was 100%, although there was a high degree of variability between samples. There was a minimal effect with P6 treatment on the progenitor population (40% increase in CFE). However only in 2/4 samples an increase in CFE was observed, after P6 treatment. The 2 samples that showed a decrease only had a minimal decrease of 20% CFE. So, the

average CFE of the progenitor cells was an increase of 40% compared to the DMSO control.

Significance was not achieved, which was probably due to limited number of samples but also patient variability as shown by the wide spread between the individual samples (Figure 3.26).

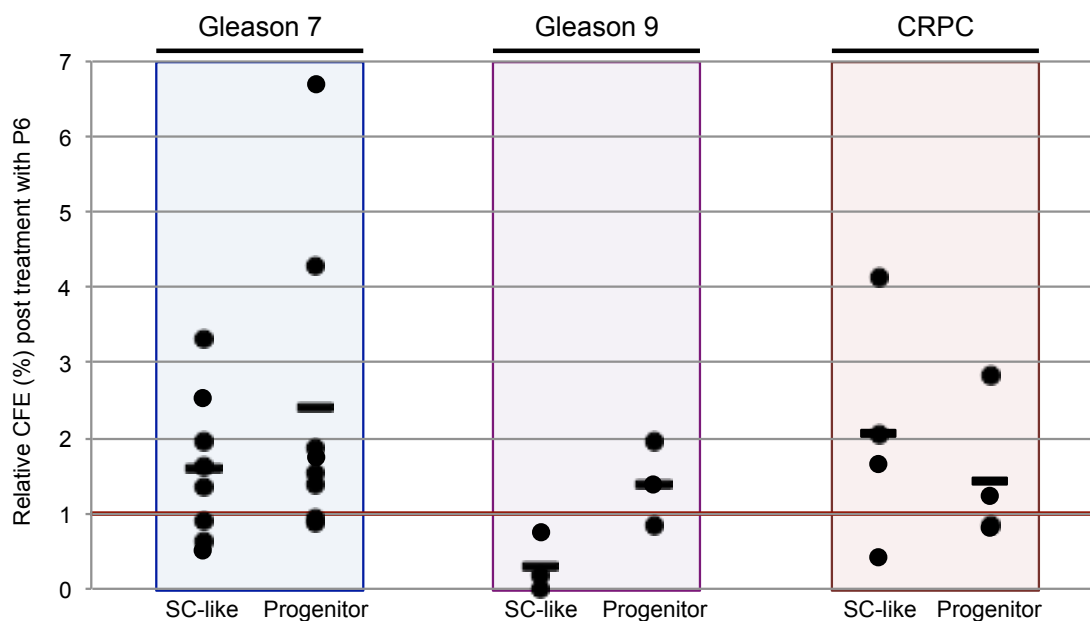


Figure 3.26. **Overall results on colony forming efficiency of a series of primary prostate cancer cell cultures, following treatment with the JAK inhibitor, P6.** Primary prostate cells, derived from high Gleason 7 (n=8), Gleason grade hormone-naïve cancer (n=3), and CRPC (n=4) samples, were treated for 48 hours with 5 μ M P6 or DMSO (vehicle control). Cells were selected for CD133⁺ (stem-like cells) and CD133⁻ (progenitor cells), and plated at a cell density of 100 cells/well in a 35mm² collagen-I coated dish together with irradiated STO feeder cells. Colonies were manually counted, using a Leica light microscope at 10x magnification. Colonies were scored if they were ≥ 32 cells. The results are expressed relative to the DMSO control (CFE=1), indicated by the red line. Each symbol represents a different patient samples, and the bar represent the average.

3.5.3. The effect of the IL-6 neutralizing antibody CNTO 328 on Colony forming efficiency of prostate primary cells

As previously observed (section 3.4.2.2), IL-6 is the primary ligand activating the JAK-STAT pathway in the prostate. To determine the functional consequences of inhibition of the ligand binding to its receptor, colony formation assays were performed after treatment with CNTO 328. Primary prostate cells, derived from high Gleason grade cancer samples, were treated with 10 µg/mL CNTO 328, for 6 days. Colonies were then scored from CD133⁺ (stem-like cells) and CD133⁻ (progenitor cells) The CFE of the cancer stem-like population, showed a significant inhibition ($P < 0.05$) compared to the untreated control. This was observed in 3/3 samples analysed, with an average 50% decrease in CFE compared to the control. However, the progenitor cells were more variable in terms of their response to CNTO328 treatment as 2 out of 3 patients tested had an increased ability to form colonies (Figure 3.27A).

3.5.4. The effect of treatment with the STAT3 inhibitor, LLL12 on colony forming efficiency

Another inhibitor, LLL12, which directly inhibits STAT3 activation, was next used and as shown previously (Figure 3.21), had a significant effect on the levels of pSTAT3 in primary prostate cells. Therefore it was important to determine the functional consequences of this inhibition, using a colony formation assay. Primary prostate cancer cells, derived from high Gleason grade cancers, were treated with 1 µM LLL12, for 24 hours. The ability to form colonies was significantly decreased for the stem-like cells (CD133⁺) ($P < 0.05$) as well as the progenitor cells (CD133⁻) ($P < 0.005$), with treatment (Figure 3.27B). This decrease in CFE was observed in 4/4 samples analysed, with a 75% decrease in CFE in the stem-like population and an even greater decrease of 90% in the progenitor population.

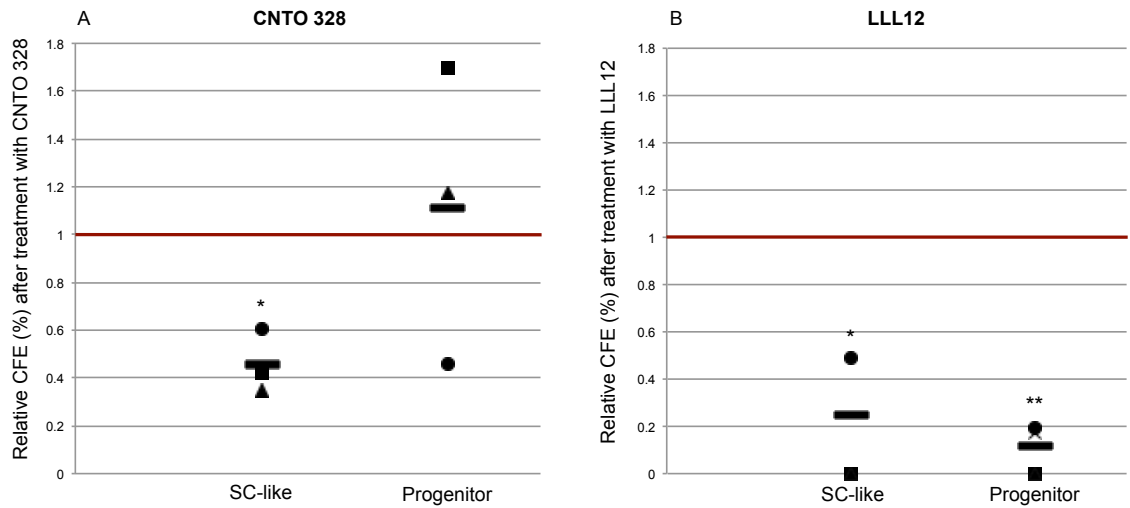


Figure 3.27. Colony formation efficiency of primary prostate cancer cells following treatment with CNTO 328 and LLL12. Primary prostate cells, derived from high Gleason grade cancers, were treated with 10 $\mu\text{g}/\text{mL}$ CNTO 328 for 6 days ($n=3$) (A) or 1 μM LLL12 for 24 hours ($n=4$) (B). Selected cells, CD133^+ (stem-like cells (SC-like)) and CD133^- (progenitor cells) were plated at a density of 100 cells/well in 35mm² collagen-I coated dishes in the presence of irradiated STO feeder cells. Colonies were manually counted when > 32 cells using a Leica light microscope at 10x magnification and colony forming efficiency (CFE) was calculated relative to the DMSO control (CFE=1), indicated by the red line. Each symbol represents a different patient and the bar represents the average CFE. Students t-test was used to test for statistical significance, * $P<0.05$ ** $P<0.005$.

Chapter 4

Results II

4. Results II

Targeting STAT3 in a ‘near patient’ xenograft model

4.1. Optimisation of protocol to determine the effect of LLL12 on tumour growth in a ‘near patient’ xenograft

To determine whether JAK-STAT signalling is important for prostate cancer (stem) cells *in vivo*, we used a unique xenograft model. Dr. Anne Collins developed this xenograft model, in which xenografts were established by engrafting prostate biopsies into Rag2^{-/-}γC^{-/-} mice, as described previously (Maitland et al., 2011). They are ‘near-patient’, low passage and can be re-derived from frozen cells. The tumours are routinely genotyped and compared to patient’s lymphocytes to confirm their identity.

The small molecule inhibitor LLL12 was used in this set of experiments to inhibit STAT3 phosphorylation. It was used at two concentrations: 5 mg/kg and 2.5 mg/kg as recommended by our collaborator Prof. Pui-Kai (Tom) Li, who kindly donated this molecule. Previous publications had also shown the molecule to be active in breast cancer xenografts and glioblastoma at those concentrations (Lin et al., 2010). As illustrated in Figure 4.1, serially-transplantable xenografts were dissociated into single cells and depleted of mouse hematopoietic lineage positive and endothelial cells before engrafting human Lin⁻/CD31⁻ cells into recipient mice, normally in groups of 10 to determine the effect of LLL12 on tumour growth. The mice were supplemented with slow-release DHT (up to 90 day release) at tumour initiation. Treatment was initiated once the tumour had become established (approximately 5 mm) (Figure 4.1). The number of tumour cells required to initiate tumour growth varied between xenografts and depended upon tumour frequency calculation. Tumour frequencies for those xenografts used in this set of experiments are shown in **Table 5**.

Table 5. Tumour initiation frequency of “near patients” xenografts used in this study. Data was kindly provided by Dr. Anne Collins.

Xenograft	pathology	Tumour frequency (95% confidence interval)
Y019	CRPC	1:433 (1:124 – 1:1,515)
Y018	CRPC	1:15,518,198 (1:370,036 – 1:650,786,317)
H027	CRPC	1:28,397 (1:3,089 – 1:202,166)

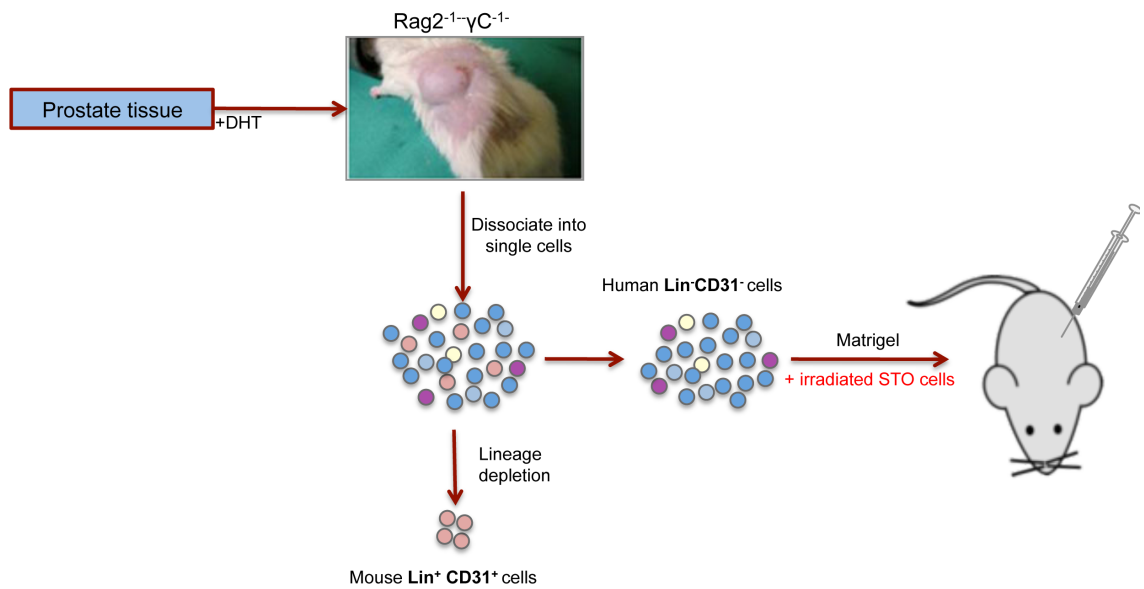


Figure 4.1. **Overview of the *in vivo* protocol to determine the effect of LLL12 on tumour growth.** Serially-transplantable xenografts, maintained in Rag2^{-/-}γC^{-/-} mice, were dissociated into single cells and depleted of mouse Lin⁺/CD31⁺ cells (see section 2.5.2.1) before implanting Lin⁻/CD31⁻ cells back into recipient Rag2^{-/-}γC^{-/-} mice supplemented with slow-release DHT pellets (right flank). Tumour cells were implanted sub-cutaneous in Matrigel together with irradiated STO feeder cells (left flank) in 30 mice as 10 mice per group were used for each experiment.

4.2. Levels of STAT3 phosphorylation in a panel of 'near patient' xenografts

It has been reported that LLL12 is most effective in tumours expressing high levels of pSTAT3 (Lin et al., 2010). Therefore, the levels of pSTAT3 were determined in a panel of 7 'near patient' xenografts.

As shown in Figure 4.2A, three of the xenograft tumours were derived from patients with Gleason grade 7 prostate cancers, and four were from CRPC. Quantification of Western blot analysis for total and pSTAT3 showed that 4/7 xenografts had high levels, compared to the expression of pSTAT3 in primary prostate cells, 2/7 had lower levels of pSTAT3 and one xenograft had undetectable levels of pSTAT3 (Figure 4.2C). Primary prostate cell lysate (which was included as a positive control) expressed one band for pSTAT3. However, the xenograft tumour cells showed two bands for pSTAT3, which are possibly two different isoforms: STAT3 α and STAT3 β (Caldenhoven et al., 1996). The sample with undetectable levels of pSTAT3 (H016) also had undetectable levels of total STAT3 and the β -actin loading control was considerable lower compared to the other xenograft samples. So it could be that insufficient amount of protein was loaded onto the gels, but as the results gave an indication of the pSTAT3 status in the panel of xenografts, no further optimization was performed. There was also no correlation between Gleason grade and pSTAT3 status.

A

Xenograft	Pathology
H024	Gleason 4+3
Y042	Gleason 7
H027	CRPC
Y019	CRPC
H016	CRPC
H042	Gleason 7
Y018	CRPC

B



C

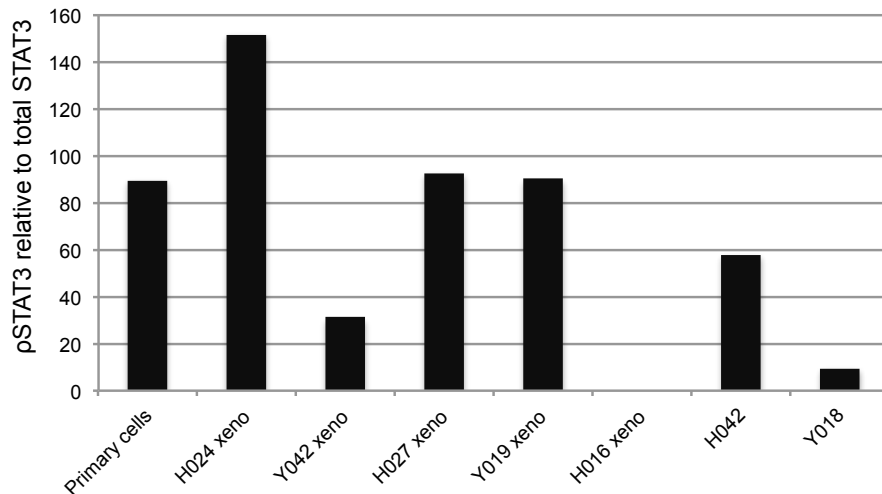


Figure 4.2. **Levels of phosphorylated STAT3 in a series of 'near patient' xenografts.** A. Table of xenografts and the patient's diagnosis, Tx: unable to evaluate Gleason grade of tumour. B. Western blot analysis for pSTAT3, total STAT3 and β-actin (loading control) of several xenograft samples and primary prostate cells derived from a cancer (positive control). C. Quantification of Western blot, which is expressed as for pSTAT3 relative to total STAT3. The amount of protein expressed was quantified using Image J software.

4.3. Inhibition of tumour growth using the pSTAT3 inhibitor LLL12

4.3.1. Treatment of tumours derived from Y019 xenograft with LLL12

The effect of LLL12 on tumour growth of Y019 was determined. This xenograft was chosen because it expresses high levels of pSTAT3 (Figure 4.2). Unfortunately, tumour incidence was particularly low in this experiment (Figure 4.3), and therefore it was impossible to draw any conclusion from this data. Firstly, only 3/10 mice grew tumours in the control group, 5/10 mice in the 2.5 mg/kg LLL12 treatment group and 3/10 in the 5 mg/kg LLL12 treatment group. The tumour volumes for all mice were also asynchronous, although treatment for all groups was started simultaneously. Thus, the relative change (percentage increase) in tumour growth was recorded. This meant that the control group had reached their end point after only 10 days of treatment. Despite these setbacks, it was observed that LLL12 at 5 mg/kg, halted tumour growth, in all 3 mice. Unfortunately, there were serious side effects at this dose and all mice in this group were culled, eight days after treatment. It was clear that there was no significant difference in the growth of tumours between the vehicle control and the group treated with 2.5 mg/kg LLL12 after 8 days of treatment (Figure 4.3). Due to limited number of tumours per group, only 1/3 from the vehicle control group, 5/7 of the 2.5 mg/kg LLL12 treatment group and 1/3 of the 5 mg/kg LLL12 treatment group were analysed by flow cytometry, to determine the basal (CD44⁺) and luminal (CD24⁺) phenotype after treatment.

For flow cytometry, the gating strategy is shown in Figure 4.4. Firstly, doublets and debris were gated out using pulse width (Figure 4.4A) and dead cells were gated out using a live/dead stain (Sytox Blue) (Figure 4.4B). Finally, only cells of the correct size and granularity for epithelial cells were included in the analysis (Figure 4.4C). Prior to flow cytometry the tumour xenografts were depleted for mouse endothelial cells and lineage positive blood cells.

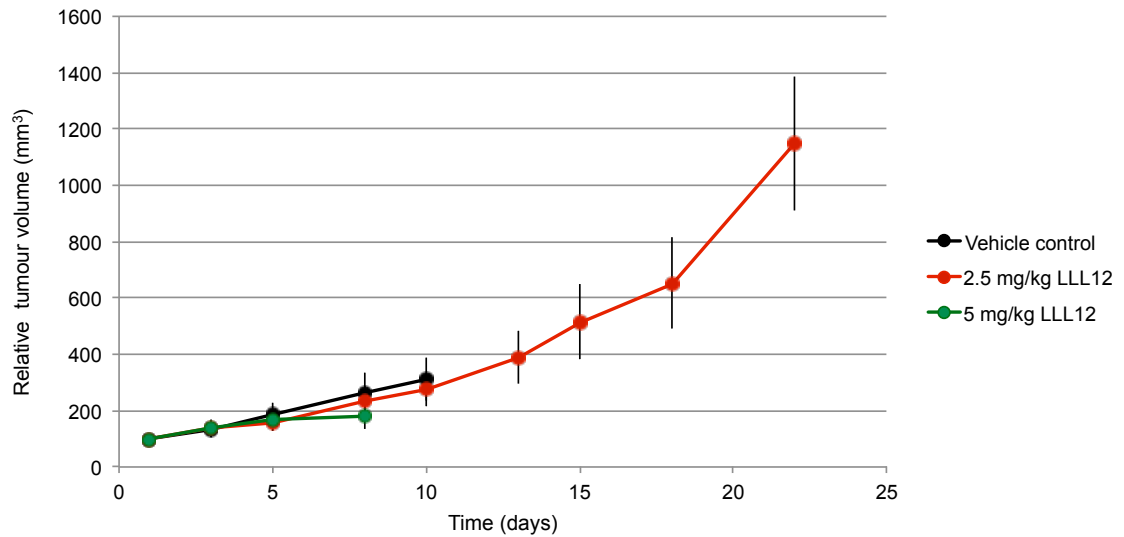


Figure 4.3. **Growth curve of Y019 xenograft after treatment with LLL12.** Mice were injected with 9.4×10^4 human tumour cells, once tumours were approximately 5mm, mice were treated with daily IP injections of either vehicle control (n=3), 2.5 mg/kg LLL12 (n=5) or 5 mg/kg LLL12 (n=3), which started at day 58 post initiation of tumour. Mice treated with 5 mg/kg, fell ill after 8 days of treatment, as these were emaciated and lost > 10% BW, and has to be culled. Tumour volume (mm³) was calculated using the Ellipsoidal formula: $1/2(\text{length} \times \text{width}^2)$. Results are expressed as the percentage increase between each measurement. The starting volume of the tumour was normalized to 100 mm³ to standardize between different tumour volumes. The error bars are represented by the SEM.

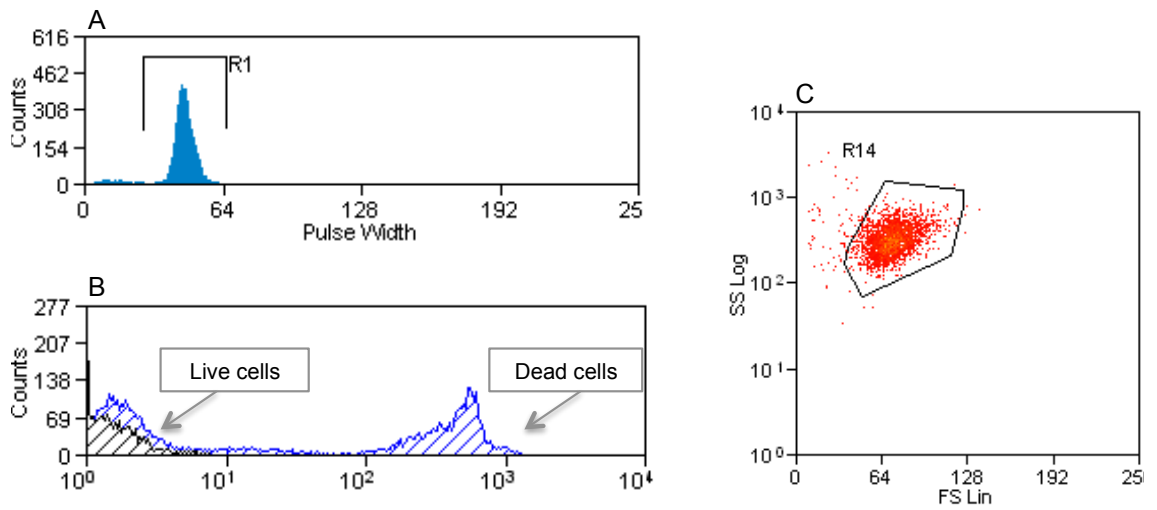


Figure 4.4. **Flow cytometry gating strategy.** Single Lin⁷/CD31⁺ human tumour were labelled for cell surface markers: CD44(-FITC) and CD24(-PE). A. Histogram of pulse width to exclude debris and doublets B. Histogram plot of cells stained with Sytox blue (blue) to exclude dead cells relative to unlabelled cells (black). C. Dot-plot of Forward (cell size) and Side Scatter (cell granularity) to include cells with the correct size and granularity i.e. exclude debris.

Results showed that 2/5 tumours, from the 2.5 mg/kg LLL12 treatment group, had a decrease in CD44⁺ expressing cells compared to the vehicle control, as these samples showed an average of 1.5% CD44⁺ cells (range 0.61– 2.4%), compared to the control, in which 25% of cells expressed CD44⁺. Moreover, in 2/5 tumours from the 2.5 mg/kg LLL12 treatment group, an increase in CD24⁺ content was observed, 13.1% (range 5.2 – 21.4%) compared to 1.9% from the vehicle control (Figure 4.5) (Appendix 6). However this was observed in one tumour control but it does indicate that inhibition of STAT3 phosphorylation potentially changes the cellular composition of the xenograft tumours.

The second xenograft used was H027. However only 1/30 mice formed a tumour. As these ‘near-patient’ xenografts are low passage, they are unpredictable in terms of growth incidence and latency unlike the “classical” cell line models that have been serially transplanted in mice for decades and are likely to bear little resemblance to human prostate cancer (van Weerden et al., 2009).

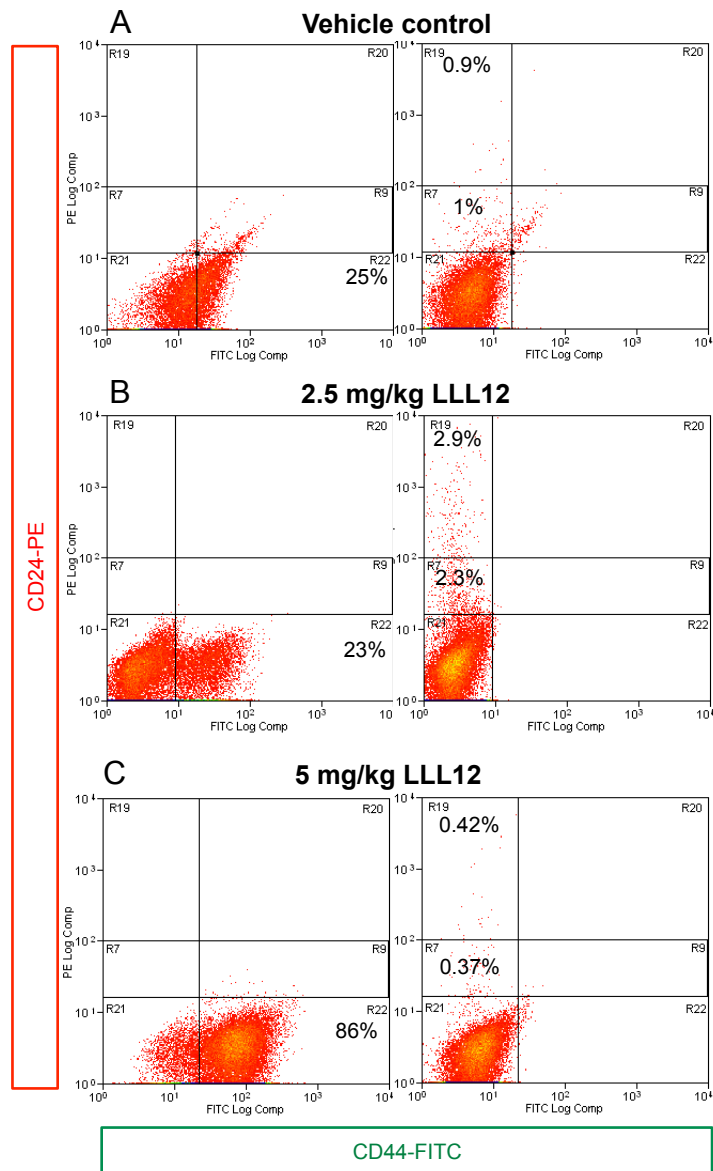


Figure 4.5. **Flow cytometry analysis of Y019 xenograft tumour cells after treatment with LLL12.** Representative flow cytometry analysis of Y019 xenograft tumours, after treatment with vehicle control (n=1), 2.5 mg/kg LLL12 (n=5) and 5 mg/kg LLL12 (n=1). Dot-plots of human Lin⁻ CD31⁻ cells dual labelled for CD44-FITC (x-axis), which labelled the cells with a basal phenotype and CD24-PE (y-axis), which labelled cells with a luminal phenotype. The number of cells expressing each marker was set against an IgG isotype control or cells only control.

4.3.2. Treatment of tumours derived from YO18 xenograft with LLL12

The above experiment was repeated with YO18, which also expresses pSTAT3, but at low levels (Figure 4.2B/C). Tumours were initiated from 3.6×10^5 Lin⁻/CD31⁻ tumour cells, randomized into 10 mice per group. Treatment started when tumours were approximately 5 mm (day 37 after engraftment). 27/30 mice grew tumours, however two mice were too ill (>10% weight loss, emaciated) after three days of treatment with 5 mg/kg LLL12 and had to be taken out of the study. After one-day of recovery for the remaining mice, the dose was lowered to 3.75 mg/kg to minimize this cytotoxic effect. This resulted in 9/10 mice for the vehicle control group, 9/10 mice for the 2.5 mg/kg LLL12 treatment group and 7/10 mice for the 3.75 mg/kg LLL12 treatment group.

The results show that with treatment there was a difference in the rate of tumour growth between the control group and those mice treated with either 2.5 or 3.75 mg/kg LLL12. This was most noticeable at day 15, with a 40 - 50 % difference in tumour volume (Figure 4.6). However this difference in tumour volume was not significant, due to the variability in tumour volume between individual mice, which was most significant in the control group. The results shown in the growth curve are until day 15, however it is worth mentioning that the treatment time did go up to day 39, but after day 15 the number of mice per group declined rapidly and this resulted in inaccurate growth curve due to high variability.

The survival curve shows that the average survival for mice in the control group was 22 days and, 22.5 days for the 2.5 mg/kg LLL12 treatment group and 25 days for the 3.75 mg/kg LLL12 treatment group (Figure 4.7). Although there was a small survival advantage with LLL12 treatment, this was not significant compared to the control.

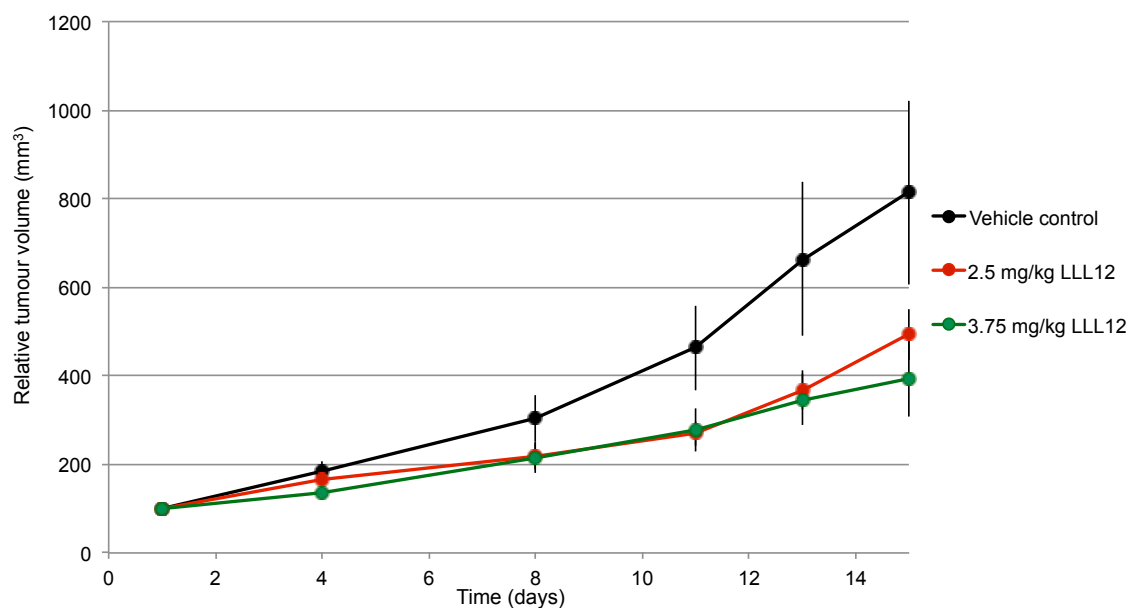


Figure 4.6. **Growth curve of Y018 xenograft after treatment with LLL12.** Mice were injected with 3.6×10^5 human tumour cells, once tumours were approximately 5 mm, mice were treated with daily IP injections of either vehicle control (n=9), 2.5 mg/kg LLL12 (n=9) or 5 mg/kg LLL12 (n=7), which started at day 37 post initiation of tumour. Mice treated with 5 mg/kg, fell ill after 3 days of treatment as these were emaciated and lost > 10% BW, and 2 mice were lost from this group. The treatment dose was lowered to 3.75 mg/kg LLL12. Tumour volume (mm³) was calculated using the Ellipsoidal formula: $1/2(\text{length} \times \text{width}^2)$. Results are expressed as the percentage increase between each measurement. The starting volume of the tumour was normalized to 100 mm³ to standardize between different tumour volumes as starting point. The error bars are represented by the SEM.

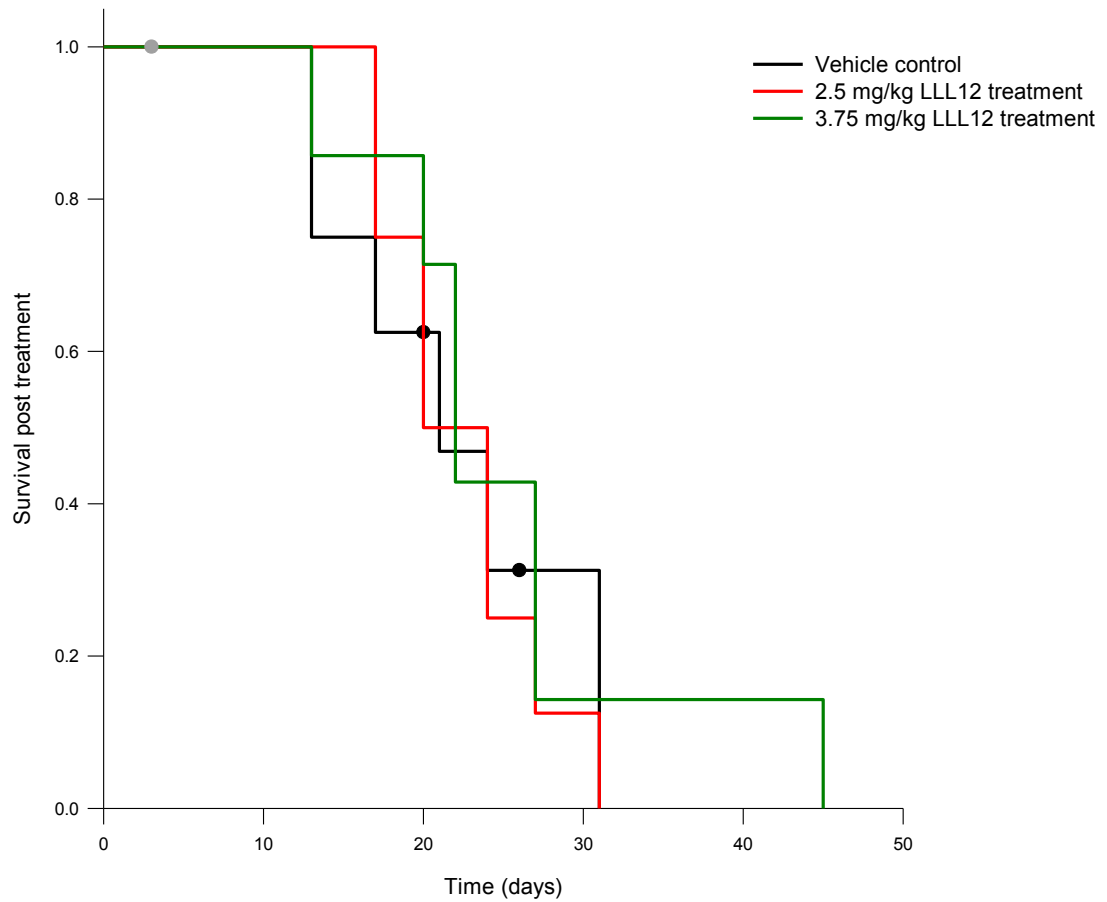


Figure 4.7. **Survival curves of Y018 xenograft after treatment with LLL12.** Mice were injected with 3.6×10^5 human tumour cells, once tumours were approximately 5 mm, mice were treated with daily IP injections of vehicle control, 2.5 mg/kg LLL12 and 3.75 mg/kg LLL12. A Kaplan-Meier curve was generated using Sigma Plot software. Tumours were taken when they reached 15 mm. The dark circles indicate censored mice, due to weight loss with therapy.

4.3.2.1. Histological analysis of Y018 xenograft post treatment

Tumour tissue of Y018 xenograft was analysed by H&E staining to determine if any morphological changes occurred after treatment with LLL12. Representative results are shown in Figure 4.8, the results show that there was no obvious difference in tumour morphology following treatment with LLL12 (Figure 4.8). Xenograft tumours, from each treatment group, had areas of tightly packed tumour cells with areas of obvious necrosis. However, there was no observable difference in necrosis between controls and treatment groups.

4.3.2.2. Flow cytometry analysis of Y018 xenograft post treatment

Using cell surface antigens (CD133, CD44 and CD24), changes in cell content with treatment were analysed: CD44 was used to label the basal cells and CD24 was used to label luminal cells within the xenograft tumours. However, due to high auto fluorescence of cells, which was most apparent in the APC channel (results not shown), we were not able to get enough cell counts for CD133 for an accurate result. Therefore it was decided to focus on the expression of CD44 and CD24, as previous results (section 5.3.1.) suggested that treatment had an effect on the proportion of these cells.

The number of xenograft tumours analysed by flow cytometry were: 4/9 from the vehicle control group, 6/9 from the 2.5 mg/kg LLL12 treatment group and 3/7 from the 3.75 mg/kg LLL12 treatment group (Appendix 7). The remaining tumours retrieved from this experiment were not analysed by flow cytometry as the Lin⁻/CD31⁻ yield was too low.

As shown in Figure 4.4, dead cells were excluded from the analysis, using a live/dead stain. Using these data it was shown that there was a slight increase in percentage of dead cells after treatment with LLL12. The vehicle group showed 45.5% (range 22.7 - 60.8%) cell death, compared to 57% (range 46.2 - 65.2%) in the 2.5 mg/kg treatment group and 56.7% (range 43.3 - 82.5%) in the 3.75 mg/kg LLL12 treatment group. However, this increase of 25% dead cells, after treatment with LLL12 compared to the vehicle control, was not significant (Figure 4.9A).

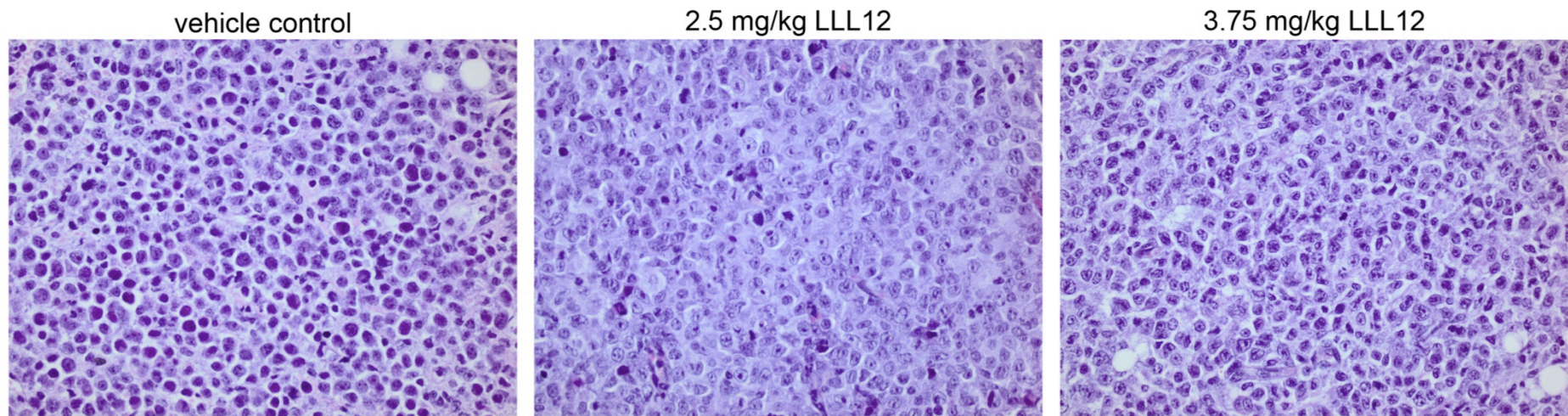
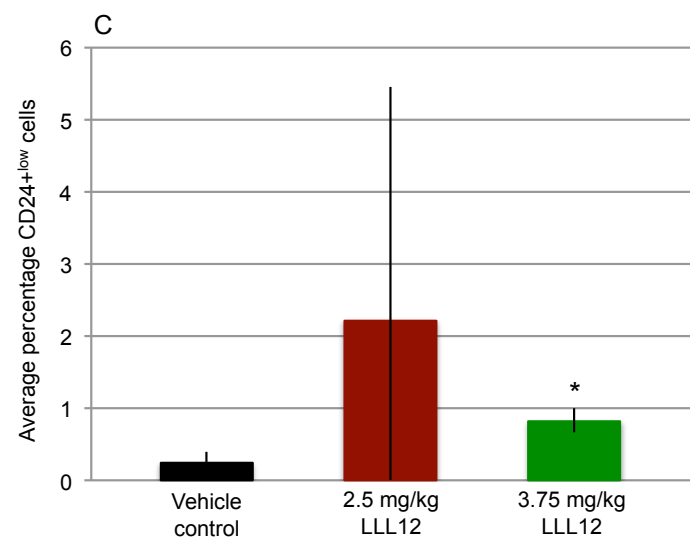
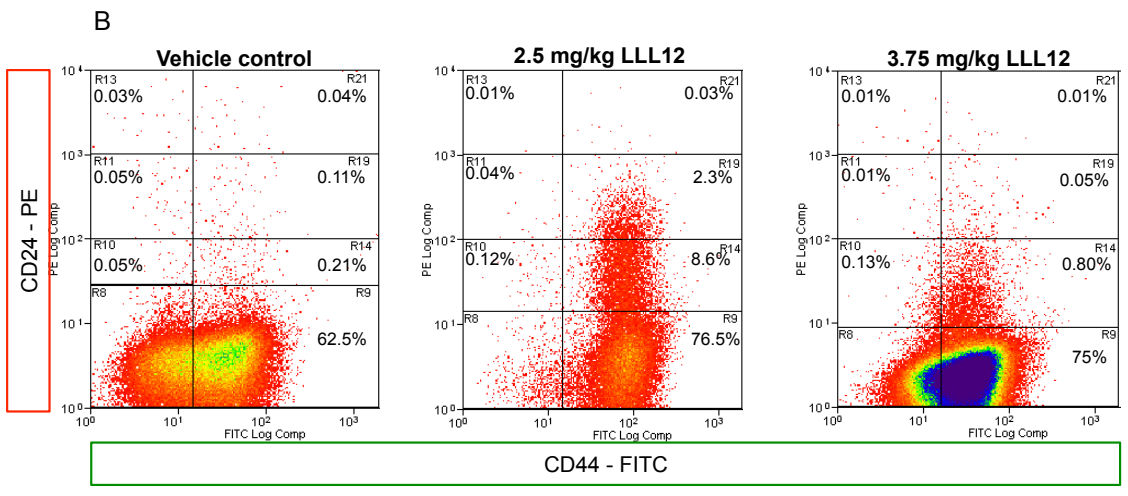
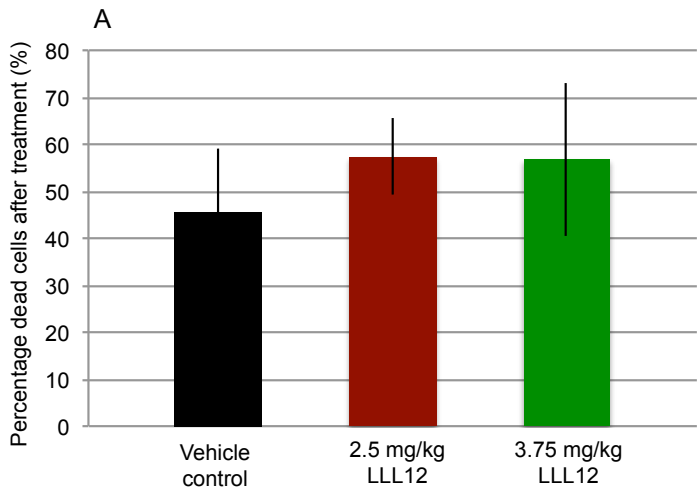


Figure 4.8. **H&E staining of Y018 xenograft paraffin embedded tissue sections.** H&E staining of representative tissue sections of Y018 xenograft tumours after treatment with vehicle control (n=5), 2.5 mg/kg LLL12 (n=8) or 3.75 mg/kg LLL12 (n=6). Images were taken using an Olympus BX51 light microscope at 40x magnification.

The results showed that there was no difference in the number of cells expressing CD44 after LLL12 treatment. CD44 was expressed by ~66% (range 51 – 80%) in the control group, ~70% (range 54 – 86%) in the 2.5 mg/kg LLL12 treatment group and ~64% (range 33 – 85%) in the higher dose of 3.75 mg/kg LLL12 group (Figure 4.9B) (Appendix 7). However, there was a significant difference ($P < 0.05$) in the expression of CD24 after treatment with LLL12. The percentage of cells expressing CD24 in the control group was 0.67% (range 0.25 – 1.12%) compared to a 4-fold increase to 2.84% of the CD24⁺ population (range 0.24 – 11.1%) in the 2.5 mg/kg group and a 2-fold increase to 1.34% (range 1.01 – 1.57%) of the CD24⁺ population in the 3.75 mg/kg LLL12 treatment group (Figure 4.9B). Although there was a 4-fold increase in the percentage of cells expressing CD24 with 2.5mg/kg treatment, this effect was not significant due to the variability in expression between tumours. Only 3/6 tumours showed this increase in CD24 content in this group. In contrast, 2/3 tumours derived from 3.75 mg/kg LLL12 treatment group had increased CD24 content and this effect achieved significance ($P < 0.05$).

The cells expressing CD24 were heterogeneous in the vehicle control, but this increase in CD24 content, with LLL12 treatment, was only observed by cells expressing low levels of CD24 (Figure 4.9B). When comparing the low-expressing CD24 cells (1 decade shift in expression), the difference became more apparent as the percentage of cells in the vehicle control expressing CD24 was 0.24% (range 0.08 – 0.48%) compared to 2.22% in the 2.5 mg/kg LLL12 treatment group, which is a 9-fold increase and 0.83% (range 0.69 – 1%) in the 3.75 mg/kg LLL12 treatment group which is a 3-fold increase in content. 4/6 tumours analysed from the 2.5 mg/kg group and 3/3 from the 3.75 mg/kg LLL12 treatment group showed this increase in CD24 content, which was a significant increase compared to the vehicle control ($P < 0.05$) (Figure 4.9C).

Figure 4.9. Flow cytometry analysis of Y018 xenograft tumour cells after treatment with LLL12. Flow cytometry analysis of Y018 xenograft tumours of vehicle control (n=4), 2.5 mg/kg LLL12 (n=6) and 3.75 mg/kg LLL12 (n=3). A. Percentage of dead cells after treatment with vehicle control or LLL12, using sytox live/dead stain. B. Representative dot-plots of human Lin⁻ CD31⁻ cells dual labeled for CD44-FITC (x-axis), which labelled the cells with a basal phenotype and CD24-PE (y-axis), which labelled cells with a luminal phenotype. Analysis was performed as described in section 5.3.1. The number of cells expressing each marker was set against an IgG isotype control or cells only control. C. Quantification of the percentage of cells expressing CD24 in the vehicle control group (n=4) 2.5 mg/kg LLL12 group (n=6) and the 3.75 mg/kg LLL12 (n=3) group. The error bars represent the standard deviation and a student t-test was performed to test for significance between groups, *P<0.05.



4.3.2.3. Levels of phosphorylated STAT3 in Y018 xenograft post treatment

The levels of phosphorylated STAT3 from Y018 tumours following treatment were analysed by Western blot. 9/9 tumours from the vehicle control group, 8/9 from the 2.5 mg/kg LLL12 treatment group and 8/9 from the 3.75 mg/kg LLL12 treatment group were analysed for levels of pSTAT3.

The results showed that 2/9 tumours from the vehicle control group, 2/8 from the 2.5 mg/kg LLL12 treatment group and 2/8 from the 3.75 mg/kg LLL12 treatment group had detectable levels of pSTAT3 (Figure 4.10). Although the same number of tumours cells ($\sim 2 \times 10^5$) was used to make cell lysates, the protein concentration loaded onto the SDS-PAGE gel was variable as shown by the β -actin loading control. It was therefore difficult to draw any conclusion from this analysis. For example, only 3 of the tumours analysed in the vehicle control group had detectable levels of pSTAT3, Despite treatment, some tumours had detectable levels of pSTAT3; 3 in the 2.5 mg/kg group and 2 in the 3.75 mg/kg group suggesting that in these mice, delivery of the drug was not optimal.

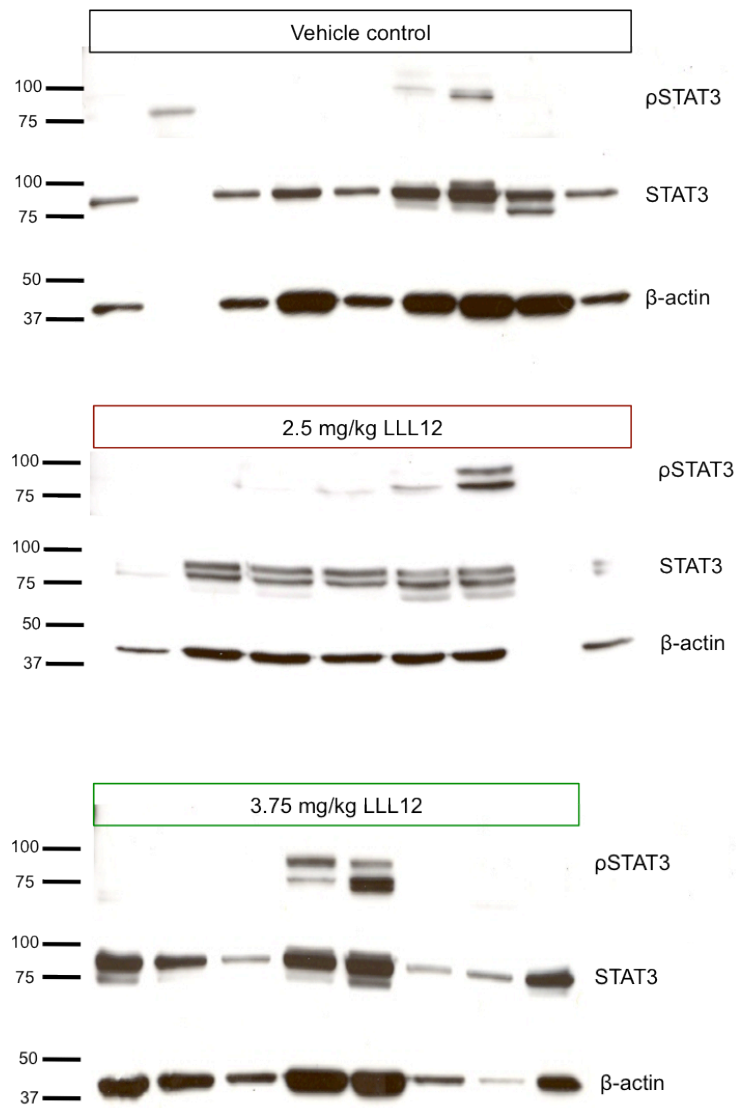


Figure 4.10. **Effect on phosphorylated STAT3 levels after *in vivo* treatment of Y018 xenograft tumours.** Western blot of Lin⁻CD31⁻ tumour cell lysate from xenograft Y018 from the vehicle control group (n=9), 2.5 mg/kg LLL12 group (n=8) and the 3.75 mg/kg LLL12 treatment group (n=8) were loaded onto a SDS-page gel and probed for pSTAT3, total STAT3 and β-actin (loading control).

4.3.3. Flow cytometry analysis for levels of phosphorylated STAT3 in xenograft tumour cells

As shown in Figure 4.10, Western blot analysis was not sensitive enough to detect levels of pSTAT3 in xenograft tumour cells, due to the cell numbers required. Therefore it was decided to detect the levels of pSTAT3 in xenograft tumours by flow cytometry. The protocol is as described previously in section 3.4.3.4 and shown to be successful for primary prostate cells (Figure 3.22C). Analysis of Y018 xenograft (vehicle control) of the previous experiment (section 4.3.2) showed that only 8% of cells expressed pSTAT3 (Figure 4.11A). This appeared to correspond to the results of the initial Western blot for the levels of pSTAT3 in a range of xenografts, shown in Figure 4.2. Further analysis was performed, using a different xenograft, H027, in which pSTAT3 levels were highly expressed as shown previously (Figure 4.2). However, low to undetectable pSTAT3 was observed by flow cytometry (Figure 4.11A). It was therefore likely that the method used to detect pSTAT3 by flow cytometry was suboptimal. Krutzik et al. showed that staining for phospho-proteins should be carried out using a combination of formaldehyde and methanol fixation rather than PFA and saponin as used for the initial analysis on YO18 and H027 xenografts (Figure 4.11A) (Krutzik and Nolan, 2003). Subsequent analysis using this combination of fixation steps resulted in the observation that 96% of YO19 xenograft tumour cells express pSTAT3 (Figure 4.11B). Unfortunately this protocol was only optimized after all the tumours from the previous experiment (section 4.3.2.) had been analysed.

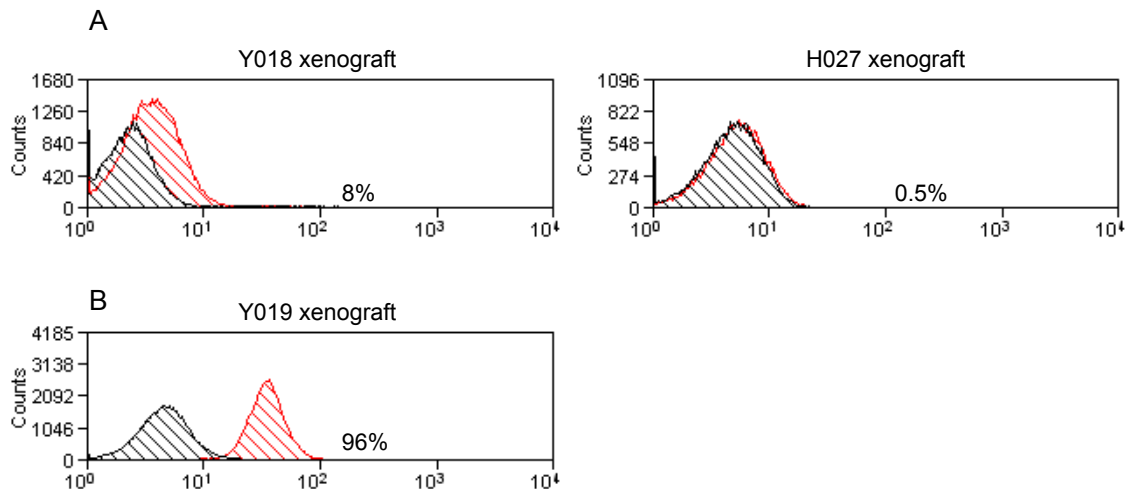


Figure 4.11. Flow cytometry analysis, of xenograft tumour cells, for levels of phosphorylated STAT3. Depleted Lin⁻CD31⁻ human tumour cells from xenografts tumour were labelled for phosphorylated-STAT3 (-APC). A. Cells were fixed with 0.5% paraformaldehyde and permeabilised with 0.05% freshly made saponin from xenograft samples Y018 and H027. B. Cells were fixed with 0.5% formaldehyde and permeabilised with ice-cold methanol from xenograft sample Y019. Cells were subsequently labelled with a pSTAT3-APC antibody (red), and analyses were performed to the unlabelled control (black) after dead cells and debris were gated out.

4.4. Tumour initiation frequency following *ex vivo* treatment of xenograft tumour cells

4.4.1. *Ex vivo* treatment of xenograft cells with LLL12

As shown in a previous experiment, Figure 4.6, there was a modest decrease in tumour growth following treatment with 2.5 and 3.75 mg/kg LLL12, however this decrease was not statistically significant. In that experiment, the effect of LLL12 was observed on established tumours. In this series of experiments, the effect on tumour initiation was studied.

As the *ex vivo* treatment of human tumour cells depleted from xenografts was novel, it was essential to determine whether the cells were viable following *ex vivo* treatment. Therefore tumour cells were treated with DMSO (vehicle control) or LLL12 (10 nM – 10 µM) overnight and the cells were counted using trypan blue exclusion, to exclude dead cells. The results showed that when cells were left untreated, treated with DMSO or 10 nM LLL12, 40% of the cells were still viable. However when cells were treated with 100 nM, 1 µM or 10 µM LLL12 there was a further decrease of 50% in viability to 19, 15 and 13% respectively, compared to the untreated or vehicle control (Figure 4.12). These results were encouraging and the effect of LLL12 on tumour initiation of xenograft cells was carried out.

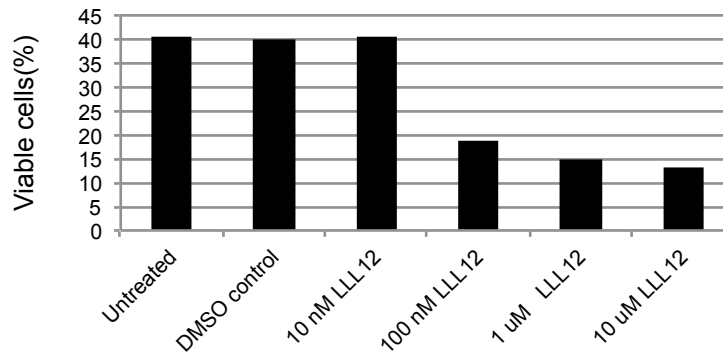


Figure 4.12. **Effect on the viability of xenograft tumour cells, following *ex vivo* treatment.** Lin⁻CD31⁻ human tumour cells were extracted from a serially transplantable YO19 xenograft, treated overnight with 10 nm – 10 μ M LLL12, DMSO or left untreated in SCM. After overnight (16 hours) treatment at 37°C 5%CO₂, the percentage of viable cells was determined using trypan blue exclusion.

4.4.2. Effect of *ex vivo* treatment of the STAT3 inhibitor LLL12 on tumour initiation of Y019 xenograft.

To determine if xenograft tumour cells were able to establish tumours following *ex vivo* treatment with LLL12, tumour cells were injected at limiting dilutions to determine tumour-initiating frequency. The results showed that xenograft tumour cells were still able to initiate tumours after treatment with the vehicle control, but tumours were not observed when cells were pre-treated with 10 μ M LLL12 (**Table 6**). Moreover, the tumour initiating cell frequency of the vehicle control treated cells was very similar to those observed from directly engrafting Y019 Lin⁻/CD31⁻ cells at limiting dilution; 1:1:433 (1:124 - 1:1,515) (results obtained with kind permission from Dr. Anne Collins). Also, the latency was similar: 37 days for directly engrafted cells and 35 days for *ex vivo* treated cells.

Table 6. Tumour initiation frequency of Y019 xenograft, following *ex vivo* treatment.

	10 ⁵	10 ⁴	10 ³	10 ²	10 ¹	Tumour initiation frequency (95% confidence interval)
DMSO control	2/2	2/2	2/2	1/2	0/2	1:161 (1:26 – 1:984)
10 μ M LLL12	0/2	0/2	0/2	0/2	0/2	-

The difference in tumour initiation became more obvious in the survival curve, the effect of *ex vivo* treatment with LLL12 was clearly significant (P<0.05) compared to the vehicle control (Figure 4.13) and also compared to the effect on established tumours (Figure 4.7).

4.4.3. Flow cytometry analysis of xenograft tumours initiated following *ex vivo* treatment

As the establishment of the xenograft tumours following *ex vivo* treatment was a novel approach, it was important to determine if there was a change in the content of different cells by phenotype. Tumours were analysed by flow cytometry for the expression of CD44, CD24 and levels of pSTAT3 as shown in Figure 4.14. Results show that there were 54% CD44 expressing cells and 0.6% CD24 expressing cells. The majority of the cells (80%) also expressed pSTAT3. These levels were similar to the levels observed from tumours that were established from directly engrafted Lin⁻ CD31⁻ human tumour cells (Figure 4.9B, vehicle control).

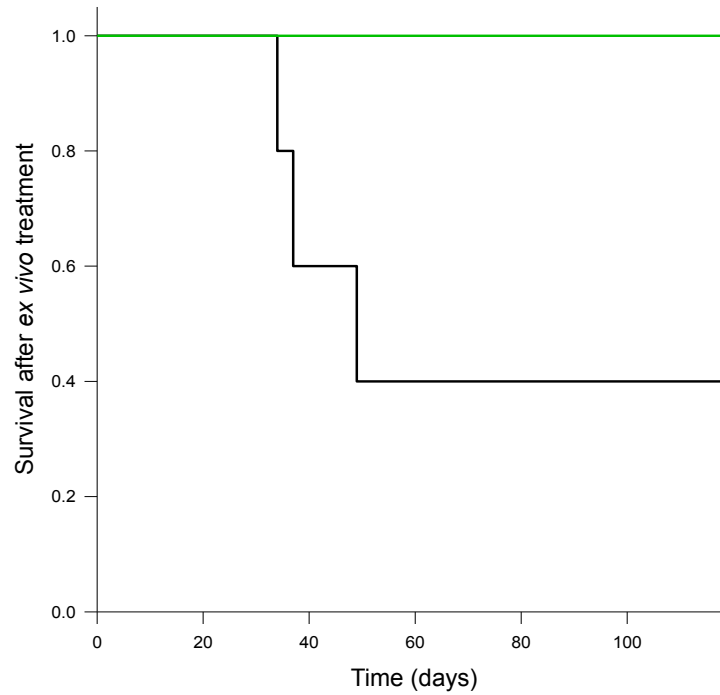


Figure 4.13. **Survival curve of Y019 xenograft, following *ex vivo* treatment of tumour cells.** Xenograft tumours cells were engrafted after overnight treatment with 10 μ M LLL12 or DMSO as vehicle control, tumour cells were then engrafted into Rag2^{-/-} γ C^{-/-} mice at limiting dilutions (10^5 – 10^1 cells). A. Kaplan-Meier survival rate is shown, with LLL12 treated (green) compared to the vehicle control (DMSO) (black). Tumours were followed out to 120 days after engraftment. The Log-Rank test was performed for statistical analysis, $P < 0.05$.

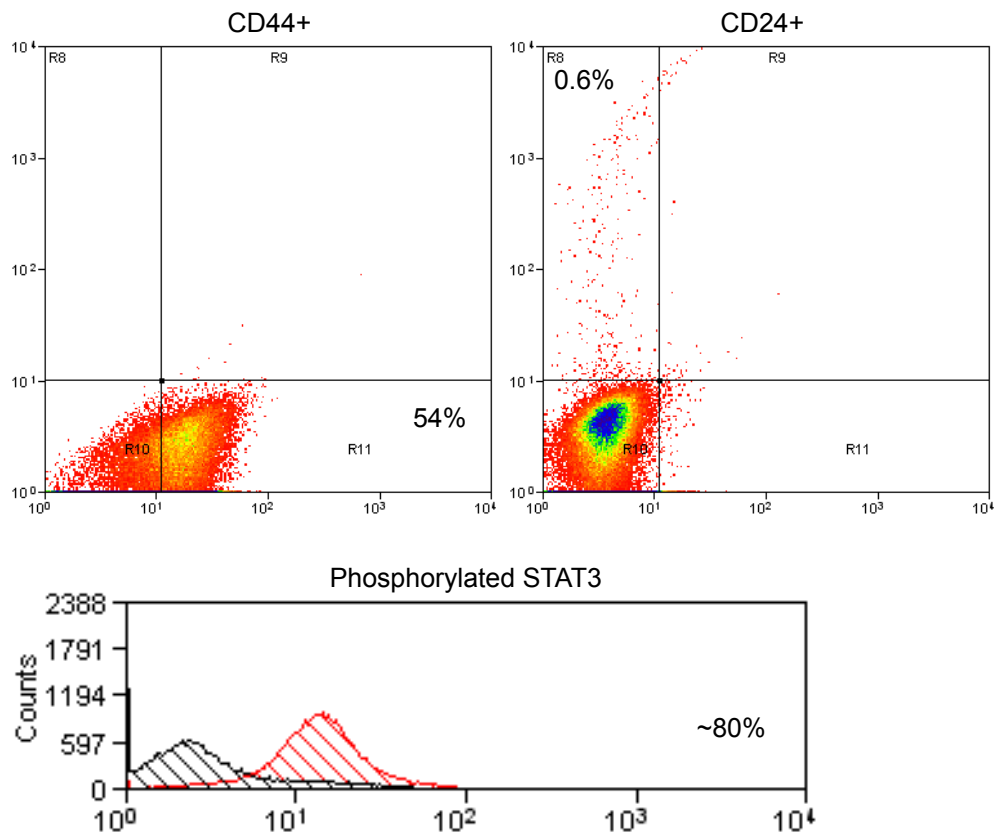


Figure 4.14. **Flow cytometry analysis, of xenograft tumour initiated after overnight *ex vivo* treatment.** Depleted Lin⁻CD31⁻ human tumour cells from Y019 xenograft tumour, which was established after overnight treatment with DMSO, were labelled for CD44 (-FITC), CD24 (-PE) and phosphorylated STAT3 (-APC). Analysis was performed with debris and dead cells gated out, and relative to the unlabelled control. Overlay APC plot shows levels of phosphorylated STAT3 (red) relative to unlabelled control (black).

Chapter 5

Discussion

5. Discussion

The aim of this study was to determine the importance of the JAK-STAT signalling pathway for the maintenance of prostate cancer cells, and more specifically the undifferentiated $\alpha_2\beta_1^{\text{hi}}/\text{CD133}^+$ cells, which are enriched for a more clonogenic and possibly tumour-initiating population. It has already been shown that IL-6, the IL-6 specific receptor gp80 and the activation of the associated JAK-STAT signalling pathway is correlated with prostate cancer progression (Twilley et al., 1995; Hobisch et al., 2000; Mora et al., 2002). However, these studies were carried out on paraffin embedded prostate tissue or prostate cancer cell lines, whilst this study was performed on low-passage primary cell cultures, and 'near-patient' xenografts of prostate cancer, which is likely a better representation of the patient's tumour compared to long-term cultured cell lines and cell line-derived xenografts. Previous work from our laboratory showed that IL-6 is overexpressed in the $\alpha_2\beta_1^{\text{hi}}/\text{CD133}^+$ (stem-like) population (Birnie et al., 2008). Therefore, further analysis was required to validate these findings.

5.1. IL-6 is highly expressed by undifferentiated prostate cancer cells

The results of this study have shown that the most undifferentiated cells (stem-like and TA cells) from a study of hormone-naïve and CRPC primary cultures expressed more IL-6 than the more differentiated CB cells (Figure 3.6). However this difference was only observed at the protein level. This may be due to patient variability and more consistent results might have been obtained if the same samples had been used for both (mRNA and protein) analyses. Due to the limited numbers of passages primary prostate cell cultures can undergo, this could not be achieved. It also became apparent that there was such variability between different patient's samples, with the same disease status, that more samples need to be analysed to confirm these findings.

Nonetheless, this analysis has shown that overall IL-6 expression is higher from hormone-naïve cultures compared to those from CRPC (Figure 3.2 / Figure 3.6). This is in contrast to other studies that show a positive correlation between IL-6 expression and Gleason grade (Twilley et al., 1995; Adler et al., 1999; Drachenberg et al., 1999; Royuela et al., 2004). However, those studies were immunohistochemical analysis of prostate tissue sections, and serum levels of IL-6 in prostate cancer patients. As the majority of cells in a primary culture are basal it is perhaps not surprising that these results do not correlate. Prostate cancer is characterized as an expansion of luminal cells with loss of the basal cells (Nagle et al., 1987). Unfortunately the luminal cells

(from both BPH and cancer samples) cannot be maintained in culture as they are non clonogenic (Collins et al., 2001). Interestingly, Royuelle and colleagues have shown that, in normal prostate tissue, IL-6 staining is mainly observed in the cytoplasm of the luminal cells with low intensity staining of the basal cells. This pattern was also observed in BPH tissue, where IL-6 was mainly observed on the luminal side of the epithelia, suggesting that IL-6 is mainly secreted by the luminal cells (Royuela et al., 2004). Taken together, IL-6 is likely to be secreted by the majority of prostate cancer cells as well as from the inflammatory cells within the microenvironment (Hobisch et al., 2000; Smith et al., 2001; Hodge et al., 2005; Corn, 2012). However, the rare cancer stem-like cells, within the basal population of prostate epithelial cells, also secrete high levels of IL-6 compared to the more committed basal cells (Figure 3.6). It has been accepted that IL-6 is an important growth factor for prostate cancer epithelial cells and IL-6 is clinically significant as elevated levels of IL-6 are associated with poor outcome (Giri et al., 2001; Smith et al., 2001). Nonetheless, the rare cancer stem-like cells also secrete high levels of IL-6, which might act as a survival factor as well as promoting cancer initiation through autocrine signalling. However, as surrounding cancer cells and cells from the tumour microenvironment also secrete IL-6, it is also likely that the cancer stem-like cells signal through paracrine signalling.

As mentioned above, IL-6 levels correlate with disease progression, with IL-6 elevated in serum of patients with (metastatic) prostate cancer (Drachenberg et al., 1999). Moreover it has also been shown that the IL-6 concentration, in prostate cancer tissue, is increased (18-fold) compared to normal prostatic tissue (Giri et al., 2001). This analysis, by Giri and co-workers, was performed on protein extracts prepared from frozen sections (and analysed by ELISA) as compared to this study, where the levels of secreted IL-6 were analysed from cultured basal cells derived from primary samples. Nevertheless, the data shown here confirm that IL-6 is highly expressed in cells derived from prostate cancer samples compared to benign disease.

These data suggest that IL-6 may act as a growth factor for prostate cancer cells, as well as facilitating prostate cancer progression to androgen-independent disease, since IL-6 is able to activate the AR in the absence of androgens (Lin et al., 2001; Lee et al., 2003). It may also be involved in bone metastasis, as the levels of IL-6 are elevated in patients with evident metastases compared to localized prostate cancer (Adler et al., 1999). IL-6 is also overexpressed in other types of malignancies, including multiple myeloma (Klein et al., 1995), renal cell carcinoma (Aoyagi et al., 1996), Kaposi's sarcoma (Aoki et al., 1999), colorectal cancer (Kinoshita et al., 1999); suggesting that IL-6 is involved in basic mechanisms of tumourigenesis. However the molecular and cellular mechanisms by which inflammation influences malignancy is not fully

understood, which explains why treatment with anti-inflammatory drugs has not been fully exploited in prostate cancer (Bardia et al., 2009). This emphasises why further detailed investigation is necessary to understand the involvement of IL-6 in prostate cancer.

It has also been suggested that IL-6 protects prostate cancer cells from cell death induced by certain chemotherapeutic agents, through activation of STAT3 (Lee et al., 2004). This correlates with the expression levels of IL-6 by the stem-like cells from prostate cancer samples, since it has been shown in other tissues that the CSCs are more resistant to chemotherapeutic agents (Murat et al., 2008).

Studies have also shown that IL-6 is important to maintain the “stemness” of adult tissue stem cells. It was demonstrated in a transgenic mouse model of IL-6 overexpression that there was a decrease in proliferation of neuroblasts with enhanced NSC self-renewal (Vallieres et al., 2002). Also, IL-6 enhances proliferation and protects undifferentiated bone marrow-derived MSCs from serum starvation-induced apoptosis, as well as inhibiting differentiation into adipocytes and chondrocytes (Pricola et al., 2009). It has also been shown that IL-6 is secreted by basal-like breast cancer stem cells. As these cells also express high levels of STAT3 this suggests activation of the pathway via an autocrine loop (Marotta et al., 2011). Other reports have also shown that IL-6 is associated with a cancer stem cell phenotype with activation via an autocrine signalling loop (Sansone et al., 2007) or a paracrine feedback loop (Wang et al., 2009a).

5.2. IL-6 receptor is expressed in a rare subpopulation of undifferentiated prostate cancer cells

Although IL-6 is secreted by prostate cancer epithelial cells, and particularly prostate cancer stem-like cells, in order to activate the associated JAK-STAT signalling pathway the cells need to express the IL-6 specific receptor (gp80) (Heinrich et al., 2003). Initially, the presence of the IL-6 receptor, gp80 was detected in cell lines using Western blotting (Figure 3.7). The prostate cancer cell line PC-3 did not express the L-6 receptor, in contrast to other findings (Santer et al., 2010). However Santer and colleagues detected the soluble IL-6 receptor, which might explain the results reported here, in which cell lysates were analysed rather than conditioned medium (Santer et al., 2010).

The IL-6 receptor gp80 was not detected in primary prostate cells when analysed by Western blot (Figure 3.7). However it has been shown that the IL-6 receptor is present in benign and malignant prostate tissue, by immunohistochemistry (Hobisch et al., 2000). Therefore it could be that Western blot analysis was not an appropriate method to detect the IL-6 receptor in unselected primary prostate cells. In addition, Western blot analysis is not sensitive enough to detect protein in the stem-like population, due to limited cell numbers.

It has been shown previously that the majority of the samples tested showed that less than 10% of the basal cells expressed the IL-6 receptor, whilst in most samples that were tested ~50% of the luminal cells expressed the IL-6 receptor. Moreover the IL-6 receptor was expressed in all the prostate cancer samples that were analysed (Hobisch et al., 2000). The results shown in this study confirm these results, as all the secretory luminal cells, in benign prostate tissue, expressed the IL-6 receptor. However, it was also clear that rare cells within the basal layer also expressed the receptor (Figure 3.9C). Although this study shows that in BPH tissue, all the luminal cells express the IL-6 receptor, compared to 50% expression observed by Hobisch (Hobisch et al., 2000), only one benign tissue sample was analysed and quantification of the number of IL-6 receptor positive cells was not performed. Further analysis on prostate tissue sections was not performed, as the aim was to determine if the IL-6 receptor was indeed expressed, and in which cells.

In order to determine which basal cells express the IL-6 receptor, selected cells (from primary prostate cell cultures) were stained for the IL-6 receptor. The initial results show that the IL-6 receptor was present in >60% of the stem cells from benign samples, compared to >90% from a cancer sample (Figure 3.11D). Analysis of more samples is necessary to determine if this is a significant difference. These results also showed that expression of the IL-6 receptor decreased with differentiation, confirming the finding, by IHC, that only rare cells within the basal layer express the IL-6 receptor and explaining why detection of the IL-6 receptor by Western blot was unsuccessful.

Flow cytometry was used to quantify the levels of IL-6 receptor expression. Primary cells were labelled with CD49b, which binds to the basal population and includes the transit amplifying and stem-like cells. The results showed that only a small proportion, 2.3%, of the CD49b-positive cells expressed the IL-6 receptor, whilst ~20% of the CD49b-negative cells, which would include the more differentiated fraction, expressed the IL-6 receptor (Figure 3.12). As CD49b binds all basal cells, the finding that only 2% of this population expresses the IL-6 receptor backs up the data obtained by direct

immunofluorescence staining of selected cells (Figure 3.11). However this does not explain why a proportion (~20%) of the CD49b negative population are IL-6 receptor positive. One explanation for this discrepancy could be the selection process. For flow cytometry, all cells within a primary culture are labelled, whereas for direct immunofluorescence, cells were selected by rapid adherence (20 minutes) to collagen-I. This process would select for stem-like cells and transit amplifying cells only (Collins et al., 2001). The remaining fraction would include all cells not adhering after 20 minutes, but would exclude the cells that had not adhered after 3 hours (when the cells are fixed for antibody staining). As the more differentiated fraction does not adhere to type I collagen; they have less integrins on their cell surface (Collins et al., 2001) and the fraction expressing the IL-6 receptor would not be detected using this method.

Samples labelled with CD133 and analysed by flow cytometry were difficult to analyse due to the rarity of the population. When triple staining this often resulted in 'quenching' of the CD133 signal. Moreover, autofluorescence in the APC channel was also problematic and most likely led to underestimation of the CD133 content. Studies have suggested that flow cytometry staining for CD133 expression is accurate, robust and specific but there are limitations due to the barely detectable levels compared to sorting using microbeads (Clement et al., 2009). Nevertheless, when flow cytometry analysis was performed on pre-selected $\alpha_2\beta_1^{\text{hi}}$ and $\alpha_2\beta_1^{\text{low}}$ cells and dual stained for CD133 and the IL-6 receptor, the results confirmed the results observed by immunofluorescence: i.e. that all the CD133 expressing cells also expressed the IL-6 receptor (Figure 3.14).

This study is the first to show that rare stem-like cells in prostate cancer express the IL-6 receptor as well as secreting high levels of IL-6. These data suggest that IL-6 signalling plays an important role in prostate cancer stem-like cells, possibly via autocrine signalling. As the progenitor transit amplifying and more committed basal cells also secrete IL-6, although to a less extent, it is also possible that the more differentiated cells in prostate cancer support stem-like cell survival via paracrine signalling. These results support the evidence in glioblastoma, in which it was shown that the IL-6 receptor is elevated in GSCs compared to the non-stem glioma cells (Wang et al., 2009a). This study also showed that IL-6 is elevated in the non-stem glioma cells compared to the GSC and it was suggested that there was autocrine IL-6 signalling in GSC as well as paracrine signalling between non-stem glioma cells and GSCs.

The JAK-STAT pathway can also be activated through cytokines other than IL-6, such as LIF and OSM (Heinrich et al., 2003). It has been shown previously that the LIF receptor is exclusively expressed in the epithelium of BPH tissue (Royuela et al.,

2004), but in that study no distinction was made between the basal and secretory luminal cells. Interestingly, their results also showed that the LIF receptor was only expressed in low Gleason grade cancer. Our results show that the LIF receptor is expressed solely on the secretory luminal cells in the normal gland (Figure 3.10). No further analysis was performed on selected populations of prostate cancer cell cultures or tissue as no evidence was found that rare basal cells expressed the receptor.

It has also been shown that the OSM receptor is expressed in prostate (Royuela et al., 2004). Royuela and colleagues found expression in the stromal and epithelial cells of benign prostate tissue by immunohistochemistry (Royuela et al., 2004). However we were not able to reproduce these results, despite using a number of different antibodies; staining was never observed. The study by Royuela does not distinguish between OSM receptor expression in basal or secretory luminal cells. However, as our results have shown that the stem-like cells expressed the IL-6 receptor and these cells also secreted high levels of IL-6, no further investigation toward the LIF- and OSM receptor was performed.

5.3. STAT3 is constitutively activate in primary prostate cells

As IL-6/IL-6R complex is directly associated with the JAK-STAT signalling pathway, we wanted to determine the activation status of this pathway. Binding of IL-6 to the IL-6 receptor initiates activation of JAK kinase, which phosphorylates and activates STATs (Heinrich et al., 2003). There are seven different STAT family members, but IL-6 is only able to activate STAT1 and STAT3 (reviewed in (Ihle, 2001)). Several studies have shown that STAT3 is constitutively active in a variety of human malignancies, including leukaemia (Gouilleux-Gruart et al., 1996), head and neck squamous cell carcinoma (Grandis et al., 1998), melanoma (Niu et al., 2002a), glioblastoma (Rahaman et al., 2002), breast (Garcia et al., 2001), lung (Song et al., 2003), colorectal (Corvinus et al., 2005) and prostate cancer (Dhir et al., 2002; Mora et al., 2002). It has also been shown that STAT3 is constitutively active in lymph node and bone metastases of clinical prostate cancers, so it is thought that STAT3 is involved in the progression of prostate cancer metastasis (Abdulghani et al., 2008).

It has been shown that STAT3 is constitutively active in human prostate tumours, as well as cell lines. Moreover increased levels of activated STAT3 correlates with high Gleason grade prostate cancer (Mora et al., 2002). The results in this study confirm that STAT3 (Tyr705) is constitutively active in several primary prostate cell cultures derived from benign and malignant disease (Figure 3.15). The results also show that 3 out of 5 cancer samples analysed, have higher levels of pSTAT3 compared to two

benign samples analysed. However, the cancer samples from low Gleason grade (3+3) tumours expressed higher levels of pSTAT3 compared to two samples from higher Gleason grade (4+4) tumours, which conflicts with data from Mora and colleagues. However in that study, the levels of pSTAT3 were analysed in prostate cancer tissue samples, which mainly consist of luminal cells (Mora et al., 2002), compared to the levels of pSTAT3 in amplified basal cells, shown in our study. Due to variation between patients it is likely that many more samples should be analysed before drawing any conclusions from this data regarding STAT3 activation and Gleason score in prostate cancer.

In addition to its role in tumorigenesis, STAT3 is also an important regulator of stem cells. It has been shown that STAT3 activation is important for the self-renewal and maintenance of mES cells, although activation is dependent on LIF (Niwa et al., 1998; Matsuda et al., 1999). However STAT3 activation is not required to maintain hES in an undifferentiated state (Daheron et al., 2004; Humphrey et al., 2004; Ying et al., 2008). Furthermore, there is data which suggests that STAT3 activation is important for tissue specific stem cells, such as neural stem cells (Gu et al., 2005) and small-intestine crypt stem cells (Matthews et al., 2011), and more recent studies show the importance of STAT3 activation for cancer stem-like cell populations of glioblastoma (Sherry et al., 2009), breast cancer (Zhou et al., 2007) and liver cancer (Tang et al., 2008). So far, the link between STAT3 activation and prostate cancer stem-like cell maintenance has not been shown.

Unfortunately, we have not been able to show activation of STAT3 in enriched stem-like cells from primary prostate cells. One reason being that Western blot analysis is not sensitive enough to detect protein in the rare stem-like population (0.1%). Another method that was used to detect the levels of pSTAT3 and total STAT3 in cells was a cell-based ELISA. However, this method required at least 10,000 cells and was not sensitive enough to determine the activation status of stem-like cells. Flow cytometry and immunofluorescence are able to detect the expression levels of pSTAT3 at a single cell level. However, at the time of analysis, it would not have been straightforward to detect the levels of pSTAT3 relative to total STAT3 at a single cell level. Since then, kits have become commercially available (Millipore) that allow the monitoring of changes in protein expression and post-translational modification, simultaneously, using flow cytometry. As IL-6 and the IL-6 receptor are highly expressed by the undifferentiated stem-like cells, and STAT3 is constitutively active in whole populations of primary prostate cells it is plausible that the pathway is activated in the stem-like population. However, so far this has not been confirmed.

5.4. Successful inhibition of STAT3 phosphorylation, using an anti-IL-6 antibody and small molecule inhibitor

As STAT3 is constitutively active in prostate cells, in both benign and malignant disease, the effect of inhibiting STAT3 phosphorylation on cell fate was determined. A widely used inhibitor of the JAK-STAT signalling pathway is P6, which is a reversible ATP inhibitor and has been found to inhibit JAKs in the low nanomolar range (IC_{50} , 1 - 15 nmol/L) which is 100-fold more effective than previously developed compounds (Thompson et al., 2002). It has been shown that P6 is able to inhibit pSTAT3 in a variety of malignancies including, prostate cancer cell lines (Pedranzini et al., 2006; Azare et al., 2007; Berishaj et al., 2007; Song et al., 2011). We confirmed that treatment of primary prostate cells, with 5 μ M P6 for 16 hours, resulted in 98% inhibition of STAT3 phosphorylation compared to the vehicle control (Figure 3.16). Those results were from whole cell lysates, but we also wanted to determine if P6 was able to inhibit nuclear translocation of phosphorylated STAT3. This is important as pSTAT3 in the nucleus activates gene transcription, such as activation of SOCS3. SOCS3 is induced via the JAK-STAT signalling pathway and subsequently inhibits STAT3-mediated signal transduction; a classical feedback inhibitor (Starr et al., 1997; Heinrich et al., 2003). The expression of SOCS3 is increased in prostate cancer, suggesting inactivation of JAK-STAT signalling (Puhr et al., 2009), however a patients subgroup have been identified with methylated SOCS3 status and correlated absence of SOCS3 and these patients have an aggressive cancer phenotype and poor prognosis (Pierconti et al., 2011). It has also been shown that another regulator of JAK-STAT signalling, PIA1, is overexpressed in prostate cancer, which has been suggested to act as a regulator of cell proliferation (Hoefler et al., 2012). So even though these proteins are known as tumour suppressors in many types of cancer, the function in prostate cancer appears to be different.

Nevertheless, in order to determine if pSTAT3 is inhibited in the nucleus of primary prostate cells, we used the expression of SOCS3 as a control. Our results show that SOCS3 is expressed in a primary cancer culture (Gleason 3+3), as SOCS3 was not inhibited after 16 hours of treatment with P6, even though inhibition of pSTAT3 in the nucleus was observed. The treatment needed to be extended to 48 hours in order to observe inhibition of the SOCS3 target gene (Figure 3.17). Although this was observed in one sample, the results could not be reproduced in different samples. This was because the staining for the nuclear loading control (TBP) was inconsistent, so the results could not be quantified (results not shown). It is important to determine if inhibitors are able to prevent STAT3 activation and translocation to the nucleus, as this is where it can activate target genes such as SOCS3 but also several proliferating

genes, such as c-myc, and cyclin-D, anti-apoptotic genes such as Bcl-xl and survivin, or angiogenic genes such as vascular endothelial growth factor (VEGF) (Bromberg et al., 1999; Kiuchi et al., 1999; Puthier et al., 1999; Niu et al., 2002b; Gritsko et al., 2006).

One approach to targeting STAT3 is through direct inhibition using antisense or siRNA molecules, or small molecule inhibitors. Another approach would be to target the upstream ligands responsible for STAT3 activation. It has been shown in malignancies, including prostate cancer cell lines, that IL-6 is responsible for activation of STAT3 (Lou et al., 2000; Gao et al., 2007; Grivennikov et al., 2009), which is perhaps not surprising as IL-6 is an inflammatory cytokine and the link between cancer and inflammation has been widely accepted (Coussens and Werb, 2002; De Marzo et al., 2007; Maitland and Collins, 2008a). Moreover, it has been shown that IL-6 is involved in the growth and progression of prostate cancer (Smith and Keller, 2001).

In this study, commercially available neutralizing antibodies were used to target STAT3, but did not result in a significant decrease in pSTAT3 levels, not even when the dose was increased, since the effect of a neutralizing antibody does depend on the amount of ligand being expressed. However, compared to the IgG control, which showed a non-specific effect, there was no decrease in levels of pSTAT3 with a higher dose of neutralizing antibody (Figure 3.18). Most studies have used an anti-IL-6 antibody from Centocor, which is a chimeric monoclonal anti-IL-6 antibody with specific neutralizing activity (Steiner et al., 2006; Guo et al., 2010; Song et al., 2011). CNTO 328 has been used in a number of phase I/II clinical trials including CRPC (Tripathi et al., 2003; Wallner et al., 2006; Fizazi et al., 2012) where it was well tolerated. It was confirmed in this study that CNTO 328 was able to decrease pSTAT3 levels in primary prostate cells (Figure 3.20). These results confirmed that STAT3 is activated upon stimulation of IL-6 in primary prostate cell cultures. The effect of CNTO 328 treatment on prostate cell lines is intriguing. When a subline of LNCaP cells: LNCaP-IL-6⁺, which does not respond to androgen ablation (Hobisch et al., 2001), were treated with CNTO328, an increase in pSTAT3 was observed. However, the growth stimulatory effect of IL-6 in this cell line is associated with stimulation of the MAPK or PI3K pathway (Chung et al., 2000; Steiner et al., 2003). Treatment of LNCaP-IL-6⁺ tumours with CNTO 328, resulted in a decrease in tumour volume, but significance was not achieved. Nonetheless, there was a decrease in the number of Ki67⁺ cells (Steiner et al., 2006). This insignificant decrease in an androgen-independent xenograft, after treatment with CNTO 328, does correlate with results shown in a phase II clinical trial where patients with CRPC were treated with CNTO 328, but did not show an improvement in clinical outcome (Fizazi et al., 2012). It is thought that IL-6 regulates the transformation to CRPC, as an increase in IL-6 has been observed, and IL-6 has

been shown to activate AR mediated gene expression (Chen et al., 2000). It has also been shown that overexpression of IL-6, through activation of STAT3, protects LNCaP cells from undergoing apoptosis induced by androgen deprivation therapy (Lee et al., 2004). However, the underlying molecular mechanisms behind this are poorly understood.

When LuCaP-35 cells and androgen-dependent xenografts were treated with CNTO 328 there was a significant decrease in tumour growth and cell proliferation with an associated increase in apoptosis (Wallner et al., 2006). In this study, the primary prostate cells that showed a decrease in pSTAT3 levels with treatment, were derived from hormone-naïve samples (Figure 3.20). These, and data from other groups, suggest that anti-IL-6 therapy may be beneficial only for a subgroup of prostate cancer patients. In this study it was not investigated whether treatment of primary prostate cells with CNTO 328 resulted in a decrease in proliferation, using Ki67 staining, or if it increased apoptosis. However, there was an effect on the clonogenic ability of hormone-naïve as well as CRPC samples following treatment with CNTO 328 (Figure 3.27). This result confirms other findings in prostate cancer cell lines, in which the proliferative ability was affected (Steiner et al., 2006; Wallner et al., 2006). However for future experiments, it would be interesting to determine CNTO 328 effects on proliferation and apoptosis using primary prostate cancer cells.

As P6 and CNTO 328 are not direct STAT3 inhibitors, a recently developed small molecule that directly targets STAT3, was used. LLL12 has been shown to inhibit constitutively activated STAT3 in a variety of human cancer cells, including breast (Lin et al., 2010) pancreatic cancer (Liu et al., 2011), glioblastoma (Ball et al., 2011) and multiple myeloma (Lin et al., 2012). The results of this study are the first to confirm that LLL12 is able to decrease pSTAT3 levels in primary prostate cancer cells (Figure 3.22). The results also suggest that the cells undergo apoptosis (Figure 3.22A), but this has not been confirmed quantitatively. Nonetheless other studies confirmed that treatment with LLL12 impaired cell proliferation and viability (Ball et al., 2011; Wei et al., 2011; Lin et al., 2012). This is not surprising, as activation of STAT3 plays an essential role in preventing apoptosis through activation of anti-apoptotic proteins (Catlett-Falcone et al., 1999).

5.5. Inhibition of STAT3 phosphorylation resulted in a decrease in the cell survival of the undifferentiated stem-like cells from primary cancer samples

The intention of this study was to determine the importance of STAT3 activation on the fate of the rare stem-like population. Although treatment with STAT3 inhibitors resulted in a significant decrease in pSTAT3 levels in primary prostate cancer cells, there was variability in the effect on colony forming recovery post treatment. There was a distinct difference between the CFE of the stem-like and TA/CB population, and the trend between the TA and CB population was always similar (Figure 3.24). Therefore the selection process was minimized to CD133 selection, resulting in CD133⁺ (stem-like) cells and CD133⁻ (progenitor) cells.

As shown in Figure 3.24A/B, there was a decrease in the colony formation ability of the undifferentiated stem-like cells (CD133⁺) when STAT3 phosphorylation was inhibited using P6, with cells derived from high Gleason grade hormone-naïve prostate cancer. These results suggest that prostate cancer stem-like cells require STAT3 phosphorylation for survival. Interestingly, the progenitor (CD133⁻) cells showed an increase in CFE, suggesting that treatment had increased the number of differentiated TA/CB cell type. However it would be important to determine if these progenitor cells have the properties of cancer stem-like cells, such as tumour initiation and therapy resistance (Dean et al., 2005).

It has been shown previously that CD133⁺ cells from benign prostate undergo fewer population doublings than CD133⁺ cells from primary and metastatic tumours (Collins et al., 2005). It was therefore not surprising that the CFE from the different cell populations derived from benign disease was lower than those from cancers. It has also been shown that the CFE from primary cultures of prostate epithelial cells is very variable; 0.9 – 18% from unselected epithelial cells. (Hudson et al., 2000). Our results confirm these results, as the stem-like cells, derived from primary cancer samples, varied from 0.72 – 20.5 (average 6.4%), when cells were treated with DMSO (control). However to improve the CFE of selected primary prostate epithelial cells, a Rho-ROCK inhibitor was used as it has been shown to improve the CFE of murine prostate stem/progenitor cells (Zhang et al., 2011). As shown in Figure 3.25, treatment with a ROCK inhibitor only showed improvement in the CFE of the TA population. These results indicate that human prostate progenitor cells, and not stem cells, are susceptible to dissociation induced apoptosis.

The increase in colony formation, following treatment with P6, was also observed in Gleason 7 and CRPC samples, in both populations (CD133⁺ and CD133⁻) (Figure 3.24 / Figure 3.26). This is in contrast to a study on multiple myeloma that showed growth inhibition of cancer cells with P6 treatment (Pedranzini et al., 2006). In the study by Pedranzini and colleagues, cell viability decreased by 40% with treatment. There was also a lot of variability between patient's samples, but nonetheless, the results shown here are surprising as it is known that STAT3 activation correlates with prostate cancer progression, and antisense STAT3 oligonucleotides have been shown (in prostate cancer cell lines) to induce growth inhibition and apoptosis (Mora et al., 2002). Moreover, activation of STAT3 increased expression of anti-apoptotic genes (Catlett-Falcone et al., 1999).

In contrast to P6, treatment with either anti-IL-6 antibody or a specific phospho-STAT3 inhibitor (LLL12) did result in a significant decrease ($P < 0.05$) in colony formation efficiency of the stem-like population (Figure 3.27). The differences observed could be due to the lower half-life of P6. P6 is rapidly taken up by cells, and has a half-life of at least 6 hours (Pedranzini et al., 2006), compared to an average of 17.3 days for CNTO 328 (Trikha et al., 2003). As the cells are only pre-treated and not maintained in the presence of the inhibitor for the colony formation assays, it could be that the cells treated with P6 become STAT3 activated again and therefore no significant inhibition of colony formation was observed.

Treatment with the anti-IL-6 antibody (CNTO 328) resulted in a decrease in colony formation in the stem-like population (Figure 3.27). The progenitor (CD133⁻) cells showed more variability but overall there was no significant difference compared to the control. These results are not unexpected as it is thought that the prostate cancer stem-like cells are likely to depend more on IL-6 for survival due to the overexpression of IL-6 in this cell population. These data confirms that the stem-like cells require STAT3 activation, through IL-6, for survival. This is similar to work on Glioma stem cells, although this study used a different approach: an IL-6 specific receptor knockdown. Nevertheless, the results did show that the GSC knockdown cells had a decreased ability to form neurospheres (Wang et al., 2009a).

LLL12 treatment has been shown to inhibit STAT3 activation in breast cancer, medulloblastoma and glioblastoma cell lines (Lin et al., 2010; Ball et al., 2011). Most studies have shown that LLL12 inhibits growth of (unselected) cancer cells, although one study has shown that STAT3 is necessary for the proliferation and survival of cancer initiating cells in colon cancer (Lin et al., 2011).

5.6. *In vivo inhibition of STAT3 phosphorylation, using LLL12, resulted in a decrease in tumour growth*

For decades, preclinical cancer therapeutics have been based on the use of human cancer cell line cultures and of xenografts derived from these cell lines. Neither of these models consistently predict efficacy in clinical trials, resulting in two major barriers to the successful translation of new cancer therapeutics, (1) drug development research is based on these models that ultimately fail in clinical trials and (2) many potentially beneficial therapies that might be valuable in humans are discarded because they fail to show efficacy in these conventional cell cultures and xenograft models (Daniel et al., 2009). Therefore it is important to use a preclinical model that has closer characteristics to the patients' tumour. The unique xenograft model used in this study was established by engrafting fresh prostate biopsies into Rag2^{-/-}γC^{-/-} mice. The xenografts are i) near patient, ii) established from primary tumours and iii) have been derived in NK null mice, which has been shown to result in higher rates of engraftment (Shultz et al., 1995; Goldman et al., 1998). The resulting tumours are largely of an intermediate phenotype (CD44⁺/CD24⁺/AR⁺). The lack of structure within the tumour mass in the xenograft model used in this study is typical of mouse xenografts of prostate cancer (Wang et al., 2005; van Weerden et al., 2009). Nonetheless, it has already been shown that using a patient-derived human tumour tissue xenograft model, more accurately reflects the *in vivo* situation than cancer cell line derived xenografts (Huynh et al., 2006).

With the use of the 'near patient' prostate cancer xenograft model, it was shown that treatment with LLL12, resulted in a modest growth inhibition compared to the vehicle control, however significance was not reached. This was mainly due to the high variability observed between mice, despite using ten mice per group. This modest inhibition in tumour growth with LLL12 was also observed in a variety of other malignancies, including breast cancer, glioblastoma, osteosarcoma and colon cancer (Lin et al., 2010; Lin et al., 2011; Onimoe et al., 2012). To our knowledge, this is the first data that shows inhibition in tumour growth after treatment with LLL12, in prostate cancer xenografts. The results published by other studies, show a growth inhibition of 2.5 – 5 fold following treatment with LLL12. The growth inhibition shown here was very similar; ~2 fold decrease in growth compared to the vehicle control at day 15 (Figure 4.6). Even though the concentration of LLL12, used in this study, was lower (3.75 – 2.5 mg/kg) compared to most studies (10 – 5 mg/kg), as the Rag2^{-/-}γC^{-/-} mice did not tolerate the drug as well as NUDE or NOD/SCID mice (Lin et al., 2011; Onimoe et al., 2012). Also, due to the high variability observed, this 2-fold decrease was not

significant and highlights one disadvantage of using a model, which is 'near patient' as these models are less predictable and much harder to synchronise for growth studies than conventional cell lines. Nonetheless, they are more likely to reflect the patients' tumour and future studies will have to be carried out with more mice per group to reflect this variability. Also, even though the cells were derived from the same xenograft and were set up simultaneously, the established tumours did not synchronize, which made the treatment with LLL12 more challenging. It also resulted in failure of the first two experiments, as only 11/30 and 1/30 mice grew tumours. Nonetheless, with the third experiment (reported here) more success was achieved as 27/30 mice grew tumours.

Due to the low passage of these 'near patients' xenografts, the resultant tumour does accurately reproduce the heterogeneity of the human cancer. However it also results in a model that is somewhat unpredictable in terms of growth incidence and tumour latency, which becomes apparent when setting up a large experiment. This will be one of the challenges that need to be overcome once this model is regularly used for testing preclinical drugs.

Another challenge was that the tumours were asynchronous, this meant that the treatment had to be delayed until enough mice (>5 per group) had measurable tumours. Ideally treatment would start when tumours were 5mm, therefore a compromise had to be found between enough mice per group in order to get enough data, but minimal variation in tumour size. The growth curve was calculated as the relative change in tumour growth (percentage between to measurements), to minimize this effect.

The high variability observed, in tumour growth, within the same treatment groups made it impossible to determine if LLL12 affected tumour growth. Although measurement of tumour size is important in preclinical animal studies when assessing drug response, it is known that calculation of tumour size using direct caliper-based measurements are often affected by errors due to variability in tumour shape, skin thickness and subcutaneous fat layer thickness. It has been shown that microCT scanning is more accurate than external caliper measurements and microPET scanning (Jensen et al., 2008). Unfortunately this technique was not available to us in this study. Therefore, the results were also represented by a Kaplan-Meier survival curve (Figure 4.7). These results show that there was a small survival advantage, after treatment with LLL12, however again significance was not achieved.

Despite the modest effect of STAT3 inhibition on tumour growth the data correlates with results with a number of prostate xenografts: the PC-3 cell line (Smith and Keller,

2001), the LNCaP-IL-6⁺ cell line (Steiner et al., 2006) and LuCAP 35 xenografts (Wallner et al., 2006). Wallner and colleagues have also shown that treatment with CNTO 328 prevents conversion of the androgen-dependent phenotype to an androgen-independent phenotype.

The variation in tumour growth, within the same treatment group, could also be due to the inefficient inhibition of STAT3 phosphorylation. It has been challenging to show the status of STAT3 phosphorylation after treatment, as shown in Figure 4.10. Some of the mice from the control group had undetectable levels of pSTAT3, although this could be due to limited protein concentration. However, pSTAT3 was detected in a number of tumour lysates from the treatment group, suggesting that there is variability in bioavailability of the drug between mice. However there is currently no evidence to suggest that this small molecule is unstable or has poor cell permeability. The Western blot analysis for levels of pSTAT3, on a number of tumour cell lysates, after treatment with LLL12, showed two bands for pSTAT3 (Figure 4.10). This might have been contaminating mouse cells, reacting with the antibody, however it could also be that it represents two STAT3 isoforms: alpha and beta. Whereby the STAT3 α is the full-length isoform and STAT3 β is the truncated isoform, which lacks the C-terminal activation domain and is generally considered the dominant negative form (Caldenhoven et al., 1996). It has also been shown that the STAT3 α isoform seems to modulate IL-6 signalling (Maritano et al., 2004) and STAT3 β has shown to be involved in granulocytic differentiation (Hevehan et al., 2002). So each isoform might have its specific function. However there is no evidence for the differentiation effect in prostate cancer.

STAT3 has also been shown to regulate VEGF expression, which is involved in angiogenic signalling and overexpression of VEGF is involved in prostate cancer metastasis (Balbay et al., 1999). It has been shown in osteosarcoma that *in vivo* treatment with LLL12 resulted in tumour inhibition but also in decreased expression of VEGF (Bid et al., 2012), suggesting that treatment with LLL12 can also decrease the angiogenic activity and potentially prevent metastasis. In this study, the effect of STAT3 inhibition, using LLL12, on the expression of VEGF has not been investigated. However it would be of interest as metastasis is linked to the cells with a stem-like phenotype, and moreover metastasis is the predominant cause of lethality in cancer patients (Patrawala et al., 2006; Visvader and Lindeman, 2008). This would require investigation about the rate of metastasis in our tumour model, which is currently unknown.

5.7. Treatment of Y018 xenograft with LLL12 resulted in an increase in cells with a luminal phenotype

Following treatment with LLL12, there was a significant increase in the number of CD24⁺ cells (Figure 4.9), which is a marker for the luminal cells in prostate tissue. This could also explain why there was only a modest inhibition in tumour growth with LLL12 treatment, as inhibition of STAT3 activation might not result in cell death (in the majority of cells) but instead result in differentiation to a more luminal phenotype. As reported here and supported by others, CSCs secrete high levels of IL-6, and appear to be constitutively active, yet the non-stem cell fraction secrete much lower levels of IL-6 (Marotta et al., 2011). This suggests that the undifferentiated CD44⁺CD24⁻ cells require high levels of pSTAT3 for survival and that these cells differentiate into CD44⁻CD24⁺ cells when the levels of pSTAT3 are decreased.

In vitro inhibition of STAT3 has also been shown to reduce the number of CD44⁺ cells, and this was associated with an increase in apoptosis. This decrease in CD44⁺ was also coupled with an improvement in sensitivity to radiotherapy (Chen et al., 2010). Therefore CD44 promotes the viability of stem-like cells, in addition to marking them (Gotte and Yip, 2006). Our data also shows an increase in cell death after LLL12 treatment but this effect was not significant. This was shown using the percentage dead cells using a live/dead stain. However there was no distinct difference in morphology from the H&E tissue sections, such as necrotic areas (Figure 4.8). Although this does need to be confirmed in a quantifiable manner, using apoptotic markers. That inhibition of STAT3 resulted in cell death is not unexpected, as IL-6/STAT3 signalling activates the regulation of several anti-apoptotic genes.

High levels of activated STAT3 are associated with higher Gleason scores (>7), which is indicative of more aggressive and poorly differentiated tumours (Mora et al., 2002). These poorly differentiated cells express high levels of CD44 (Murant et al., 1997), and this cell population is enriched for prostate cancer tumour stem/progenitor cells (Collins et al., 2005; Patrawala et al., 2006). Our results confirm that inhibition of STAT3 activation can lead to an increase in the number of luminal cells, but there was no decrease in the number of CD44⁺ cells. This was puzzling, but it has been reported that LLL12 treatment is mostly effective in tumours with high levels of pSTAT3 (Lin et al., 2010). Future analysis on tumours with variable levels of pSTAT3 should address this point. It has been shown previously that CD24⁺ cells express high levels of AR and are dependent on AR for their survival (Kyprianou and Isaacs, 1988a; Sar et al., 1990), which means that these cells are susceptible to therapies that target the AR. It has been hypothesised that AR targeted treatments will eradicate the bulk of the non-

tumour-initiating (CD24⁺) cells, whilst the AR-negative cancer stem-like population will be resistant and tumours will regrow (Collins and Maitland, 2006). So therefore it would be important to determine if treatment with LLL12, which resulted in an increase in CD24⁺ expressing cells, results in tumours that are more susceptible to conventional treatment strategies.

Confirmation that inhibition of STAT3 activation, after *in vivo* treatment of an established xenograft tumour, potentially results in more differentiated luminal cells, which are non-tumourigenic, is to carry out secondary tumour formation assays. An increase in CD24⁺ cells would be expected to delay tumour initiation as CD44⁺ cells are able to initiate tumours at low cell numbers compared to CD24⁺ cells (Hurt et al., 2008; Maitland et al., 2011) suggesting that the CD44⁺ fraction contains the cancer stem cell.

5.8. Ex vivo treatment of xenograft tumour cells with LLL12 resulted in improved survival

If STAT3 inhibition does result in differentiation to a non-tumourigenic phenotype, then as mentioned above this would result in a reduction in the frequency of tumour *initiation*. Indeed, it was observed that *ex vivo* treatment with LLL12 resulted in the complete inhibition of tumour formation in the mice. This was not due to cell death after treatment, as trypan blue exclusion was used to determine the percentage of live cells engrafted. The concentration of drug used in this analysis was 10-fold higher to that used for the *in vitro* clonogenic recovery assays, as the initial experiments showed was no difference in cell viability at both concentrations (Figure 4.12). As tumour initiation was completely abolished there is some uncertainty, thus treating the cells with a lower dose is important to determine if this effect can be repeated at a lower dose. The most recent data, performed Dr. Anne Collins, also showed complete abolishment of tumour initiation when xenograft tumour cells were treated *ex vivo* with 5 μ M LLL12. Tumours were only observed from the DMSO-control group and from *ex vivo* treatment with 0.5 and 1 μ M LLL12. Pairwise tests for differences in tumour frequencies determined that treatment with 1 μ M LLL12, but not 0.5mM LLL12 significantly reduced the ability to initiate tumours ($P < 0.01$). Characterisation of tumours, from *ex vivo* treatment 1 μ M LLL12, showed that treatment induced differentiation to a more luminal phenotype as the majority of cells expressed CD24. Interestingly only 1% of the cancer cells expressed pSTAT3 following treatment. These data confirm the initial results shown here (Figure 4.13) and demonstrate that LLL12 is potent at suppressing tumour initiation of human prostate cancer cells *in vivo*.

These results also show that xenograft tumour cells can survive in culture and maintain tumorigenic potential. The latency, tumour initiation frequency and cell content of the established tumour did not change compared to a tumour that was established from directly engrafted Lin⁻/CD31⁻ cells (**Table 6** / Figure 4.14). These results show that treatment can be useful for drug/compound testing in cells derived from 'near patient' xenografts, but it will be important to establish if these xenograft cells can be treated for a longer period of time as certain drug/compounds might require this. This could be an important tool for screening compounds in a more relevant pre-clinical model (Figure 5.1). Especially as we are currently unable to culture primary prostate epithelium long term *in vitro*, and re-xenograft efficiently into Rag2^{-/-}γC^{-/-} mice (Maitland et al., 2011).

The results shown in this study indicate that STAT3 activation is important for prostate cancer stem-like cell survival. This became evident when xenograft tumour cells were unable to initiate tumour growth, after *ex vivo* treatment with a STAT3 inhibitor. If inhibition of STAT3 only has an effect on the survival of the stem-like population, within prostate cancer, it is not surprising that there was no significant inhibition observed on tumour growth of an already established tumour, particularly as this stem cell population is very rare within the bulk population of the tumour. This data also correlates with results shown in phase II clinical trials, whereby patients with CRPC were treated with CNTO 328, but unfortunately did not show any improvement in their overall survival (Dorff et al., 2010; Fizazi et al., 2012).

It will also be important to investigate if *ex vivo* treatment with LLL12 affects all the different cells types within the tumour mass or if a specific population is more susceptible. This can be done by treating unselected cells *ex vivo*, followed by cell sorting and engrafting CD44⁺ and CD24⁺ cells. It has been shown that expression of CD44 is correlated with radio sensitivity (Chen et al., 2010), again suggesting that targeting the CD44⁺CD24⁻ cells could be potential therapeutic target.

Thus, the 'near patient' prostate cancer xenograft model, used in this study, can be used to (1) treat established tumours to determine the effect of newly developed therapeutics on tumour growth, and (2) to determine the effect of therapeutics on the tumour initiation population, which can be done by treating the xenograft tumour cells *ex vivo* prior to engraftment. If there is an effect on the tumour initiation (CSC) population, this will become apparent in the (secondary) tumour formation frequency (Figure 5.1).

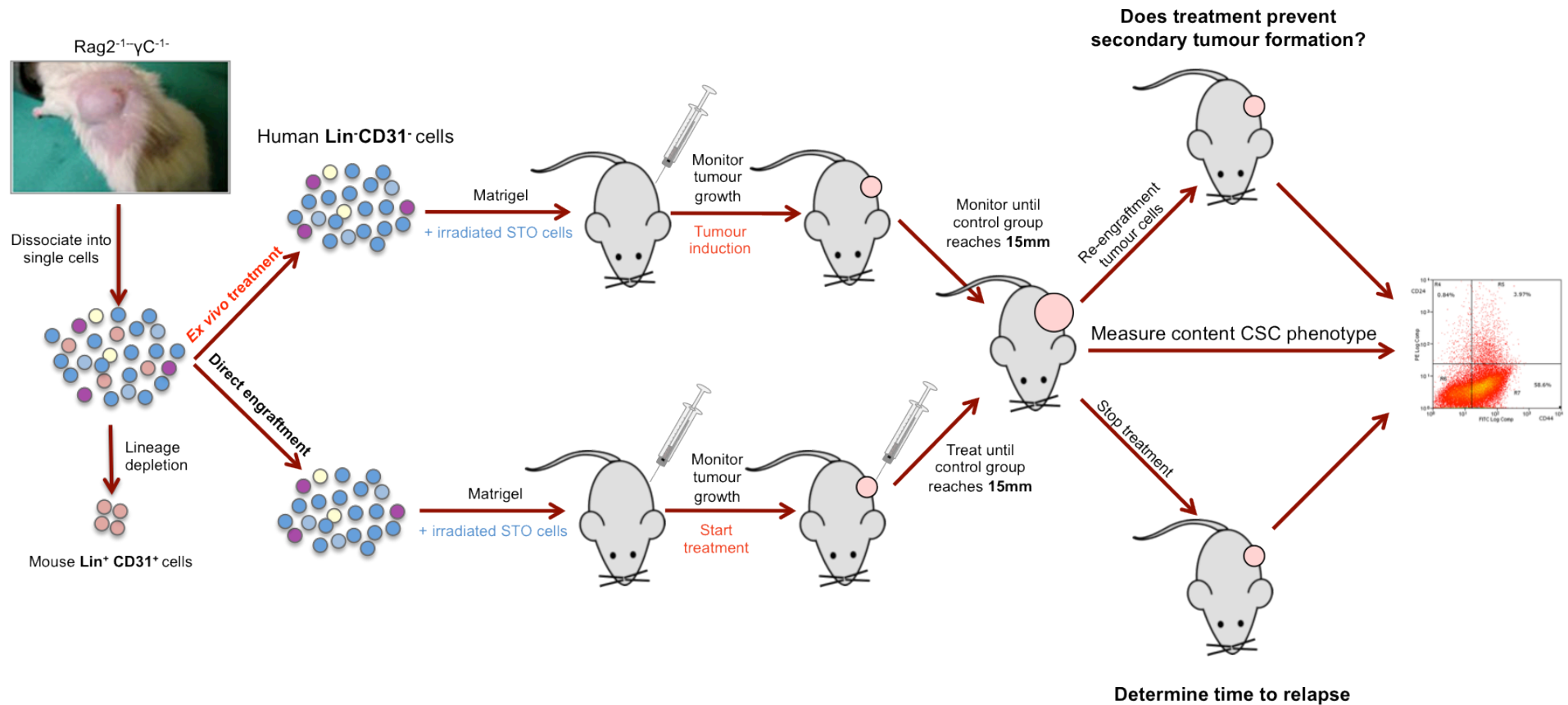


Figure 5.1. **In vivo pre-clinical model for testing prostate cancer stem cells therapeutics.** Serial transplantable ‘near patient’ xenograft tumours are dissociated into single cells and depleted for mouse Lin⁺CD31⁺ cells. The Lin⁻CD31⁻ human tumour cells can either be treated with newly developed therapeutics overnight or directly engrafted back into the Rag2^{-/-}γC^{-/-} mice. Tumour growth will be monitored and treatment starts when the established tumour reaches 5 mm. Once the tumour is 15 mm in size, the Lin⁻CD31⁻ cells will be depleted and analysed for the content of cell phenotypes, re-enuffred for secondary tumour formation, or treatment stopped to determine time to relapse.

5.9. Summary

In this study, evidence has been presented which shows that the stem-like cells from primary prostate samples (cancer and benign disease) have constitutively active JAK-STAT signalling, and that this activation is most likely via IL-6 stimulation. Elevated levels of IL-6 were observed in the prostate cancer stem-like population, which also express the IL-6 receptor, suggest that activation of the JAK-STAT signalling pathway in this population is important for cell survival. More evidence for this hypothesis was demonstrated when cells were treated with anti-IL-6 and small molecule inhibitors against STAT3 (Tyr705), which resulted in a significant reduction in the ability of stem-like cells to form colonies. Moreover, *ex vivo* treatment resulted in an abolition of tumour initiation. This is the first report on the importance of IL-6/STAT3 in cancer stem-like cells in the prostate, and correlates with what has been shown in glioblastoma and colon cancer (Wang et al., 2009a; Lin et al., 2011). The autocrine loop of IL-6 signalling might also play an important role in the transformation to CRPC, as the stem-like cells are protected from undergoing apoptosis during standard of care treatment. As IL-6 is able to activate AR gene expression this could lead to an androgen-independent cell type, which expands in a castrate-resistant tumour. Therefore targeting IL-6 might prevent progression to CRPC as well as eradicating targeting the stem-like cells within the tumour.

A model is proposed in which undifferentiated prostate cancer stem-like cells have high levels of pSTAT3 due to elevated levels of IL-6. Activation of STAT3 can occur either via an autocrine route or paracrine activation via other cell types, such as the progenitor cells or inflammatory cells (Figure 5.2). In this study, the levels of IL-6 or activated STAT3 have not been determined in the secretory luminal cells, but has previously been shown to express the IL-6 receptor. As these cells are difficult to grow in culture and do not engraft, it is impossible to determine their role. Nonetheless, the data presented here supports the evidence supporting a functional role for the high levels of IL-6 and STAT3 activation that is found in more aggressive and advanced prostate tumours.

As STAT3 is activated through an autocrine loop in the undifferentiated stem-like cells, it is likely that these cells require this pathway for their survival. When STAT3 activity is inhibited, these cells can no longer remain in their undifferentiated state and are pushed to differentiate into a more committed cell type. This would mean that treatment with an anti-IL-6 antibody would not result in eradication of the tumour if it was applied as a mono-therapy, as the bulk of tumour cells might not be affected. However once

the undifferentiated stem-like cells are pushed from their tumorigenic phenotype into a more differentiated cell, they could be targeted with conventional treatment.

Our study has provided evidence that inhibiting IL-6/STAT3 signalling should be considered for further exploitations in therapeutic development for patients with prostate cancer. Especially because the outlook for patients with advanced prostate cancer remains poor. This is because the current treatment methods are aimed towards a homogeneous population of cancer cells. Even though scientific evidence has shown that prostate tumours consist of a heterogeneous mass of cells, including a small population of rare cancer stem cells, which are thought to be responsible for tumour initiation, maintenance and metastasis. This study has shown that targeting IL-6/STAT3 signalling may results in the elimination of the prostate cancer stem-like cells and therefore provides a promising approach for treating patients with advanced prostate cancer. Thus, combination treatment strategy might result in a more desirable response to current standard of care therapies.

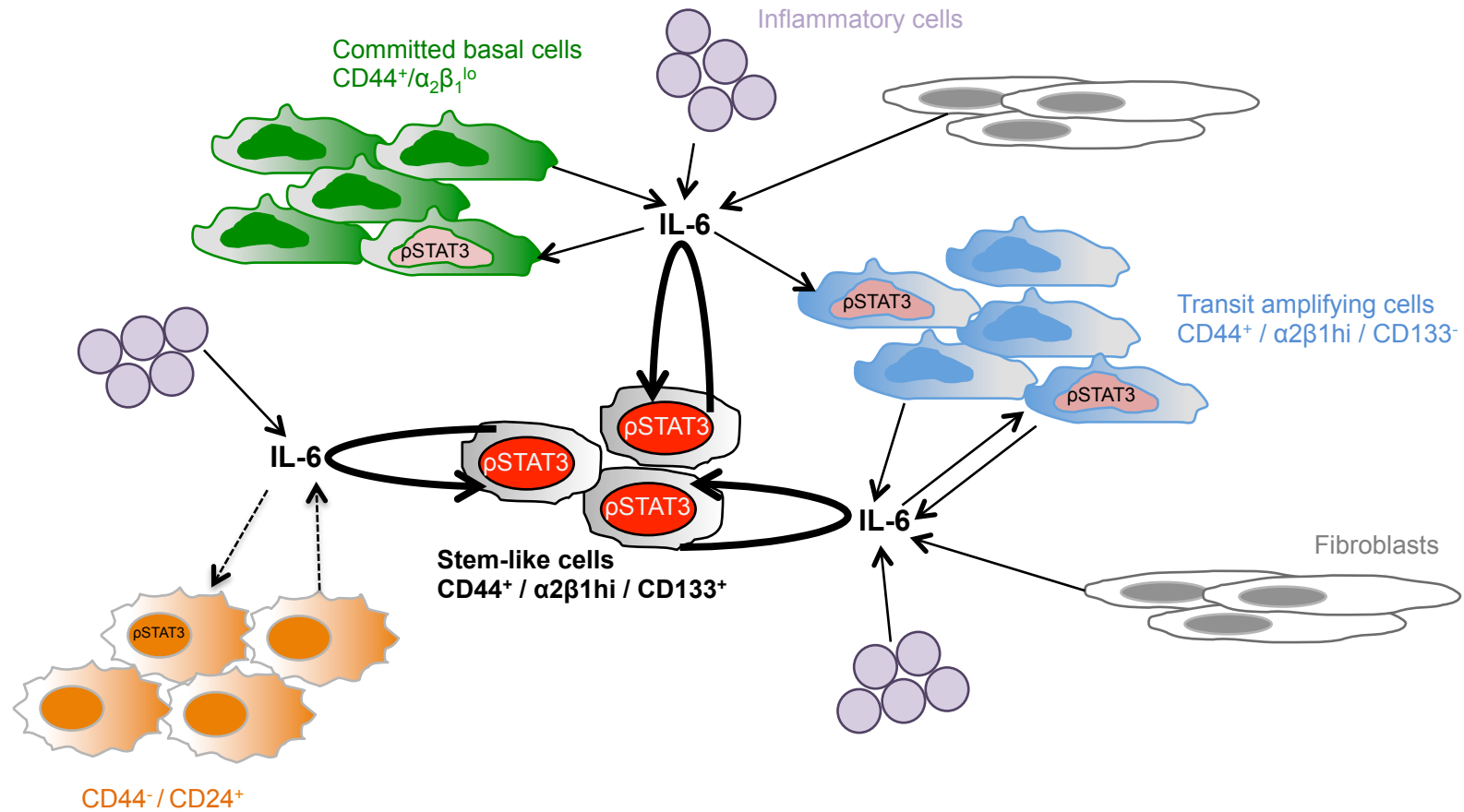


Figure 5.2. **Proposed model of STAT3 activation in prostate cancer.** The $CD44^+/\alpha_2\beta_1^{hi}/CD133^+$ stem-like cells have constitutively pSTAT3 due to the overexpression of IL-6. Other cancer cells types, from the basal and possible luminal cells, are sometimes pSTAT3 activated due to the uptake of IL-6 secreted by themselves, neighbouring cells or inflammatory cells.

Abbreviations

%	percentage
°C	degree celcius
ABM	antibiotic-antimycotic
ACT	alpha-1-antichymotrypsin
AML	acute myeloid leukemia
APC	adenomatous polypopis coli
APC	allophycocyanin
APES	3'aminopropyl triehoxysaline
AR	androgen receptor
ATCC	American Type Culture Collection
ATP	adenosine triphosphate
BCA	bicinchoninic acid
BER	base excision repair
BP	base pair
BPH	benign prostatic hyperplasia
BSA	bovine serum albumin
BSF	biological service facility
BW	body weight
CB	committed basal
CD	cluster designation
CFE	colony formation efficiency
CK	cytokeratins
CLC	cardiotrophin-like cytokine
CNTF	ciliary neutrotrophic factor
CRPC	castrate resistant prostate cancer
CSC	cancer stem cells
CT	cardiotrophin
DAB	3,3'diaminobenzidine
DHT	dihydrotestosterone
DMSO	dimethyl sulfoxide
DNA	deoxyribonucleic acid
DRE	digital rectal examination
DSB	double strand break
DTT	dithiothreitol
ECACC	European Collection of Animal Cell Culture
EGF	epidermal growth factor

ELISA	enzyme-linked immunosorbent assay
ELISPOT	enzyme-linked immunosorbent spot
ES	embryonic stem
EtOH	ethanol
FITC	fluorescein isothiocyanate
FSC	fetal calf serum
g	gram
GAPDH	glyceraldehyde 3-phosphate dehydrogenase
GEMM	genetically engineered mouse model
GM-CSF	granulocyte-macrophage colony-stimulating factor
GP	glycoprotein
GSC	glioblastoma stem cell
Gy	gray
H	hours
H&E	hematoxylin and eosin
HCl	hydrogen chloride
HeLa	Henrietta Lacks
HIFU	high-intensity focussed ultrasound
HPV	human papillomavirus-18
HR	homologous recombination
HS	high sensitivity
hTERT	human telomerase reverse transcriptase
I.E.	id est
IL	Interleukin
INF- γ	interferon gamma
IP	intraperitoneal
JAK	janus kinase
Kg	kilogram
KSFM	keratinocyte serum-free medium
LIF	leukemia inhibitory factor
LPS	Lypopolysaccharide
LSM	lymphocyte separation medium
LUTS	lower urinary tract symptoms
m	marker
M	molair
MeOH	methanol
mg	milligram
mL	millilitre

mm	millimetre
MMR	mismatch repair
NBT/BCIP	nitro-blue tetrazolium chloride/5-bromo-4-chloro-3'-indolyphosphatase p-toluidine salt
NER	nucleotide excision repair
NF-κB	nuclear factor-kappaB
ng	nano
NK	natural killer
OSM	oncostatin m
P	P-value
P6	Pyridone-6
PAP	prostatic acid phosphatase
PBS	phosphate buffered saline
PE	phycoerythrin
PEG400	poly(ethylene glycol)400
PFA	paraformaldehyde
PIA	proliferative inflammatory atrophy
PIA	protein inhibitor of activated STATs
PIN	prostate intraepithelial neoplastic
PSA	prostate specific antigen
PTEN	phosphatase and tensin homolog
PTP	protein tyrosine phosphatase
R	receptor
RFU	relative fluorescent units
RNA	ribonucleic acid
RNA	ribonucleic acid
ROCK	rho-associated kinase
RPM	revolutions per minute
RPMI	roswell park memorial institute-1640
RT	room temperature
S	soluble
SC	stem cells
SCM	stem cell medium
SDS	sodium dodecyl sulphate
SDS-PAGE	sodium dodecyl sulphate polyacrylamide gel electrophoresis
SEM	standard error of mean
sh	short hairpin
SNP	single nucleotide polymorphisms

SOCS	suppressor of cytokine signaling
STAT	signal transducer and activator of transcription
STO	a continuous line of SIM mouse embryonic fibroblasts
SV40	simian virus
TA	transit amplifying
TAM	tumour associated macrophages
TBP	tata binding protein
TBS	tris-buffered saline
TBS-T	tris-buffered saline / 0.1% tween-20
TF	technology facility
TRAMP	transgenic adenocarcinoma of the mouse prostate
TRUS	transrectal ultrasonography
TURP	transurethral resection of the prostate
TYK	tyrosine-kinase
U	unit
UK	United Kingdom
UMG	urogenital sinus mesenchyme
UT	untreated
V	volt
v/v	volume to volume
VEGF	vascular endothelial growth factor
w/v	weight to volume
α	alpha
β	beta
μ	micro
ρ	phosphorylated

Appendices

Appendix 1. List of Medium

Name	Content
H7	Ham's F-12 medium (Lonza) 7% FSC (PAA) 2 mM L-glutamine (Invitrogen)
K2	Keratinocyte Serum-Free Medium (Invitrogen) 2% FCS 2mM L-glutamine 5 ng/mL EGF (Invitrogen) 50 µg/mL bovine pituitary extract (Invitrogen)
R5	Roswell Park Memorial Institute 1640 (Invitrogen) 5% FSC 2 mM L-glutamine
R10	Roswell Park Memorial Institute 1640 10% FCS 2mM L-glutamine
SCM	Keratincoty Serum-Free Medium 5 ng/mL EGF 50 µg/mL bovine pituitary extract 2 mM L-Glutamine 2 ng/mL stem cell factor (First Link) 1 ng/mL GM-CSF (Miltenyi Biotec) 100 ng/mL cholera toxin (Sigma-Aldrich)

Appendix 2. Details of Patients' samples used in the *in vitro* experiments

	Patient ID	Age	Operation	Diagnosis
Figure 13 Optimisation of RT-PCR analysis	PEY025/07	68	R	Cancer Gleason 8 (4+4)
	PEY028/07	72	T	Cancer Gleason 8 (4+4) on hormones
	PEY006/09	82	T	Benign
	PEH016/09	-	R	Cancer Gleason 7
Figure 14 Overall levels of IL-6 mRNA, by qRT-PCR	PE690	79	C	Benign
	PE693	75	T	Benign
	PEY006/09	82	T	Benign
	PEY081/06	63	C	Benign
	PEY082/06	73	C	Benign
	PE434	59	R	Cancer Gleason 8/9
	PE525	63	R	Cancer Gleason 8 (4+4)
	PE550	65	R	Cancer Gleason 8 (4+4)
	PEH016/09	-	R	Cancer Gleason 7
	PEY025/07	68	R	Cancer Gleason 8 (4+4)
	PE704	64	T	Cancer Gleason 7 (4+3) on hormones
	PEY091/09	81	T	Cancer on hormones
	PEY028/07	72	T	Cancer Gleason 8 (4+4) on hormones
	Figure 15 ELISPOT analysis	PEY002/08	67	R
Figure 16 and 17 Optimisation of ELISA	PEY090/09	80	T	Cancer on hormones
	PEY035/09	83	T	Benign
	PE667	47	R	Cancer Gleason 6 (3+3)
	PEY091/09	81	T	Cancer on hormones
Figure 19 Overall results of IL-6 protein level, by ELISA	PEY030/09	70	T	Benign
	PEY035/09	83	T	Benign
	PEY047/09	60	T	Benign
	PEY088/09	71	T	Benign
	PEY006/09	82	T	Benign
	PE360	64	R	Cancer Gleason 6 (3+3)
	PE519	79	C	Cancer Gleason 6 (3+3)
	PE524	56	R	Cancer Gleason 6 (3+3)
	PE531	57	R	Cancer Gleason 9 (4+5)
	PE667	47	R	Cancer Gleason 6 (3+3)

	PE671	62	R	Cancer Gleason 7 (3+4)
	PEH016/09	-	R	Cancer Gleason 7
	PEY061/06	70	R	Cancer Gleason 6 (3+3)
	PEY020/10	54	T	Cancer on hormones
	PEY090/09	80	T	Cancer on hormones
	PEY091/09	81	T	Cancer on hormones
Figure 19 Western blot for the IL-6 receptor	PEY008/08	62	T	Benign
	PEY042/08	75	T	Benign
Figure 20 IHC for the IL-6 receptor	PEY109/06	70	T	Benign
Figure 21 IF for CK5 and IL-6R on tissue	PEY109/09	70	T	Benign
Figure 22 IHC for the LIF receptor	PEY109/09	70	T	Benign
Figure 23 Immunofluorescence for the IL-6 receptor on selected cells	PEH030/10	-	C	Benign
	PE671	62	R	Cancer Gleason 7 (3+4)
	PEY025/11	75	T	Benign
Figure 24 - 26 Flow cytometry for the IL-6 receptor and CD133 expressing cells	PE531 (x2)	57	R	Cancer Gleason 9 (4+5)
	PE524	56	R	Cancer Gleason 6 (3+3)
	PE569	67	R	Cancer Gleason 8 (3+5)
Figure 27 Western blot analysis for levels of pSTAT3 in primary prostate cells	PEY042/08	75	T	Benign
	PEY006/09	82	T	Benign
	PEY107/06	68	R	Cancer Gleason 6 (3+3)
	PEY008/06	59	R	Cancer Gleason 6 (3+3)
	PEY025/07	68	R	Cancer Gleason 8 (4+4)
	PEY028/07	72	T	Cancer Gleason 8 (4+4) on hormones
	PEH008/08	-	R	Cancer
Figure 28 Inhibition of pSTAT3 with P6	PEY020/10	54	T	Cancer on hormones
	PEH047/11	-	R	Cancer Gleason 9 (4+5)
	PEH069/11	65	R	Cancer Gleason 7 (3+4)
Figure 29 Time course treatment with P6	PE524	56	R	Cancer Gleason 6 (3+3)
Figure 30 Treatment with neutralizing Abs	PE531	57	R	Cancer Gleason 9 (4+5)
	PEH050/11	-	T	Cancer Gleason 7 (3+4)
Figure 31 Optimisation of CNTO 328	PEH052/11	-	R	Cancer Gleason 7 (3+4)
Figure 32 Treatment with CNTO 328	PEH052/11	-	R	Cancer Gleason 7 (3+4)
	PEH047/11	-	R	Cancer Gleason 9 (4+5)

	PEH069/11	65	R	Cancer Gleason 7 (3+4)
Figure 33 Optimisation of LLL12	PEH052/11	-	R	Cancer Gleason 7 (3+4)
Figure 34 Western blot and flow cytometry after LLL12 treatment	PEY055/11	76	T	Benign
	PEH020/11	58	R	Cancer Gleason 6 (3+3)
Figure 35 Images of cell colonies	PE531	57	R	Cancer Gleason 9 (4+5)
Figure 36 Colony formation assay after treatment with P6	PE531	57	R	Cancer Gleason 9 (4+5)
	PE671	62	R	Cancer Gleason 7 (3+4)
	PEY006/09	82	T	Benign
Figure 37 Colony formation assay with/without rho-ROCK inhibitor	PEH035/11	-	R	Cancer Gleason 7 (3+4)
Figure 38 Overall results of colony formation assay following treatment with P6, relative to DMSO (control)	PE531	57	R	Cancer Gleason 9 (4+5)
	PEH039/11	-	R	Cancer Gleason 9 (4+5)
	PEH047/11	-	R	Cancer Gleason 9 (4+5)
	PE671	62	R	Cancer Gleason 7 (3+4)
	PEH035/11	-	R	Cancer Gleason 7 (3+4)
	PEH043/11	-	R	Cancer Gleason 7 (4+3)
	PEH044/11	-	R	Cancer Gleason 7 (3+4)
	PEH050/11	-	T	Cancer Gleason 7 (3+4)
	PEH051/11	-	R	Cancer Gleason 7 (3+4)
	PEH087/11	68	R	Cancer
	PEH116/11	64	R	Cancer Gleason 7 (3+4)
	PEY089/09	85	T	Cancer on hormones
	PEY062/11	61	T	Cancer Gleason 9 (5+4) on hormones
	PEH135/11	56	T	Cancer Gleason 9 (5+4) on hormones
	PEH149/11	-	R	Cancer Gleason 9 (4+5) on hormones
Figure 39 Overall results of colony formation assay following treatment with CNTO 328 and LLL12	PEH046/11	-	R	Cancer Gleason 8 (3+5)
	PEH47/11	-	R	Cancer Gleason 9 (4+5)
	PEH149/11	-	R	Cancer Gleason 9 (4+5) on hormones
	PEY062/11	61	T	Cancer Gleason 9 (5+4) on hormones

Appendix 3. List of Primers

Table A. PCR primers

Name	Primer sequence 5' to 3'
IL-6 F	TCT GGA TTC AAT GAG GAG AC
IL-6 R	TGA GAT GAG TTG TCA TGT CC
GAPDH sense	AAG GTG AAG GTC GGA GTC AA
GAPDH antisense	GGA CAC GGA AGG CCA TGC CA

Table B. TaqMan gene expression array

Target	TaqMan® Gene Expression Assay	Dye
IL-6	Hs00174131_m1	FAM
RPLP0	Hs99999902_m1	FAM

Appendix 4. List of antibodies

Table A. Primary antibodies

Target	Isotype	Clone	Manufacturer	Application	Concentration
β -actin	Mouse mAb	AC-74	Sigma #A5316	WB	1:10,000
CD133/2-APC	Mouse mAb	293/C3	Miltenyi Biotec	FC	1:10
CD24-PE	Mouse mAb IgG1	32D12	Miltenyi Biotec	FC	1:10
CD44-FITC	Mouse mAb IgG1	DB105	Miltenyi Biotec	FC	1:10
CD49b-PE	IgG1	AK7	AbD serotec #MCA743PET	FC	1:10
CK5	Mouse mAb IgG1	XM26	Vector Laboratories VP-C400	IHC	1:100
Anti-IL-6	Mouse IgG1	6708	R&D systems MAB206	N	5-50 μ g/mL
IL-6R-FITC	Mouse mAb	B-R6	Abcam	FC	10 μ L for 10 ⁶ cells
IL-6R	Mouse mAb IgG1	17506	R&D systems MAB227	WB	1:500
IL-6R α	Rabbit	C-20	Santa Cruz Biotechnology	IHC IF FC	1:50-1:100 1:50-1:100 1:10
Anti-OSM	Mouse IgG2a	17001	R&D systems MAB295	N	5-50 μ g/mL
OSM-R	Goat IgG	Not provided	Santa Cruz biotechnology	IHC	1:100 – 1:25
OSM-R	Mouse IgG1	469221	R&D systems MAB4389	IHC	1:100 – 1:25
Anti-LIF	Goat IgG	Not provided	R&D systems AB-250-NA	N	5-50 μ g/mL
LIF-R α	Goat IgG	Not provided	R&D systems AF-249-NA	IHC	1:50
Pan cytokeratin	Mouse mAb	mixture	Sigma C2562	IHC	1:800
PhosphoSTAT3 (Tyr705)	Mouse mAb IgG1	not provided	Cell signalling #9138	WB	1:500
PhosphoSTAT3 (Tyr705) - alexa 647	Mouse mAb	not provided	BD Pharmingen #557815	FC	20 μ L per test
STAT3	Rabbit	not provided	Cell signalling #9132	WB	1:1000
Tata-binding protein	Mouse mAb IgG1	1TBP18	Abcam #Ab818	WB	1:3000

Table B. Negative control antibodies

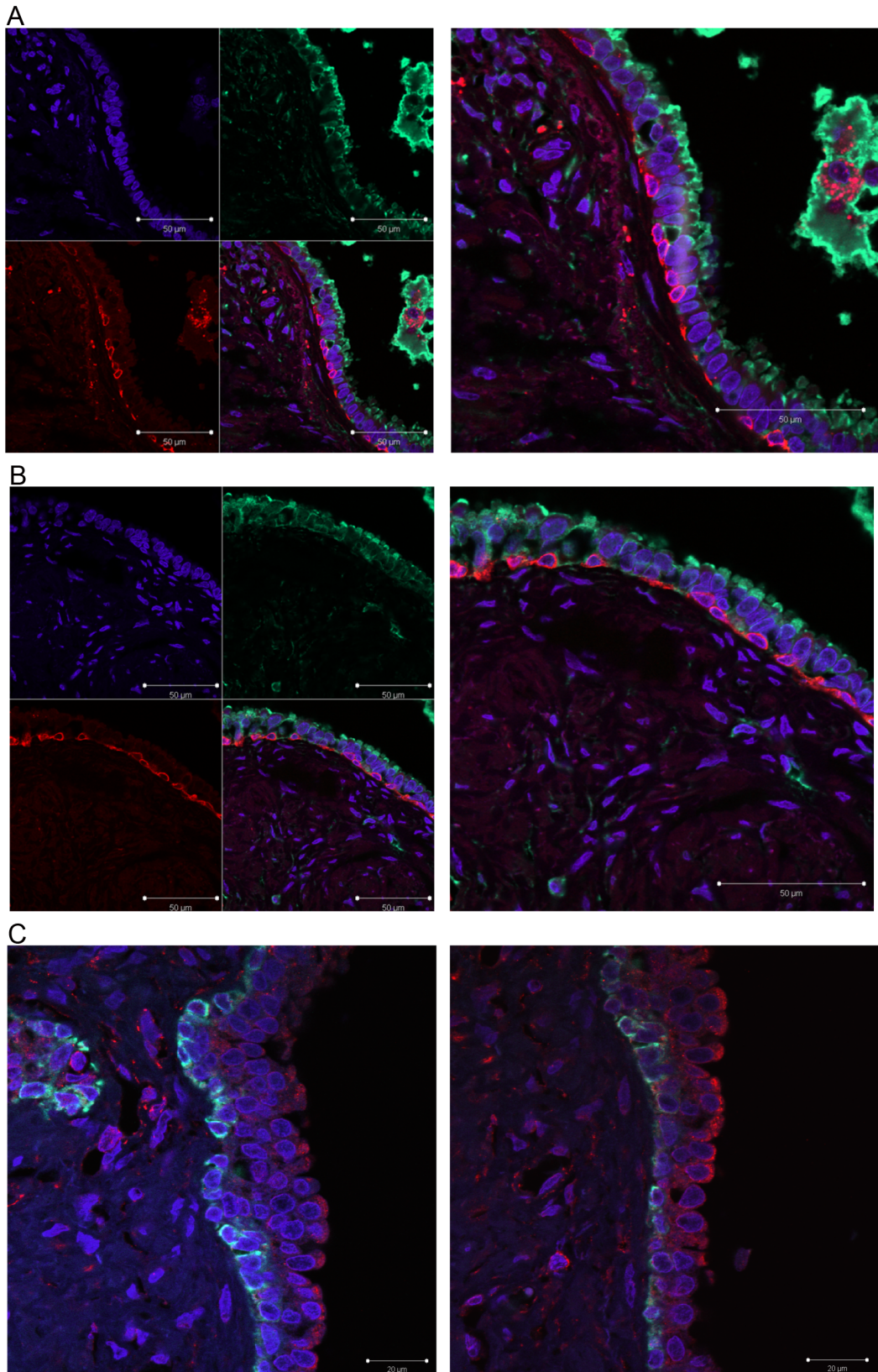
Target	Isotype	Clone	Manufacturer	Application	Concentration
IgG mouse	IgG1	Not provided	DAKO	IHC	1:100
IgG mouse	IgG1a	11711	R&D systems MAB002	N	5-50 µg/mL
IgG mouse	IgG2a	20102	R&D systems MAB003	N	5-50 µg/mL
IgG I rabbit	Rabbit IgG	not provided	Sigma # I5006	IF	1:2500
IgG goat	Goat	Not provided	R&D systems	IHC N	1:100 5-50 µg/mL

Table C. Secondary antibodies

Reactivity	Conjugate	Manufacturer	Application	Concentration
Sheep anti-mouse	POD	Sigma # 5906	WB	1:5000
Goat anti-rabbit	HRP	Cell signalling # 7074	WB	1:5000
Goat anti-rabbit	Biotin	DAKO # E0432	IHC	1:100
Rabbit anti-mouse	Biotin	DAKO # E0464	IHC	1:100
Rabbit anti-goat	Biotin	DAKO # E0466	IHC	1:100
Goat anti-mouse	Alexa568	Invitrogen # A11031	IHC	1:200
Goat anti-rabbit	Alexa568	Invitrogen # A11036	IHC	1:200
Donkey anti-goat	Alexa555	Invitrogen # A21432	IHC	1:200
Goat anti-mouse	Alexa488	Invitrogen # A11001	IHC	1:200
Goat anti-rabbit	Alexa488	Invitrogen # A11008	IHC, FC, IF	1:200
Rabbit anti-goat	Alexa488	Invitrogen # A11078	IHC	1:200

FC=flow cytometry, WB=Western blot, IF=immunofluorescence, IHC=immunofluorescence, N=neutralizing

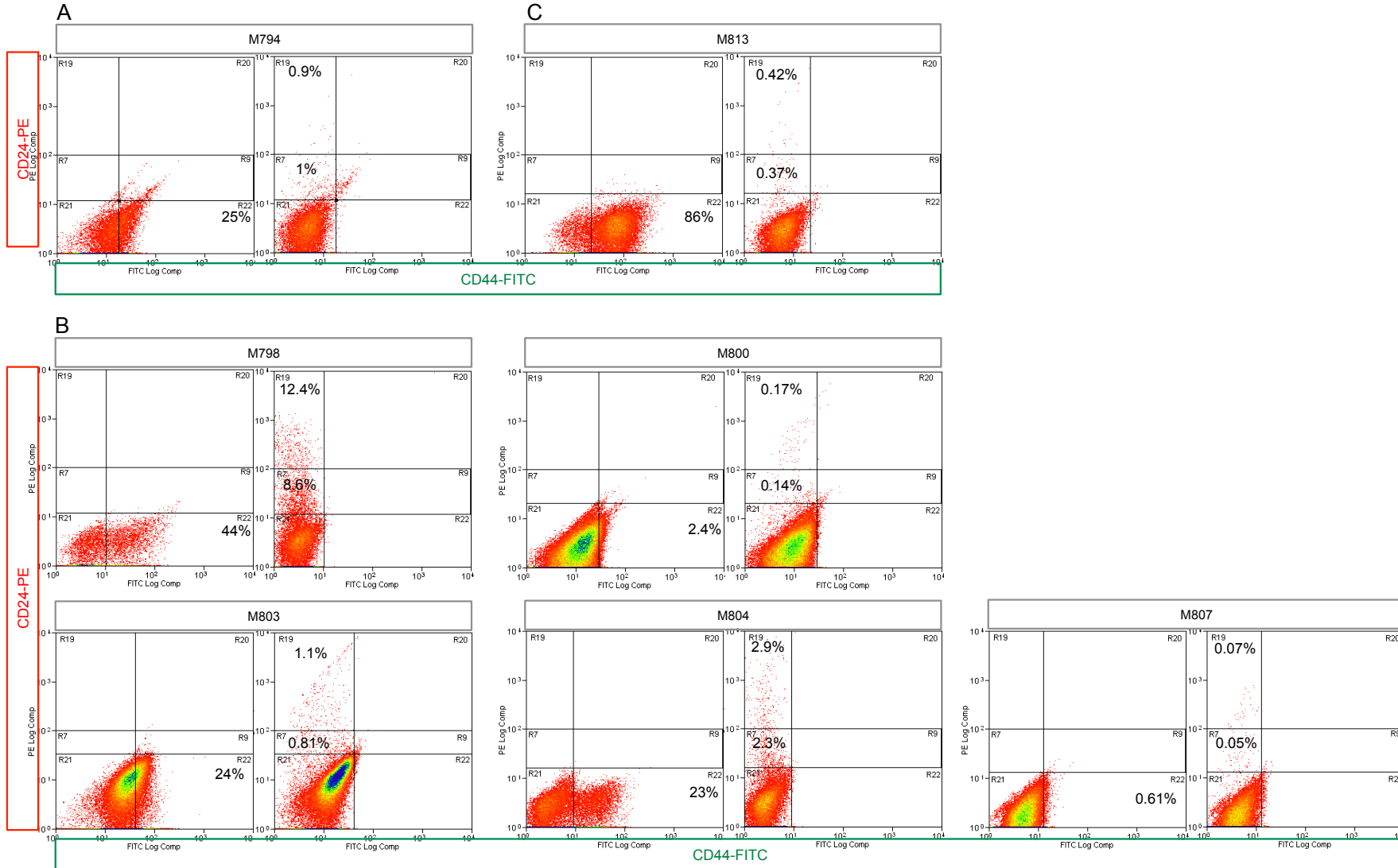
Appendix 5. Supplementary images immunofluorescence IL-6 receptor



Representative images of Immunofluorescence on paraffin embedded benign prostate sections stained for IL-6 receptor (-Alexa448) and CK5 (-Alexa538) (A-B) or IL-6 receptor (-Alexa548) and CK5 (-Alexa488) (C). Images were taken using a Zeiss LSM 510 meta confocal microscope at 63x magnification.

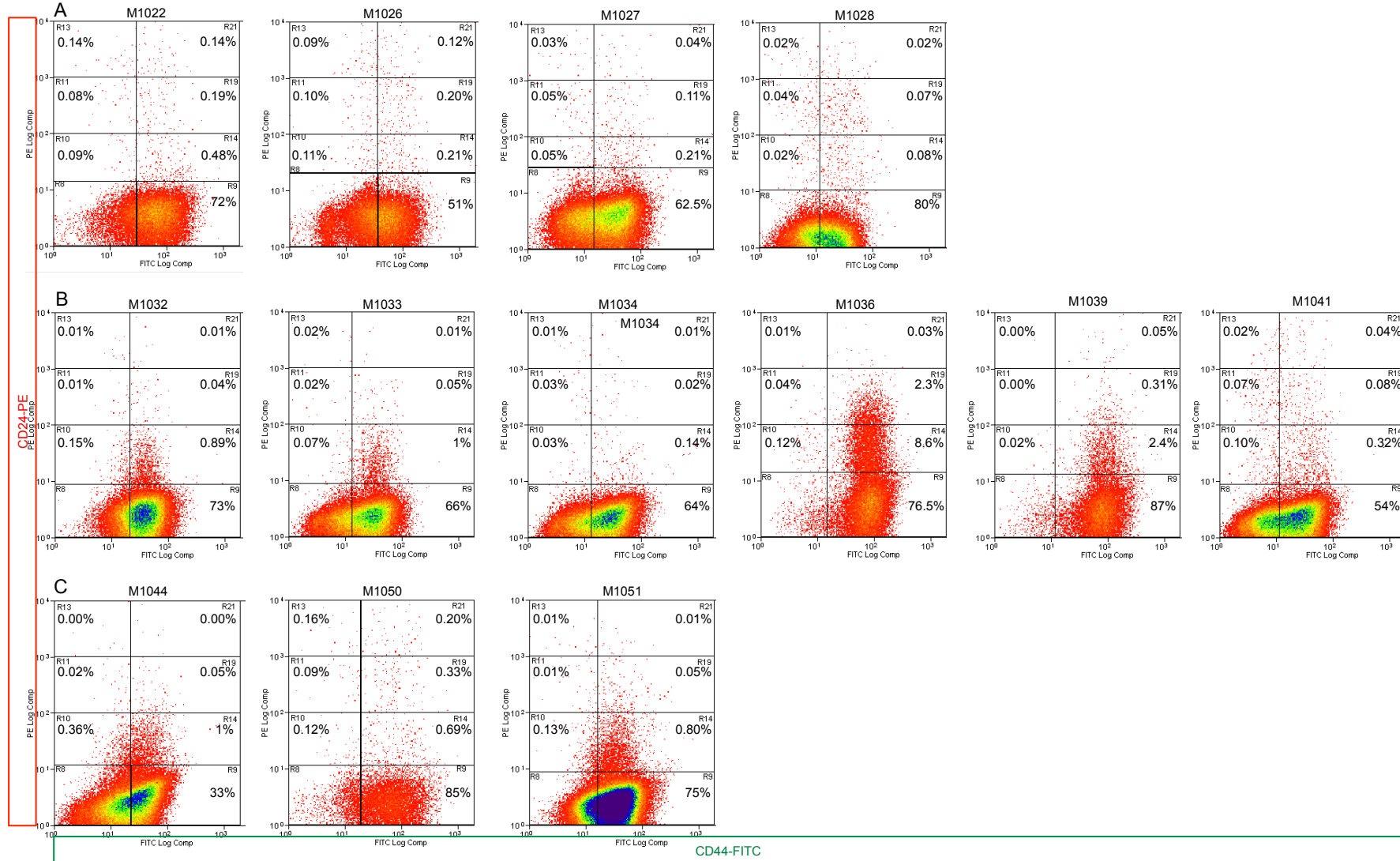
Appendix 6. Flow cytometry analysis for Y019 xenograft tumour cells post treatment with LLL12. Flow cytometry analysis of Y019 xenograft tumours of vehicle control (n=1) (A), 2.5 mg/kg LLL12 (n=5) (B) or 5 mg/kg LLL12 (n=1)(C). Dot plots of human Lin⁻CD31⁻ tumour cells dual labelled for CD44-FITC (x-axis), which labels the basal cells, and CD24-PE (y-axis), which labels the cells with a luminal phenotype. The number of cells expressing each marker were set against an IgG control or cells only control.

Appendix 6. Flow cytometry analysis of Y019 xenograft post treatment.



Appendix 7. Flow cytometry analysis for Y018 xenograft tumour cells post treatment with LLL12. Flow cytometry analysis of Y018 xenograft tumours of vehicle control (n=4) (A), 2.5 mg/kg LLL12 (n=6) (B) or 3.75 mg/kg LLL12 (n=3)(C). Dot plots of human Lin⁻CD31⁻ tumour cells dual labelled for CD44-FITC (x-axis), which labels the basal cells, and CD24-PE (y-axis), which labels the cells with a luminal phenotype. The number of cells expressing each marker were set against an IgG control or cells only control.

Appendix 7. Flow cytometry analysis of Y018 xenograft post treatment.



References

Abate-Shen, C., and Shen, M.M. (2000). Molecular genetics of prostate cancer. *Genes & development* *14*, 2410-2434.

Abdulghani, J., Gu, L., Dagvadorj, A., Lutz, J., Leiby, B., Bonuccelli, G., Lisanti, M.P., Zellweger, T., Alanen, K., Mirtti, T., et al. (2008). Stat3 promotes metastatic progression of prostate cancer. *The American journal of pathology* *172*, 1717-1728.

Abrahamsson, P.A. (1999). Neuroendocrine cells in tumour growth of the prostate. *Endocrine-related cancer* *6*, 503-519.

Adler, H.L., McCurdy, M.A., Kattan, M.W., Timme, T.L., Scardino, P.T., and Thompson, T.C. (1999). Elevated levels of circulating interleukin-6 and transforming growth factor-beta1 in patients with metastatic prostatic carcinoma. *The Journal of urology* *161*, 182-187.

Aggarwal, B.B., Vijayalekshmi, R.V., and Sung, B. (2009). Targeting inflammatory pathways for prevention and therapy of cancer: short-term friend, long-term foe. *Clinical cancer research : an official journal of the American Association for Cancer Research* *15*, 425-430.

Ahmed, H.U., Hindley, R.G., Dickinson, L., Freeman, A., Kirkham, A.P., Sahu, M., Scott, R., Allen, C., Van der Meulen, J., and Emberton, M. (2012). Focal therapy for localised unifocal and multifocal prostate cancer: a prospective development study. *The lancet oncology* *13*, 622-632.

Alison, M., Golding, M., Lalani, E.N., Nagy, P., Thorgeirsson, S., and Sarraf, C. (1997). Wholesale hepatocytic differentiation in the rat from ductular oval cells, the progeny of biliary stem cells. *Journal of hepatology* *26*, 343-352.

Amaral, T.M., Macedo, D., Fernandes, I., and Costa, L. (2012). Castration-resistant prostate cancer: mechanisms, targets, and treatment. *Prostate cancer* *2012*, 327253.

Amin, M., Khalid, A., Tazeen, N., and Yasoob, M. (2010). Zonal Anatomy of Prostate. *ANNALS* *16*, 138-142.

Angele, S., Falconer, A., Foster, C.S., Taniere, P., Eeles, R.A., and Hall, J. (2004). ATM protein overexpression in prostate tumors: possible role in telomere maintenance. *American journal of clinical pathology* *121*, 231-236.

Aoki, Y., Jaffe, E.S., Chang, Y., Jones, K., Teruya-Feldstein, J., Moore, P.S., and Tosato, G. (1999). Angiogenesis and hematopoiesis induced by Kaposi's sarcoma-associated herpesvirus-encoded interleukin-6. *Blood* *93*, 4034-4043.

Aoyagi, T., Takishima, K., Hayakawa, M., and Nakamura, H. (1996). Gene expression of TGF- α , EGF and IL-6 in cultured renal tubular cells and renal cell carcinoma. *International journal of urology : official journal of the Japanese Urological Association* 3, 392-396.

Attard, G., Rizzo, S., Ledaki, I., Clark, J., Reid, A.H., Thompson, A., Khoo, V., de Bono, J.S., Cooper, C.S., and Hudson, D.L. (2009). A novel, spontaneously immortalized, human prostate cancer cell line, Bob, offers a unique model for pre-clinical prostate cancer studies. *The Prostate* 69, 1507-1520.

Aumuller, G. (1991). Postnatal development of the prostate. *Bulletin de l'Association des anatomistes* 75, 39-42.

Aus, G. (2006). Current status of HIFU and cryotherapy in prostate cancer--a review. *European urology* 50, 927-934; discussion 934.

Azare, J., Leslie, K., Al-Ahmadie, H., Gerald, W., Weinreb, P.H., Violette, S.M., and Bromberg, J. (2007). Constitutively activated Stat3 induces tumorigenesis and enhances cell motility of prostate epithelial cells through integrin beta 6. *Molecular and cellular biology* 27, 4444-4453.

Balbay, M.D., Pettaway, C.A., Kuniyasu, H., Inoue, K., Ramirez, E., Li, E., Fidler, I.J., and Dinney, C.P. (1999). Highly metastatic human prostate cancer growing within the prostate of athymic mice overexpresses vascular endothelial growth factor. *Clinical cancer research : an official journal of the American Association for Cancer Research* 5, 783-789.

Balk, S.P. (2002). Androgen receptor as a target in androgen-independent prostate cancer. *Urology* 60, 132-138; discussion 138-139.

Balkwill, F., and Mantovani, A. (2001). Inflammation and cancer: back to Virchow? *Lancet* 357, 539-545.

Ball, S., Li, C., Li, P.K., and Lin, J. (2011). The small molecule, LLL12, inhibits STAT3 phosphorylation and induces apoptosis in medulloblastoma and glioblastoma cells. *PLoS one* 6, e18820.

Bao, S., Wu, Q., McLendon, R.E., Hao, Y., Shi, Q., Hjelmeland, A.B., Dewhirst, M.W., Bigner, D.D., and Rich, J.N. (2006). Glioma stem cells promote radioresistance by preferential activation of the DNA damage response. *Nature* 444, 756-760.

Bardia, A., Platz, E.A., Yegnasubramanian, S., De Marzo, A.M., and Nelson, W.G. (2009). Anti-inflammatory drugs, antioxidants, and prostate cancer prevention. *Current opinion in pharmacology* 9, 419-426.

Barker, N., Ridgway, R.A., van Es, J.H., van de Wetering, M., Begthel, H., van den Born, M., Danenberg, E., Clarke, A.R., Sansom, O.J., and Clevers, H. (2009). Crypt stem cells as the cells-of-origin of intestinal cancer. *Nature* 457, 608-611.

Baron, J.A., and Sandler, R.S. (2000). Nonsteroidal anti-inflammatory drugs and cancer prevention. *Annual review of medicine* 51, 511-523.

Becher, O.J., and Holland, E.C. (2006). Genetically engineered models have advantages over xenografts for preclinical studies. *Cancer research* 66, 3355-3358, discussion 3358-3359.

Beedassy, A., and Cardi, G. (1999). Chemotherapy in advanced prostate cancer. *Seminars in oncology* 26, 428-438.

Bellido, M., and Te Boekhorst, P.A. (2012). JAK2 Inhibition: Reviewing a New Therapeutical Option in Myeloproliferative Neoplasms. *Advances in hematology* 2012, 535709.

Berishaj, M., Gao, S.P., Ahmed, S., Leslie, K., Al-Ahmadie, H., Gerald, W.L., Bornmann, W., and Bromberg, J.F. (2007). Stat3 is tyrosine-phosphorylated through the interleukin-6/glycoprotein 130/Janus kinase pathway in breast cancer. *Breast cancer research : BCR* 9, R32.

Berry, P.A., Maitland, N.J., and Collins, A.T. (2008). Androgen receptor signalling in prostate: effects of stromal factors on normal and cancer stem cells. *Molecular and cellular endocrinology* 288, 30-37.

Berthon, P., Cussenot, O., Hopwood, L., Leduc, A., and Maitland, N. (1995). Functional expression of sv40 in normal human prostatic epithelial and fibroblastic cells - differentiation pattern of nontumorigenic cell-lines. *Int J Oncol* 6, 333-343.

Bhatia-Gaur, R., Donjacour, A.A., Sciavolino, P.J., Kim, M., Desai, N., Young, P., Norton, C.R., Gridley, T., Cardiff, R.D., Cunha, G.R., et al. (1999). Roles for Nkx3.1 in prostate development and cancer. *Genes & development* 13, 966-977.

Bid, H.K., Oswald, D., Li, C., London, C.A., Lin, J., and Houghton, P.J. (2012). Anti-angiogenic activity of a small molecule STAT3 inhibitor LLL12. *PLoS one* 7, e35513.

Bill-Axelson, A., Holmberg, L., Filen, F., Ruutu, M., Garmo, H., Busch, C., Nordling, S., Haggman, M., Andersson, S.O., Bratell, S., et al. (2008). Radical prostatectomy versus watchful waiting in localized prostate cancer: the Scandinavian prostate cancer group-4 randomized trial. *Journal of the National Cancer Institute* 100, 1144-1154.

Bingle, L., Brown, N.J., and Lewis, C.E. (2002). The role of tumour-associated macrophages in tumour progression: implications for new anticancer therapies. *The Journal of pathology* 196, 254-265.

Birnie, R., Bryce, S.D., Roome, C., Dussupt, V., Droop, A., Lang, S.H., Berry, P.A., Hyde, C.F., Lewis, J.L., Stower, M.J., et al. (2008). Gene expression profiling of human prostate cancer stem cells reveals a pro-inflammatory phenotype and the importance of extracellular matrix interactions. *Genome Biol* 9, R83.

Blacklock, N.J. (1991). The anatomy of the prostate: relationship with prostatic infection. *Infection 19 Suppl 3*, S111-114.

Bonkhoff, H., and Remberger, K. (1993). Widespread distribution of nuclear androgen receptors in the basal cell layer of the normal and hyperplastic human prostate. *Virchows Archiv A, Pathological anatomy and histopathology 422*, 35-38.

Bonkhoff, H., Stein, U., and Remberger, K. (1994). The proliferative function of basal cells in the normal and hyperplastic human prostate. *The Prostate 24*, 114-118.

Bonkhoff, H., Stein, U., and Remberger, K. (1995). Endocrine-paracrine cell types in the prostate and prostatic adenocarcinoma are postmitotic cells. *Human pathology 26*, 167-170.

Bonkhoff, H., Wernert, N., Dhom, G., and Remberger, K. (1991). Basement membranes in fetal, adult normal, hyperplastic and neoplastic human prostate. *Virchows Archiv A, Pathological anatomy and histopathology 418*, 375-381.

Bonnet, D., and Dick, J.E. (1997). Human acute myeloid leukemia is organized as a hierarchy that originates from a primitive hematopoietic cell. *Nature medicine 3*, 730-737.

Borrello, M.G., Alberti, L., Fischer, A., Degl'innocenti, D., Ferrario, C., Gariboldi, M., Marchesi, F., Allavena, P., Greco, A., Collini, P., et al. (2005). Induction of a proinflammatory program in normal human thyrocytes by the RET/PTC1 oncogene. *Proceedings of the National Academy of Sciences of the United States of America 102*, 14825-14830.

Bristow, R.G., Ozcelik, H., Jalali, F., Chan, N., and Vesprini, D. (2007). Homologous recombination and prostate cancer: a model for novel DNA repair targets and therapies. *Radiotherapy and oncology : journal of the European Society for Therapeutic Radiology and Oncology 83*, 220-230.

Bromberg, J. (2002). Stat proteins and oncogenesis. *The Journal of clinical investigation 109*, 1139-1142.

Bromberg, J.F., Wrzeszczynska, M.H., Devgan, G., Zhao, Y., Pestell, R.G., Albanese, C., and Darnell, J.E., Jr. (1999). Stat3 as an oncogene. *Cell 98*, 295-303.

Bruce, W.R., and Van Der Gaag, H. (1963). A Quantitative Assay for the Number of Murine Lymphoma Cells Capable of Proliferation in Vivo. *Nature 199*, 79-80.

Buchanan, G., Greenberg, N.M., Scher, H.I., Harris, J.M., Marshall, V.R., and Tilley, W.D. (2001). Collocation of androgen receptor gene mutations in prostate cancer. *Clinical cancer research : an official journal of the American Association for Cancer Research 7*, 1273-1281.

Burke, W.M., Jin, X., Lin, H.J., Huang, M., Liu, R., Reynolds, R.K., and Lin, J. (2001). Inhibition of constitutively active Stat3 suppresses growth of human ovarian and breast cancer cells. *Oncogene* 20, 7925-7934.

Caldenhoven, E., van Dijk, T.B., Solari, R., Armstrong, J., Raaijmakers, J.A., Lammers, J.W., Koenderman, L., and de Groot, R.P. (1996). STAT3beta, a splice variant of transcription factor STAT3, is a dominant negative regulator of transcription. *The Journal of biological chemistry* 271, 13221-13227.

Catalona, W.J., Partin, A.W., Slawin, K.M., Brawer, M.K., Flanigan, R.C., Patel, A., Richie, J.P., deKernion, J.B., Walsh, P.C., Scardino, P.T., et al. (1998). Use of the percentage of free prostate-specific antigen to enhance differentiation of prostate cancer from benign prostatic disease: a prospective multicenter clinical trial. *JAMA : the journal of the American Medical Association* 279, 1542-1547.

Catalona, W.J., Richie, J.P., Ahmann, F.R., Hudson, M.A., Scardino, P.T., Flanigan, R.C., deKernion, J.B., Ratliff, T.L., Kavoussi, L.R., Dalkin, B.L., et al. (1994). Comparison of digital rectal examination and serum prostate specific antigen in the early detection of prostate cancer: results of a multicenter clinical trial of 6,630 men. *The Journal of urology* 151, 1283-1290.

Catlett-Falcone, R., Landowski, T.H., Oshiro, M.M., Turkson, J., Levitzki, A., Savino, R., Ciliberto, G., Moscinski, L., Fernandez-Luna, J.L., Nunez, G., et al. (1999). Constitutive activation of Stat3 signaling confers resistance to apoptosis in human U266 myeloma cells. *Immunity* 10, 105-115.

Cerveira, N., Ribeiro, F.R., Peixoto, A., Costa, V., Henrique, R., Jeronimo, C., and Teixeira, M.R. (2006). TMPRSS2-ERG gene fusion causing ERG overexpression precedes chromosome copy number changes in prostate carcinomas and paired HGPIN lesions. *Neoplasia* 8, 826-832.

Chen, J., Li, Y., Yu, T.S., McKay, R.M., Burns, D.K., Kernie, S.G., and Parada, L.F. (2012). A restricted cell population propagates glioblastoma growth after chemotherapy. *Nature* 488, 522-526.

Chen, L., Elahi, A., Pow-Sang, J., Lazarus, P., and Park, J. (2003). Association between polymorphism of human oxoguanine glycosylase 1 and risk of prostate cancer. *The Journal of urology* 170, 2471-2474.

Chen, T., Wang, L.H., and Farrar, W.L. (2000). Interleukin 6 activates androgen receptor-mediated gene expression through a signal transducer and activator of transcription 3-dependent pathway in LNCaP prostate cancer cells. *Cancer research* 60, 2132-2135.

Chen, Y.W., Chen, K.H., Huang, P.I., Chen, Y.C., Chiou, G.Y., Lo, W.L., Tseng, L.M., Hsu, H.S., Chang, K.W., and Chiou, S.H. (2010). Cucurbitacin I suppressed stem-like property and enhanced radiation-induced apoptosis in head and

neck squamous carcinoma--derived CD44(+)ALDH1(+) cells. *Molecular cancer therapeutics* 9, 2879-2892.

Cheng, A.L., Hsu, C.H., Lin, J.K., Hsu, M.M., Ho, Y.F., Shen, T.S., Ko, J.Y., Lin, J.T., Lin, B.R., Ming-Shiang, W., et al. (2001). Phase I clinical trial of curcumin, a chemopreventive agent, in patients with high-risk or pre-malignant lesions. *Anticancer research* 21, 2895-2900.

Chodak, G.W., Thisted, R.A., Gerber, G.S., Johansson, J.E., Adolfsson, J., Jones, G.W., Chisholm, G.D., Moskovitz, B., Livne, P.M., and Warner, J. (1994). Results of conservative management of clinically localized prostate cancer. *The New England journal of medicine* 330, 242-248.

Chung, T.D., Yu, J.J., Kong, T.A., Spiotto, M.T., and Lin, J.M. (2000). Interleukin-6 activates phosphatidylinositol-3 kinase, which inhibits apoptosis in human prostate cancer cell lines. *The Prostate* 42, 1-7.

Chung, T.D., Yu, J.J., Spiotto, M.T., Bartkowski, M., and Simons, J.W. (1999). Characterization of the role of IL-6 in the progression of prostate cancer. *The Prostate* 38, 199-207.

Clement, V., Dutoit, V., Marino, D., Dietrich, P.Y., and Radovanovic, I. (2009). Limits of CD133 as a marker of glioma self-renewing cells. *International journal of cancer Journal international du cancer* 125, 244-248.

Clevers, H. (2011). The cancer stem cell: premises, promises and challenges. *Nature medicine* 17, 313-319.

Coffey, D.S., and Pienta, K.J. (1987). New concepts in studying the control of normal and cancer growth of the prostate. *Progress in clinical and biological research* 239, 1-73.

Coffey, D.S., and Walsh, P.C. (1990). Clinical and experimental studies of benign prostatic hyperplasia. *The Urologic clinics of North America* 17, 461-475.

Cohen, R.J., Shannon, B.A., McNeal, J.E., Shannon, T., and Garrett, K.L. (2005). *Propionibacterium acnes* associated with inflammation in radical prostatectomy specimens: a possible link to cancer evolution? *The Journal of urology* 173, 1969-1974.

Collins, A.T., Berry, P.A., Hyde, C., Stower, M.J., and Maitland, N.J. (2005). Prospective identification of tumorigenic prostate cancer stem cells. *Cancer research* 65, 10946-10951.

Collins, A.T., Habib, F.K., Maitland, N.J., and Neal, D.E. (2001). Identification and isolation of human prostate epithelial stem cells based on alpha(2)beta(1)-integrin expression. *Journal of cell science* 114, 3865-3872.

Collins, A.T., and Maitland, N.J. (2006). Prostate cancer stem cells. *Eur J Cancer* 42, 1213-1218.

Cook, M.G. (1992). The significance of inflammation and regression in melanoma. *Virchows Archiv A, Pathological anatomy and histopathology* 420, 113-115.

Corn, P.G. (2012). The tumor microenvironment in prostate cancer: elucidating molecular pathways for therapy development. *Cancer management and research* 4, 183-193.

Cornelissen, C., Luscher-Firzlaff, J., Baron, J.M., and Luscher, B. (2012). Signaling by IL-31 and functional consequences. *European journal of cell biology* 91, 552-566.

Corvinus, F.M., Orth, C., Moriggi, R., Tsareva, S.A., Wagner, S., Pfitzner, E.B., Baus, D., Kaufmann, R., Huber, L.A., Zatloukal, K., et al. (2005). Persistent STAT3 activation in colon cancer is associated with enhanced cell proliferation and tumor growth. *Neoplasia* 7, 545-555.

Coussens, L.M., and Werb, Z. (2002). Inflammation and cancer. *Nature* 420, 860-867.

Craft, N., Chhor, C., Tran, C., Beldegrun, A., DeKernion, J., Witte, O.N., Said, J., Reiter, R.E., and Sawyers, C.L. (1999). Evidence for clonal outgrowth of androgen-independent prostate cancer cells from androgen-dependent tumors through a two-step process. *Cancer research* 59, 5030-5036.

Cress, A.E., Rabinovitz, I., Zhu, W., and Nagle, R.B. (1995). The alpha 6 beta 1 and alpha 6 beta 4 integrins in human prostate cancer progression. *Cancer metastasis reviews* 14, 219-228.

Croker, B.A., Kiu, H., and Nicholson, S.E. (2008). SOCS regulation of the JAK/STAT signalling pathway. *Seminars in cell & developmental biology* 19, 414-422.

Cuddihy, A.R., and Bristow, R.G. (2004). The p53 protein family and radiation sensitivity: Yes or no? *Cancer metastasis reviews* 23, 237-257.

Culig, Z., Bartsch, G., and Hobisch, A. (2002). Interleukin-6 regulates androgen receptor activity and prostate cancer cell growth. *Molecular and cellular endocrinology* 197, 231-238.

Culig, Z., Hobisch, A., Cronauer, M.V., Radmayr, C., Trapman, J., Hittmair, A., Bartsch, G., and Klocker, H. (1994). Androgen receptor activation in prostatic tumor cell lines by insulin-like growth factor-I, keratinocyte growth factor, and epidermal growth factor. *Cancer research* 54, 5474-5478.

Cunha, G.R., Battle, E., Young, P., Brody, J., Donjacour, A., Hayashi, N., and Kinbara, H. (1992). Role of epithelial-mesenchymal interactions in the differentiation and spatial organization of visceral smooth muscle. *Epithelial Cell Biol* 1, 76-83.

Cunha, G.R., Donjacour, A.A., Cooke, P.S., Mee, S., Bigsby, R.M., Higgins, S.J., and Sugimura, Y. (1987). The endocrinology and developmental biology of the prostate. *Endocrine reviews* 8, 338-362.

Custer, R.P., Bosma, G.C., and Bosma, M.J. (1985). Severe combined immunodeficiency (SCID) in the mouse. Pathology, reconstitution, neoplasms. *The American journal of pathology* 120, 464-477.

Daheron, L., Opitz, S.L., Zaehres, H., Lensch, M.W., Andrews, P.W., Itskovitz-Eldor, J., and Daley, G.Q. (2004). LIF/STAT3 signaling fails to maintain self-renewal of human embryonic stem cells. *Stem Cells* 22, 770-778.

Daniel, V.C., Marchionni, L., Hierman, J.S., Rhodes, J.T., Devereux, W.L., Rudin, C.M., Yung, R., Parmigiani, G., Dorsch, M., Peacock, C.D., et al. (2009). A primary xenograft model of small-cell lung cancer reveals irreversible changes in gene expression imposed by culture in vitro. *Cancer research* 69, 3364-3373.

Darnell, J.E., Jr. (1997). STATs and gene regulation. *Science* 277, 1630-1635.

Darnell, J.E., Jr., Kerr, I.M., and Stark, G.R. (1994). Jak-STAT pathways and transcriptional activation in response to IFNs and other extracellular signaling proteins. *Science* 264, 1415-1421.

de Bono, J.S., Logothetis, C.J., Molina, A., Fizazi, K., North, S., Chu, L., Chi, K.N., Jones, R.J., Goodman, O.B., Jr., Saad, F., et al. (2011). Abiraterone and increased survival in metastatic prostate cancer. *The New England journal of medicine* 364, 1995-2005.

De Marzo, A.M., Marchi, V.L., Epstein, J.I., and Nelson, W.G. (1999). Proliferative inflammatory atrophy of the prostate: implications for prostatic carcinogenesis. *The American journal of pathology* 155, 1985-1992.

De Marzo, A.M., Nelson, W.G., Meeker, A.K., and Coffey, D.S. (1998). Stem cell features of benign and malignant prostate epithelial cells. *The Journal of urology* 160, 2381-2392.

De Marzo, A.M., Platz, E.A., Sutcliffe, S., Xu, J., Gronberg, H., Drake, C.G., Nakai, Y., Isaacs, W.B., and Nelson, W.G. (2007). Inflammation in prostate carcinogenesis. *Nature reviews Cancer* 7, 256-269.

de Visser, K.E., Eichten, A., and Coussens, L.M. (2006). Paradoxical roles of the immune system during cancer development. *Nature reviews Cancer* 6, 24-37.

Dean, M., Fojo, T., and Bates, S. (2005). Tumour stem cells and drug resistance. *Nature reviews Cancer* 5, 275-284.

Demichelis, F., and Rubin, M.A. (2007). TMPRSS2-ETS fusion prostate cancer: biological and clinical implications. *Journal of clinical pathology* 60, 1185-1186.

Dhir, R., Ni, Z., Lou, W., DeMiguel, F., Grandis, J.R., and Gao, A.C. (2002). Stat3 activation in prostatic carcinomas. *The Prostate* 51, 241-246.

Di Cristofano, A., Pesce, B., Cordon-Cardo, C., and Pandolfi, P.P. (1998). Pten is essential for embryonic development and tumour suppression. *Nature genetics* 19, 348-355.

di Sant'Agnese, P.A. (1992). Neuroendocrine differentiation in carcinoma of the prostate. Diagnostic, prognostic, and therapeutic implications. *Cancer* 70, 254-268.

di Sant'Agnese, P.A. (1998). Neuroendocrine cells of the prostate and neuroendocrine differentiation in prostatic carcinoma: a review of morphologic aspects. *Urology* 51, 121-124.

Dillon, S.R., Sprecher, C., Hammond, A., Bilsborough, J., Rosenfeld-Franklin, M., Presnell, S.R., Haugen, H.S., Maurer, M., Harder, B., Johnston, J., et al. (2004). Interleukin 31, a cytokine produced by activated T cells, induces dermatitis in mice. *Nature immunology* 5, 752-760.

Djakiew, D. (2000). Dysregulated expression of growth factors and their receptors in the development of prostate cancer. *The Prostate* 42, 150-160.

Dong, J.T. (2006). Prevalent mutations in prostate cancer. *Journal of cellular biochemistry* 97, 433-447.

Dorff, T.B., Goldman, B., Pinski, J.K., Mack, P.C., Lara, P.N., Jr., Van Veldhuizen, P.J., Jr., Quinn, D.I., Vogelzang, N.J., Thompson, I.M., Jr., and Hussain, M.H. (2010). Clinical and correlative results of SWOG S0354: a phase II trial of CNT0328 (siltuximab), a monoclonal antibody against interleukin-6, in chemotherapy-pretreated patients with castration-resistant prostate cancer. *Clinical cancer research : an official journal of the American Association for Cancer Research* 16, 3028-3034.

Drach, G.W., Fair, W.R., Meares, E.M., and Stamey, T.A. (1978). Classification of benign diseases associated with prostatic pain: prostatitis or prostatodynia? *The Journal of urology* 120, 266.

Drachenberg, D.E., Elgamal, A.A., Rowbotham, R., Peterson, M., and Murphy, G.P. (1999). Circulating levels of interleukin-6 in patients with hormone refractory prostate cancer. *The Prostate* 41, 127-133.

Drewa, T., and Styczynski, J. (2008). Can conception of prostate cancer stem cells influence treatment dedicated to patients with disseminated disease? *Medical hypotheses* 71, 694-699.

Driessens, G., Beck, B., Caauwe, A., Simons, B.D., and Blanpain, C. (2012). Defining the mode of tumour growth by clonal analysis. *Nature* 488, 527-530.

Eastham, J.A., Stapleton, A.M., Gousse, A.E., Timme, T.L., Yang, G., Slawin, K.M., Wheeler, T.M., Scardino, P.T., and Thompson, T.C. (1995). Association of p53 mutations with metastatic prostate cancer. *Clinical cancer research : an official journal of the American Association for Cancer Research* 1, 1111-1118.

Ekbom, A., Helmick, C., Zack, M., and Adami, H.O. (1990). Ulcerative colitis and colorectal cancer. A population-based study. *The New England journal of medicine* 323, 1228-1233.

Engels, E.A. (2008). Inflammation in the development of lung cancer: epidemiological evidence. *Expert review of anticancer therapy* 8, 605-615.

Eyler, C.E., and Rich, J.N. (2008). Survival of the fittest: cancer stem cells in therapeutic resistance and angiogenesis. *Journal of clinical oncology : official journal of the American Society of Clinical Oncology* 26, 2839-2845.

Fabian, A., Barok, M., Vereb, G., and Szollosi, J. (2009). Die hard: are cancer stem cells the Bruce Willises of tumor biology? *Cytometry Part A : the journal of the International Society for Analytical Cytology* 75, 67-74.

Farmer, H., McCabe, N., Lord, C.J., Tutt, A.N., Johnson, D.A., Richardson, T.B., Santarosa, M., Dillon, K.J., Hickson, I., Knights, C., et al. (2005). Targeting the DNA repair defect in BRCA mutant cells as a therapeutic strategy. *Nature* 434, 917-921.

Farrow, B., and Evers, B.M. (2002). Inflammation and the development of pancreatic cancer. *Surgical oncology* 10, 153-169.

Feldman, B.J., and Feldman, D. (2001). The development of androgen-independent prostate cancer. *Nature reviews Cancer* 1, 34-45.

Feng, S., Tang, Q., Sun, M., Chun, J.Y., Evans, C.P., and Gao, A.C. (2009). Interleukin-6 increases prostate cancer cells resistance to bicalutamide via TIF2. *Molecular cancer therapeutics* 8, 665-671.

Fidler, I.J. (1990). Critical factors in the biology of human cancer metastasis: twenty-eighth G.H.A. Clowes memorial award lecture. *Cancer research* 50, 6130-6138.

Finegood, D.T., Scaglia, L., and Bonner-Weir, S. (1995). Dynamics of beta-cell mass in the growing rat pancreas. Estimation with a simple mathematical model. *Diabetes* 44, 249-256.

Fizazi, K., De Bono, J.S., Flechon, A., Heidenreich, A., Voog, E., Davis, N.B., Qi, M., Bandekar, R., Vermeulen, J.T., Cornfeld, M., et al. (2012). Randomised phase II study of siltuximab (CNTO 328), an anti-IL-6 monoclonal antibody, in combination with mitoxantrone/prednisone versus mitoxantrone/prednisone alone in metastatic castration-resistant prostate cancer. *Eur J Cancer* 48, 85-93.

Flanagan, S.P. (1966). 'Nude', a new hairless gene with pleiotropic effects in the mouse. *Genetical research* 8, 295-309.

Frame, F.M., Hager, S., Pellacani, D., Stower, M.J., Walker, H.F., Burns, J.E., Collins, A.T., and Maitland, N.J. (2010). Development and limitations of lentivirus vectors as tools for tracking differentiation in prostate epithelial cells. *Experimental cell research* 316, 3161-3171.

Frank, N.Y., Schatton, T., and Frank, M.H. (2010). The therapeutic promise of the cancer stem cell concept. *The Journal of clinical investigation* 120, 41-50.

Gao, S.P., Mark, K.G., Leslie, K., Pao, W., Motoi, N., Gerald, W.L., Travis, W.D., Bornmann, W., Veach, D., Clarkson, B., et al. (2007). Mutations in the EGFR kinase domain mediate STAT3 activation via IL-6 production in human lung adenocarcinomas. *The Journal of clinical investigation* 117, 3846-3856.

Garcia, R., Bowman, T.L., Niu, G., Yu, H., Minton, S., Muro-Cacho, C.A., Cox, C.E., Falcone, R., Fairclough, R., Parsons, S., et al. (2001). Constitutive activation of Stat3 by the Src and JAK tyrosine kinases participates in growth regulation of human breast carcinoma cells. *Oncogene* 20, 2499-2513.

Gingrich, J.R., Barrios, R.J., Morton, R.A., Boyce, B.F., DeMayo, F.J., Finegold, M.J., Angelopoulou, R., Rosen, J.M., and Greenberg, N.M. (1996). Metastatic prostate cancer in a transgenic mouse. *Cancer research* 56, 4096-4102.

Giovannucci, E., Rimm, E.B., Colditz, G.A., Stampfer, M.J., Ascherio, A., Chute, C.C., and Willett, W.C. (1993). A prospective study of dietary fat and risk of prostate cancer. *Journal of the National Cancer Institute* 85, 1571-1579.

Giri, D., Ozen, M., and Ittmann, M. (2001). Interleukin-6 is an autocrine growth factor in human prostate cancer. *The American journal of pathology* 159, 2159-2165.

Gleason, D.F. (1966). Classification of prostatic carcinomas. *Cancer chemotherapy reports Part 1* 50, 125-128.

Goldman, J.P., Blundell, M.P., Lopes, L., Kinnon, C., Di Santo, J.P., and Thrasher, A.J. (1998). Enhanced human cell engraftment in mice deficient in RAG2 and the common cytokine receptor gamma chain. *British journal of haematology* 103, 335-342.

Gormley, G.J., Stoner, E., Bruskewitz, R.C., Imperato-McGinley, J., Walsh, P.C., McConnell, J.D., Andriole, G.L., Geller, J., Bracken, B.R., Tenover, J.S., et al. (1992). The effect of finasteride in men with benign prostatic hyperplasia. The Finasteride Study Group. *The New England journal of medicine* 327, 1185-1191.

Gotte, M., and Yip, G.W. (2006). Heparanase, hyaluronan, and CD44 in cancers: a breast carcinoma perspective. *Cancer research* 66, 10233-10237.

Gouilleux-Gruart, V., Gouilleux, F., Desaint, C., Claisse, J.F., Capiod, J.C., Delobel, J., Weber-Nordt, R., Dusanter-Fourt, I., Dreyfus, F., Groner, B., et al. (1996). STAT-related transcription factors are constitutively activated in peripheral blood cells from acute leukemia patients. *Blood* 87, 1692-1697.

Grandis, J.R., Drenning, S.D., Chakraborty, A., Zhou, M.Y., Zeng, Q., Pitt, A.S., and Tweardy, D.J. (1998). Requirement of Stat3 but not Stat1 activation for epidermal growth factor receptor- mediated cell growth In vitro. *The Journal of clinical investigation* 102, 1385-1392.

Greenberg, N.M., DeMayo, F., Finegold, M.J., Medina, D., Tilley, W.D., Aspinall, J.O., Cunha, G.R., Donjacour, A.A., Matusik, R.J., and Rosen, J.M. (1995). Prostate cancer in a transgenic mouse. *Proceedings of the National Academy of Sciences of the United States of America* 92, 3439-3443.

Gritsko, T., Williams, A., Turkson, J., Kaneko, S., Bowman, T., Huang, M., Nam, S., Eweis, I., Diaz, N., Sullivan, D., et al. (2006). Persistent activation of stat3 signaling induces survivin gene expression and confers resistance to apoptosis in human breast cancer cells. *Clinical cancer research : an official journal of the American Association for Cancer Research* 12, 11-19.

Grivennikov, S., Karin, E., Terzic, J., Mucida, D., Yu, G.Y., Vallabhapurapu, S., Scheller, J., Rose-John, S., Cheroutre, H., Eckmann, L., et al. (2009). IL-6 and Stat3 are required for survival of intestinal epithelial cells and development of colitis-associated cancer. *Cancer cell* 15, 103-113.

Gronberg, H. (2003). Prostate cancer epidemiology. *Lancet* 361, 859-864.

Gu, F., Hata, R., Ma, Y.J., Tanaka, J., Mitsuda, N., Kumon, Y., Hanakawa, Y., Hashimoto, K., Nakajima, K., and Sakanaka, M. (2005). Suppression of Stat3 promotes neurogenesis in cultured neural stem cells. *Journal of neuroscience research* 81, 163-171.

Gu, G., Yuan, J., Wills, M., and Kasper, S. (2007). Prostate cancer cells with stem cell characteristics reconstitute the original human tumor in vivo. *Cancer research* 67, 4807-4815.

Guo, Y., Nemeth, J., O'Brien, C., Susa, M., Liu, X., Zhang, Z., Choy, E., Mankin, H., Hornicek, F., and Duan, Z. (2010). Effects of siltuximab on the IL-6-induced signaling pathway in ovarian cancer. *Clinical cancer research : an official journal of the American Association for Cancer Research* 16, 5759-5769.

Guo, Y., Xu, F., Lu, T., Duan, Z., and Zhang, Z. (2012). Interleukin-6 signaling pathway in targeted therapy for cancer. *Cancer treatment reviews* 38, 904-910.

Hagemann, T., Lawrence, T., McNeish, I., Charles, K.A., Kulbe, H., Thompson, R.G., Robinson, S.C., and Balkwill, F.R. (2008). "Re-educating" tumor-associated macrophages by targeting NF-kappaB. *The Journal of experimental medicine* 205, 1261-1268.

Hall, P.A., and Watt, F.M. (1989). Stem cells: the generation and maintenance of cellular diversity. *Development* 106, 619-633.

Hamburger, A.W., and Salmon, S.E. (1977). Primary bioassay of human tumor stem cells. *Science* 197, 461-463.

Hayward, S.W., Rosen, M.A., and Cunha, G.R. (1997). Stromal-epithelial interactions in the normal and neoplastic prostate. *British journal of urology* 79 Suppl 2, 18-26.

He, B., You, L., Uematsu, K., Zang, K., Xu, Z., Lee, A.Y., Costello, J.F., McCormick, F., and Jablons, D.M. (2003). SOCS-3 is frequently silenced by hypermethylation and suppresses cell growth in human lung cancer. *Proceedings of the National Academy of Sciences of the United States of America* 100, 14133-14138.

Heinrich, P.C., Behrmann, I., Haan, S., Hermanns, H.M., Muller-Newen, G., and Schaper, F. (2003). Principles of interleukin (IL)-6-type cytokine signalling and its regulation. *The Biochemical journal* 374, 1-20.

Heinrich, P.C., Behrmann, I., Muller-Newen, G., Schaper, F., and Graeve, L. (1998). Interleukin-6-type cytokine signalling through the gp130/Jak/STAT pathway. *The Biochemical journal* 334 (Pt 2), 297-314.

Hevehan, D.L., Miller, W.M., and Papoutsakis, E.T. (2002). Differential expression and phosphorylation of distinct STAT3 proteins during granulocytic differentiation. *Blood* 99, 1627-1637.

Hobisch, A., Ramoner, R., Fuchs, D., Godoy-Tundidor, S., Bartsch, G., Klocker, H., and Culig, Z. (2001). Prostate cancer cells (LNCaP) generated after long-term interleukin 6 (IL-6) treatment express IL-6 and acquire an IL-6 partially resistant phenotype. *Clinical cancer research : an official journal of the American Association for Cancer Research* 7, 2941-2948.

Hobisch, A., Rogatsch, H., Hittmair, A., Fuchs, D., Bartsch, G., Jr., Klocker, H., Bartsch, G., and Culig, Z. (2000). Immunohistochemical localization of interleukin-6 and its receptor in benign, premalignant and malignant prostate tissue. *The Journal of pathology* 191, 239-244.

Hodge, D.R., Hurt, E.M., and Farrar, W.L. (2005). The role of IL-6 and STAT3 in inflammation and cancer. *Eur J Cancer* 41, 2502-2512.

Hoefler, J., Schafer, G., Klocker, H., Erb, H.H., Mills, I.G., Hengst, L., Puhr, M., and Culig, Z. (2012). PIAS1 is increased in human prostate cancer and enhances proliferation through inhibition of p21. *The American journal of pathology* 180, 2097-2107.

Horoszewicz, J.S., Leong, S.S., Chu, T.M., Wajsman, Z.L., Friedman, M., Papsidero, L., Kim, U., Chai, L.S., Kakati, S., Arya, S.K., et al. (1980). The LNCaP cell line--a new model for studies on human prostatic carcinoma. *Progress in clinical and biological research* 37, 115-132.

Hsing, A.W., and Chokkalingam, A.P. (2006). Prostate cancer epidemiology. *Frontiers in bioscience : a journal and virtual library* 11, 1388-1413.

Hu, Y., and Fu, L. (2012). Targeting cancer stem cells: a new therapy to cure cancer patients. *American journal of cancer research* 2, 340-356.

Huang, M., Page, C., Reynolds, R.K., and Lin, J. (2000). Constitutive activation of stat 3 oncogene product in human ovarian carcinoma cells. *Gynecologic oncology* 79, 67-73.

Hudson, D.L., O'Hare, M., Watt, F.M., and Masters, J.R. (2000). Proliferative heterogeneity in the human prostate: evidence for epithelial stem cells. *Laboratory investigation; a journal of technical methods and pathology* 80, 1243-1250.

Huggins, C. (1967). Endocrine-induced regression of cancers. *Science* 156, 1050-1054.

Humphrey, R.K., Beattie, G.M., Lopez, A.D., Bucay, N., King, C.C., Firpo, M.T., Rose-John, S., and Hayek, A. (2004). Maintenance of pluripotency in human embryonic stem cells is STAT3 independent. *Stem Cells* 22, 522-530.

Hurt, E.M., Kawasaki, B.T., Klarmann, G.J., Thomas, S.B., and Farrar, W.L. (2008). CD44+ CD24(-) prostate cells are early cancer progenitor/stem cells that provide a model for patients with poor prognosis. *British journal of cancer* 98, 756-765.

Huynh, H., Soo, K.C., Chow, P.K., Panasci, L., and Tran, E. (2006). Xenografts of human hepatocellular carcinoma: a useful model for testing drugs. *Clinical cancer research : an official journal of the American Association for Cancer Research* 12, 4306-4314.

Ihle, J.N. (2001). The Stat family in cytokine signaling. *Current opinion in cell biology* 13, 211-217.

Isaacs, J.T., and Coffey, D.S. (1989). Etiology and disease process of benign prostatic hyperplasia. *The Prostate Supplement* 2, 33-50.

Isaacs, T.J. (1985). Control of cell proliferation and cell death in the normal and neoplastic prostate: a stem cell model. Rodgers CH, Coffey DS, Gunha G, Grayhack JT, Hinman Jr F, Horton R, editors, *Benign prostatic hyperplasia*, Department of Health and Human Services, NIH, Washington (DC) 87-2881, 85-94.

Iwahori, K., Serada, S., Fujimoto, M., Nomura, S., Osaki, T., Lee, C.M., Mizuguchi, H., Takahashi, T., Ripley, B., Okumura, M., et al. (2011). Overexpression of SOCS3 exhibits preclinical antitumor activity against malignant pleural mesothelioma. *International journal of cancer Journal international du cancer* 129, 1005-1017.

Iwamaru, A., Szymanski, S., Iwado, E., Aoki, H., Yokoyama, T., Fokt, I., Hess, K., Conrad, C., Madden, T., Sawaya, R., et al. (2007). A novel inhibitor of the STAT3 pathway induces apoptosis in malignant glioma cells both in vitro and in vivo. *Oncogene* 26, 2435-2444.

Jemal, A., Bray, F., Center, M.M., Ferlay, J., Ward, E., and Forman, D. (2011). Global cancer statistics. *CA: a cancer journal for clinicians* 61, 69-90.

Jensen, M.M., Jorgensen, J.T., Binderup, T., and Kjaer, A. (2008). Tumor volume in subcutaneous mouse xenografts measured by microCT is more accurate and reproducible than determined by 18F-FDG-microPET or external caliper. *BMC medical imaging* 8, 16.

Kaighn, M.E., Narayan, K.S., Ohnuki, Y., Lechner, J.F., and Jones, L.W. (1979). Establishment and characterization of a human prostatic carcinoma cell line (PC-3). *Investigative urology* 17, 16-23.

Kanda, N., Seno, H., Konda, Y., Marusawa, H., Kanai, M., Nakajima, T., Kawashima, T., Nanakin, A., Sawabu, T., Uenoyama, Y., et al. (2004). STAT3 is constitutively activated and supports cell survival in association with survivin expression in gastric cancer cells. *Oncogene* 23, 4921-4929.

Karkera, J., Steiner, H., Li, W., Skradski, V., Moser, P.L., Riethdorf, S., Reddy, M., Puchalski, T., Safer, K., Prabhakar, U., et al. (2011). The anti-interleukin-6 antibody siltuximab down-regulates genes implicated in tumorigenesis in prostate cancer patients from a phase I study. *The Prostate* 71, 1455-1465.

Kassen, A., Sutkowski, D.M., Ahn, H., Sensibar, J.A., Kozlowski, J.M., and Lee, C. (1996). Stromal cells of the human prostate: initial isolation and characterization. *The Prostate* 28, 89-97.

Kellokumpu-Lehtinen, P., Santti, R., and Pelliniemi, L.J. (1979). Early cytodifferentiation of human prostatic urethra and Leydig cells. *The Anatomical record* 194, 429-443.

Kellokumpu-Lehtinen, P., Santti, R., and Pelliniemi, L.J. (1980). Correlation of early cytodifferentiation of the human fetal prostate and Leydig cells. *The Anatomical record* 196, 263-273.

Kellokumpu-Lehtinen, P., Santti, R.S., and Pelliniemi, L.J. (1981). Development of human fetal prostate in culture. *Urological research* 9, 89-98.

Kinbara, H., Cunha, G.R., Boutin, E., Hayashi, N., and Kawamura, J. (1996). Evidence of stem cells in the adult prostatic epithelium based upon responsiveness to mesenchymal inductors. *The Prostate* 29, 107-116.

Kinoshita, T., Ito, H., and Miki, C. (1999). Serum interleukin-6 level reflects the tumor proliferative activity in patients with colorectal carcinoma. *Cancer* 85, 2526-2531.

Kiuchi, N., Nakajima, K., Ichiba, M., Fukada, T., Narimatsu, M., Mizuno, K., Hibi, M., and Hirano, T. (1999). STAT3 is required for the gp130-mediated full activation of the c-myc gene. *The Journal of experimental medicine* 189, 63-73.

Klein, B., Zhang, X.G., Lu, Z.Y., and Bataille, R. (1995). Interleukin-6 in human multiple myeloma. *Blood* 85, 863-872.

Kleinerman, D.I., Troncso, P., Lin, S.H., Pisters, L.L., Sherwood, E.R., Brooks, T., von Eschenbach, A.C., and Hsieh, J.T. (1995). Consistent expression of

an epithelial cell adhesion molecule (C-CAM) during human prostate development and loss of expression in prostate cancer: implication as a tumor suppressor. *Cancer research* 55, 1215-1220.

Klotz, L., Zhang, L., Lam, A., Nam, R., Mamedov, A., and Loblaw, A. (2010). Clinical results of long-term follow-up of a large, active surveillance cohort with localized prostate cancer. *Journal of clinical oncology : official journal of the American Society of Clinical Oncology* 28, 126-131.

Krieger, J.N., Lee, S.W., Jeon, J., Cheah, P.Y., Liong, M.L., and Riley, D.E. (2008). Epidemiology of prostatitis. *International journal of antimicrobial agents* 31 *Suppl 1*, S85-90.

Kroon, P., Pellacani, D., Frame, F.M., Maitland, N.J., and Collins, A.T. (2011). Cancer Stem Cells in Prostate Cancer. In *Cancer Stem Cells in Solid Tumors*, A.L. Allan, ed. (Springer Science + Business Media), pp. 99-116.

Krutzik, P.O., and Nolan, G.P. (2003). Intracellular phospho-protein staining techniques for flow cytometry: monitoring single cell signaling events. *Cytometry Part A : the journal of the International Society for Analytical Cytology* 55, 61-70.

Kumar, V.L., and Majumder, P.K. (1995). Prostate gland: structure, functions and regulation. *International urology and nephrology* 27, 231-243.

Kwabi-Addo, B., Ozen, M., and Ittmann, M. (2004). The role of fibroblast growth factors and their receptors in prostate cancer. *Endocrine-related cancer* 11, 709-724.

Kyprianou, N., and Isaacs, J.T. (1988a). Activation of programmed cell death in the rat ventral prostate after castration. *Endocrinology* 122, 552-562.

Kyprianou, N., and Isaacs, J.T. (1988b). Identification of a cellular receptor for transforming growth factor-beta in rat ventral prostate and its negative regulation by androgens. *Endocrinology* 123, 2124-2131.

Lang, S.H., Frame, F.M., and Collins, A.T. (2009). Prostate cancer stem cells. *The Journal of pathology* 217, 299-306.

Lang, S.H., Stark, M., Collins, A., Paul, A.B., Stower, M.J., and Maitland, N.J. (2001). Experimental prostate epithelial morphogenesis in response to stroma and three-dimensional matrigel culture. *Cell growth & differentiation : the molecular biology journal of the American Association for Cancer Research* 12, 631-640.

Lawson, D.A., Xin, L., Lukacs, R.U., Cheng, D., and Witte, O.N. (2007). Isolation and functional characterization of murine prostate stem cells. *Proceedings of the National Academy of Sciences of the United States of America* 104, 181-186.

Laxman, B., Morris, D.S., Yu, J., Siddiqui, J., Cao, J., Mehra, R., Lonigro, R.J., Tsodikov, A., Wei, J.T., Tomlins, S.A., et al. (2008). A first-generation multiplex

biomarker analysis of urine for the early detection of prostate cancer. *Cancer research* 68, 645-649.

Lee, J.T., and Herlyn, M. (2007). Old disease, new culprit: tumor stem cells in cancer. *Journal of cellular physiology* 213, 603-609.

Lee, S.O., Lou, W., Hou, M., de Miguel, F., Gerber, L., and Gao, A.C. (2003). Interleukin-6 promotes androgen-independent growth in LNCaP human prostate cancer cells. *Clinical cancer research : an official journal of the American Association for Cancer Research* 9, 370-376.

Lee, S.O., Lou, W., Johnson, C.S., Trump, D.L., and Gao, A.C. (2004). Interleukin-6 protects LNCaP cells from apoptosis induced by androgen deprivation through the Stat3 pathway. *The Prostate* 60, 178-186.

Leong, K.G., Wang, B.E., Johnson, L., and Gao, W.Q. (2008). Generation of a prostate from a single adult stem cell. *Nature* 456, 804-808.

Lepor, H. (2004). Management of clinically localized prostate cancer. *Reviews in urology* 6 *Suppl* 2, S3-S12.

Levy-Lahad, E., and Friedman, E. (2007). Cancer risks among BRCA1 and BRCA2 mutation carriers. *British journal of cancer* 96, 11-15.

Li, J., Yen, C., Liaw, D., Podsypanina, K., Bose, S., Wang, S.I., Puc, J., Miliareis, C., Rodgers, L., McCombie, R., et al. (1997). PTEN, a putative protein tyrosine phosphatase gene mutated in human brain, breast, and prostate cancer. *Science* 275, 1943-1947.

Liao, C.P., Adisetiyo, H., Liang, M., and Roy-Burman, P. (2010). Cancer-associated fibroblasts enhance the gland-forming capability of prostate cancer stem cells. *Cancer research* 70, 7294-7303.

Libermann, T.A., and Baltimore, D. (1990). Activation of interleukin-6 gene expression through the NF-kappa B transcription factor. *Molecular and cellular biology* 10, 2327-2334.

Licastro, F., Bertaccini, A., Porcellini, E., Chiappelli, M., Perneti, R., Sanguedolce, F., Marchiori, D., and Martorana, G. (2008). Alpha 1 antichymotrypsin genotype is associated with increased risk of prostate carcinoma and PSA levels. *Anticancer research* 28, 395-399.

Lilja, H., and Abrahamsson, P.A. (1988). Three predominant proteins secreted by the human prostate gland. *The Prostate* 12, 29-38.

Lin, D.L., Whitney, M.C., Yao, Z., and Keller, E.T. (2001). Interleukin-6 induces androgen responsiveness in prostate cancer cells through up-regulation of androgen receptor expression. *Clinical cancer research : an official journal of the American Association for Cancer Research* 7, 1773-1781.

Lin, L., Benson, D.M., Jr., DeAngelis, S., Bakan, C.E., Li, P.K., Li, C., and Lin, J. (2012). A small molecule, LLL12 inhibits constitutive STAT3 and IL-6-induced STAT3 signaling and exhibits potent growth suppressive activity in human multiple myeloma cells. *International journal of cancer Journal international du cancer* 130, 1459-1469.

Lin, L., Hutzen, B., Li, P.K., Ball, S., Zuo, M., DeAngelis, S., Foust, E., Sobo, M., Friedman, L., Bhasin, D., et al. (2010). A novel small molecule, LLL12, inhibits STAT3 phosphorylation and activities and exhibits potent growth-suppressive activity in human cancer cells. *Neoplasia* 12, 39-50.

Lin, L., Liu, A., Peng, Z., Lin, H.J., Li, P.K., Li, C., and Lin, J. (2011). STAT3 is necessary for proliferation and survival in colon cancer-initiating cells. *Cancer research* 71, 7226-7237.

Liu, A., Liu, Y., Li, P.K., Li, C., and Lin, J. (2011). LLL12 inhibits endogenous and exogenous interleukin-6-induced STAT3 phosphorylation in human pancreatic cancer cells. *Anticancer research* 31, 2029-2035.

Liu, A.Y., Nelson, P.S., van den Engh, G., and Hood, L. (2002). Human prostate epithelial cell-type cDNA libraries and prostate expression patterns. *The Prostate* 50, 92-103.

Liu, A.Y., True, L.D., LaTray, L., Nelson, P.S., Ellis, W.J., Vessella, R.L., Lange, P.H., Hood, L., and van den Engh, G. (1997). Cell-cell interaction in prostate gene regulation and cytodifferentiation. *Proceedings of the National Academy of Sciences of the United States of America* 94, 10705-10710.

Lou, H., and Dean, M. (2007). Targeted therapy for cancer stem cells: the patched pathway and ABC transporters. *Oncogene* 26, 1357-1360.

Lou, W., Ni, Z., Dyer, K., Tweardy, D.J., and Gao, A.C. (2000). Interleukin-6 induces prostate cancer cell growth accompanied by activation of stat3 signaling pathway. *The Prostate* 42, 239-242.

Lucet, I.S., Fantino, E., Styles, M., Bamert, R., Patel, O., Broughton, S.E., Walter, M., Burns, C.J., Treutlein, H., Wilks, A.F., et al. (2006). The structural basis of Janus kinase 2 inhibition by a potent and specific pan-Janus kinase inhibitor. *Blood* 107, 176-183.

Ma, S., Lee, T.K., Zheng, B.J., Chan, K.W., and Guan, X.Y. (2008). CD133+ HCC cancer stem cells confer chemoresistance by preferential expression of the Akt/PKB survival pathway. *Oncogene* 27, 1749-1758.

Maitland, N.J., and Collins, A.T. (2008a). Inflammation as the primary aetiological agent of human prostate cancer: a stem cell connection? *Journal of cellular biochemistry* 105, 931-939.

Maitland, N.J., and Collins, A.T. (2008b). Prostate cancer stem cells: a new target for therapy. *Journal of clinical oncology : official journal of the American Society of Clinical Oncology* 26, 2862-2870.

Maitland, N.J., Frame, F.M., Polson, E.S., Lewis, J.L., and Collins, A.T. (2011). Prostate cancer stem cells: do they have a basal or luminal phenotype? *Hormones & cancer* 2, 47-61.

Maitland, N.J., Macintosh, C.A., Hall, J., Sharrard, M., Quinn, G., and Lang, S. (2001). In vitro models to study cellular differentiation and function in human prostate cancers. *Radiat Res* 155, 133-142.

Mancino, A., and Lawrence, T. (2010). Nuclear factor-kappaB and tumor-associated macrophages. *Clinical cancer research : an official journal of the American Association for Cancer Research* 16, 784-789.

Mantovani, A., Allavena, P., Sica, A., and Balkwill, F. (2008). Cancer-related inflammation. *Nature* 454, 436-444.

Mantovani, A., Bottazzi, B., Colotta, F., Sozzani, S., and Ruco, L. (1992). The origin and function of tumor-associated macrophages. *Immunology today* 13, 265-270.

Marcelli, M., Tilley, W.D., Wilson, C.M., Griffin, J.E., Wilson, J.D., and McPhaul, M.J. (1990). Definition of the human androgen receptor gene structure permits the identification of mutations that cause androgen resistance: premature termination of the receptor protein at amino acid residue 588 causes complete androgen resistance. *Mol Endocrinol* 4, 1105-1116.

Maritano, D., Sugrue, M.L., Tininini, S., Dewilde, S., Strobl, B., Fu, X., Murray-Tait, V., Chiarle, R., and Poli, V. (2004). The STAT3 isoforms alpha and beta have unique and specific functions. *Nature immunology* 5, 401-409.

Marotta, L.L., Almendro, V., Marusyk, A., Shipitsin, M., Schemme, J., Walker, S.R., Bloushtain-Qimron, N., Kim, J.J., Choudhury, S.A., Maruyama, R., et al. (2011). The JAK2/STAT3 signaling pathway is required for growth of CD44(+)CD24(-) stem cell-like breast cancer cells in human tumors. *The Journal of clinical investigation* 121, 2723-2735.

Martinon, F., Petrilli, V., Mayor, A., Tardivel, A., and Tschopp, J. (2006). Gout-associated uric acid crystals activate the NALP3 inflammasome. *Nature* 440, 237-241.

Masuda, M., Suzui, M., Yasumatu, R., Nakashima, T., Kuratomi, Y., Azuma, K., Tomita, K., Komiyama, S., and Weinstein, I.B. (2002). Constitutive activation of signal transducers and activators of transcription 3 correlates with cyclin D1 overexpression and may provide a novel prognostic marker in head and neck squamous cell carcinoma. *Cancer research* 62, 3351-3355.

Matsuda, T., Nakamura, T., Nakao, K., Arai, T., Katsuki, M., Heike, T., and Yokota, T. (1999). STAT3 activation is sufficient to maintain an undifferentiated state of mouse embryonic stem cells. *The EMBO journal* 18, 4261-4269.

Matthews, J.R., Sansom, O.J., and Clarke, A.R. (2011). Absolute requirement for STAT3 function in small-intestine crypt stem cell survival. *Cell death and differentiation* 18, 1934-1943.

McNeal, J.E. (1981). Normal and pathologic anatomy of prostate. *Urology* 17, 11-16.

McNeal, J.E. (1988). Normal anatomy of the prostate and changes in benign prostatic hypertrophy and carcinoma. *Seminars in ultrasound, CT, and MR* 9, 329-334.

McNeal, J.E., Redwine, E.A., Freiha, F.S., and Stamey, T.A. (1988). Zonal distribution of prostatic adenocarcinoma. Correlation with histologic pattern and direction of spread. *Am J Surg Pathol* 12, 897-906.

Meeker, A.K., Hicks, J.L., Platz, E.A., March, G.E., Bennett, C.J., Delannoy, M.J., and De Marzo, A.M. (2002). Telomere shortening is an early somatic DNA alteration in human prostate tumorigenesis. *Cancer research* 62, 6405-6409.

Michaud, D.S. (2007). Chronic inflammation and bladder cancer. *Urologic oncology* 25, 260-268.

Mohler, J.L., Gregory, C.W., Ford, O.H., 3rd, Kim, D., Weaver, C.M., Petrusz, P., Wilson, E.M., and French, F.S. (2004). The androgen axis in recurrent prostate cancer. *Clinical cancer research : an official journal of the American Association for Cancer Research* 10, 440-448.

Mora, L.B., Buettner, R., Seigne, J., Diaz, J., Ahmad, N., Garcia, R., Bowman, T., Falcone, R., Fairclough, R., Cantor, A., et al. (2002). Constitutive activation of Stat3 in human prostate tumors and cell lines: direct inhibition of Stat3 signaling induces apoptosis of prostate cancer cells. *Cancer research* 62, 6659-6666.

Morrison, S.J., and Spradling, A.C. (2008). Stem cells and niches: mechanisms that promote stem cell maintenance throughout life. *Cell* 132, 598-611.

Murant, S.J., Handley, J., Stower, M., Reid, N., Cussenot, O., and Maitland, N.J. (1997). Co-ordinated changes in expression of cell adhesion molecules in prostate cancer. *Eur J Cancer* 33, 263-271.

Murat, A., Migliavacca, E., Gorlia, T., Lambiv, W.L., Shay, T., Hamou, M.F., de Tribolet, N., Regli, L., Wick, W., Kouwenhoven, M.C., et al. (2008). Stem cell-related "self-renewal" signature and high epidermal growth factor receptor expression associated with resistance to concomitant chemoradiotherapy in glioblastoma. *Journal of clinical oncology : official journal of the American Society of Clinical Oncology* 26, 3015-3024.

Nagle, R.B., Ahmann, F.R., McDaniel, K.M., Paquin, M.L., Clark, V.A., and Celniker, A. (1987). Cytokeratin characterization of human prostatic carcinoma and its derived cell lines. *Cancer research* 47, 281-286.

Ni, Z., Lou, W., Leman, E.S., and Gao, A.C. (2000). Inhibition of constitutively activated Stat3 signaling pathway suppresses growth of prostate cancer cells. *Cancer research* 60, 1225-1228.

Niu, G., Bowman, T., Huang, M., Shivers, S., Reintgen, D., Daud, A., Chang, A., Kraker, A., Jove, R., and Yu, H. (2002a). Roles of activated Src and Stat3 signaling in melanoma tumor cell growth. *Oncogene* 21, 7001-7010.

Niu, G., Wright, K.L., Huang, M., Song, L., Haura, E., Turkson, J., Zhang, S., Wang, T., Sinibaldi, D., Coppola, D., et al. (2002b). Constitutive Stat3 activity up-regulates VEGF expression and tumor angiogenesis. *Oncogene* 21, 2000-2008.

Niwa, H., Burdon, T., Chambers, I., and Smith, A. (1998). Self-renewal of pluripotent embryonic stem cells is mediated via activation of STAT3. *Genes & development* 12, 2048-2060.

Norris, A.M., Gentry, M., Peehl, D.M., D'Agostino, R., Jr., and Scarpinato, K.D. (2009). The elevated expression of a mismatch repair protein is a predictor for biochemical recurrence after radical prostatectomy. *Cancer epidemiology, biomarkers & prevention : a publication of the American Association for Cancer Research, cosponsored by the American Society of Preventive Oncology* 18, 57-64.

Nowell, P.C. (1976). The clonal evolution of tumor cell populations. *Science* 194, 23-28.

Oesterling, J.E. (1991). Prostate-specific antigen: a valuable clinical tool. *Oncology (Williston Park)* 5, 107-122; discussion 122, 125-106, 128.

Oldridge, E.E., Pellacani, D., Collins, A.T., and Maitland, N.J. (2012). Prostate cancer stem cells: Are they androgen-responsive? *Molecular and cellular endocrinology* 360, 14-24.

Onimoe, G.I., Liu, A., Lin, L., Wei, C.C., Schwartz, E.B., Bhasin, D., Li, C., Fuchs, J.R., Li, P.K., Houghton, P., et al. (2012). Small molecules, LLL12 and FLLL32, inhibit STAT3 and exhibit potent growth suppressive activity in osteosarcoma cells and tumor growth in mice. *Investigational new drugs* 30, 916-926.

Parkin, D.M. (2011). 2. Tobacco-attributable cancer burden in the UK in 2010. *British journal of cancer* 105 Suppl 2, S6-S13.

Patrawala, L., Calhoun, T., Schneider-Broussard, R., Li, H., Bhatia, B., Tang, S., Reilly, J.G., Chandra, D., Zhou, J., Claypool, K., et al. (2006). Highly purified CD44+ prostate cancer cells from xenograft human tumors are enriched in tumorigenic and metastatic progenitor cells. *Oncogene* 25, 1696-1708.

Pedranzini, L., Dechow, T., Berishaj, M., Comenzo, R., Zhou, P., Azare, J., Bornmann, W., and Bromberg, J. (2006). Pyridone 6, a pan-Janus-activated kinase inhibitor, induces growth inhibition of multiple myeloma cells. *Cancer research* 66, 9714-9721.

Peehl, D.M. (1992). Culture of Human Prostatic Epithelial Cells. In *CULTURE OF EPITHELIAL CELLS*, R.I. Freshney, ed. (Wiley-Liss, Inc), pp. 159 - 180.

Peehl, D.M. (2005). Primary cell cultures as models of prostate cancer development. *Endocrine-related cancer* 12, 19-47.

Persson, B.E., and Ronquist, G. (1996). Evidence for a mechanistic association between nonbacterial prostatitis and levels of urate and creatinine in expressed prostatic secretion. *The Journal of urology* 155, 958-960.

Pflanz, S., Timans, J.C., Cheung, J., Rosales, R., Kanzler, H., Gilbert, J., Hibbert, L., Churakova, T., Travis, M., Vaisberg, E., et al. (2002). IL-27, a heterodimeric cytokine composed of EBI3 and p28 protein, induces proliferation of naive CD4(+) T cells. *Immunity* 16, 779-790.

Phillips, T.M., McBride, W.H., and Pajonk, F. (2006). The response of CD24(-/low)/CD44+ breast cancer-initiating cells to radiation. *Journal of the National Cancer Institute* 98, 1777-1785.

Pienta, K.J., and Bradley, D. (2006). Mechanisms underlying the development of androgen-independent prostate cancer. *Clinical cancer research : an official journal of the American Association for Cancer Research* 12, 1665-1671.

Pierconti, F., Martini, M., Pinto, F., Cenci, T., Capodimonti, S., Calarco, A., Bassi, P.F., and Larocca, L.M. (2011). Epigenetic silencing of SOCS3 identifies a subset of prostate cancer with an aggressive behavior. *The Prostate* 71, 318-325.

Pisters, L.L., Troncoso, P., Zhau, H.E., Li, W., von Eschenbach, A.C., and Chung, L.W. (1995). c-met proto-oncogene expression in benign and malignant human prostate tissues. *The Journal of urology* 154, 293-298.

Poletti, F., Medici, M.C., Alinovi, A., Menozzi, M.G., Sacchini, P., Stagni, G., Toni, M., and Benoldi, D. (1985). Isolation of Chlamydia trachomatis from the prostatic cells in patients affected by nonacute abacterial prostatitis. *The Journal of urology* 134, 691-693.

Potten, C.S. (1981). Cell replacement in epidermis (keratopoiesis) via discrete units of proliferation. *International review of cytology* 69, 271-318.

Pricola, K.L., Kuhn, N.Z., Haleem-Smith, H., Song, Y., and Tuan, R.S. (2009). Interleukin-6 maintains bone marrow-derived mesenchymal stem cell stemness by an ERK1/2-dependent mechanism. *Journal of cellular biochemistry* 108, 577-588.

Puhr, M., Santer, F.R., Neuwirt, H., Susani, M., Nemeth, J.A., Hobisch, A., Kenner, L., and Culig, Z. (2009). Down-regulation of suppressor of cytokine signaling-

3 causes prostate cancer cell death through activation of the extrinsic and intrinsic apoptosis pathways. *Cancer research* 69, 7375-7384.

Puthier, D., Derenne, S., Barille, S., Moreau, P., Harousseau, J.L., Bataille, R., and Amiot, M. (1999). Mcl-1 and Bcl-xL are co-regulated by IL-6 in human myeloma cells. *British journal of haematology* 107, 392-395.

Putzi, M.J., and De Marzo, A.M. (2000). Morphologic transitions between proliferative inflammatory atrophy and high-grade prostatic intraepithelial neoplasia. *Urology* 56, 828-832.

Rahaman, S.O., Harbor, P.C., Chernova, O., Barnett, G.H., Vogelbaum, M.A., and Haque, S.J. (2002). Inhibition of constitutively active Stat3 suppresses proliferation and induces apoptosis in glioblastoma multiforme cells. *Oncogene* 21, 8404-8413.

Rembrink, K., Romijn, J.C., van der Kwast, T.H., Rubben, H., and Schroder, F.H. (1997). Orthotopic implantation of human prostate cancer cell lines: a clinically relevant animal model for metastatic prostate cancer. *The Prostate* 31, 168-174.

Reya, T., Morrison, S.J., Clarke, M.F., and Weissman, I.L. (2001). Stem cells, cancer, and cancer stem cells. *Nature* 414, 105-111.

Richardson, G.D., Robson, C.N., Lang, S.H., Neal, D.E., Maitland, N.J., and Collins, A.T. (2004). CD133, a novel marker for human prostatic epithelial stem cells. *Journal of cell science* 117, 3539-3545.

Risbridger, G.P., Bianco, J.J., Ellem, S.J., and McPherson, S.J. (2003). Oestrogens and prostate cancer. *Endocrine-related cancer* 10, 187-191.

Robinson, E.J., Neal, D.E., and Collins, A.T. (1998). Basal cells are progenitors of luminal cells in primary cultures of differentiating human prostatic epithelium. *The Prostate* 37, 149-160.

Roehrborn, C.G. (2002). Reporting of acute urinary retention in BPH treatment trials: importance of patient follow-up after discontinuation and case definitions. *Urology* 59, 811-815.

Royuela, M., Ricote, M., Parsons, M.S., Garcia-Tunon, I., Paniagua, R., and de Miguel, M.P. (2004). Immunohistochemical analysis of the IL-6 family of cytokines and their receptors in benign, hyperplastic, and malignant human prostate. *The Journal of pathology* 202, 41-49.

Rybicki, B.A., Conti, D.V., Moreira, A., Cicek, M., Casey, G., and Witte, J.S. (2004). DNA repair gene XRCC1 and XPD polymorphisms and risk of prostate cancer. *Cancer epidemiology, biomarkers & prevention : a publication of the American Association for Cancer Research, cosponsored by the American Society of Preventive Oncology* 13, 23-29.

Sansone, P., Storci, G., Tavorari, S., Guarnieri, T., Giovannini, C., Taffurelli, M., Ceccarelli, C., Santini, D., Paterini, P., Marcu, K.B., et al. (2007). IL-6 triggers malignant features in mammospheres from human ductal breast carcinoma and normal mammary gland. *The Journal of clinical investigation* 117, 3988-4002.

Santer, F.R., Malinowska, K., Culig, Z., and Cavarretta, I.T. (2010). Interleukin-6 trans-signalling differentially regulates proliferation, migration, adhesion and maspin expression in human prostate cancer cells. *Endocrine-related cancer* 17, 241-253.

Sar, M., Lubahn, D.B., French, F.S., and Wilson, E.M. (1990). Immunohistochemical localization of the androgen receptor in rat and human tissues. *Endocrinology* 127, 3180-3186.

Schafer, Z.T., and Brugge, J.S. (2007). IL-6 involvement in epithelial cancers. *The Journal of clinical investigation* 117, 3660-3663.

Schepers, A.G., Snippert, H.J., Stange, D.E., van den Born, M., van Es, J.H., van de Wetering, M., and Clevers, H. (2012). Lineage tracing reveals Lgr5+ stem cell activity in mouse intestinal adenomas. *Science* 337, 730-735.

Scherl, A., Li, J.F., Cardiff, R.D., and Schreiber-Agus, N. (2004). Prostatic intraepithelial neoplasia and intestinal metaplasia in prostates of probasin-RAS transgenic mice. *The Prostate* 59, 448-459.

Shackleton, M., Quintana, E., Fearon, E.R., and Morrison, S.J. (2009). Heterogeneity in cancer: cancer stem cells versus clonal evolution. *Cell* 138, 822-829.

Sherry, M.M., Reeves, A., Wu, J.K., and Cochran, B.H. (2009). STAT3 is required for proliferation and maintenance of multipotency in glioblastoma stem cells. *Stem Cells* 27, 2383-2392.

Sherwood, E.R., Theyer, G., Steiner, G., Berg, L.A., Kozlowski, J.M., and Lee, C. (1991). Differential expression of specific cytokeratin polypeptides in the basal and luminal epithelia of the human prostate. *The Prostate* 18, 303-314.

Shodeinde, A.L., and Barton, B.E. (2012). Potential use of STAT3 inhibitors in targeted prostate cancer therapy: future prospects. *OncoTargets and therapy* 5, 119-125.

Shuai, K. (2006). Regulation of cytokine signaling pathways by PIAS proteins. *Cell research* 16, 196-202.

Shuai, K., and Liu, B. (2003). Regulation of JAK-STAT signalling in the immune system. *Nature reviews Immunology* 3, 900-911.

Shultz, L.D., Schweitzer, P.A., Christianson, S.W., Gott, B., Schweitzer, I.B., Tennent, B., McKenna, S., Mobraaten, L., Rajan, T.V., Greiner, D.L., et al. (1995). Multiple defects in innate and adaptive immunologic function in NOD/LtSz-scid mice. *J Immunol* 154, 180-191.

Sica, A., Saccani, A., Bottazzi, B., Polentarutti, N., Vecchi, A., van Damme, J., and Mantovani, A. (2000). Autocrine production of IL-10 mediates defective IL-12 production and NF-kappa B activation in tumor-associated macrophages. *J Immunol* 164, 762-767.

Siegall, C.B., Schwab, G., Nordan, R.P., FitzGerald, D.J., and Pastan, I. (1990). Expression of the interleukin 6 receptor and interleukin 6 in prostate carcinoma cells. *Cancer research* 50, 7786-7788.

Signoretti, S., Waltregny, D., Dilks, J., Isaac, B., Lin, D., Garraway, L., Yang, A., Montironi, R., McKeon, F., and Loda, M. (2000). p63 is a prostate basal cell marker and is required for prostate development. *The American journal of pathology* 157, 1769-1775.

Slack, J.M. (2000). Stem cells in epithelial tissues. *Science* 287, 1431-1433.

Smith, P.C., Hobisch, A., Lin, D.L., Culig, Z., and Keller, E.T. (2001). Interleukin-6 and prostate cancer progression. *Cytokine & growth factor reviews* 12, 33-40.

Smith, P.C., and Keller, E.T. (2001). Anti-interleukin-6 monoclonal antibody induces regression of human prostate cancer xenografts in nude mice. *The Prostate* 48, 47-53.

Snowdon, D.A., Phillips, R.L., and Choi, W. (1984). Diet, obesity, and risk of fatal prostate cancer. *American journal of epidemiology* 120, 244-250.

Sommerfeld, H.J., Meeker, A.K., Piatyszek, M.A., Bova, G.S., Shay, J.W., and Coffey, D.S. (1996). Telomerase activity: a prevalent marker of malignant human prostate tissue. *Cancer research* 56, 218-222.

Song, L., Rawal, B., Nemeth, J.A., and Haura, E.B. (2011). JAK1 activates STAT3 activity in non-small-cell lung cancer cells and IL-6 neutralizing antibodies can suppress JAK1-STAT3 signaling. *Molecular cancer therapeutics* 10, 481-494.

Song, L., Turkson, J., Karras, J.G., Jove, R., and Haura, E.B. (2003). Activation of Stat3 by receptor tyrosine kinases and cytokines regulates survival in human non-small cell carcinoma cells. *Oncogene* 22, 4150-4165.

Southam, C., and Brunschwig A. (1961). Quantitative studies of autotransplantation of human cancer. *Cancer* 14, 461-563.

Spangrude, G.J., Heimfeld, S., and Weissman, I.L. (1988). Purification and characterization of mouse hematopoietic stem cells. *Science* 241, 58-62.

Stahel, R.A., Mabry, M., Sabbath, K., Speak, J.A., and Bernal, S.D. (1985). Selective cytotoxicity of murine monoclonal antibody LAM2 against human small-cell carcinoma in the presence of human complement: possible use for in vitro elimination of tumor cells from bone marrow. *International journal of cancer Journal international du cancer* 35, 587-592.

Starr, R., Willson, T.A., Viney, E.M., Murray, L.J., Rayner, J.R., Jenkins, B.J., Gonda, T.J., Alexander, W.S., Metcalf, D., Nicola, N.A., et al. (1997). A family of cytokine-inducible inhibitors of signalling. *Nature* 387, 917-921.

Steiner, H., Cavarretta, I.T., Moser, P.L., Berger, A.P., Bektic, J., Dietrich, H., Zaki, M.H., Nakada, M., Hobisch, A., Nemeth, J.A., et al. (2006). Regulation of growth of prostate cancer cells selected in the presence of interleukin-6 by the anti-interleukin-6 antibody CNTO 328. *The Prostate* 66, 1744-1752.

Steiner, H., Godoy-Tundidor, S., Rogatsch, H., Berger, A.P., Fuchs, D., Comuzzi, B., Bartsch, G., Hobisch, A., and Culig, Z. (2003). Accelerated in vivo growth of prostate tumors that up-regulate interleukin-6 is associated with reduced retinoblastoma protein expression and activation of the mitogen-activated protein kinase pathway. *The American journal of pathology* 162, 655-663.

Stevermer, J.J., and Easley, S.K. (2000). Treatment of prostatitis. *American family physician* 61, 3015-3022, 3025-3016.

Stone, K.R., Mickey, D.D., Wunderli, H., Mickey, G.H., and Paulson, D.F. (1978). Isolation of a human prostate carcinoma cell line (DU 145). *International journal of cancer Journal international du cancer* 21, 274-281.

Sugimura, Y., Cunha, G.R., and Donjacour, A.A. (1986). Morphogenesis of ductal networks in the mouse prostate. *Biology of reproduction* 34, 961-971.

Sutherland, K.D., Lindeman, G.J., Choong, D.Y., Wittlin, S., Brentzell, L., Phillips, W., Campbell, I.G., and Visvader, J.E. (2004). Differential hypermethylation of SOCS genes in ovarian and breast carcinomas. *Oncogene* 23, 7726-7733.

Takeda, K., Noguchi, K., Shi, W., Tanaka, T., Matsumoto, M., Yoshida, N., Kishimoto, T., and Akira, S. (1997). Targeted disruption of the mouse Stat3 gene leads to early embryonic lethality. *Proceedings of the National Academy of Sciences of the United States of America* 94, 3801-3804.

Tang, Y., Kitisin, K., Jogunoori, W., Li, C., Deng, C.X., Mueller, S.C., Resson, H.W., Rashid, A., He, A.R., Mendelson, J.S., et al. (2008). Progenitor/stem cells give rise to liver cancer due to aberrant TGF-beta and IL-6 signaling. *Proceedings of the National Academy of Sciences of the United States of America* 105, 2445-2450.

Tannock, I.F., de Wit, R., Berry, W.R., Horti, J., Pluzanska, A., Chi, K.N., Oudard, S., Theodore, C., James, N.D., Turesson, I., et al. (2004). Docetaxel plus prednisone or mitoxantrone plus prednisone for advanced prostate cancer. *The New England journal of medicine* 351, 1502-1512.

Terracciano, D., Bruzzese, D., Ferro, M., Autorino, R., di Lorenzo, G., Buonerba, C., Mariano, A., Macchia, V., Altieri, V., and di Carlo, A. (2011). Soluble interleukin-6 receptor to interleukin-6 (sIL6R/IL-6) ratio in serum as a predictor of high Gleason sum at radical prostatectomy. *Oncology letters* 2, 861-864.

Terzic, J., Grivennikov, S., Karin, E., and Karin, M. (2010). Inflammation and colon cancer. *Gastroenterology* 138, 2101-2114 e2105.

Thompson, I.M., Pauler, D.K., Goodman, P.J., Tangen, C.M., Lucia, M.S., Parnes, H.L., Minasian, L.M., Ford, L.G., Lippman, S.M., Crawford, E.D., et al. (2004). Prevalence of prostate cancer among men with a prostate-specific antigen level \leq 4.0 ng per milliliter. *The New England journal of medicine* 350, 2239-2246.

Thompson, J.E., Cubbon, R.M., Cummings, R.T., Wicker, L.S., Frankshun, R., Cunningham, B.R., Cameron, P.M., Meinke, P.T., Liverton, N., Weng, Y., et al. (2002). Photochemical preparation of a pyridone containing tetracycline: a Jak protein kinase inhibitor. *Bioorganic & medicinal chemistry letters* 12, 1219-1223.

Thompson, T.C., Southgate, J., Kitchener, G., and Land, H. (1989). Multistage carcinogenesis induced by ras and myc oncogenes in a reconstituted organ. *Cell* 56, 917-930.

Tomlins, S.A., Rhodes, D.R., Perner, S., Dhanasekaran, S.M., Mehra, R., Sun, X.W., Varambally, S., Cao, X., Tchinda, J., Kuefer, R., et al. (2005). Recurrent fusion of TMPRSS2 and ETS transcription factor genes in prostate cancer. *Science* 310, 644-648.

Trikha, M., Corringham, R., Klein, B., and Rossi, J.F. (2003). Targeted anti-interleukin-6 monoclonal antibody therapy for cancer: a review of the rationale and clinical evidence. *Clinical cancer research : an official journal of the American Association for Cancer Research* 9, 4653-4665.

Trzeciak, A.R., Nyaga, S.G., Jaruga, P., Lohani, A., Dizdaroglu, M., and Evans, M.K. (2004). Cellular repair of oxidatively induced DNA base lesions is defective in prostate cancer cell lines, PC-3 and DU-145. *Carcinogenesis* 25, 1359-1370.

Tsujimura, A., Koikawa, Y., Salm, S., Takao, T., Coetzee, S., Moscatelli, D., Shapiro, E., Lepor, H., Sun, T.T., and Wilson, E.L. (2002). Proximal location of mouse prostate epithelial stem cells: a model of prostatic homeostasis. *The Journal of cell biology* 157, 1257-1265.

Twillie, D.A., Eisenberger, M.A., Carducci, M.A., Hsieh, W.S., Kim, W.Y., and Simons, J.W. (1995). Interleukin-6: a candidate mediator of human prostate cancer morbidity. *Urology* 45, 542-549.

Uemura, N., Okamoto, S., Yamamoto, S., Matsumura, N., Yamaguchi, S., Yamakido, M., Taniyama, K., Sasaki, N., and Schlemper, R.J. (2001). Helicobacter pylori infection and the development of gastric cancer. *The New England journal of medicine* 345, 784-789.

Umbas, R., Isaacs, W.B., Bringuier, P.P., Schaafsma, H.E., Karthaus, H.F., Oosterhof, G.O., Debruyne, F.M., and Schalken, J.A. (1994). Decreased E-cadherin

expression is associated with poor prognosis in patients with prostate cancer. *Cancer research* 54, 3929-3933.

Valkenburg, K.C., and Williams, B.O. (2011). Mouse models of prostate cancer. *Prostate cancer* 2011, 895238.

Vallieres, L., Campbell, I.L., Gage, F.H., and Sawchenko, P.E. (2002). Reduced hippocampal neurogenesis in adult transgenic mice with chronic astrocytic production of interleukin-6. *The Journal of neuroscience : the official journal of the Society for Neuroscience* 22, 486-492.

van den Hoogen, C., van der Horst, G., Cheung, H., Buijs, J.T., Lippitt, J.M., Guzman-Ramirez, N., Hamdy, F.C., Eaton, C.L., Thalmann, G.N., Cecchini, M.G., et al. (2010). High aldehyde dehydrogenase activity identifies tumor-initiating and metastasis-initiating cells in human prostate cancer. *Cancer research* 70, 5163-5173.

van Leenders, G., Dijkman, H., Hulsbergen-van de Kaa, C., Ruiter, D., and Schalken, J. (2000). Demonstration of intermediate cells during human prostate epithelial differentiation in situ and in vitro using triple-staining confocal scanning microscopy. *Laboratory investigation; a journal of technical methods and pathology* 80, 1251-1258.

van Weerden, W.M., Bangma, C., and de Wit, R. (2009). Human xenograft models as useful tools to assess the potential of novel therapeutics in prostate cancer. *British journal of cancer* 100, 13-18.

van Zaanen, H.C., Koopmans, R.P., Aarden, L.A., Rensink, H.J., Stouthard, J.M., Warnaar, S.O., Lokhorst, H.M., and van Oers, M.H. (1996). Endogenous interleukin 6 production in multiple myeloma patients treated with chimeric monoclonal anti-IL6 antibodies indicates the existence of a positive feed-back loop. *The Journal of clinical investigation* 98, 1441-1448.

van Zaanen, H.C., Lokhorst, H.M., Aarden, L.A., Rensink, H.J., Warnaar, S.O., van der Lelie, J., and van Oers, M.H. (1998). Chimaeric anti-interleukin 6 monoclonal antibodies in the treatment of advanced multiple myeloma: a phase I dose-escalating study. *British journal of haematology* 102, 783-790.

Veldscholte, J., Berrevoets, C.A., Ris-Stalpers, C., Kuiper, G.G., Jenster, G., Trapman, J., Brinkmann, A.O., and Mulder, E. (1992). The androgen receptor in LNCaP cells contains a mutation in the ligand binding domain which affects steroid binding characteristics and response to antiandrogens. *The Journal of steroid biochemistry and molecular biology* 41, 665-669.

Verhagen, A.P., Ramaekers, F.C., Aalders, T.W., Schaafsma, H.E., Debruyne, F.M., and Schalken, J.A. (1992). Colocalization of basal and luminal cell-type cytokeratins in human prostate cancer. *Cancer research* 52, 6182-6187.

Visakorpi, T., Hyytinen, E., Koivisto, P., Tanner, M., Keinanen, R., Palmberg, C., Palotie, A., Tammela, T., Isola, J., and Kallioniemi, O.P. (1995). In vivo amplification of the androgen receptor gene and progression of human prostate cancer. *Nature genetics* 9, 401-406.

Visvader, J.E., and Lindeman, G.J. (2008). Cancer stem cells in solid tumours: accumulating evidence and unresolved questions. *Nature reviews Cancer* 8, 755-768.

Voorhees, P.M., Chen, Q., Kuhn, D.J., Small, G.W., Hunsucker, S.A., Strader, J.S., Corringham, R.E., Zaki, M.H., Nemeth, J.A., and Orlowski, R.Z. (2007). Inhibition of interleukin-6 signaling with CNTO 328 enhances the activity of bortezomib in preclinical models of multiple myeloma. *Clinical cancer research : an official journal of the American Association for Cancer Research* 13, 6469-6478.

Walboomers, J.M., Jacobs, M.V., Manos, M.M., Bosch, F.X., Kummer, J.A., Shah, K.V., Snijders, P.J., Peto, J., Meijer, C.J., and Munoz, N. (1999). Human papillomavirus is a necessary cause of invasive cervical cancer worldwide. *The Journal of pathology* 189, 12-19.

Wallner, L., Dai, J., Escara-Wilke, J., Zhang, J., Yao, Z., Lu, Y., Trikha, M., Nemeth, J.A., Zaki, M.H., and Keller, E.T. (2006). Inhibition of interleukin-6 with CNTO328, an anti-interleukin-6 monoclonal antibody, inhibits conversion of androgen-dependent prostate cancer to an androgen-independent phenotype in orchiectomized mice. *Cancer research* 66, 3087-3095.

Walsh, P.C. (2007). The discovery of the cavernous nerves and development of nerve sparing radical retropubic prostatectomy. *The Journal of urology* 177, 1632-1635.

Wang, G., Wang, Z., Sarkar, F.H., and Wei, W. (2012). Targeting prostate cancer stem cells for cancer therapy. *Discovery medicine* 13, 135-142.

Wang, H., Lathia, J.D., Wu, Q., Wang, J., Li, Z., Heddleston, J.M., Eyler, C.E., Elderbroom, J., Gallagher, J., Schuschu, J., et al. (2009a). Targeting interleukin 6 signaling suppresses glioma stem cell survival and tumor growth. *Stem Cells* 27, 2393-2404.

Wang, S., Gao, J., Lei, Q., Rozengurt, N., Pritchard, C., Jiao, J., Thomas, G.V., Li, G., Roy-Burman, P., Nelson, P.S., et al. (2003). Prostate-specific deletion of the murine Pten tumor suppressor gene leads to metastatic prostate cancer. *Cancer cell* 4, 209-221.

Wang, X., Kruithof-de Julio, M., Economides, K.D., Walker, D., Yu, H., Halili, M.V., Hu, Y.P., Price, S.M., Abate-Shen, C., and Shen, M.M. (2009b). A luminal epithelial stem cell that is a cell of origin for prostate cancer. *Nature* 461, 495-500.

Wang, Y., Xue, H., Cutz, J.C., Bayani, J., Mawji, N.R., Chen, W.G., Goetz, L.J., Hayward, S.W., Sadar, M.D., Gilks, C.B., et al. (2005). An orthotopic metastatic prostate cancer model in SCID mice via grafting of a transplantable human prostate tumor line. *Laboratory investigation; a journal of technical methods and pathology* 85, 1392-1404.

Watanabe, K., Ueno, M., Kamiya, D., Nishiyama, A., Matsumura, M., Wataya, T., Takahashi, J.B., Nishikawa, S., Nishikawa, S., Muguruma, K., et al. (2007). A ROCK inhibitor permits survival of dissociated human embryonic stem cells. *Nature biotechnology* 25, 681-686.

Watson, C.J., and Miller, W.R. (1995). Elevated levels of members of the STAT family of transcription factors in breast carcinoma nuclear extracts. *British journal of cancer* 71, 840-844.

Watt, K.W., Lee, P.J., M'Timkulu, T., Chan, W.P., and Loor, R. (1986). Human prostate-specific antigen: structural and functional similarity with serine proteases. *Proceedings of the National Academy of Sciences of the United States of America* 83, 3166-3170.

Webber, M.M., Bello, D., and Quader, S. (1996). Immortalized and tumorigenic adult human prostatic epithelial cell lines: characteristics and applications. Part I. Cell markers and immortalized nontumorigenic cell lines. *The Prostate* 29, 386-394.

Weber-Nordt, R.M., Egen, C., Wehinger, J., Ludwig, W., Gouilleux-Gruart, V., Mertelsmann, R., and Finke, J. (1996). Constitutive activation of STAT proteins in primary lymphoid and myeloid leukemia cells and in Epstein-Barr virus (EBV)-related lymphoma cell lines. *Blood* 88, 809-816.

Wei, C.C., Ball, S., Lin, L., Liu, A., Fuchs, J.R., Li, P.K., Li, C., and Lin, J. (2011). Two small molecule compounds, LLL12 and FLLL32, exhibit potent inhibitory activity on STAT3 in human rhabdomyosarcoma cells. *Int J Oncol* 38, 279-285.

Wen, Z., Zhong, Z., and Darnell, J.E., Jr. (1995). Maximal activation of transcription by Stat1 and Stat3 requires both tyrosine and serine phosphorylation. *Cell* 82, 241-250.

Wernert, N., Seitz, G., and Achtstatter, T. (1987). Immunohistochemical investigation of different cytokeratins and vimentin in the prostate from the fetal period up to adulthood and in prostate carcinoma. *Pathology, research and practice* 182, 617-626.

Wicha, M.S., Liu, S., and Dontu, G. (2006). Cancer stem cells: an old idea--a paradigm shift. *Cancer research* 66, 1883-1890; discussion 1895-1886.

Winquist, R.J., Boucher, D.M., Wood, M., and Furey, B.F. (2009). Targeting cancer stem cells for more effective therapies: Taking out cancer's locomotive engine. *Biochemical pharmacology* 78, 326-334.

Woodward, W.A., Bristow, R.G., Clarke, M.F., Coppes, R.P., Cristofanilli, M., Duda, D.G., Fike, J.R., Hambardzumyan, D., Hill, R.P., Jordan, C.T., et al. (2009). Radiation Therapy Oncology Group translational research program stem cell symposium: incorporating stem cell hypotheses into clinical trials. *International journal of radiation oncology, biology, physics* 74, 1580-1591.

Wu, T., Giovannucci, E., Welge, J., Mallick, P., Tang, W.Y., and Ho, S.M. (2011). Measurement of GSTP1 promoter methylation in body fluids may complement PSA screening: a meta-analysis. *British journal of cancer* 105, 65-73.

Xu, J., Zheng, S.L., Turner, A., Isaacs, S.D., Wiley, K.E., Hawkins, G.A., Chang, B.L., Blecker, E.R., Walsh, P.C., Meyers, D.A., et al. (2002). Associations between hOGG1 sequence variants and prostate cancer susceptibility. *Cancer research* 62, 2253-2257.

Xue, Y., Smedts, F., Debruyne, F.M., de la Rosette, J.J., and Schalken, J.A. (1998). Identification of intermediate cell types by keratin expression in the developing human prostate. *The Prostate* 34, 292-301.

Yang, A., Kaghad, M., Wang, Y., Gillett, E., Fleming, M.D., Dotsch, V., Andrews, N.C., Caput, D., and McKeon, F. (1998). p63, a p53 homolog at 3q27-29, encodes multiple products with transactivating, death-inducing, and dominant-negative activities. *Molecular cell* 2, 305-316.

Yeh, C.C., Lee, C., and Dahiya, R. (2001). DNA mismatch repair enzyme activity and gene expression in prostate cancer. *Biochemical and biophysical research communications* 285, 409-413.

Yin, A.H., Miraglia, S., Zanjani, E.D., Almeida-Porada, G., Ogawa, M., Leary, A.G., Olweus, J., Kearney, J., and Buck, D.W. (1997). AC133, a novel marker for human hematopoietic stem and progenitor cells. *Blood* 90, 5002-5012.

Ying, Q.L., Wray, J., Nichols, J., Batlle-Morera, L., Doble, B., Woodgett, J., Cohen, P., and Smith, A. (2008). The ground state of embryonic stem cell self-renewal. *Nature* 453, 519-523.

Yoshikawa, H., Matsubara, K., Qian, G.S., Jackson, P., Groopman, J.D., Manning, J.E., Harris, C.C., and Herman, J.G. (2001). SOCS-1, a negative regulator of the JAK/STAT pathway, is silenced by methylation in human hepatocellular carcinoma and shows growth-suppression activity. *Nature genetics* 28, 29-35.

Yu, C.L., Meyer, D.J., Campbell, G.S., Larner, A.C., Carter-Su, C., Schwartz, J., and Jove, R. (1995). Enhanced DNA-binding activity of a Stat3-related protein in cells transformed by the Src oncoprotein. *Science* 269, 81-83.

Zabaleta, J., Su, L.J., Lin, H.Y., Sierra, R.A., Hall, M.C., Sartor, A.O., Clark, P.E., Hu, J.J., and Ochoa, A.C. (2009). Cytokine genetic polymorphisms and prostate cancer aggressiveness. *Carcinogenesis* 30, 1358-1362.

Zhang, L., Valdez, J.M., Zhang, B., Wei, L., Chang, J., and Xin, L. (2011). ROCK inhibitor Y-27632 suppresses dissociation-induced apoptosis of murine prostate stem/progenitor cells and increases their cloning efficiency. *PloS one* 6, e18271.

Zheng, S.L., Liu, W., Wiklund, F., Dimitrov, L., Balter, K., Sun, J., Adami, H.O., Johansson, J.E., Sun, J., Chang, B., et al. (2006). A comprehensive association study for genes in inflammation pathway provides support for their roles in prostate cancer risk in the CAPS study. *The Prostate* 66, 1556-1564.

Zhou, J., Wulfkuhle, J., Zhang, H., Gu, P., Yang, Y., Deng, J., Margolick, J.B., Liotta, L.A., Petricoin, E., 3rd, and Zhang, Y. (2007). Activation of the PTEN/mTOR/STAT3 pathway in breast cancer stem-like cells is required for viability and maintenance. *Proceedings of the National Academy of Sciences of the United States of America* 104, 16158-16163.

Zietman, A.L., DeSilvio, M.L., Slater, J.D., Rossi, C.J., Jr., Miller, D.W., Adams, J.A., and Shipley, W.U. (2005). Comparison of conventional-dose vs high-dose conformal radiation therapy in clinically localized adenocarcinoma of the prostate: a randomized controlled trial. *JAMA : the journal of the American Medical Association* 294, 1233-1239.

Zynger, D.L., and Yang, X. (2009). High-grade prostatic intraepithelial neoplasia of the prostate: the precursor lesion of prostate cancer. *International journal of clinical and experimental pathology* 2, 327-338.